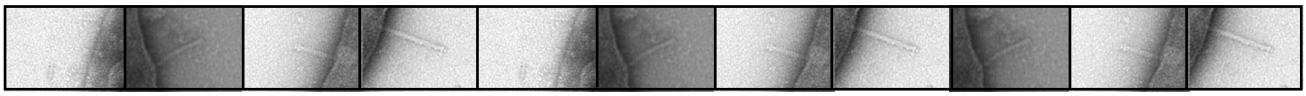

Length control of the *Yersinia* injectisome

Inauguraldissertation

zur

Erlangung der Würde eines Doktors der Philosophie

vorgelegt der

Philosophisch-Naturwissenschaftlichen Fakultät

der Universität Basel von

Stefanie Wagner

aus Mörfelden-Walldorf, Deutschland

Basel, 2010

Genehmigt von der Philosophisch-Naturwissenschaftlichen Fakultät auf Antrag von:

Prof. Dr. Guy R. Cornelis

Prof. Dr. Urs Jenal

Basel, den 8. Dezember 2009

Prof. Dr. Eberhard Parlow, Dekan

Bungestrasse 18
CH-4055 Basel
Switzerland

Table of Contents

Abstract

Many pathogenic bacteria harbor a type III secretion system to translocate effector proteins from the bacterium into the host cell cytosol. This one-step translocation requires a nanomachinery which was termed injectisome. It consists of a basal body, spanning the two bacterial membranes, and a needle-like structure, bridging the distance between the bacterium and the target cell. Control of the length of the type III secretion injectisome needle is crucial for a correct function.
In *Yersinia*, the YscP protein is involved in needle length control: the number of YscP residues directly correlates with needle length. In this thesis, this correlation was shown to be dependent on the secondary structure of YscP. By substitution of individual residues, needle length could be altered without changing the number of residues in YscP. The molecular ruler model was proposed for length control of the *Yersinia* injectisome needle. There are, however, two possibilities for the molecular ruler model regarding the amount of YscP needed for regulation of the needle length of one injectisome. In the static model, only one molecule of YscP and in a more dynamic model, several proteins are required for length control of one needle. Here, it was demonstrated that partially diploid bacteria, expressing a short and a long YscP simultaneously assemble distinct sets of short and long needles. These results suggest that only one YscP molecule is required for length control of one needle. In *Yersinia*, the YscU protein (a member of the export machinery) was suggested to be involved in the substrate specificity switch. Here, YscU was demonstrated to play a role in substrate recognition but not in substrate switching. Taken together, a refined model for length control of the *Yersinia* injectisome needle is proposed in this thesis, confirming the role of YscP as a molecular ruler.

Introduction

Type III secretion

Type III secretion is a protein export pathway (Figure 1) which is found in many pathogenic or symbiotic bacteria such as *Yersinia spp.*, *Salmonella spp.*, *Pseudomonas aeruginosa*, *Shigella spp.*, the enteropathogenic *Escherichia coli* (EPEC) as well as in plant pathogens like *Erwinia amylovora*, *Mesorhizobium loti* or *Pseudomonas syringae* [1].

The type III secretion pathway is involved in both the assembly of the flagellum and the virulence-associated injectisomes [2]. It enables bacteria to secrete proteins across the inner bacterial membrane, the periplasm and the outer bacterial membrane, independent of the sec-pathway and without a periplasmic intermediate (Figure 1; [3]).

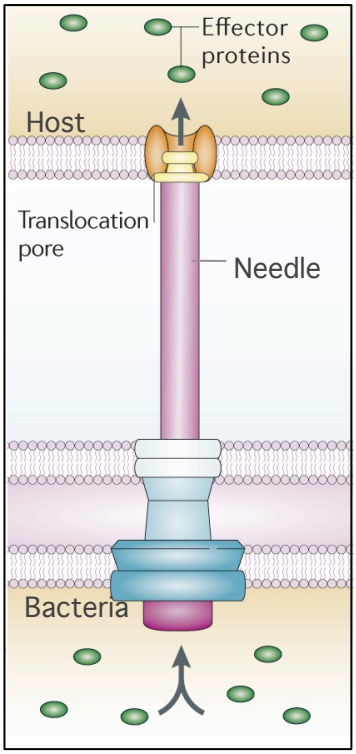

Figure 1

The type III secretion system
Upon contact with the host cell membrane, the tip complex assists with the assembly of the translocation pore, serving as an assembly platform. The effector proteins can now be translocated into the host cell cytosol.
Reprinted by permission from Macmillan Publishers Ltd: *Nature Reviews Microbiology* (Cornelis, 2006, *Nature Reviews Microbiology* **4**, 811–825) ©2006

After contact with the target cell *in vivo* [4 - 6] the virulence-associated type III secretion allows bacteria to inject virulence proteins (effectors) across the eukaryotic plasma membrane into the target cell cytosol. The translocated effectors then alter host-cell functions like cytoskeletal architecture, signal transduction or immune response.

Yersinia

The genus *Yersinia* belongs to the group of gram-negative *coccobacillus*-shaped bacteria in the family of *Enterobacteriaceae*. Three species among the genus *Yersinia* are known human pathogens: *Y. pestis*, *Y. pseudotuberculosis* and *Y. enterocolitica*. Although their route of infection differs, they share the ability to reach the lymphoid tissue by a common tropism while avoiding the host's nonspecific immune response and killing by polymorphonuclear neutrophils (PMNs) [7 - 12]. Within the host tissue *Yersinia* proliferate as extracellular pathogens [13 - 15]. *Y. pestis* is transmitted by flea bites, distributed via the blood stream and causes bubonic plaque. In contrast, *Y. pseudotuberculosis* and *Y. enterocolitica* are food-borne pathogens, that enter the lymphatic system via M cells of the small intestine upon ingestion [16, 17]. They invade the Payer's patches which are gut-associated lymphoid follicles, and finally reach the mesenteric lymph nodes [18]. *Y. enterocolitica* infections in humans lead to gastrointestinal symptoms like diarrhea or mesenteric lymphadenitis. In addition, *Y. pseudotuberculosis* causes a mesenteric adenitis in humans, mimics appendicitis or induces a septicemia [19 - 21].

The ability to cause infections is dependent on the 70 kb virulence plasmid, called pYV (plasmid involved in *Yersinia* Virulence, [22]) in all three species. The pYV plasmid encodes for the complete type III secretion system and the virulence proteins (effectors), which are injected into the cytosol of the target cell by a nanomachine called injectisome. The virulence proteins, so called Yops (for *Yersinia* outer proteins), are further divided into two groups. The first group consists of translocators which are responsible for the formation of a pore-like structure into the plasma membrane of the target cell. The second group includes effector proteins that are injected through the hypothetical pore into the host cell where they alter several host-cell

functions [23]. Furthermore, the pYV plasmid harbors genes encoding chaperones (Syc; [24]), adhesion proteins (e.g., YadA), an arsenite resistance [25] and proteins involved in regulation and assembly of the injectisome. While the Yop effectors and their chaperones are spread all over the plasmid, the genes encoding the machinery (Yscs, for Yop secretion) and the translocators are clustered in operons.

The *Yersinia* injectisome

The type III secretion system consists of a membrane embedded basal body, spanning the two bacterial membranes and the periplasmic space, and a hollow needle protruding from the bacterial surface into the extracelluar space (Figure 2; [26 - 31]). The distinct length of the needle is strictly controlled in order to allow injection of the effectors into the target cell cytosol [32]. In some other pathogens the extracelluar structure is replaced by either a pilus (plant pathogens; [33]) or a filament (enteropathogenic *E. coli*, [34 - 36]).

The basal structure is composed of two connected pairs of rings each spanning one bacterial membrane [30, 37, 38]. The outer membrane ring is built by YscC, a member of the secretin superfamily which form pores into outer membranes [39, 40]. In analogy to the flagellum the inner membrane ring is called MS ring. It consists of a periplasmic lipoprotein which is a member of the highly conserved YscJ familiy and another protein called YscD. The latter one is less conserved among the injectisomes, but its centrally located hydrophobic domain led to the speculation that it is the homolog of PrgH, which is part of the MS ring in *Salmonella typhimurium* [28, 41]. The cytoplasmic ring (C-ring) of the flagellum is built by FliM and FliN. These flagellar proteins share sequence similarities to YscQ, which belongs to a highly conserved protein family of injectisome proteins. Although experimental evidence is missing for injectisomes, YscQ is assumed to build the C-ring linked to the MS-ring. This hypothesis is supported by immunogold experiments, showing the localization of the *Shigella* YscQ homologue Spa33 at the cytoplasmic side of injectisomes [38].

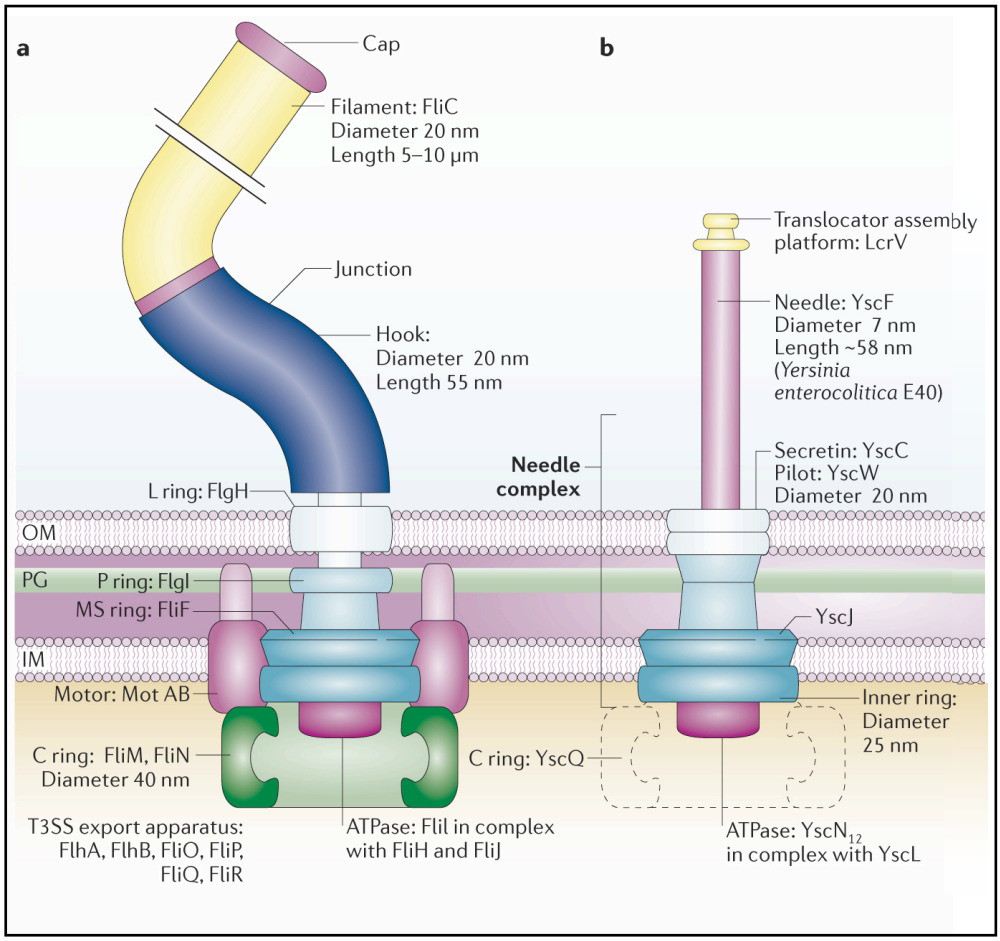

Figure 2

Structure of the bacterial flagellum and the type III secretion injectisome.

Schematic representation of the flagellum (a) and the Ysc injectisome of Yersinia (b). For the injectisome, the C ring is represented by a dashed line as information on this component is still scarce. IM, inner membrane; OM, outer membrane; PG, peptidoglycan.

Assembly of the macroscopic structures beyond the cytoplasmic membrane and secretion of effector proteins requires an export apparatus, which is conserved among all type III secretion systems [42]. It is composed of five predicted inner membrane proteins (YscR, YscS, YscT, YscU, YscV), supposedly located within the cylindrical structure of the MS ring. Three additional proteins (YscK, YscL, YscN), predicted to be either cytoplasmic or peripherally associated to the membrane complete the export machinery. YscN is a membrane associated ATPase, a member of the AAA^+ family [43]. Its essential role might be the detachment of chaperones and

the unfolding of the export substrates [44]. The precise stoichiometry and localization of the export apparatus are still unknown.

The extracellular structure of the *Yersinia* injectisome consists of a hollow tube with an inner diameter of 2 to 3 nm and an outer diameter of about 7 nm. It is built by helical polymerization of about 140 subunits of the YscF protein [26, 45]. At the distal end, the needle structure terminates in a tip structure built by a pentamer of the translocator protein LcrV [45 - 47]. The hydrophilic LcrV is thought to act as assembly platform for the pore [45], which is formed by two other translocators (YopB, YopD) upon cell contact *in vivo*. Both, YopB and YopD, have hydrophobic domains [48] and insert into membranes, but also the third translocator LcrV is neccessary for pore formation [49 - 52]. The injectisome needle has a defined length [53], which is necessary to bridge the distance between the bacterium and the target cell [32].

Length control in microorganisms

Length control is a common feature in biology, and it is encountered in many complex biological structures. Length control must be ensured by the organism to allow a proper assembly and functionality. Consequently, a number of mechanisms evolved for structures adopting a narrow size distribution. Most studies focus on length control of linear structures, built by polymerization of single building blocks.

Examples for length control in microorganisms are the bacteriophage tail, the flagellar hook, the type III secretion system injectisome needle, and the lipopolysaccharide (LPS) O-antigen.

The bacteriophage tail

The tail of bacteriophage lambda is a thin flexible tube of 150 nm length consisting of 32 disks [54], each of which is a ring-like hexamer of the major tail subunit gpV [55, 56]. Eleven genes are required for the assembly of the bacteriophage lambda tail (genes Z, U, V, G, T, H, M, L, K, I, and J [57 - 60]) and three models for length determination of the tail were proposed. First, the Cumulative model suggests an increase in deformation of subunits, which polymerize at the growing end of the tail and therefore, ultimately, a blocking of further addition of subunits. Here, tail length is determined by the intrinsic properties of the subunits [61, 62]. Second, in the Vernier model, an internal element supposedly co-measures length by elongation alongside the growing tail. When both macromolecular structures reach the same length, elongation of the tail stops and thereby a binding site for a terminator molecule is created [63]. Finally, in the ruler model the length of the phage tail is determined by a ruler or tape measure protein (TMP) around which the tail subunits polymerize. Here, the length of the tail is in direct correlation to the length of the ruler protein [64]. Mutations in the tail subunit gpV such as deletions or amino acid substitutions do not affect tail length [65], whereas deletions and insertions in the 92-kDa α-helical protein (60% helical content) encoded by gene H (gpH) result in shorter or elongated tails, respectively [66]. Additionally, the tail length is proportional to the amino acid sequence length of gpH mutants [67]. Alterations in the C-terminal part of gpH,

which is needed for initiator assembly [68], do not change the length of the phage tail. These newer findings clearly supported the Ruler model (Figure 3). Polymerization of the tail subunit gpV on the baseplate is initiated by six gpH proteins [56, 69] which attach to the baseplate as a supramolecular assembly *via* their C-termini. During polymerization of gpV around the six gpH molecules, the TMPs supposedly unfold and serve as tape measure and scaffold at the same time [66]. The growing end of the tail is thought to be protected by the N-terminal part of gpH. Once the tail has reached the length of the stretched gpH protein, the continuously growing gpH-unprotected end would be available for the terminator protein gpU. As a result, stopping of the gpV assembly (Figure 3) [70] and cleavage of gpH [71, 72] is initiated. This two-step process includes a molecular ruler controlling the tail length and a growth terminator locking it in the correct length.

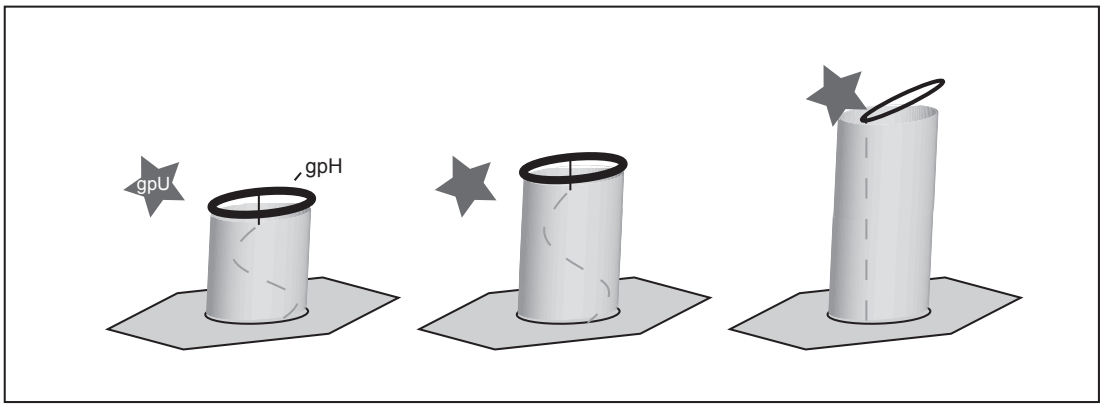

Figure 3
Determination of phage tail length in bacteriophage lambda
During polymerization of the tail subunits, the TMPs (gpH) unfold and serve as tape measure and scaffold. The N-terminal parts of the TMPs protect the growing end of the tail from the terminator protein (gpU). The unprotected tail is available for the terminator protein, which stops polymerization of the tail subunits.

A similar mechanism for tail length determination was found for bacteriophage T4 (reviewed in [73]). Although the organization is more complex, the sequence length of TMP gp29 was found to be proportional to the tail length. Furthermore, structure predictions suggested that the stretched 64 kDa protein gp29 would be sufficiently long to act as a molecular ruler [74]. A strain lacking protein gp3 showed the same phenotype as *ΔgpU* in bacteriophage lambda: a slow and aberrant

elongation of the tail tube, suggesting gp3 as counterpart of gpU acting as a terminator of tail assembly [75]. This hypothesis was validated by showing that gp3 forms a hexameric ring, terminating the tail once it has reached its correct length [76]. In contrast to gpH from bacteriophage lambda, gp29 is supposedly attached to the baseplate via its C-terminus and to the tip of the growing tail via its N-terminus during tail elongation.

Several other studies revealed that TMPs are found in almost all bacteriophages with flexible non-contractile tails, e.g., lambdoid [68] and T phages [73], mycobacteriophages [77] and lactococcal bacteriophages [78]. The length of the TMP proteins are in direct correlation to the corresponding tail length [67, 73]. However, for some phages the TMP is longer than a tail spanning α-helix. This suggests that some regions of these proteins do not participate in length determination [77]. The *tmp* genes are generally encoded on the same locus, though gene length and sequence of TMPs differs even within the same group of bacteriophages [77].

A comparative genomic analysis of 14 mycobacteriophages revealed conserved motifs related to known small proteins which are unrelated to phage or prophage genomes. The role of these motifs is still unclear, suggesting an additional function for TMPs [77]. For mycobacteriophage TM4 it was suggested that the TMP spanning the tail is involved in triggering DNA-injection into bacteria [79]. More recently, the phage T4 TMP containing motif 3 (mt3) was shown to have a peptidoglycan-hydrolyzing activity facilitating efficient infection of stationary phase bacterial cells [80]. A recent study on phage T5 proposes TMP Pb2, besides its role as molecular ruler, sensing the contact to the phage receptor and then triggers the opening of the head-tail connector for peptidoglycan degradation [81]. In this model the TMP acts as molecular ruler, remains attached, and spans the tail. The contact between phage T5 and its receptor then results in a conformational change of the coiled-coil domain (tape measure domain) of the TMP. This conformational change would be the sensor for the opening of the head-tail connector. After DNA release from the capsid, the C-terminus of the TMP supposedly gains access to the bacterial outer membrane. The conformational changes of the TMP finally result in local

degradation of the peptidoglycan and pore formation by fusion of the two bacterial membranes [81].

These findings suggest a general mechanism for length control of the bacteriophage tail by a molecular ruler. This ruler or TMP consists of two domains, one binding the site of tail assembly initiation and a second domain that tracks the growing end of the tail and prevents binding of the growth-terminating protein. When the tail becomes longer than the TMP, the terminator can bind and lock the tail in its correct length. Moreover, the TMPs might have additional functions in the infection process besides their general characteristics of a molecular ruler.

The flagellum

The bacterial flagellum is a highly complex motility organelle with a built in type III secretion machinery [82]. It consists of the basal body spanning the bacterial membranes, the hook junction and the flagellum filament (Figure 2; reviewed in [83 - 85]).

The flagellar basal body consists of three membrane rings (an outer membrane ring (L-ring), a periplasmic ring (P-ring) [86, 87], an integral membrane ring (MS-ring) [87, 88], a rod spanning the periplasmic space [87] and a cytoplasmic ring (C-ring) [89]. The rod is divided into the proximal rod (FlgB, FlgC, FlgF) and a distal rod (FlgG) [87, 90]. The basal body is surrounded by a stator, which consists of multiple copies of an integral membrane structure made of MotA and MotB. The stator is noncovalently attached to the peptidoglycan layer, whereas the rotor consisting of multiple copies of FliG is noncovalently attached to the MS-ring. The stator and the rotor form the flagellar motor, which is responsible for torque generation (reviewed in [85]). The flagellar base also incorporates the type III secretion system which is used to export flagellar proteins during flagellar assembly (reviewed in [84, 91]).

An export apparatus, mounted within the cytoplasmic side of the MS-ring, translocates most external proteins of the flagellum to their site of assembly through a narrow channel of the structure [92 - 94]. It is a multi-protein complex, structurally and evolutionarily related to the virulence associated type III secretion system [27, 91, 95], and it is composed of six membrane proteins (FlhA, FlhB, FliO, FliP, FliQ, FliR)

and three soluble proteins (FliI, FliH, FliJ) [95]. The ATPase complex consisting of FliI (ATPase), FliH, and the chaperone FliJ, is thought to deliver the substrates for the export [96].

The flagellum filament is a long and cylindrical structure of helical shape. The filament is of variable length (5-10 µm), but has a constant diameter of ~ 20 nm. The major subunit of the filament is FliC (flagellin). In contrast to the hook cap, the filament capping protein FliD, which enables flagellin subunits to polymerize at the distal end, remains attached [97 - 99].

The hook is a cylindrical hollow structure serving as a joint between the basal body and the filament. It consists of ~ 130 subunits of FlgE [87]. Assembly of the flagellar hook depends on the hook capping protein FlgD which acts as a scaffold [100 - 102]. Control of hook length was postulated to be essential for proper function and behavior of the cell. The distinct hook length was found to be 55 +/- 6 nm [103] which is necessary to generate a sufficient bend angle for efficient transmission of the torque [104, 105]. To date several theories have been proposed to explain the mechanism how hook length is controlled.

The *fliK* gene was the first gene identified as a regulator of hook length in a broad screen of mutants [106]. The Δ*fliK* mutants were non-motile with hooks of uncontrolled length (ranging from 40 – 900 nm) and no filament attached. The described phenotype was named superhooks [106] later renamed polyhooks [103]. The failure to terminate the hook at its proper length and to initiate filament assembly in Δ*fliK* mutants suggested that FliK is a bi-functional protein [105].

Indeed sequence analysis of the 405 amino acid long protein [104, 107] revealed at least three functional regions: a moderately conserved N-terminus ($FliK_N$, residues 1-180), a proline-rich central part serving as linker ($FliK_L$, residues 181-205) and a highly conserved C-terminal region rich in glutamine residues (residues 206-405), which is thought to be of high conformational flexibility [104, 108]. The C-terminal region consists of a highly stable, compactly folded region (residues 206-370 $FliK_C$) and a partially unfolded stretch from residue 371-405 ($FliK_{CT}$) [109]. Residues 265 to 405 are particularly involved in the switching process, as shown by mutagenesis analysis [109]. The identified domain is highly conserved among the

YscP/FliK familiy [110] and was therefore named T3S4 (Type Three Secretion Substrate Specificity Switch) in FliK [107] and YscP [110].

Furthermore, full length FliK is exported into the culture medium by the flagellum type III secretion pathway. The N-terminal first 40 amino acids seem essential for export of FliK [111]. Export of FliK is important for termination of hook elongation and initiation of filament formation and thus is part of the switch [109]. It should be noted, that some N-terminally truncated FliK variants were not secreted but still switched substrate specificity [112]. However, their switching ability was dependent on their expression level [112]. Therefore, the role of the N-terminus of FliK remains unclear. Moreover, FliK secretion was reported to be independent from hook length control [113].

Many pseudorevertants showing a polyhook-filament phenotype [104, 105, 114] were observed and extragenic suppressor mutations were always mapped in *flhB* [103, 115]. The majority of mutations lay towards the 3' end of *flhB,* leading to a disruption of the predicted cytoplasmic domain of the integral membrane component of the export apparatus [105]. FlhB was reported to be involved in the substrate specificity switch by an autoproteolytic cleavage [116]. It was proposed that FliK measures hook length and senses it to FlhB to switch the export substrate specificity [105].

Observations that mutations leading to short hooks were not within the *filK* gene (as it would be expected in the case of a molecular ruler mechanism) but mapped in *fliM*, *fliG* or *fliN*, encoding for three proteins that form the so-called C-ring beneath the basal body led to another model for length control. The measuring cup model [117] (Figure 4) proposes that the C-ring forms some kind of a cup providing binding sites for all hook subunits (FlgE) and thereby controlling hook length. Upon clearance of the measuring cup, the export machinery is accessible for a switching protein resulting in export of the filament subunits.

In this model, hook length is not determined by FliK but by the number of FlgE proteins fitting into the cup. However, FliK is necessary to switch substrate specificity and finally terminate hook elongation. Interestingly, in *ΔflgD* mutants (hook cap) the hook subunits do not assemble on the rod. Furthermore, the hook subunits are

secreted, but the substrate specificity switch by FliK does not take place [100]. Additionally, the model can not explain a lack of a severe effect in case of overproduction of hook subunits [108, 118]. Moreover, as described by Chevance & Hughes [119], the C-ring cup has only room for max. 50 subunits of FlgE [119, 120]. In this calculation, the space required for the ATPase complex FliHIJ is not considered, and it is unknown if FlgE has associated chaperones. Thus, for a functional cup model, the cup must for example fill and empty 4 times with 30 subunits in order to produce a 120-subunit-long hook. This suggests a more complicated mechanism and imposes a higher complexity for the C-ring than a simple measuring cup device to control hook length [119]. Nevertheless, it should be noted that overproduction of FlgE increases the frequency of polyhook phenotype [118].

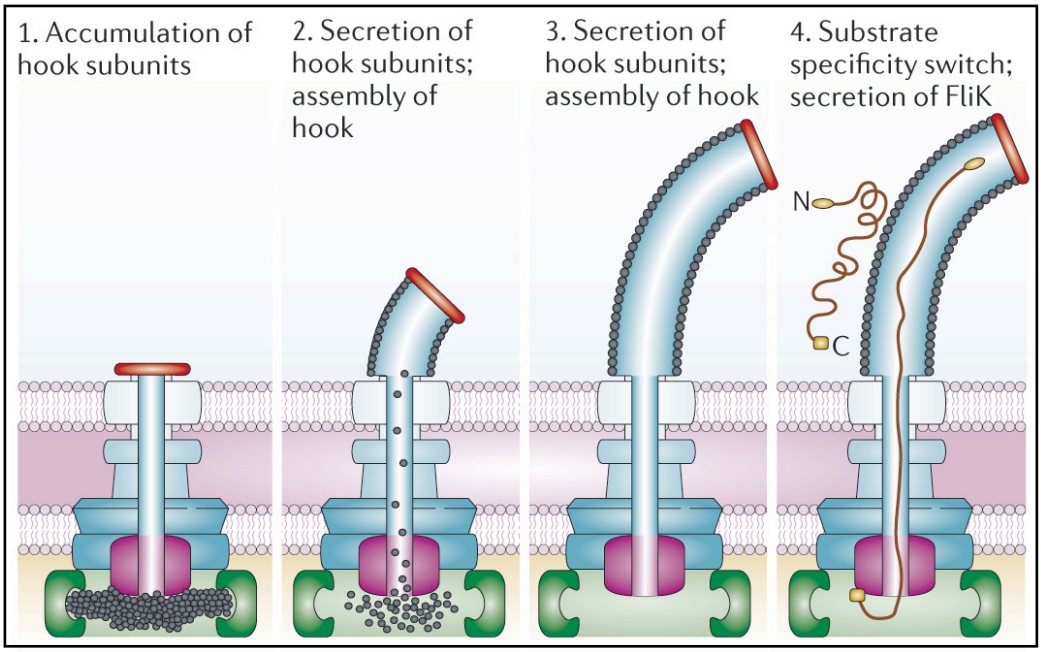

Figure 4

The cup model [117]: The C ring of the basal body is filled with hook subunits (1); the subunits are exported and the hook elongates (2); FliK switches the substrate specificity (3); flagellin is exported and the filament grows (4).

A further model for hook length control was proposed by Moriya *et al*. [118]. In the molecular clock model [118], a dual hook-length control mechanism is proposed, dependent on the rate of hook elongation and on an intrinsic timing device. This timing device either programs the export machinery to switch substrate specificity or slows down the export of hook subunits, independent of hook length. Nevertheless, a complete switch to export filament subunits still depends on an infrequent ruler protein or a tape measure protein [118]. Evidence for the molecular clock model is based on the following observations: *flgE* mutants are defective in polymerization and therefore hook growth rate is slowed down and the timing device stops elongation earlier which results in shorter hooks compared to wild type. Over-expression of the FlgE mutants restores growth to wild type level, supposedly due to an increased polymerization rate. Over-expression of wild type FlgE leads to elongated hooks with a broader length distribution likely due to a increased polymerization rate and decreased interaction between FliK and FlhB [118]. Finally, this model accounts for the observed small peak of normal hook length distribution in a knock-out *fliK* mutant ([121]; although there is a broad distribution): the timing device always switches substrate specificity after a fixed time, based on the average from initiation of hook polymerization. Auto-cleavage of the FlhB C-terminal domain [116] was suggested to be the timing device, the molecular clock. The cleavage slows down hook subunit export before $FliK_{T3S4}$ and $FlhB_C$ interact and the resulting conformational change in FlhB leads to the switch [118].

Interactions between $FliK_N$ and the cytoplasmic domain of FlhB ($FlhB_C$), were reported [109, 116]. Subsequently, it was suggested that $FliK_N$, recognized as export substrate, senses the hook length reaching its mature length to $FliK_C$, which leads to structural conformational changes in $FlhB_C$ [109]. In addition, interactions between $FliK_N$ and the hook capping protein FlgD (high affinity), and the hook subunit FlgE (low affinity) were demonstrated [118] supporting the hypothesis that the N-terminus directly monitors hook length and is required for an effective $FliK_C$ and $FlhB_C$ interaction to switch the substrate specificity.

An appropriate frequency of FliK export is necessary to explain the effect of cellular FliK concentrations on hook length. Overproduction of FliK increases the

chance of $FliK_{T3S4}$-$FlhB_C$ at a slightly earlier timing and therefore shortens hook length, while the decrease of FliK levels also decreases the probability of FliK measuring the growing hook, leading to polyhooks and polyhook filaments [108, 118]. Subsequently, FliK was thought to act as a flexible ruler, a 'molecular tape measure' [118]. Insertion and deletions within the FliK ruler should therefore result in longer and shorter hooks, respectively. Appropriate results were obtained for FliK, but the majority of the deletions led to a loss of function phenotype [113]. This suggests that length control of the flagellar hook does not involve a conventional molecular ruler like for the phage tail. However, most of the deletions in $FliK_N$ result in polyhooks [113] and hence impair the ruler function of FliK. It should be noted that three FliK deletion variants producing shorter hooks were neither detected in culture supernatant nor in the cytoplasm [113]. Therefore, Shibata's conclusion of FliK as the internal ruler and the fact that its secretion is not required for the export specificity switch is not conclusive [113]. In contrast, Minamino *et al*. [122] found that the interaction of $FliK_N$ with the hook and the hook cap is important for an efficient switching process, suggesting that FliK measures hook length inside the hook during the process of FliK secretion.

Hook and filament assembly is a well studied field, but the exact mechanism how FliK measures and controls hook length needs further investigation.

Type III secretion injectisome

The injectisome needle has a defined length of ~ 60 nm for the *Yersinia enterocolitica* Ysc injectisome [53], ~ 30-50 nm for the *Salmonella enterica* type III secretion system [41, 123] and ~ 45 nm for the *Shigella* needle complex [31]. The flagellar hook must be of certain length for mechanical function [104, 105], whereas needle length is optimized to bridge the distance between bacterium and target cell [32]. For length control of the injectisome needle, several hypotheses have been proposed.

The needle length of the type III secretion injectisome is genetically determined as shown for the bacteriophage tail and the flagellar hook. Knock out mutation of *spa32* in *Shigella* [124], *invJ* in *Samonella enterica* (*Salmonella* pathogenicity island 1, SPI-1) [28] and of *yscP* in *Yersinia* [53] lead to needles of undefined length and loss of

effector export. This phenotype evokes the one described for *fliK* knock out mutants in the flagellum (polyhook structures and no export of filament subunits) [105].

YscP a molecular ruler?

The YscP protein is an early substrate of the injectisome [125]. It is exported by the type III secretion machinery into the culture supernatant, also under non-permissive conditions (high calcium concentrations) for effector release. Under such conditions it is loosely attached to the bacterial surface [125]. YscP harbors two independent secretion signals in the N-terminal region [126] (S1: residues 1-35, S2: residues 97-137), and both differ from the export signals of the effector proteins (Figure 5). The two signals, S1 and S2, seem to be redundant for the secretion of YscP, but both are needed for tight length control of the injectisome needle [126]. This observation was also made for InvJ and FliK. It was shown that secretion of InvJ is essential for length control [127], and that export of FliK during hook assembly seems to be important for length determination [111]. Nevertheless, the export of YscP is not required for switching substrate specificity [126]. However, the secretion signals of both proteins are different from those of YscP [111, 127].

Furthermore, an extragenic suppressor mutation in the f*lhB* homolog *yscU* is also capable to restore effector secretion [128]. YscU also undergoes autoproteolytic cleavage as observed for FlhB [129]. Thus, it is likely that YscP and its orthologs fulfil a similar switch function as FliK. This function was assigned to residues 405-500 of the 515 residues YscP [110]. This domain is predicted to have a globular structure, an original α/β fold, a proline-x-leucine-glycine signature and no catalytic activity. Despite limited sequence similarity, the predicted structure is well conserved among the C-terminal region of length-measuring proteins in many injectisomes as well as in the flagellum. Representing a new protein domain, it is called type III secretion substrate specificity switch domain (T3S4) [110].

Deletions of amino acids between residues 36-96 and 222-306 and insertions of additional amino acids between residues 49-50 revealed shorter and longer needles, respectively. Furthermore, a linear relationship for needle length *versus* number of YscP residues was observed. In addition to S1 and S2 of YscP which link

export of YscP with length determination, and the T3S4 domain, two other regions were assigned as ruler regions involved in length control. One builds the spacer between S1 and S2 (residues 36-96) and the other extends from S2 to the T3S4 domain (residues 138-381) [53].

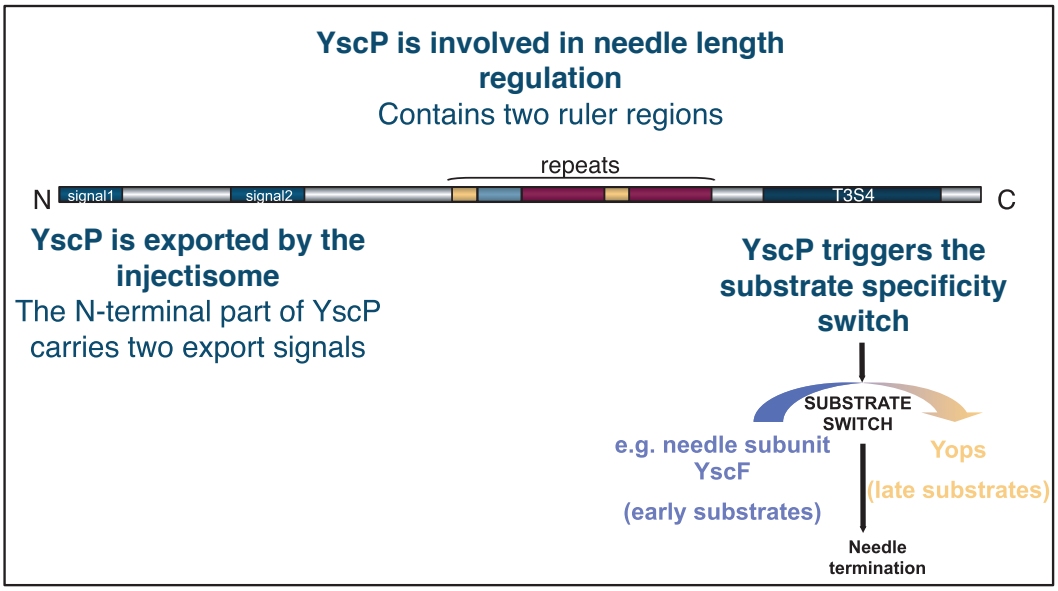

Figure 5

Schematic representation of YscP showing the export signal(s) localized in the amino-terminal part of the protein, and the T3S4 domain localized in the carboxy-terminal part of the protein. A repeat region is localized in the central ruler domain.

The molecular ruler model for YscP is based on the previous findings. According to this hypothesis, length control involves a two-step process: measurement of needle length and switching of substrate specificity. However, two possible explanations were proposed [52, 131].

The initial model is static and proposes that one molecule of the ruler is anchored by its N-terminus to the growing end of the needle and gradually stretches while the needle elongates. In the fully elongated state, the ruler senses the stretch to the T3S4 domain, located inside the basal body, resulting in a switch in substrate specificity. Here, the ruler occupies the channel in an extended form, while the needle subunits simultaneously travel through the channel to the growing end (Figure 6) [53].

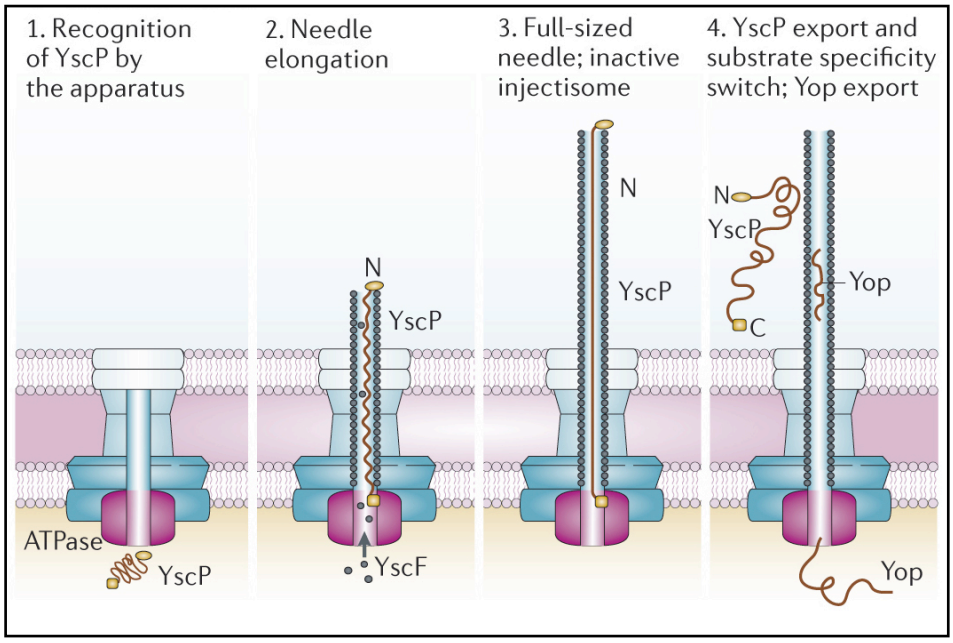

Figure 6

The ruler model [53]

YscP enters the channel after completion of the basal structure (1); the needle subunits are exported and polymerize, leading to the extension of the ruler component of YscP (2); the needle assembly is completed (3); the T3S4 domain of YscP switches the substrate specificity to effector secretion and the ruler is released (4).

Reprinted by permission from Macmillan Publishers Ltd: *Nature Reviews Microbiology* (Cornelis, 2006, *Nature Reviews Microbiology* **4**, 811–825) ©2006

The inner diameter of the needle is only 2-3 nm, raising the question whether the ruler and the needle subunit could occupy the channel simultaneously. A few elements do not perfectly fit with this ruler model. Indeed, it was shown that over-expression of YscP can improve length control [126, 130]. Consequently, a more dynamic version of the ruler model was proposed (Figure 7a; [131]). Here, the needle length is monitored by more than one ruler, which is exported in alternation with the needle subunit. And as proposed for FliK [118] the ruler can only switch substrate specificity, when the needle structure reaches the correct length (Figure 7a).

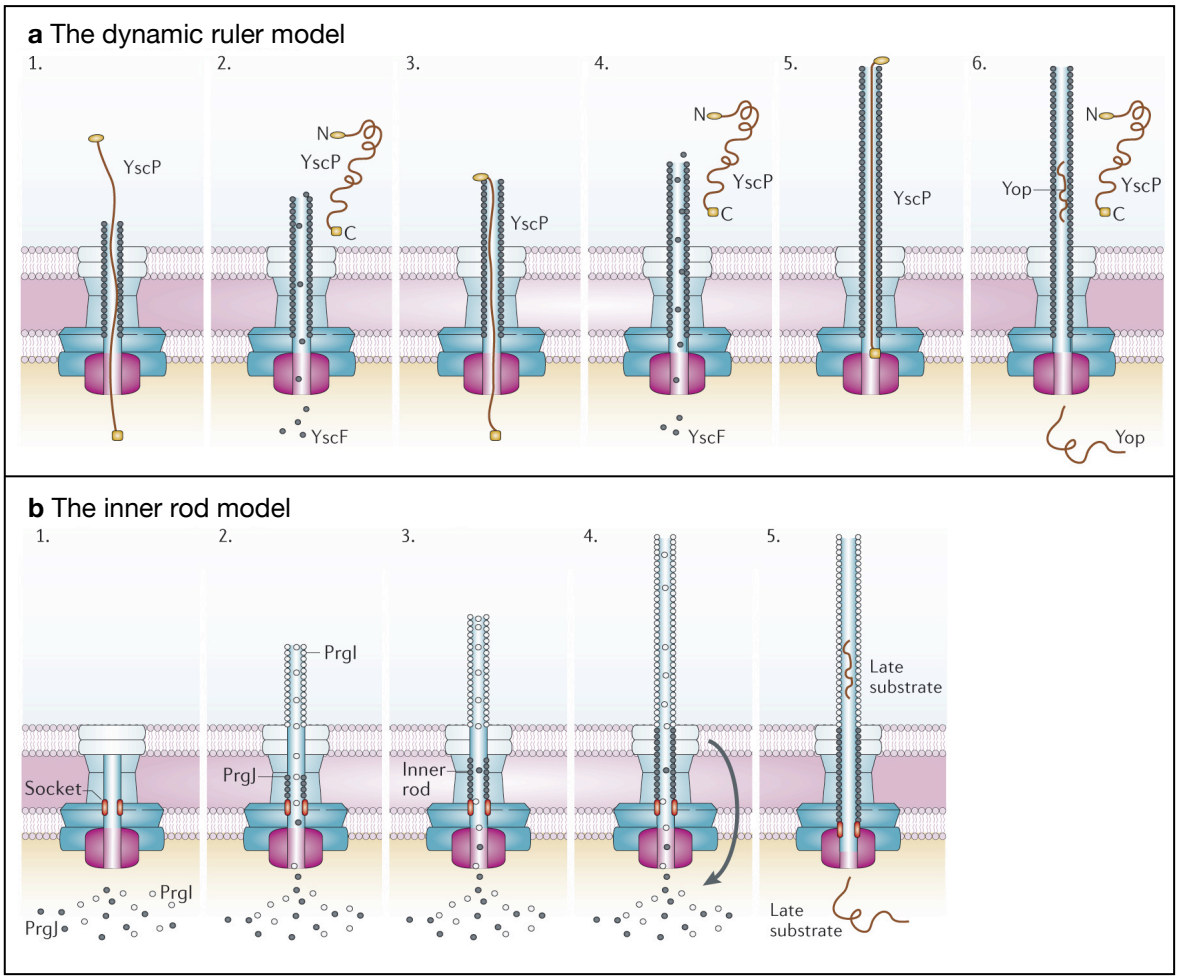

Figure 7

Alternative models for needle length control

a | The dynamic ruler model [131]: Here, ruler and needle subunit molecules are exported alternately (1 to 4). The ruler checks the length while traveling through the channel (1 and 3). When the exact length is reached, the ruler switches the substrate specificity (5), leaving the injectisome ready for translocator and effector protein (Yop) export (6). b | The inner rod model [123]: Needle length control by timing of substrate switching. In this model, InvJ stabilizes the socket substructure (shown in red (1)), which is necessary for the assembly of the inner rod (black subunits composed of PrgJ). Note that the needle (white subunits, composed of PrgI) assembles simultaneously (2, 3). Termination of the inner rod results in conformational changes that lead to substrate switching (4). Late substrates are then exported (5).

So far, a correlation between needle length and length of the ruler protein is known only for the *Y. enterocolitica* injectisome [53]. For the *Shigella* injectisome needle it was suggested that Spa32, an YscP homolog, acts rather as a tape measure protein than as a molecular ruler [132]. The molecular ruler is suggested to

stretch during needle growth, whereas the tape measure protein is secreted during needle elongation. Finally, investigation of the *Salmonella* SPI-1 injectisome led to another hypothesis. Marlovits *et al*. [123] proposed for *Salmonella enterica* (SPI-1) that assembly of the inner rod determines the length of the type III secretion injectisome needle. The 'Inner Rod model' suggests for InvJ, a counterpart of YscP, a new function in respect of length control. In *invJ* knockout mutants a socket like structure, acting as linker between the inner rod and the base of the basal body, is missing and the needles easily break off. InvJ is proposed to stabilize the socket and thus allows proper assembly and anchoring of the rod and the needle. In a previous study, Marlovits *et al*. [37] showed significant conformational changes on the cytoplasmic face of the basal body upon completion of the injectisome. These changes were suggested as structural basis for the substrate specificity switch. It was suggested that a properly anchored rod is necessary for switching the substrate specificity (Figure 7b).

Many questions on the mechanism have been addressed and there is given evidence for the ruler model as the appropriate one for the *Y. enterocolitica* injectisome needle. However, experimental evidence for one or the other molecular ruler model is still lacking.

The O-antigen of the lipopolysaccharide

Another example of length control in microorganisms exists for the O-antigen chain of the lipopolysaccharide (LPS). LPS represents the major surface structure of Gram-negative bacteria and consists of a polysaccharide O-antigen chain, a core oligosaccharide and lipid A which anchors the LPS molecule in the outer membrane (reviewed in [133]). LPS isolated from exponentially growing bacteria is heterogeneous in size, as seen by characteristic ladder patterns in gel electrophoresis [134 - 136]. Although the size of the O-antigen varies to a certain extend, there is a characteristic strain-specific modal chain length. In general, O-antigens are assembled by the so-called Wzy-dependent pathway (reviewed in [137]), where the O-antigen is synthesized on a polyisoprenoid lipid carrier at the cytoplasmic side of the inner membrane. The intermediates are then translocated

across the inner membrane with the help of the integral membrane protein Wzx. These lipid-linked oligosaccharides are polymerized en bloc in a periplasmic reaction, involving the integral membrane protein Wzy. In the final stage of LPS biosynthesis the O-antigen is linked to a preformed lipid A-core molecule prior to surface translocation of the completed molecule.

The integral inner membrane protein Wzz determines the O-antigen chain length [138, 139] and is a homolog to the polysaccharide co-polymerase (PCP) protein (class 1). These proteins have a regulatory role in polymerization [140, 141]. PCP family members (including families PCP-1, PCP-2, and PCP-3) share a conserved membrane topology. They consist of two transmembrane (TM) helices that flank a large hydrophilic periplasmic domain (PD), which contains amino acid sequences predicted to form coiled-coils (CCs) and which possesses a proline-rich consensus motif at the C-terminal TM span (TM2) [142 - 146].

The SDS-PAGE profiles of LPS isolated from wzz-null mutants are non-modal, where polymerization is terminated prematurely and a random distribution of O-antigen chain length, favoring a low number of repeat units in the polysaccharide, is observed. In complementation experiments, expression of heterologous wzz genes in a wzz-deficient background results in O-antigens with chain lengths characteristic for the source of the wzz gene [139, 143, 147, 148].

The mode of action of these proteins, however, remains obscure but two possible regulatory strategies have been postulated: a ‘molecular stopwatch’ [143] and a ‘molecular ruler’ [144]. To obtain insight into the Wzz mechanism, crystal structures were obtained for the periplasmic domains of three Wzz homologs (WzzPD) [149]. In each case, the domain forms an extended α-helical hairpin connected to an α/β base domain. The protomers assemble into complexes containing three, five, eight, or nine subunits (depending on the particular Wzz homolog) [149]. From these structural studies it was proposed that the oligomerization state of Wzz homologs defines the molecular ruler responsible for determining O-antigen chain length [149]. However, Larue *et al.* [150] studied various full-length Wzz homologs and observed different oligomeric states compared to those of the periplasmic domains alone [149, 151]. In case of a reconstitution in a

lipid bilayer, the full-length Wzz homologs all display the same quaternary structure, which contradicts the molecular ruler hypothesis.

Nilsson *et al*. [152] showed that *Helicobacter pylori* varies its LPS fucosylation pattern and that alteration of the number of heptad repeats in the fucosyltransferase sequence results in a corresponding size change of the glycosylated O-antigen chain. They demonstrated that one heptad repeat in the fucosyltransferase corresponds to one *N*-acetyl-lactosamine unit in the O-antigen polysaccharide, which supports the molecular ruler model [152].

Substrate specificity switch

YscU/FlhB

Mutations affecting FliK, the flagellar YscP homolog, lead to extra-long hooks (called polyhooks) but no filament and hence bacteria are not motile [103]. Motile revertants appear as a consequence of extragenic suppressive mutations in the integral membrane protein FlhB, suggesting a role for FlhB in specificity switching [105, 115]. FlhB has a long C-terminal cytosolic domain, which undergoes an autoproteolytic cleavage between N269 and P270; the resulting subdomains however, remain tightly associated with each other [116, 153, 154]. This cleavage is abolished by the mutation N269A and cells producing $FlhB_{N269A}$ assemble polyhook structures lacking filaments. It was proposed that cleavage and interaction of the two fragments generates conformational changes important for the specificity switching process (reviewed by [155]).

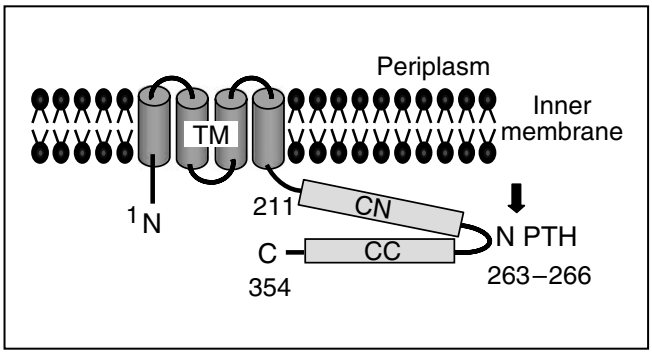

Figure 8

Schematic representation of YscU based on the studies by Allaoui *et al.* [156] and Lavander *et al.* [129]. The black arrow represents the putative cleavage site. N-terminus (N); C-terminus (C); conserved NPTH motif (NPTH); transmembrane domain (TM); N-terminal part of the C-terminal domain (CN); C-terminal part of C-terminal domain (CC). Numbers indicate amino acid position in YscU from *Y. enterocolitica* W22703.

The FlhB homolog in the *Yersinia* injectisome is called YscU, a 354-residue polypeptide with four transmembrane helices and a long cytoplasmic tail [156]. As observed for FlhB, YscU undergoes autoproteolytic cleavage before P264,

generating a 10-kDa C-terminal fragment [129]. YscUN263A is resistant to this cleavage, but interestingly retains the capacity to secrete Yops [129].

The position of LcrV at the tip of the needle implies that LcrV is exported immediately after YscF but before the Yops. Thus, the hierarchy of secretion must consist of at least three categories of substrates and not only two as in the flagellum. There are, however, no genetic data to support this assumption.

Aim of the Thesis

The aim of this PhD thesis is to understand the mechanism of needle length control in the *Yersinia* injectisome. It was previously shown that the number of residues of the protein YscP correlates to the length of the injectisome needle, suggesting that YscP might act as a molecular ruler determining the needle length. Moreover, YscP has two N-terminal secretion signals and it was demonstrated that YscP itself needs to be exported to fulfill its function. In addition to length determination of the injectisome needle, YscP was shown to be required to switch on the export of late substrates. This function was assigned to the C-terminal domain, called substrate specificity switch domain (T3S4). However, the exact mechanism and the interacting partners still remain unclear. The protein FlhB, a homolog of YscU and a transmembrane protein in the flagellum was shown to be involved in this switching. Therefore, the role of the FlhB homolog in *Yersinia* (YscU) was investigated.

The original ruler model suggested that YscP and the needle subunit YscF travel at the same time inside the growing needle. However, some data suggest a more dynamic model, where several YscP molecules are released alternating with YscF proteins.

Therefore, the main questions addressed in this thesis are the following:

1. How does YscP measure the length of the injectisome needle - what is the role of the ruler domains?
2. How many YscP proteins are needed to control the length of a single needle?
3. What is the role of YscU in needle length control and substrate specificity switching?
4. Does YscP act as a molecular ruler or as a timer?
5. Which other proteins are involved in needle length control?

Results

How does YscP measure the length of the injectisome needle?

What is the role of the ruler domains?

The helical content of the YscP molecular ruler determines the length of the *Yersinia* injectisome

Stefanie Wagner[1], Isabel Sorg[1], Matteo Degiacomi[2], Laure Journet[1], Matteo Dal Peraro[2] and Guy R. Cornelis[1]*

[1] Biozentrum der Universität Basel, Basel, Switzerland.

[2] Laboratory for Biomolecular Modeling, Institute of Bioengineering, School of Life Sciences, EPF Lausanne, Switzerland.

Author contributions

SW, LJ and GC conceived the experiments. SW, LJ, MDP and GC designed the experiments. SW, IS, MD and LJ performed the experiments. SW, MDP and GC analyzed the data. SW, MDP and GC wrote the the paper.

The length of the *Yersinia* injectisome needle is determined by the protein YscP, which could act as a molecular ruler. The analysis of the correlation between the size of YscP and the needle length in seven wild-type strains of *Yersinia enterocolitica* reinforced this hypothesis but hinted that the secondary structure of YscP might influence needle length. Hence, 11 variants of $YscP_{515}$ were generated by multiple Pro or Gly substitutions. The needle length changed in inverse function of the helical content, indicating that not only the number of residues but also their structure controls length. Taking the secondary motifs into account, Pro/Gly-variants were subjected to *in silico* modelling to simulate the extension of YscP upon needle growth. The calculated lengths when the helical content is preserved correlated strikingly with the measured needle length, with a constant difference of ~29 nm, which corresponds approximately to the size of the basal body. These data support the ruler model and show that the functional ruler has a helical structure.

Molecular Microbiology (2008) ■ doi:10.1111/j.1365-2958.2008.06556.x

The helical content of the YscP molecular ruler determines the length of the *Yersinia* injectisome

Stefanie Wagner,[1] Isabel Sorg,[1] Matteo Degiacomi,[2] Laure Journet,[1†] Matteo Dal Peraro[2] and Guy R. Cornelis[1*]
[1]*Biozentrum der Universität Basel, Basel, Switzerland.*
[2]*Laboratory for Biomolecular Modeling, Institute of Bioengineering, School of Life Sciences, EPF Lausanne, Switzerland.*

Summary

The length of the *Yersinia* injectisome needle is determined by the protein YscP, which could act as a molecular ruler. The analysis of the correlation between the size of YscP and the needle length in seven wild-type strains of *Yersinia enterocolitica* reinforced this hypothesis but hinted that the secondary structure of YscP might influence needle length. Hence, 11 variants of $YscP_{515}$ were generated by multiple Pro or Gly substitutions. The needle length changed in inverse function of the helical content, indicating that not only the number of residues but also their structure controls length. Taking the secondary motifs into account, Pro/Gly-variants were subjected to *in silico* modelling to simulate the extension of YscP upon needle growth. The calculated lengths when the helical content is preserved correlated strikingly with the measured needle length, with a constant difference of ~29 nm, which corresponds approximately to the size of the basal body. These data support the ruler model and show that the functional ruler has a helical structure.

Introduction

Size determination represents a fundamental problem for multi-component biological structures with a complex architecture including tubular components (Marshall, 2004). In few cases, like the tail of bacteriophages, it appears that one protein acts as a tape measure or a molecular ruler (Katsura and Hendrix, 1984; Katsura, 1987; Pedulla *et al*., 2003). The molecular ruler, in its elongated state, determines the number of subunits of another protein that are allowed to polymerize to create the tubular structure. The same concept has been proposed to determine the length of the needle of the bacterial injectisome (Journet *et al*., 2003) and of the flagellar hook (Moriya *et al*., 2006). In the latter cases, the situation is more complex than in bacteriophages because the needle and hook are assembled outside from the bacterial cytosol and the exact mechanism remains a matter of debate. The flagellar hook-length control and assembly have been recently comprehensively reviewed (Waters *et al*., 2007; Chevance and Hughes, 2008).

The injectisome or needle complex allows pathogenic or symbiotic bacteria to inject effector proteins across eukaryotic cell membranes, a process called type III secretion (T3S). This nanomachine, which is evolutionary related to the flagellum (Macnab, 2003), consists of a basal body surmounted by a hollow stiff needle (Kubori *et al*., 1998; 2000; Blocker *et al*., 1999; 2001; Hoiczyk and Blobel, 2001), a filament (Knutton *et al*., 1998; Daniell *et al*., 2001; Crepin *et al*., 2005) or a pilus (Van Gijsegem *et al*., 2000) that projects from the bacterial surface into the exterior milieu. The basal body is made of several rings embedded in the two bacterial membranes (Blocker *et al*., 1999; 2001; Marlovits *et al*., 2004; Morita-Ishihara *et al*., 2006). The MS ring, spanning the plasma membrane, contains a number of integral membrane proteins constituting the core of the T3S export apparatus (reviewed by Tampakaki *et al*., 2004; Cornelis, 2006; Galan and Wolf-Watz, 2006; Yip and Strynadka, 2006).

The *Yersinia enterocolitica* Ysc injectisome terminates with a 65-nm-long stiff hollow needle, made of ~140 copies of the 9 kDa YscF protein (Hoiczyk and Blobel, 2001). At the tip of the needle, a pentamer of LcrV (Mueller *et al*., 2005; Broz *et al*., 2007) forms a tip structure serving as an assembly platform for the translocation pore (Goure *et al*., 2005; Mueller *et al*., 2008). In *Y. enterocolitica*, the needle detaches very easily from the bacterium and the detached needles have a constant length, implying that they detach from their origin or brake always at the same point (Journet *et al*., 2003). During morphogenesis, the needle components, like the hook and the filament of the flagellum are sequentially exported by the T3S apparatus itself (Sukhan *et al*., 2001), travelling through the growing structure and polymerizing at its

Accepted 17 November, 2008. *For correspondence. E-mail guy.cornelis@unibas.ch; Tel. secretary (+41) 61 267 21 21; direct (+41) 61 267 21 10; Fax (+41) 61 267 21 18. †Present address: UMR7175-LC1, CNRS-Université, Strasbourg 1, France.

distal end (Li *et al.*, 2002; Macnab, 2003). There is no clear hierarchy in the synthesis of the injectisome components and substrates. Thus, the export apparatus is expected to switch its substrate specificity over time so that needle subunits (early substrates) are exported before LcrV (intermediate substrate) and the effectors (late substrates). This substrate specificity switch presumably leads to the arrest of needle growth (Ferris and Minamino, 2006).

The switch to export late substrates is triggered by a protein, which is itself exported, FliK for the flagellum (Hirano *et al.*, 1994; Minamino *et al.*, 1999; 2004) and YscP for the *Yersinia* spp. injectisome. More precisely, this switch function was assigned to residues 405–500 of the 515-residue YscP (Agrain *et al.*, 2005a). This domain, predicted to have a globular structure, an original α/β fold, a P-x-LG signature and no catalytic activity, is called T3S4 for Type 3 Secretion Substrate Specificity Switch (Agrain *et al.*, 2005a). The T3S4 domain is thought to interact with YscU (FlhB in the flagellum), a component of the basal body that is also involved in setting the hierarchy of export (Hirano *et al.*, 1994; Sorg *et al.*, 2007). Overexpression of the T3S4 domain alone allows the system to switch on the export of late substrates but it does not lead to needle length control, implying that the N-terminus of YscP is necessary to determine at which stage the switch has to occur (Agrain *et al.*, 2005b). YscP is itself an early substrate of the machine (Stainier *et al.*, 2000; Riordan *et al.*, 2008) driven by two independent export signals (S1: residues 1–35 and S2: 97–137) and export is required to ensure a proper length control (Agrain *et al.*, 2005b). Deletions between residues 36–96 and 222–306 of YscP and insertions between residues 49 and 50 lead to shorter and longer needles, respectively, with a linear correlation between the size of YscP and the needle length (Journet *et al.*, 2003). This led to a model where YscP acts as a molecular ruler measuring the needle (Journet *et al.*, 2003). According to the model, export of needle subunit proteins would be allowed until the length of the needle reaches the length of the extended YscP ruler domain after which, the T3S4 domain of YscP would signal the secretion apparatus to stop exporting needle subunits. YscP is thus a protein with a dual function, ruler and substrate specificity switch. A similar correlation was observed between the size of FliK and the length of the hook but it was interpreted in a different way (Shibata *et al.*, 2007).

In this paper, we provide evidence that not only the number of residues but also the secondary structure of YscP plays a role in determining the needle length and we show that the predicted length of various YscP variants in their functional state approximates to the actual needle length that they determine. These data further support the ruler model (Journet *et al.*, 2003).

Results

The needle length is not constant in the Y. enterocolitica *species*

The needles made by *Y. enterocolitica* E40 endowed with YscP from *Yersinia pestis* KIM are shorter than the natural needles of *Y. enterocolitica* E40 (Journet *et al.*, 2003). This observation indicates that the needle length varies within the genus *Yersinia* and suggests that it might vary also within the species *Y. enterocolitica.* As this information might be valuable for the understanding of the mechanism, we sequenced the *yscP* genes in seven isolates belonging to different serotypes and biotypes of *Y. enterocolitica* (Table S1). The sequences (aligned in Fig. S1) revealed that the YscP proteins varied from one another by the number of times three different motifs are repeated (Fig. 1A). The shorter protein had only 453 residues while the longer one had 551 residues. We then measured the needles made by all these strains (Fig. S2) and, as expected, the plot of the needle length versus the number of residues of YscP (Fig. 1B) indicated a linear correlation. Interestingly, however, for two strains, the point was clearly off the regression line. In particular, needles from strain IP17, having the longest YscP (551 aa), were significantly shorter than the needles from WAT9/88, which has a 539-aa YscP. In addition, three strains, which have an YscP protein of 515 aa, did not synthesize needles of exactly the same length. All this suggested not only that the length of YscP was determining the needle length but that, possibly, another parameter could be involved. Comparing the different YscP sequences, it appeared that there were variations in the percentage of proline residues and in the content of predicted α-helices (Fig. 1A).

The needle length correlates with the helical content of the ruler part of YscP

To test the hypothesis that the helical content of YscP may influence the needle length, we turned to YscP from strain W22703, the model protein which was used in our previous work (Journet *et al.*, 2003). We first substituted four, six or eight prolines that occurred within predicted unstructured regions (Pro 174, 181, 185, 188, 237, 238, 244, 252) by alanines, which are strong helix formers (Chou and Fasman, 1978) and we replaced four, six or eight residues in the middle of putative predicted α-helices by prolines (Gln 212, 217; Leu 268, 283, 303; Glu 277, 375, 379), as schematized in Fig. 2A. The eight recombinant YscP proteins had thus the exact same number of residues as wild-type YscP (515 aa), but they determined different needle lengths (Fig. 2B and C). Although the median lengths did not differ from more than 15 nm, the differences were statistically significant and

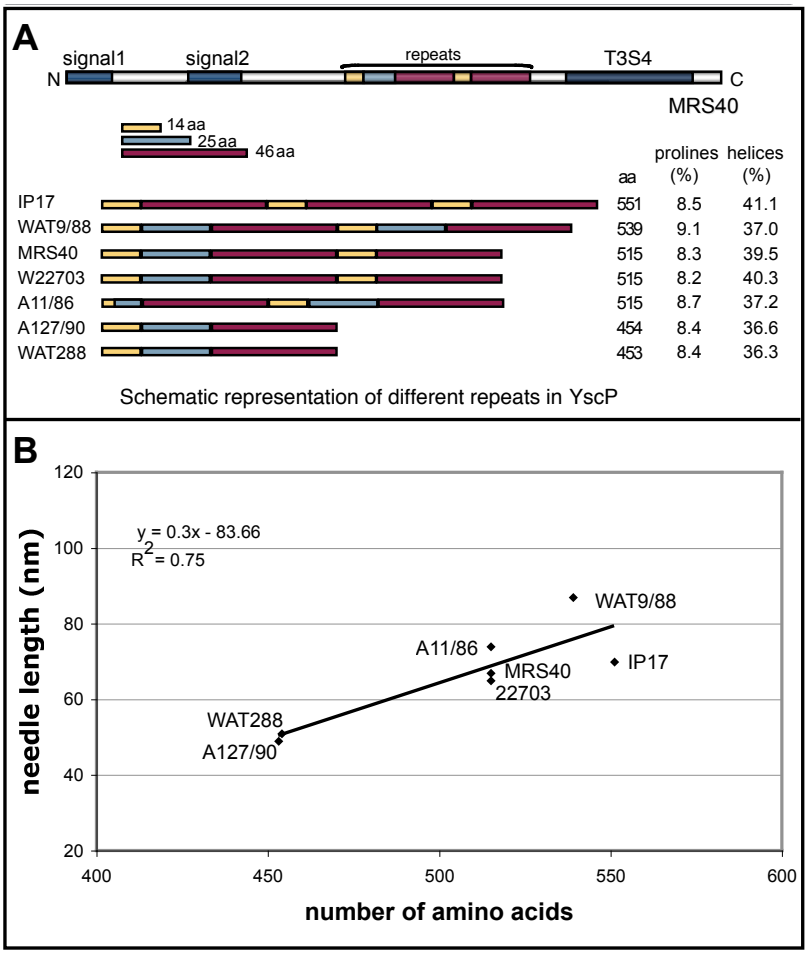

Fig. 1. Correlation between the YscP number of residues and the length of needles present in various different wild-type strains.
A. Schematic representation of the sequences of the different YscP proteins. The proteins differ by the number of repetitions of three sequences.
B. The needle length plotted against the total number of residues in YscP.

there was a linear correlation between the number of prolines in YscP and needle length (Fig. 3 lower slope). As a control, four residues in non-helical regions were also substituted by prolines (Glu 145, 151; Leu 162; Gln 165) (pSTW44) (Fig. 2B) and, in this case, substitutions did not affect the needle length (66 nm versus 65 nm for the wild type).

This result suggested that the impact of prolines might be due to the breakage of α-helices. To test this hypothesis, four residues in predicted helices (Gln 212, 217; Glu 375, 379) were substituted by glycines (pSTW46), known to be as strong helix breakers as prolines (Chou and Fasman, 1978). Here again, the substitutions had impact on needle length, which increased to 70 nm (Figs 2B and 3), suggesting that indeed the helical content of YscP within the 138–380 domain as predicted by bioinformatics tools is highly correlated with the needle length (Fig. S3). *A posteriori*, these mutagenesis results also concur to validate the initial prediction of the secondary structure for YscP protein (see *Experimental procedures*).

The length of the extended YscP is consistent with the needle length

The data presented so far suggest that the functional conformation of YscP includes α-helices. We thus tried to have an insight into the actual length of YscP in this conformation. In order to do this, an *in silico* molecular dynamics (MD) approach was used to simulate the pulling of the protein starting from a random initial conformation, which would mimic the extension of YscP upon needle growth (see *Experimental procedures*). We modelled the secondary structure of region 36–380 of YscP. This includes (i) the region between signal 1 and signal 2 (36–96) that remains invariant in the present set of simulations, (ii) signal 2, and (iii) the central ruler region (138–380), affected in the present set of YscP mutants. We submitted the wild type along with nine variants (Table S2) to a series of independent steered MD simulations both in water and *in vacuo* (see *Experimental procedures*). From the analysis of YscP extension under constant velocity

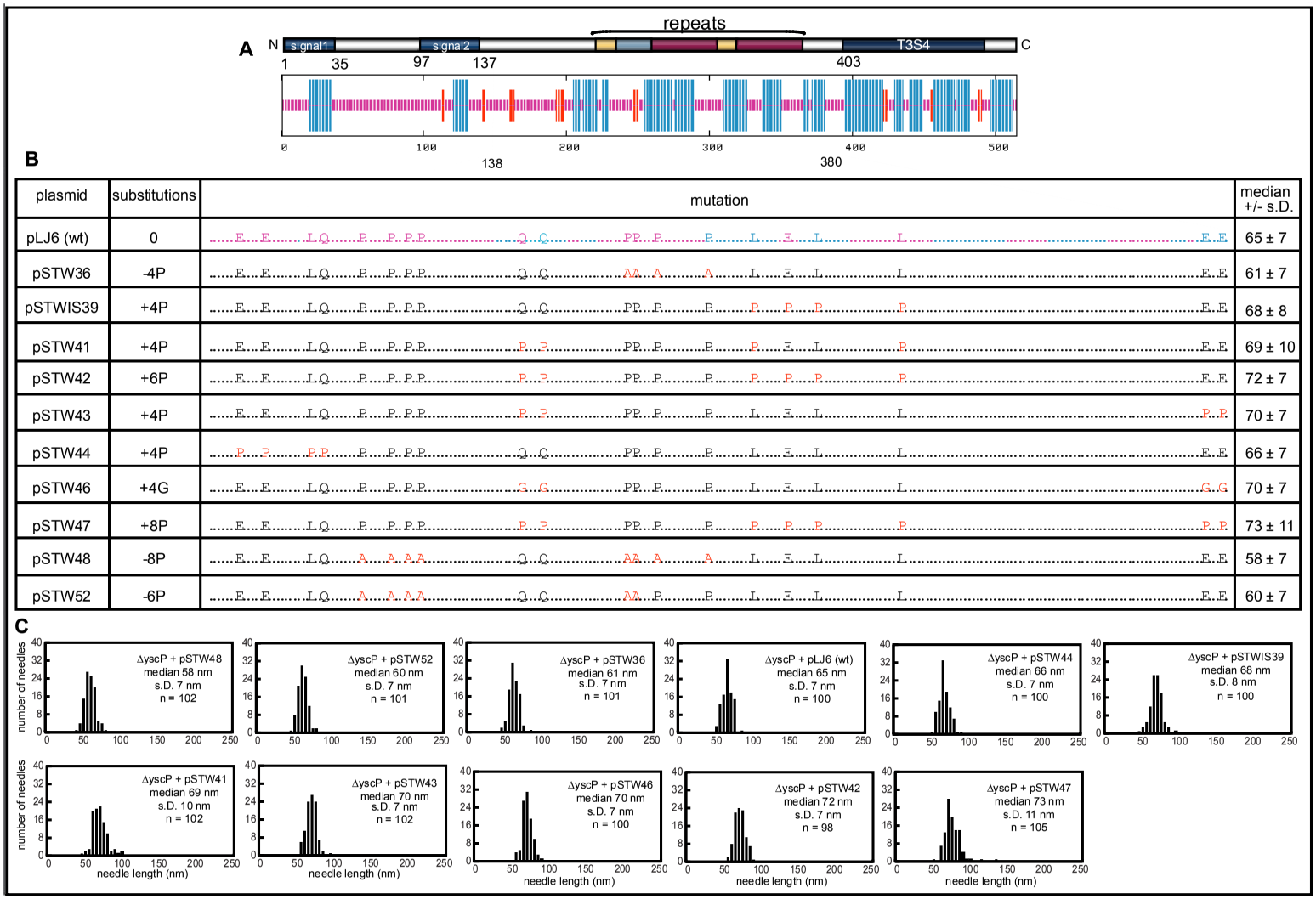

B

plasmid	substitutions	mutation	median +/- s.D.
pLJ6 (wt)	0	.....E..E.....LQ.....P....P..P.P.....Q..Q.....PP...P.....P.....L...E..L.....L.....E.E	65 ± 7
pSTW36	-4P	.....E..E.....LQ.....P....P..P.P.....Q..Q.....AA...A.....A.....L...E..L.....L.....E.E	61 ± 7
pSTWIS39	+4P	.....E..E.....LQ.....P....P..P.P.....Q..Q.....PP...P.....P.....P...P..P.....P.....E.E	68 ± 8
pSTW41	+4P	.....E..E.....LQ.....P....P..P.P.....P..P.....PP...P.....P.....P...E..L.....P.....E.E	69 ± 10
pSTW42	+6P	.....E..E.....LQ.....P....P..P.P.....P..P.....PP...P.....P.....P...P..P.....P.....E.E	72 ± 7
pSTW43	+4P	.....E..E.....LQ.....P....P..P.P.....P..P.....PP...P.....P.....L...E..L.....L.....P.P	70 ± 7
pSTW44	+4P	.....P..P.....P.P.....P....P..P.P.....Q..Q.....PP...P.....P.....L...E..L.....L.....E.E	66 ± 7
pSTW46	+4G	.....E..E.....LQ.....P....P..P.P.....G..G.....PP...P.....P.....L...E..L.....L.....G.G	70 ± 7
pSTW47	+8P	.....E..E.....LQ.....P....P..P.P.....P..P.....PP...P.....P.....P...P..P.....P.....P.P	73 ± 11
pSTW48	-8P	.....E..E.....LQ.....A....A..A.A.....Q..Q.....AA...A.....A.....L...E..L.....L.....E.E	58 ± 7
pSTW52	-6P	.....E..E.....LQ.....A....A..A.A.....Q..Q.....AA...P.....P.....L...E..L.....L.....E.E	60 ± 7

C

Fig. 2. Effect of amino acids substitutions in YscP on the needle length.
A. Schematic representation of YscP. Secondary structure predicted by SIMPA96. Blue bars = α helices; red bars = β sheets; purple bars = unstructured.
B. Table showing the substitutions introduced between residues 138 and 380. Note that prolines have been removed from unstructured domains (except for position 303) while they were inserted into predicted α-helices, except for plasmid pSTW44 where the substitutions have been made in a region predicted to be unstructured (control). Glycines were also introduced into predicted α-helices.
C. The histograms of length measurements. s.d., standard deviation; *n*, number of measured needles.

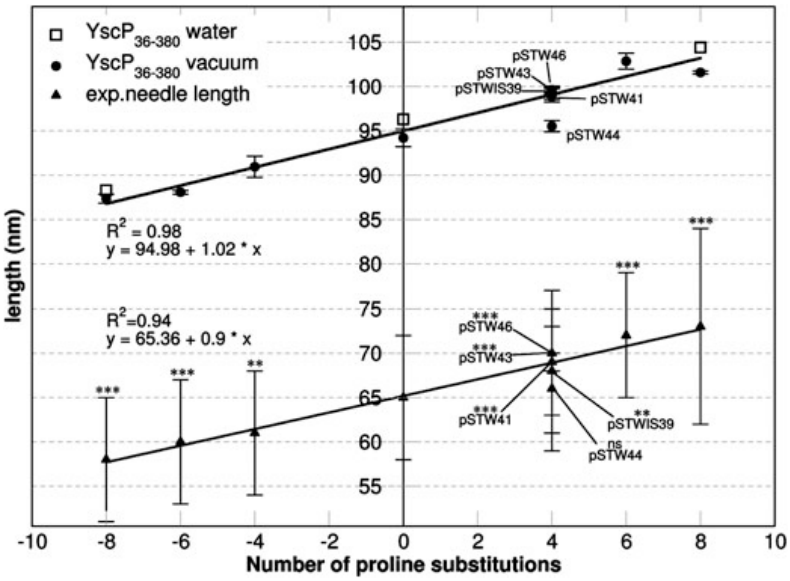

Fig. 3. Molecular modelling of YscP protein and comparison with experimental needle length. Computed lengths of the $YscP_{36–380}$ wild type and mutants are reported in circles (top), and are compared with the experimental measures of the needle (in triangles at the bottom). The computed $YscP_{36–380}$ lengths result from a series of ~20 independent steered MD trajectories for each protein; results from explicit solvent MD simulations are also reported (empty squares at the bottom). The distance between residues 36 and 380 has been measured when 90% of the helical content is conserved. Correlation between needle length and number of prolines substitutions is shown in the lower slope (triangles). Note that all the measurements align along a straight line except for pSTW44. All the values were compared with the wild-type value by the *t*-test. The stars indicate the probability of difference to wild type. NS = $P > 0.05$ (not significant). *$0.05 > P > 0.01$ (significant). **$0.01 > P > 0.001$ (very significant). ***$P < 0.001$ (extremely significant).

pulling, we found that the helical regions are conserved within the ns timescale, and upon pulling YscP models extend maintaining their initial secondary structure. As far as YscP approaches a fully linear extended conformation, α-helices abruptly start to break under mechanical stress, eventually reaching a completely extended β-strand-like conformation. The length values observed in MD simulations before the unfolding of any α-helix within region 36–380 of YscP (using a confidence threshold set to 90% of the initial helical content, see *Experimental procedures*) are plotted against the relative number of prolines in Fig. 3 (upper slope). We interestingly found that when the initial helical content of $YscP_{36–380}$ is preserved, the length of the wild-type protein (93.5 nm) along with the mutant conformations is strikingly correlated with the measured needle length, showing a constant difference of ~29 nm between the length of YscP and the length of the needle (Fig. S4). This value corresponds approximately to the distance between the cytoplasm and the surface of the basal body (26 nm) (Blocker *et al.*, 2001; Marlovits *et al.*, 2004). Hence, YscP is properly commensurate to the length of the injectisome from the inner side of the plasma membrane to the needle tip. Given the T3S4 domain of YscP is supposed to interact with the cytosolic domain of the transmembrane protein YscU, these data provide strong grounds to the ruler hypothesis.

In *Y. enterocolitica* needles are very fragile, to the extend that, even in electron microscopy analyses from non-sheared cultures, most needles appear to be detached from the bacterium. These detached needles have a constant length as shown here and in our previous work (Journet *et al.*, 2003; Agrain *et al.*, 2005a,b; Sorg *et al.*, 2007), implying that they always break at the same point. To validate our interpretation of the length measurement data, we had to ensure that detached needles have the same length as attached needles measured from the bacterial surface, in other words, that needles break at the bacterial surface. We checked this on wild-type bacteria and we measured on the same preparations 63 attached needles where the insertion point was clearly visible and 100 detached needles. As shown in Fig. 4, the length was similar (66 ± 8 nm and 65 ± 7 nm respectively), showing that indeed our interpretation of the length, supporting the ruler model, was correct.

The width of YscP is compatible with the needle channel size

The molecular modelling analysis thus confirms that the functional form of YscP consists in a succession of α-helices that modulates the needle length. The model of the molecular ruler, as presented earlier (Journet *et al.*, 2003), proposes that the ruler is located inside the growing needle. Based on the hypothesis that YscP is fully extended conserving its helical content, the width of the wild-type ruler was evaluated using our computational models for YscP. For every residue *i*, the protein's width was calculated by measuring the minimum and maximum size of the smallest box including all the atoms in residues window $[i - n, i + n]$, when the modelled YscP is fully extended (the graph in Fig. 5 shows the results for $n = 5$). The average min–max width of the ruler goes from 0.79 ± 0.10 nm to 0.95 ± 0.10 nm, and it never reaches values higher than 1.3 nm. Given that the needle is known

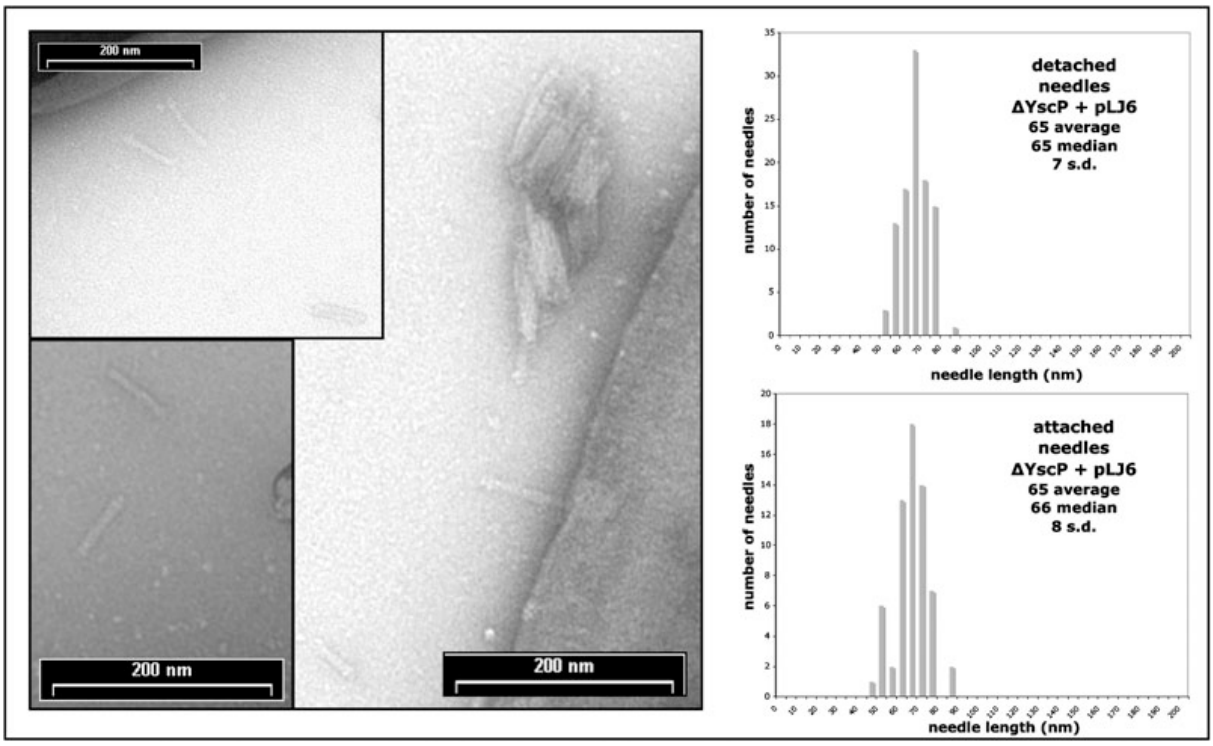

Fig. 4. Length of attached and detached needles. Left: Electron micrographs showing attached and detached needles. Right: Histograms showing the needle length *N*, number of measured needles; s.d., standard deviation.

from cryo-electron microscopy experiments to have a section of 2–3 nm (Blocker *et al.*, 2001; Mueller *et al.*, 2005), the YscP protein can be easily accommodated within the needle cavity, although presenting conserved helical motifs. Moreover, on the needle channel there would be enough space to accommodate at the same time both the YscP protein and the YscF building blocks of the needle. Based on this structural analysis, non-specific interactions between YscP and YscF proteins can likely happen during the construction of the needle.

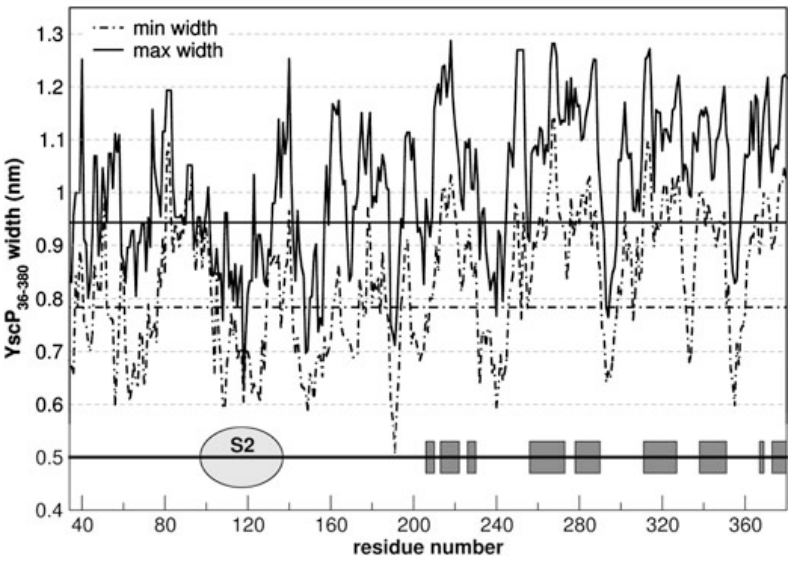

Fig. 5. Width of the extended $YscP_{36-380}$ ruler's segment. Maximum (in solid line) and minimum (in dashed line) width of $YscP_{36-380}$ using a sliding window size of $n = 5$ centred at the residue i, $[i - n, i + n]$. The average maximum (0.95 nm) and minimum (0.79 nm) values are represented by constant lines. At the bottom, a cartoon representing the secondary structure is shown: grey boxes represent predicted helices, while the oval represents the position of signal 2 domain (97–137).

Discussion

There are two simple ways to explain how the length of the YscP protein could determine the length of the needle. First, as suggested earlier (Journet *et al*., 2003), YscP could operate as a molecular ruler. In this model, YscP could stretch gradually while the needle grows, until it reaches a tension, which is transmitted to the switch domain. The switch domain then interacts with the cytosolic domain of a protein from the transmembrane export apparatus, probably YscU (Ferris *et al*., 2005; Cornelis *et al*., 2006; Chevance and Hughes, 2008). In this model, the actual length of the 'ruler' domain must be equal to the length of the protruding needle plus the distance separating the cytosol from the surface of the bacterium, which can be estimated around 30 nm (Macnab, 2003; Ogino *et al*., 2006). Alternatively, one could speculate that the progressive threading of YscP from the N-terminus to the C-terminus would act as a 'timer'. In other words, export of subunits would be allowed as long as the C-terminal switch domain (the T3S4 domain) has not reached its switch partner around the translocation channel. In this model, there is a correlation between the number of residues in YscP and the needle length but the two do not need to have the same length. A slightly different version of this 'timer' mechanism was initially proposed for FliK (Moriya *et al*., 2006). To discriminate between these two models, it would thus be interesting to have some insight into the actual length of the functional YscP.

The experiments reported in this paper show that there is a direct correlation between the number of prolines or glycines in the ruler part of YscP and the needle length, provided substitutions affected the predicted α-helical content (Fig. 2 and Table S2). The data show an inverse correlation between helical content and needle length, which supports the ruler model rather than the timer model. Indeed, helical segments contain more residues per length unit than unfolded segments. Considering the timer model, longer needles would result from a slower export of YscP and there is no obvious reason why a protein with a lower number of α-helices would be exported slower. One would eventually expect the opposite.

Therefore, we probed the actual length of the different engineered YscP proteins by using molecular simulations to calculate their extension. YscP was pulled at constant velocity mimicking the gradual extension along the needle cavity likely experienced by the protein during needle growth. As expected, the simulation results showed a strong correlation between predicted protein helical content and protein length before breaking of helices (Fig. S3). Most interestingly, the computed lengths of $YscP_{36–380}$ show a remarkable correlation with the needle lengths determined experimentally, only when considering a model for the ruler region in which the helical content is mostly conserved **(**Fig. 3). Furthermore, the computed $YscP_{36–380}$ lengths could be commensurate to the experimental measures of the needle (Fig. 3 and S4). The length of $YscP_{36–380}$ was indeed approximately equal to the length of the needle protruding outside the bacterium plus ~29 nm. This is consistent with the prediction of the ruler hypothesis, assuming that the ruler does conserve its helical content to control needle growth.

Altogether, these data on protein length support the ruler model as proposed by Journet *et al*. (2003). However, this model raises a few questions. First, a ruler can only work if it recognizes both ends of the structure it has to measure. In other words, the N-terminus of YscP (i.e. signal 1, residues 1–35) should somehow interact with the growing needle. So far, there is no experimental evidence that YscP reacts with YscF and one can exclude that it reacts with the LcrV tip complex because LcrV mutants make needles of normal length (Fig. S5). This situation is different from that of the flagellum where an interaction between FliK and the hook cap was demonstrated (Moriya *et al*., 2006). For the needle, in spite of intensive investigations, no polymerization cap was identified so far, suggesting that there could be none. The question of how would the N-terminus of YscP recognize the growing end remains thus open. A second caveat, which is often put forward, is the fact that two proteins must occupy the channel of the needle at the same time. This point must even be taken more seriously because the data presented here suggest that the proteins contain α-helices. However, as shown in Fig. 5, the width of our models of YscP makes it possible from a steric point of view to have two proteins at the time in the needle. Finally, another difficulty of the model resides in the fact that it implies that YscP and the needle subunits are translocated simultaneously across the plasma membrane. It is indeed not conceivable that the plasma membrane contains an open channel as large as the needle channel because the proton motive force would collapse. The consideration of this conceptual difficulty requires some understanding of the structure and function of the transmembrane export apparatus (YscR, S, T, U, V) and this information is, so far, totally missing.

Future work should also aim at understanding better the switch mechanism. Based on the seminal discovery of *flhB* mutations suppressing *fliK* mutations (Williams *et al*., 1996), it is generally believed that the switch results from the interaction $FliK_{C\text{-}term}$: $FlhB_{C\text{-}term}$ (Ferris *et al*., 2005), $YscP_{C\text{-}term}$: $YscU_{C\text{-}term}$ (Riordan and Schneewind, 2008). No such biochemical interaction could be detected so far for YscP or FliK. However, HpaC a non-secretable protein from *Xanthomonas campestris* which presumably acts as a T3S substrate specificity switch protein was recently shown to interact with $HcrU_{C\text{-}term}$, the *Xanthomonas*

homologue of YscU (Lorenz *et al*., 2008). As there is also evidence that the C-terminus of FlhB/YscU is involved in the recognition of some classes of substrates (Sorg *et al*., 2006; 2007) the characterization of the molecular contacts between $FliK_{C\text{-}term}$: $FlhB_{C\text{-}term}$/$YscP_{C\text{-}term}$: $YscU_{C\text{-}term}$/HpaC : $HcrU_{C\text{-}term}$ in the export machinery appears thus as a primary goal for future research.

Interestingly, the C-terminal cytosolic domain of FlhB/YscU undergoes an autoproteolytic cleavage (Ferris *et al*., 2005) and the 'clock' model proposes that this cleavage could set the time for export of early substrates (Moriya *et al*., 2006). However, a detailed molecular analysis of the reaction showed that cleavage, which occurs immediately after translation and folding in the cytoplasm, is a critical event for stabilization of these inner membrane proteins and thus that is not the switching event *per se* (Zarivach *et al*., 2008).

To summarize, the data presented here suggest that YscP maintains its helical secondary structure while exerting its function and provide support for the ruler model but more information is required to fully understand the needle length control mechanism.

Experimental procedures

Bacterial strains, genetic constructs and sequence analyses of yscP *from wild-type strains*

The different wild-type *Y. enterocolitica* strains and the plasmids encoding the different *yscP* genetic constructs used in this study are listed in Table S1. They were engineered according to standard procedures described in Sorg *et al*. (2007) using the oligonucleotides listed in Table S3.

The *yscP* gene from different wild-type strains was amplified by PCR from pYV plasmid preparations (HiSpeed Plasmid Mini kit, Qiagen) using the Pfu turbo polymerase (Startagene) and primers 3344 and 3345. The PCR products were analysed by agarose gel electrophoresis and purified from the gel with the Gel extraction kit (Sigma). Both strands of each PCR product were sequenced using a 3100-*Avant* genetic analyzer (ABI Prism) and the following oligonucleotides 3344, 3345, 3321, 3170, 3171 and 3672 (see Table S3).

Induction of the yop *regulon, Yop protein analysis and needle length measurement*

Bacterial cultures, induction of injectisomes synthesis and protein analysis was done as described in Sorg *et al*. (2007). YscPwt was overexpressed downstream the pBAD promoter in *Y. enterocolitica* E40 Δ*yscP* (LJ4036). Bacteria were analysed after 4 h of induction of the *yop* regulon at 37°C. The pBAD promoter was induced by adding 0.2% L-arabinose just before the shift to 37°C, and again 2 h later. Bacteria were harvested at 2000 *g* and resuspended gently in 20 mM Tris-HCl, pH 7.5. Droplets were applied for 1 min to freshly glow-discharged, formvar-carbon coated grids, and negatively stained with 2% (w/v) uranyl acetate. Bacteria were visualized in a Philips CM100 transmission electron microscope at a nominal magnification of 20 000× and an acceleration voltage of 80 kV. Sizes were measured with the 'Soft imaging system software' (Hamburg, Germany). For the statistical analysis, a *t*-test comparing the measurements of the mutants to those of the wild type was performed using the Macintosh Version of GraphPad Prism 5.0a (Trial) from Software MacKiev.

In silico *molecular modelling of the YscP protein*

We obtained information about YscP secondary structure for the wild type using several secondary structure predictors (see Fig. S6) and designed mutagenesis experiments and modelling based on these results. We did not get a full consensus for all the algorithms taken into account; nevertheless most of them predicted a significant helical content for YscP, with good topological similarity. We chose SIMPA96 (Levin *et al*., 1986) prediction as initial working hypothesis to interpret the results from mutagenesis experiments and molecular simulations as described below, obtaining a consistent match for the designed mutants that were supposed to break and/or form helical structure. This can also be taken as *a posteriori* indirect validation of the initial predicted helical content. These results were initially used to design the experiments on the wild type and Pro/Gly-variants of YscP. In a second stage, we sculpted based on the same information structural models of the ruler regions (from amino acid 36–380). Said models represented a partially extended protein with intact helices intercalated by unstructured coiled regions. $YscP_{36\text{–}380}$ models for wild type and its 9 Pro/Gly-mutants have been pulled ~20 times *in vacuo* at the constant velocity of 0.001 nm ps^{-1}, using steered MD (Izrailev *et al*., 1998) as implemented in NAMD molecular dynamics engine (Izrailev *et al*., 1998). CHARMM force field is used to describe the YscP protein (MacKerel *et al*., 1998). In each simulation, pulling force, helical content [determined using the DSSP algorithm (Kabsch and Sander, 1983)] and strand length are evaluated. The choice of simulating the protein *in vacuo* has been determined by the following reasons: (i) preliminary results showed that no relevant differences from results *in vacuo* could be obtained by performing the steered MD in any of the available implicit solvent models; (ii) given the length of the models (over 80 nm), the same set of simulations with the use of an explicit solvent model would have been computationally prohibitive. However, a limited set of steered MD simulations has been carried out for relevant conformations to estimate the difference on the calculated YscP length provided by neglecting explicit solvent. The wild type along with the two most extreme proline variants (+8P and −8P mutants) were simulated in explicit solvent using a TIP3P model for water. The results from single trajectory MD are also reported in Fig. 3 and Table S2, and pointed to an identical, within errors, length estimation and correlation with experimental measurements. We assessed the protein length upon unfolding of its helices by measuring the distance between the two terminal C_α-atoms (residues 36 and 380). We decided to assess the decrease of helical content during the pulling in order to determine univocally the beginning of helical unfolding. This could be achieved by counting the number h_n of residues

being part of a helix for every frame of the simulation and comparing it to the number h_i initially present in the protein. Unfolding was determined as soon as $h_i^* t > h_n$, where t is a threshold percentage. The choice of the correct threshold t being crucial, we assessed how the measure of protein length is affected by this value. We performed the measurements with a value of t between 0.8 and 0.95 and, it turned out that the outcome of the evaluation was not significantly affected by this value. This indicated that the breaking of helixes is quite abrupt. For the rest of the analysis we set $t = 0.9$.

Acknowledgements

We thank Cécile Paroz for sequencing the wild-type *yscP* genes, Yaniv Cohen for generating the *lcrV* null mutant, Gianni Morson for assistance in electron microscopy and G. Wauters (Louvain) for the gift of the wild-type *Y. enterocolitica* strains. This work was supported by the Swiss National Science Foundation (Grant 310000-113333/1 to G.C.).

References

Agrain, C., Callebaut, I., Journet, L., Sorg, I., Paroz, C., Mota, L.J., *et al.* (2005a) Characterization of a Type III secretion substrate specificity switch (T3S4) domain in YscP from *Yersinia enterocolitica*. *Mol Microbiol* **56:** 54–67.

Agrain, C., Sorg, I., Paroz, C., and Cornelis, G.R. (2005b) Secretion of YscP from *Yersinia enterocolitica* is essential to control the length of the injectisome needle but not to change the type III secretion substrate specificity. *Mol Microbiol* **57:** 1415–1427.

Blocker, A., Gounon, P., Larquet, E., Niebuhr, K., Cabiaux, V., Parsot, C., *et al.* (1999) The tripartite type III secreton of *Shigella flexneri* inserts IpaB and IpaC into host membranes. *J Cell Biol* **147:** 683–693.

Blocker, A., Jouihri, N., Larquet, E., Gounon, P., Ebel, F., Parsot, C., *et al.* (2001) Structure and composition of the *Shigella flexneri* 'needle complex', a part of its type III secreton. *Mol Microbiol* **39:** 652–663.

Broz, P., Mueller, C.A., Muller, S.A., Philippsen, A., Sorg, I., Engel, A., *et al.* (2007) Function and molecular architecture of the *Yersinia* injectisome tip complex. *Mol Microbiol* **65:** 1311–1320.

Chevance, F.F., and Hughes, K.T. (2008) Coordinating assembly of a bacterial macromolecular machine. *Nat Rev* **6:** 455–465.

Chou, P.Y., and Fasman, G.D. (1978) Prediction of the secondary structure of proteins from their amino acid sequence. *Adv Enzymol Relat Areas Mol Biol* **47:** 45–148.

Cornelis, G.R. (2006) The type III secretion injectisome. *Nat Rev* **4:** 811–825.

Cornelis, G.R., Agrain, C., and Sorg, I. (2006) Length control of extended protein structures in bacteria and bacteriophages. *Curr Opin Microbiol* **9:** 201–206.

Crepin, V.F., Shaw, R., Abe, C.M., Knutton, S., and Frankel, G. (2005) Polarity of enteropathogenic *Escherichia coli* EspA filament assembly and protein secretion. *J Bacteriol* **187:** 2881–2889.

Daniell, S.J., Takahashi, N., Wilson, R., Friedberg, D., Rosenshine, I., Booy, F.P., *et al.* (2001) The filamentous type III secretion translocon of enteropathogenic *Escherichia coli*. *Cell Microbiol* **3:** 865–871.

Ferris, H.U., and Minamino, T. (2006) Flipping the switch: bringing order to flagellar assembly. *Trends Microbiol* **14:** 519–526.

Ferris, H.U., Furukawa, Y., Minamino, T., Kroetz, M.B., Kihara, M., Namba, K., *et al.* (2005) FlhB regulates ordered export of flagellar components via autocleavage mechanism. *J Biol Chem* **280:** 41236–41242.

Galan, J.E., and Wolf-Watz, H. (2006) Protein delivery into eukaryotic cells by type III secretion machines. *Nature* **444:** 567–573.

Goure, J., Broz, P., Attree, O., Cornelis, G.R., and Attree, I. (2005) Protective anti-V antibodies inhibit *Pseudomonas* and *Yersinia* translocon assembly within host membranes. *J Infect Dis* **192:** 218–225.

Hirano, T., Yamaguchi, S., Oosawa, K., and Aizawa, S. (1994) Roles of FliK and FlhB in determination of flagellar hook length in *Salmonella typhimurium*. *J Bacteriol* **176:** 5439–5449.

Hoiczyk, E., and Blobel, G. (2001) Polymerization of a single protein of the pathogen *Yersinia enterocolitica* into needles punctures eukaryotic cells. *Proc Natl Acad Sci USA* **98:** 4669–4674.

Izrailev, S., Stepaniants, S., Isralewitz, B., Kosztin, D., Lu, H., Molnar, F., *et al.* (1998) Steered molecular dynamics. In *Computational Molecular Dynamics: Challenges, Methods, Ideas, Volume 4 of Lecture Notes in Computational Science and Engineering*. Deuflhard, P., Hermans, J., Leimkuhler, B., Mark, A.E., Reich, S., and Skeel, R.D. (eds). Berlin: Springer-Verlag, pp. 39–65.

Journet, L., Agrain, C., Broz, P., and Cornelis, G.R. (2003) The needle length of bacterial injectisomes is determined by a molecular ruler. *Science* **302:** 1757–1760.

Kabsch, W., and Sander, C. (1983) Dictionary of protein secondary structure: pattern recognition of hydrogen bonded and geometrical features. *Biopolymers* **22:** 2577–2637.

Katsura, I. (1987) determination of bacteriophage 1 tail length by a protein ruler. *Nature* **327:** 73–75.

Katsura, I., and Hendrix, R.W. (1984) Length determination in bacteriophage lambda tails. *Cell* **39:** 691–698.

Knutton, S., Rosenshine, I., Pallen, M.J., Nisan, I., Neves, B.C., Bain, C., *et al.* (1998) A novel EspA-associated surface organelle of enteropathogenic *Escherichia coli* involved in protein translocation into epithelial cells. *EMBO J* **17:** 2166–2176.

Kubori, T., Matsushima, Y., Nakamura, D., Uralil, J., Lara-Tejero, M., Sukhan, A., *et al.* (1998) Supramolecular structure of the *Salmonella typhimurium* type III protein secretion system. *Science* **280:** 602–605.

Kubori, T., Sukhan, A., Aizawa, S.I., and Galan, J.E. (2000) Molecular characterization and assembly of the needle complex of the *Salmonella typhimurium* type III protein secretion system. *Proc Natl Acad Sci USA* **97:** 10225–10230.

Levin, J., Robson, B., and Garnier, J. (1986) An algorithm for secondary structure determination in proteins based on sequence similarity. *FEBS Lett* **205:** 303–308.

Li, C.M., Brown, I., Mansfield, J., Stevens, C., Boureau, T.,

Romantschuk, M., *et al.* (2002) The Hrp pilus of *Pseudomonas syringae* elongates from its tip and acts as a conduit for translocation of the effector protein HrpZ. *EMBO J* **21:** 1909–1915.
Lorenz, C., Schulz, S., Wolsch, T., Rossier, O., Bonas, U., and Buttner, D. (2008) HpaC controls substrate specificity of the Xanthomonas type III secretion system. *PLoS Pathog* **4:** e1000094.
MacKerel Jr., A.D., Brooks III, C.L., Nilsson, L., Roux, B., Won, Y., and Karplus, M. (1998) The energy function and its parameterization with an overview of the program. In *The Encyclopedia of Computational Chemistry*, Chapter: CHARMM. von Ragué Schleyer, P. (ed.). Chichester: John Wiley & Sons, pp. 271–277.
Macnab, R.M. (2003) How bacteria assemble flagella. *Annu Rev Microbiol* **57:** 77–100.
Marlovits, T.C., Kubori, T., Sukhan, A., Thomas, D.R., Galan, J.E., and Unger, V.M. (2004) Structural insights into the assembly of the type III secretion needle complex. *Science* **306:** 1040–1042.
Marshall, W.F. (2004) Cellular length control systems. *Annu Rev Cell Dev Biol* **20:** 677–693.
Minamino, T., Gonzalez-Pedrajo, B., Yamaguchi, K., Aizawa, S.I., and Macnab, R.M. (1999) FliK, the protein responsible for flagellar hook length control in Salmonella, is exported during hook assembly. *Mol Microbiol* **34:** 295–304.
Minamino, T., Saijo-Hamano, Y., Furukawa, Y., Gonzalez-Pedrajo, B., Macnab, R.M., and Namba, K. (2004) Domain organization and function of *Salmonella* FliK, a flagellar hook-length control protein. *J Mol Biol* **341:** 491–502.
Morita-Ishihara, T., Ogawa, M., Sagara, H., Yoshida, M., Katayama, E., and Sasakawa, C. (2006) *Shigella* Spa33 is an essential C-ring component of type III secretion machinery. *J Biol Chem* **281:** 599–607.
Moriya, N., Minamino, T., Hughes, K.T., Macnab, R.M., and Namba, K. (2006) The type III flagellar export specificity switch is dependent on FliK ruler and a molecular clock. *J Mol Biol* **359:** 466–477.
Mueller, C.A., Broz, P., Muller, S.A., Ringler, P., Erne-Brand, F., Sorg, I., *et al.* (2005) The V-antigen of *Yersinia* forms a distinct structure at the tip of injectisome needles. *Science* **310:** 674–676.
Mueller, C.A., Broz, P., and Cornelis, G.R. (2008) The type III secretion system tip complex and translocon. *Mol Microbiol* **68:** 1085–1095.
Ogino, T., Ohno, R., Sekiya, K., Kuwae, A., Matsuzawa, T., Nonaka, T., *et al.* (2006) Assembly of the type III secretion apparatus of enteropathogenic *Escherichia coli*. *J Bacteriol* **188:** 2801–2811.
Pedulla, M.L., Ford, M.E., Houtz, J.M., Karthikeyan, T., Wadsworth, C., Lewis, J.A., *et al.* (2003) Origins of highly mosaic mycobacteriophage genomes. *Cell* **113:** 171–182.
Riordan, K.E., and Schneewind, O. (2008) YscU cleavage and the assembly of *Yersinia* type III secretion machine complexes. *Mol Microbiol* **68:** 1485–1501.
Riordan, K.E., Sorg, J.A., Berube, B.J., and Schneewind, O. (2008) Impassable YscP substrates and their impact on the *Yersinia enterocolitica* type III secretion pathway. *J Bacteriol* **190:** 6204–6216.
Shibata, S., Takahashi, N., Chevance, F.F., Karlinsey, J.E., Hughes, K.T., and Aizawa, S. (2007) FliK regulates flagellar hook length as an internal ruler. *Mol Microbiol* **64:** 1404–1415.
Sorg, J.A., Blaylock, B., and Schneewind, O. (2006) Secretion signal recognition by YscN, the *Yersinia* type III secretion ATPase. *Proc Natl Acad Sci USA* **103:** 16490–16495.
Sorg, I., Wagner, S., Amstutz, M., Muller, S.A., Broz, P., Lussi, Y., *et al.* (2007) YscU recognizes translocators as export substrates of the *Yersinia* injectisome. *EMBO J* **26:** 3015–3024.
Stainier, I., Bleves, S., Josenhans, C., Karmani, L., Kerbourch, C., Lambermont, I., *et al.* (2000) YscP, a Yersinia protein required for Yop secretion that is surface exposed, and released in low Ca2+. *Mol Microbiol* **37:** 1005–1018.
Sukhan, A., Kubori, T., Wilson, J., and Galan, J.E. (2001) Genetic analysis of assembly of the *Salmonella enterica* serovar Typhimurium type III secretion-associated needle complex. *J Bacteriol* **183:** 1159–1167.
Tampakaki, A.P., Fadouloglou, V.E., Gazi, A.D., Panopoulos, N.J., and Kokkinidis, M. (2004) Conserved features of type III secretion. *Cell Microbiol* **6:** 805–816.
Van Gijsegem, F., Vasse, J., Camus, J.C., Marenda, M., and Boucher, C. (2000) *Ralstonia solanacearum* produces hrp-dependent pili that are required for PopA secretion but not for attachment of bacteria to plant cells. *Mol Microbiol* **36:** 249–260.
Waters, R.C., O'Toole, P.W., and Ryan, K.A. (2007) The FliK protein and flagellar hook-length control. *Protein Sci* **16:** 769–780.
Williams, A.W., Yamaguchi, S., Togashi, F., Aizawa, S.I., Kawagishi, I., and Macnab, R.M. (1996) Mutations in fliK and flhB affecting flagellar hook and filament assembly in *Salmonella typhimurium*. *J Bacteriol* **178:** 2960–2970.
Yip, C.K., and Strynadka, N.C. (2006) New structural insights into the bacterial type III secretion system. *Trends Biochem Sci* **31:** 223–230.
Zarivach, R., Deng, W., Vuckovic, M., Felise, H.B., Nguyen, H.V., Miller, S.I., *et al.* (2008) Structural analysis of the essential self-cleaving type III secretion proteins EscU and SpaS. *Nature* **453:** 124–127.

Supporting information

Additional supporting information may be found in the online version of this article.

Please note: Wiley-Blackwell are not responsible for the content or functionality of any supporting materials supplied by the authors. Any queries (other than missing material) should be directed to the corresponding author for the article.

Wagner *et al.* Figure S1

Alignment of the sequences of YscP proteins from different *Y. enterocolitica* strains listed in Table S1

CLUSTAL W (1.83)

```
MRS40           -MNKITTRSPLEPEYQPLGKLHHDLQARADFEQALLHNNKGNRHPKEEPRRPVRPHDLGKKEGQKGDGLRAHAPLEATFQPGRKEVGLKPQHNHQNNHDLNLSPLAEGVTNRAHLYQQDS
KNG22703        -MNKITTRSPLEPEYQPLGKLHHDLQARADFEQALLHNNKGNRHPKEEPRRPVRPHDLGKKEGQKGDGLRAHAPLEATFQPGRKEVGLKPQHNHQNNHDLNLSPLAEGVTNRAHLYQQDS
A11/86          MANKITTRSPLEPEYQPLGKPHHDLQARVDFEQALLHN-KDNRHPKEEPRRPVRPHDLGKKEGQKGDGLRAHAPLAATFQPGR-EVGLKPQHNHQNNHDFNLSPLAEGATNRKHLYQQDS
WAT9/88         MANKITTRSPLEPEYQPLGKPHHDLQARVDFEQALLHN-KDNRHPKEEPRRPVRPHDLGKKEGQKGDGLRAHAPLAATFQPGR-EVGLKPQHNHQNNHDFNLSPLAEGATNRKHLYQQDS
WAT288          MANKITTRSPLEPEYQPLGKPHHDLQARVDFEQALLHN-KDNRHPKEEPRRPVRPHDLGKKEGQKGDGLRAHAPLAATFQPGR-EVGLKPQHNHQNNHDFNLSPLAEGATNRKHLYQQDS
A127/90         -MNKITTRSPLEPEYQPLGKPHHDLQARVDFEQALLHN-KDNRHPKEEPRRPVRPHDLGKKEGQKGDGLRAHAPLAATFQPGR-EVGLKPQHNHQNNHDFNLSPLAEGATNRKHLYQQDS
IP17            MANKITTRSPLEPEYQPLGKPHHDLQARADFEQALLHNNKGNRHPKEEPRRPVRPHDLGKKEGQKGDGLRAHAPLAATFQPGRKEVGLKPQHNHQNNHDFNLSPLAEGATNRKHLYQQDS
                  ****************** *******.********* *.********************************** ***  ** ***************:********.*** *******

MRS40           RFDDRVESIINALMPLAPFLKGVTCETGTSSESPCEPSGHDELFVQQSPIDSVQPVQLNTKPTVQPLNPAADGAEVIVWSVGRETPASIAKNQRDSRQKRLAEEPLPLHQEALPEVCPPA
KNG22703        RFDDRVESIINALMPLAPFLKGVTCETGTSSESPCEPSGHDELFVQQSPIDSVQPVQLNTKPTVQPLNPAADGAEVIVWSVGRETPASIAKNQRDSRQKRLAEEPLPLHQEALPEVCPPA
A11/86          RFDDRVESIINALMPLAPFLEGVTCETGTSSESPCEPFGHDELFVQQSPIDSAQPVQLNTKPTVQSLNPAADGAEVMIWSVGRDTLASIAKNQRDSRQKRLAEEPLP------------
WAT9/88         RFDDRVESIINALMPLAPFLEGVTCETGTSSESPCEPFGHDELFVQQSPIDSAQPVQLNTKPTVQSLNPAADGAEVMIWSVGRDTLASIAKNQRDSRQKRLAEEPLPLHQEALPEVCPPA
WAT288          RFDDRVESIINALMPLAPFLEGVTCETGTSSESPCEPSGHDELFVQQSPIDSAQPVQLNTKPTVQSLNPAADGAEVMISSVGRDTLASIAKNQRDSRQKRLAEEPLPLHQEALPEVCPPA
A127/90         RFDDRVESIINALMPLAPFLEGVTCETGTSSESPCEPSGHDELFVQQSPIDSAQPVQLNTKPTVQPLNPAADGAEVMIWSVGRDTLASIAKNQCDSRQKRLAEEPLPLHQEALPEVCPPA
IP17            RFDDRVESIINALMPLAPFLKGVTCETGTSSESPCEPSGHDELFVQQSPIDSVQPVQLNTKPTVQPLNPAADGAEVIVWSVGRETPASIAKNQRDSRQKRLAEEPLPLHQEALPEV----
                ********************:**************** ************.************.**********:: ****:* ******* *************

MRS40           VSATPNDHLVARWCATPVAEVAEKSARFLHKAIVQSEQLDMTELADRSQHLTDGVDSSKDTIELPRPEEPLPLHQEALPEV-----------------------------------------
KNG22703        VSATPNDHLVARWCATPVAEVAEKSARFLHKAIVQSEQLDMTELADRSQHLTDGVDSSKDTIELPRPEEPLPLHQEALPEV-----------------------------------------
A11/86          -----------RWCATPVAEVAEKSARFPHKATVQSEQLDMTELADRSQHLTDGVDSSKDTIEPPRPEEPLPLHQEALPEV-----CPPAVSTTPDDHLVARWCATPVAEV---------
WAT9/88         VSTTPDDHLVARWCATPVAEVAEKSARFPHKATVQSEQLDMTELADRSQHLTDGVDSSKDTIEPPRPEEPLPLHQEALPEV-----CPPAVSTTPDDHLVARWCATPVAEV---------
WAT288          VSTTPDDHLVARWCATPVAEVAEKSARFPHKATVQSEQLDMTELADRSQHLTDGVDSSKDTIEPPRP-----------------------------------------------------
A127/90         VSTTPDDHLVARWCATPVAEVAEKSARFPHKATVQSEQLDMTELADRSQHLTDGVDSSKDTIEPPRP-----------------------------------------------------
IP17            ----------------------AEKSARFPHKATVQSEQLDMTELAARSQYLTDGVDSSKDTIELPRPEEPLPLHQEALPEVAEKSARFPHKATVQSEQLDMTELAARSQYLTDGVDSSKD
                                       ******* *** ************ ***************** ***

MRS40           ----------------------AEKSARFPHKATVQSEQLDMTELAARSQYLTDGVDSSKDTIEPPRPEELLLPREETLLEMYSLSFTAPVVTPGDHLLATMRATRLTSVSEQLIQLAQRL
KNG22703        ----------------------AEKSARFQHKATVQSEQLDMTELAARSQYLTDGVDSSKDTIEPPRPEELLLPREETLLEMYSLSFTAPVVTPGDHLLATMRATRLTSVSEQLIQLAQRL
A11/86          ----------------------AEKSARFPHKATVQSEQLDMTELADRSQHLTDGVDSSKDTIEPPRPEELLLPREETLPEMYSLSFTAPVITPGDHLLATMRATRLASVSEQLIQLAQRL
WAT9/88         ----------------------AEKSARFPHKATVQSEQLDMTELADRSQHLTDGVDSSKDTIEPPRPEELLLPREETLPEMYSLSFTAPVITPGDHLLATMRATRLASVSEQLIQLAQRL
WAT288          ------------------------------------------------------------EELLLPREETLPEMYSLSFTAPVITPGDHLLATMRATRLASVSEQLIQLAQRL
A127/90         ------------------------------------------------------------EELLLPREETLPEMYSLSFTAPVITLGDHLLATMRATRLASVSEQLIQLAQRL
IP17            TIELPRPEEPLPLHQEALPEVAEKSARFPHKATVQSEQLDMTELAARSQYLTDGVDSSKDTIEPPRPEELLLPREETLLEMYSLSFTAPVVTPGDHLLATMRATRLTSVSEQLIQLAQRL
                                                                            *********** ***********:* *************:**************

MRS40           AVELELRGGSSQVTQLHLNLPELGAIMVRIAEIPGKLHVELIASQEALRILAQGSYDLLERLQRIEPTQLDFQASGDSEQESRQKRHVYEEWEAEE
KNG22703        AVELELRGGSSQVTQLHLNLPELGAIMVRIAEIPGKLHVELIASQEALRILAQGSYDLLERLQRIEPTQLDFQASGDSEQESRQKRHVYEEWEAEE
A11/86          AVELELRGGSSQVTQLHLNLPELGAIMVRIAEIPGKLHVELIASRETLRILAQGSYDLLERLQRIEPTQLDFQASGDSEQESRQKRHVYEEWXAEE
WAT9/88         AVELELRGGSSQVTQLHLNLPELGAIMVRIAEIPGKLHVELIASRETLRILAQGSYDLLERLQRIEPTQLDFQASGDSEQESRQKRHVYEEWEAEE
WAT288          AVELELRGGSSQVTQLHLNLPELGAIMVRIAEIPGKLHVELIASRETLRILAQGSYDLLERLQRIEPTQLDFQASGDSEQESRQKRHVYEEWEAEE
A127/90         AVELELRGGSSQVTQLHLNLPELGAIMVRIAEIPGKLHVELIASRETLRILAQGSYDLLERLQRIEPTQLDFQASGDSEQESRQKRHVYEEWEAEE
IP17            AVELELRGGSSQVTQLHLNLPELGAIMVRIAEIPGKLHVELIASQEALRILAQGSYDLLERLQRIEPTQLDFQASGDSEQESRQKRHVYEEWEAEE
                ******************************************:*:********************************************** ***
```

Wagner *et al.:* **Figure S2**

The histograms of length measurements from different *Yersinia enterocolitica* wildtype strains.
s.d., standard deviation; n, number of measured needles

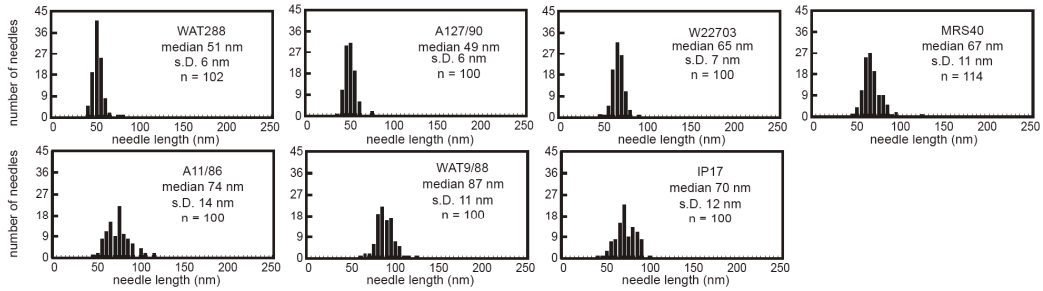

Wagner *et al.* : **Figure S3**

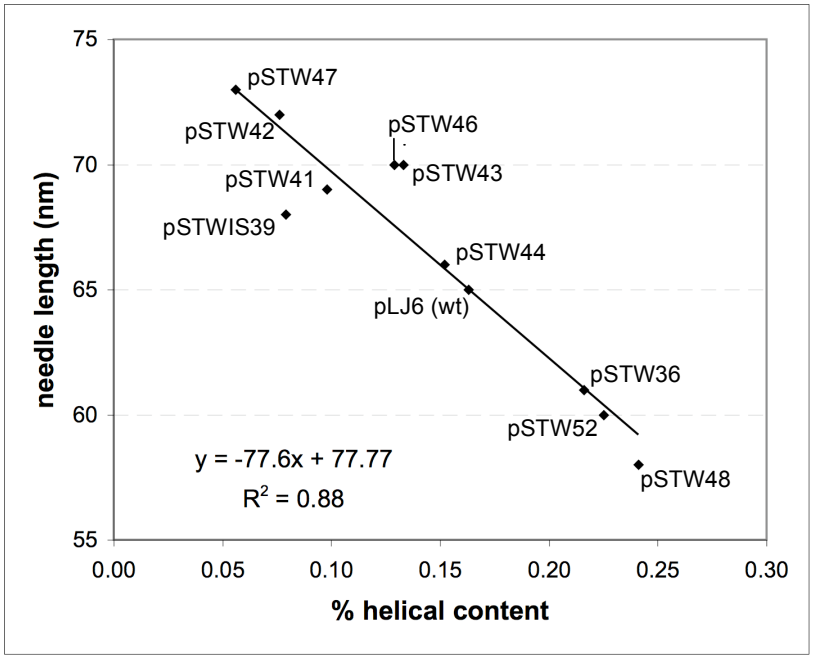

A. Correlation between the helical content of $YscP_{36-380}$ predicted by SIMPA96 and the measured needle length. Raw data is shown in Table S2.

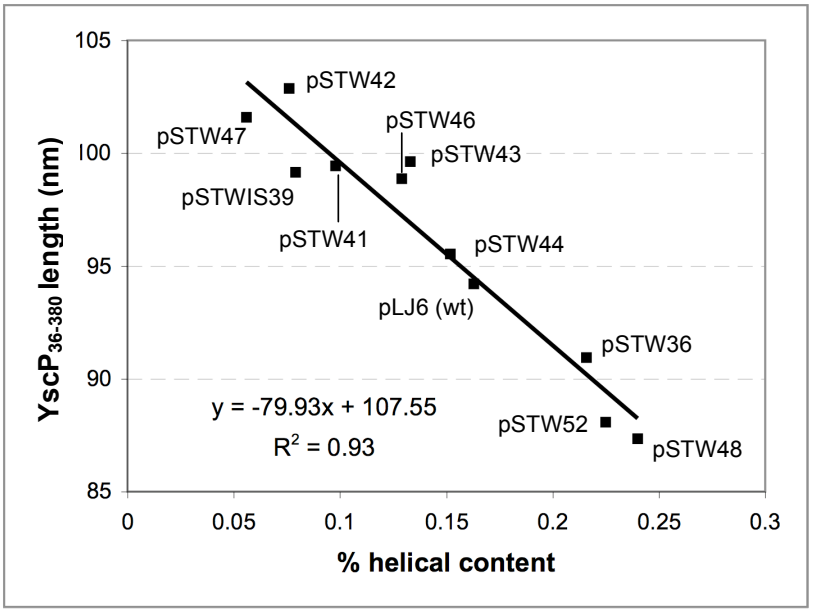

B. Correlation between the helical content of $YscP_{36-380}$ and the calculated ruler length. Raw data is shown in Table S2.

Wagner *et al.:* **Figure S4**

Correlation between the computed $YscP_{36-380}$ length and the experimental needle length.

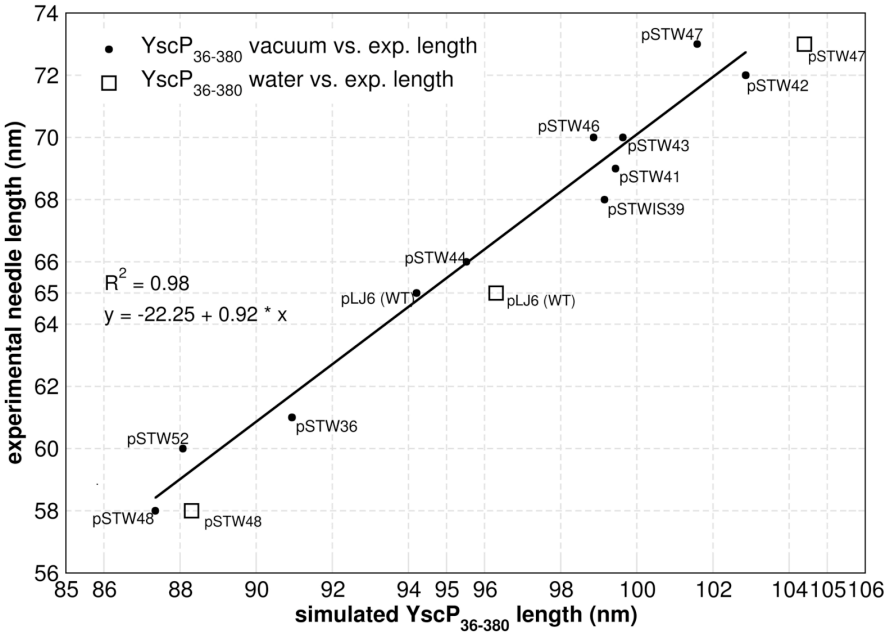

Wagner *et al.:* **Figure S5**: **Length of tipless needles**

To analyze the length difference between WT needles and needles without a tip, *Y. enterocolitica* E40 [wt], *Y. enterocolitica* E40(pYC4001) [Δ*lcrV*] , E40(pYC4001)(pPB24) [Δ*lcrV* + p*lcrV*] were analyzed exactly as described in Figure S4. Histograms showing the needle length; N, number of measured needles; s.d., standard deviation.

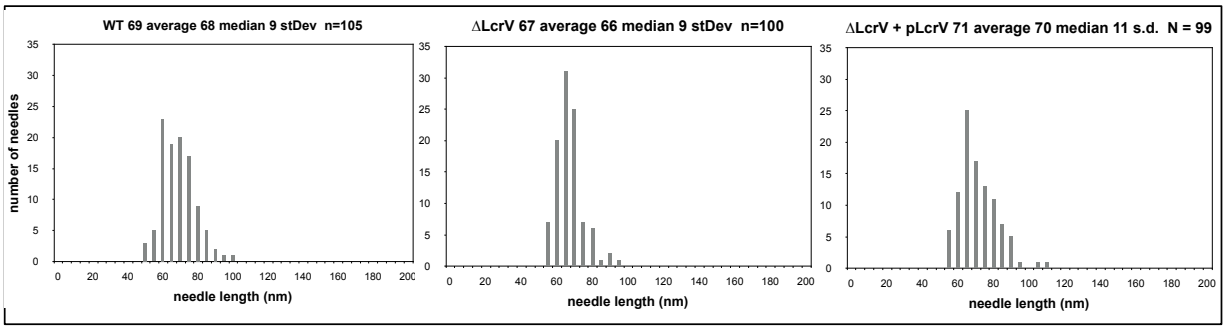

Strains and plasmids

Plasmids	Encoded protein	Genotype or description	Source or reference
pYC4001		pYV40 - *lcrV*$_{\Delta 6\text{-}319}$ (del of aa 6-319) constructed using mutator plasmid pMN3	This study
pMN3		pKNG101-*lcrV*$_{\Delta 6\text{-}319}$	Marenne *et al*., 2003
pPB42	LcrV wt	pBADMycHisA-*lcrV*	Sorg *et al*., 2007

References

Sorg I, Wagner S, Amstutz M, Muller SA, Broz P, Lussi Y, Engel A, Cornelis GR (2007) YscU recognizes translocators as export substrates of the Yersinia injectisome. *Embo J* **26:** 3015-3024

Marenne MN, Journet L, Mota LJ, Cornelis GR (2003) Genetic analysis of the formation of the Ysc-Yop translocation pore in macrophages by *Yersinia enterocolitica:* role of LcrV, YscF and YopN. *Microb Pathog*. **35**(6): 243-258

Wagner *et al.:* **Figure S6: Comparison of different algorithms for secondary structure prediction of YscP$_{1-38}$.**

The global helical content predicted by SIMPA96 (Levin *et al.*, 1986), NNPREDICT (Kneller *et al.*, 1990), PREDATOR (Frishman & Argos, 1996), JNET (Cuff & Barton, 2000), QLSSP (Munson *et al.*, 1994), PROF (Rost *et al.*, 2004) , GARNIER (Garnier *et al.*, 1978) is reported for region [1-380] of protein YscP. The export signals and the T3S4 domain are delineated according to earlier work (Agrain *et al.*, 2005a; Agrain *et al.*, 2005b). "A" indicates a position where a proline was substituted by an alanine. "P/G" indicates a position where a residue (E, L or Q) was substituted by a proline. SIMPA96 has been chosen for producing mutations and to model YscP (see Methods and Materials).

name	helical content (%)
1. SIMPA96	39.77
2. NNPREDICT	28.57
3. PREDATOR	38.99
4. JNET	18.15
5. QLSSP	37.84
6. PROF (c=0.3)	21.43
7. GARNIER	44.40

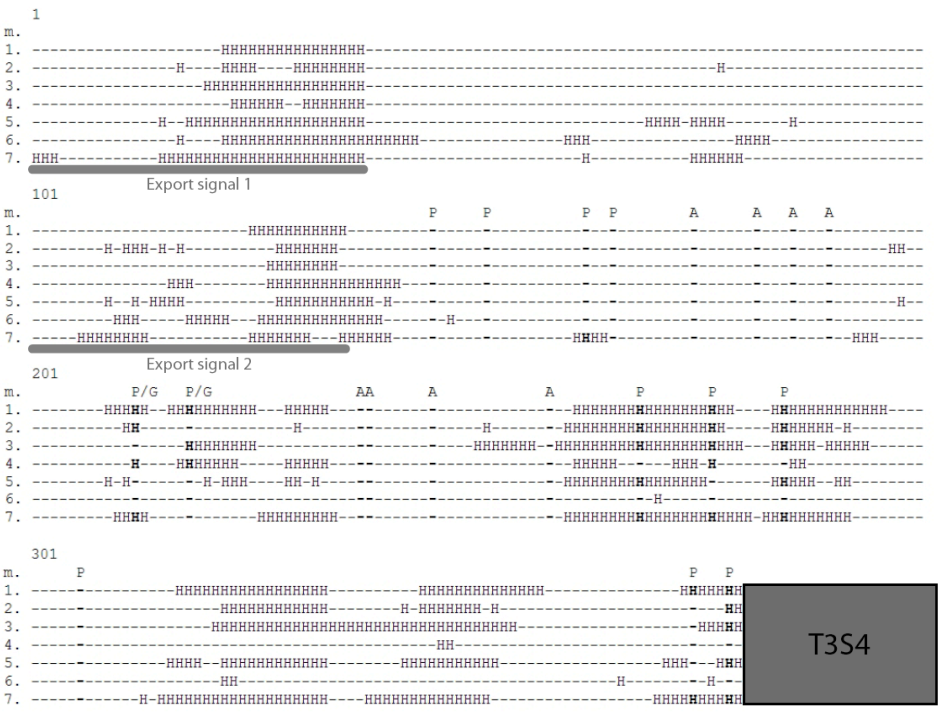

Agrain, C., I. Callebaut, L. Journet, I. Sorg, C. Paroz, L. J. Mota, et al., (2005a) Characterization of a Type III secretion substrate specificity switch (T3S4) domain in YscP from Yersinia enterocolitica. Mol Microbiol 56: 54-67.

Agrain, C., I. Sorg, C. Paroz & G. R. Cornelis, (2005b) Secretion of YscP from Yersinia enterocolitica is essential to control the length of the

injectisome needle but not to change the type III secretion substrate specificity. Mol Microbiol 57: 1415-1427.
Cuff, J. A. & G. J. Barton, (2000) Application of multiple sequence alignment profiles to improve protein secondary structure prediction. Proteins 40: 502-511.
Frishman, D. & P. Argos, (1996) Incorporation of non-local interactions in protein secondary structure prediction from the amino acid sequence. Protein engineering 9: 133-142.
Garnier, J., D. J. Osguthorpe & B. Robson, (1978) Analysis of the accuracy and implications of simple methods for predicting the secondary structure of globular proteins. Journal of molecular biology 120: 97-120.
Kneller, D. G., F. E. Cohen & R. Langridge, (1990) Improvements in protein secondary structure prediction by an enhanced neural network. Journal of molecular biology 214: 171-182.
Levin, J., B. Robson & J. Garnier, (1986) An algorithm for secondary structure determination in proteins based on sequence similarity. FEBS 205: 303-308.
Munson, P. J., V. Di francesco & R. Porrelli, (1994) Protein Secondary Structure Prediction using Periodic-Quadratic-Logistic Models: Theoretical and Practical Issues. 27tH Annual Hawaii International Conference on System Science, IEEE, Los Alamitos, CA 5: 375-384.
Rost, B., G. Yachdav & J. Liu, (2004) The PredictProtein server. Nucleic acids research 32: W321-326.

Strain	GenBank Accession number	Biotype	Serotype	Virulence	Host
WAT9/88	FJ175196	1B	O:4	high	human
A11/86	FJ175195	1B	O:21	high	human
WAT288	FJ175197	1B	O:13	high	human
A127/90	NC_004564	1B	O:8	high	human
E40	AF260705	2	O:9	low	human
W22703	NC_002120	2	O:9	low	human
IP17	FJ175198	5	O:2.3	low	hare

Plasmids	Encoded protein	Genotype or description	Source or reference
pYV plasmids			
pYV40		Wild-type virulence plasmid from strain *Y. enterocolitica* E40	Sory *et al*. (1995)
pLJ4036		pYV40 Δ*yscP* (deleted from start to stop)	Agrain *et al.* (2005)
Expression plasmids			
pBADMycHisA			Invitrogen
pLJ6	$YscP_{WT}$	*pBADMycHisA-yscP* This *yscP* gene originates from strain W22703 and differs slightly from the ortholog in strain E40.	Journet *et al.* (2003)
pSTW35	$YscP_{P237A\ ,\ P238A}$	Mutations P237A and P238A were introduced into pLJ6 by overlapping PCR using oligo pairs 3344 and 4875 and 4876 and 3345	This study
pSTW36	$YscP_{P237A,\ P238A,\ P244A,P256A}$	Mutations P237A, P238A, P244A and P256A were introduced into pLJ6 by overlapping PCR using oligo pairs 3344 and 4877 and 4878 and 3345	This study
pSTWIS38	$YscP_{L268P,L303P}$	Mutations L268P and L303P were introduced into pLJ6 by overlapping PCR using oligo pairs 3344 and 4950 and 4949 and 3345	This study
pSTWIS39	$YscP_{L268P,\ E277P,\ L283P,\ L303P}$	Mutations L268P, E277P, L283P and L303P were introduced into pLJ6 by overlapping PCR using oligo pairs 3344 and 4952 and 4951 and 3345	This study
pSTW41	$YscP_{Q212P,\ Q217P,\ L268P,\ L303P}$	Mutations Q212P, Q217P were introduced into pSTWIS38 by overlapping PCR using oligo pairs 3344 and 4948 and 4947 and 3345	This study
pSTW42	$YscP_{Q212P,\ Q217P,\ L268P,\ E277P,\ L283P,\ L303P}$	Mutations Q212P, Q217P were introduced into pSTWIS39 by overlapping PCR using oligo pairs 3344 and 4948 and 4947 and 3345	This study

pSTW43	YscP Q212P, Q217P, E375P, E379P	Mutations Q212P, Q217P, E375P and E379P were introduced into pLJ6 by overlapping PCR using oligo pairs 3344 and 4948, 4947 and 4963, and 4962 and 3345	This study
pSTW44	YscP E145P, E151P, L162P, Q165P	mutations E145P, E151P, L162P and Q165P were introduced into pLJ6 by overlapping PCR using oligo pairs 3344 and 4990 and 4989 and 3345	This study
pSTW46	YscP Q212G, Q217G, E375G,E379G	Mutations Q212G, Q217G, E375G and E379G were introduced into pLJ6 by overlapping PCR using oligo pairs 3344 and 4996, 4995 and 4998, and 4997 and 3345	This study
pSTW47	YscP Q212P, Q217P, L268P, E277P, L283P, L303P, E375P, E379P	Mutations Q212P, Q217P, E375P and E379P were introduced into pSTWIS39 by overlapping PCR using oligo pairs 3344 and 4948, 4947 and 4963, and 4962 and 3345	This study
pSTW48	YscP P174A, P181A, P185A, P188A, P237A, P238A, P244A, P256A	Mutations P174A, P181A, P185A, P188A were introduced into pSTW36 by overlapping PCR using oligo pairs 3344 and 5000 and 4999 and 3345	This study
pSTW52	YscP P174A, P181A, P185A, P188A, P237A, P238A	Mutations P174A, P181A, P185A, P188A were introduced into pSTW35 by overlapping PCR using oligo pairs 3344 and 5000 and 4999 and 3345	This study

Wagner *et al.:* **Table S2**

Table S2. Raw data from MD simulations of YscP compared with experimental needle length measurements as presented in Fig. 3 of the manuscript.

Protein	Proline substitutions	Simulated YscP length (nm)	Simulated YscP s.d. (nm)	Helical content %	Experimental needle length (nm)	Experimental needle length s.d. (nm)
Results in vacuum						
pSTW48	-8	87.35	0.5	0.24	58	7
pSTW52	-6	88.074	0.2	0.23	60	7
pSTW36	-4	90.94	1.2	0.22	61	7
wt	0	94.212	1	0.16	65	7
pSTW44	4	95.525	0.62	0.15	66	7
pSTW41	4	99.44	0.3	0.098	69	1
pSTW46	4	98.865	0.3	0.13	70	7
pSTW43	4	99.634	0.3	0.13	70	7
pSTWIS39	4	99.15	0.9	0.079	68	7
pSTW42	6	102.86	0.9	0.076	72	7
pSTW47	8	101.585	0.18	0.056	73	11
Results in explicit water						
pSTW48		88.3		0.44		
wt		96.3		0.296		
pSTW47		104.4		0.168		

How many YscP molecules are needed to control length of one injectisome needle?

The *Yersinia* injectisome needle is determined by only one molecule of YscP

Stefanie Wagner[1], Marco Stenta[2] Lisa Metzger[1], Matteo Dal Peraro[2] and Guy R. Cornelis[1]

[1] Biozentrum der Universität Basel, Basel, Switzerland.

[2] Laboratory for Biomolecular Modeling, Institute of Bioengineering, School of Life Sciences, EPF Lausanne, Switzerland

Author contributions

SW and GC conceived and designed the experiments. SW and LM performed the experiments. SW, LM and GC analyzed the data. SW and GC wrote the the paper. MS and MDP performed modeling and contributed to writing the paper.

The needle length of the *Yersinia* spp. injectisome is determined by YscP, an early substrate of the injectisome itself. There is a linear correlation between the length of YscP and needle length and thus it has been suggested, that YscP acts as a molecular ruler to control needle length. However, it is not clear whether one single molecule of YscP controls the length of one needle or whether several molecules of YscP are required for length determination of the *Yersinia* injectisome needle. In this dynamic ruler model YscP molecules are exported in alternation with the needle subunit YscF until the needle length matches the ruler length, which would result in a stop of needle growth. To address this question, bacteria expressing simultaneously a short and a long version of YscP were engineered. The experimentally obtained needle length distribution was analyzed mathematically and compared to the distributions predicted by mathematical modeling of the various possible scenarios. The experimental data are compatible with the single ruler model and not with the scenarios involving more than one ruler per needle.

Control of the length of the injectisome needle requires only one molecule of YscP

Stefanie Wagner[1§], Marco Stenta[2§], Lisa C. Metzger[1§] Matteo Dal Peraro[#2] and Guy R. Cornelis[1#†]

(1) Biozentrum der Universität Basel, Basel, Switzerland

(2) Laboratory for Biomolecular Modeling, Institute of Bioengineering, School of Life Sciences, EPF Lausanne, Switzerland

§ The three first authors contributed equally to the work.

# The two last authors contributed equally to the work

† Corresponding author

Biozentrum, Klingelbergstrasse 50, CH-4056, Basel

Tel. secretary (41) 61 267 21 21

Fax (41) 61 267 21 18

E-mail: guy.cornelis@unibas.ch

Total character count (with spaces): 26'892

Running title: One ruler per needle.

Subject category: Microbiology & Pathogens

ABSTRACT

The needle length of the *Yersinia* spp. injectisome is determined by YscP, an early substrate of the injectisome. It is proposed that YscP acts as a molecular ruler coupled to a substrate specificity switch but some data are missing to propose a precise mechanism. Here, by measuring needles made by *Yersinia enterocolitica* that express simultaneously a short and a long version of YscP, we provide evidence that only one molecule of YscP is required to control the length of one needle.

Keywords: nanomachine / type-III secretion / molecular ruler/ Yersinia

INTRODUCTION

The injectisome or needle complex allows pathogenic bacteria to inject effector proteins across eukaryotic cell membranes, a process called type III secretion (T3S). This nanomachine is evolutionary related to the flagellum and has a basal body made of several rings embedded in the two bacterial membranes (Hodgkinson *et al.*, 2009; Marlovits *et al.*, 2006) and including integral membrane proteins constituting the core of the T3S export apparatus (reviewed by (Cornelis, 2006; Galan & Wolf-Watz, 2006; Yip & Strynadka, 2006)). The *Yersinia enterocolitica* E40 Ysc injectisome terminates with a 65-nm long stiff hollow needle, made of ~ 140 copies of the 9-kDa YscF protein. At the tip of the needle, a pentamer of LcrV (Broz *et al.*, 2007; Mueller *et al*., 2005) forms a structure serving as an assembly platform for the translocation pore (Goure *et al.*, 2005).

During morphogenesis, the needle components, like the hook and the filament of the flagellum are sequentially exported by the T3S apparatus itself, travelling through the growing structure and polymerizing at its distal end (Macnab, 2003). The export apparatus is expected to switch its substrate specificity over time so that needle subunits (early substrates) are exported before LcrV (intermediate substrate) and the effectors (late substrates). The switch between early and intermediate substrates determines the arrest of needle growth and hence the needle length (Ferris & Minamino, 2006).

The control of the needle length and the switch to export intermediate substrates involves a protein, which is itself exported, YscP for the *Yersinia* spp injectisome (Journet *et al.*, 2003) and FliK for the flagellum (Hirano *et al.*, 1994; Minamino *et al*., 1999; Minamino *et al*., 2004). In the absence of this protein, injectisomes have extra-long needles (deregulated phenotype) and do not secrete LcrV and effectors, while the flagellum has extra-long hooks and no filament (polyhook phenotype). The switch function is assigned to the C-terminal domains of YscP and FliK (Agrain *et al*., 2005a; Minamino *et al*., 2004). This domain, called T3S4 for Type 3 Secretion Substrate Specificity Switch (Agrain *et al*., 2005a) is thought to interact with YscU (FlhB in the flagellum), a component of the basal body that is also involved in setting the hierarchy of export (Botteaux *et al*., 2008; Hirano *et al*., 1994;

Sorg *et al*., 2007). To control length, YscP needs to be exported by the nascent T3S export machine, a phenomenon driven by two independent N-terminal export signals (S1: residues 1-35 and S2: 97-137) separated by a short spacer (Agrain *et al*., 2005b).

The central region of YscP is proline-rich and contains repeats whose number varies from strain to strain in the genus *Yersinia* (Journet *et al.*, 2003; Wagner *et al.*, 2009). Deletions between residues 36-96 and 222-306 of YscP and insertions between residues 49 and 50 lead to shorter and longer needles, respectively, with a linear correlation between the size of YscP and the needle length, which led to a model where YscP acts as a molecular ruler measuring the needle (Journet *et al*., 2003). A similar correlation, observed between the size of FliK and the length of the hook (Shibata *et al*., 2007) was recently re-interpreted in the same way (Hirano *et al*., 2009).

The ruler model implies that the actual length of the ruler domain of YscP matches the length of the needle plus the basal body. The length of the ruler domain calculated by molecular modelling was indeed found to correlate with the measured needle length, with a constant difference of 29 nm, which corresponds approximately to the size of the basal body (Wagner *et al*., 2009). This element thus reinforces the ruler model. Still, open questions about the details of the mechanism remain. The first model to be proposed (Journet *et al*., 2003) was static, in the sense that each needle is regulated by a single ruler molecule which gradually stretches and switches substrate specificity when the needle has reached its final length and the T3S4 domain is in the right position to interact with the secretion apparatus and thereby terminate needle elongation. In this model, the YscF proteins are able to pass through the growing needle which is partially filled by YscP. A dynamic model was then proposed, in which the elongation of each needle is controlled by several rulers or "tape-measure" molecules which keep passing through the still growing needle. When the actual needle length exactly matches (or is greater than) the length of the passing ruler molecule, the latter stops elongation (Cornelis, 2006; Moriya *et al*., 2006). In this model, needle subunits and ruler or tape-measure proteins travel alternatively. In this report, we provide some genetic evidence that only one molecule

of YscP is required to control the length of one injectisome needle, which supports the static model.

RESULTS

Rational of the approach and selection of the appropriate alleles

Our approach consists in measuring the needles made by partial diploid bacteria that express simultaneously two yscP alleles -a short one and a long one- and compare the distribution of needle length to the predictions made by a mathematical analysis of the two models. As a short YscP protein, we chose $YscP_{388}$, a derivative of YscP in which the spacer between the two export signals and one copy of the repeats in the central part have been removed (Fig 1A) (Journet *et al*., 2003). To generate a long YscP, we engineered a restriction cleavage site between codons 250-251 in the central part of the *yscP* gene. We then generated $yscP_{686}$ by inserting a copy of codons 214-374, encoding the repeated region, into the restriction site (Fig 1A). The two recombinant genes, cloned on the same expression vector were then introduced in *Y. enterocolitica* LJ4036 deleted from the wt copy of *yscP* and the phenotypes were analyzed (Fig 1B). To test whether the two sorts of needles could be discriminated, equal numbers of *Y. enterocolitica* LJ4036 bacteria producing either $YscP_{388}$ or $YscP_{686}$ were mixed and 200 needles were measured. As shown in Fig 1C, the histogram of needle length distribution (nld) revealed two distinct peaks, at the expected sizes of 48 ± 6 nm and 100 ± 12 nm. Surprisingly, even though equal amounts of bacteria were mixed, about 60% of the needles measured were of the small type (Table S3). The reason for this unequal representation was not investigated. We can nevertheless exclude that long needles break down because no small needles appear in cultures producing exclusively long needles (Fig 1C).

Predicted nld for diploid bacteria according to the static and dynamic models.

In a first step, the nld of haploid bacteria was analyzed and found consistent with a normal distribution (Figs S3, Tables S3, S4). Based on this, an algorithm was developed to account for the static and dynamic models of needle length control

(see SI for details). The one ruler per needle model (scenario 1) predicts (Scheme S1) that (i) diploid bacteria will produce a mixture of long and short needles identical to a mixed culture of two different haploid strains (Fig 2A, Tables S5-S7) and that (ii) there will not be any deregulated needle

In the case of the dynamic ruler model, two scenarios can be envisioned; needle growth is interrupted when the length of the YscP travelling molecule is shorter than the needle (scenario 2), or YscP exactly matches (within a tolerance) the needle length (scenario 3). The nld was computed (Scheme S2) for scenarios 2 and 3, using ratios of [YscF]/[YscP] ranging from 1 (~100 YscP/needle) to 50 (~3 YscP/needle) (Fig S7). The [YscF] and [YscP] terms represent the "effective concentration" of needle subunits and proteins, respectively (see SI material); their ratio represents the relative probability of accessing the basal body. Ratios of [YscF]/[YscP] below 1 were considered unrealistic and not included. Full results are given in Fig 2 and S6, where the number of needles is shown as a heat map (Fig 2B, 2D). Significant slices for scenario 2 and 3 are given in Figs 2C and 2E, respectively. The percentage of rulers belonging to either the long- or short-needle distribution is also reported along with the percentage of deregulated needles produced by the model (Figs 2B and 2D).

For scenario 2, when the "effective concentration" of rulers is similar to that of needle subunits ([YscF]/[YscP] ≈ 1), the system is "over-regulated" by the short rulers which meet the stopping criterion (i.e., needle length greater than the ruler length) before the longer ones. This is evident in Figs 2B and S6A, B where a sole peak (corresponding to the smaller needles) is present for low [YscF]/[YscP] values. As [YscP] decreases ([YscF]/[YscP] up to 50), the initial peak broadens. Nonetheless, two distinct peaks were never observed, as confirmed by the Expectation-Maximization Algorithm (EMA) (Georgi *et al*., 2010) analysis (Figs 2B, C and S4, S6A, C and Table S8). Since this scenario imposes a stop whenever the needle length is greater than the passing-by ruler, even needles allowed to grow by a low measurement frequency (low [YscP]) will be stopped as soon as a ruler is allowed to enter the needle. Hence the scenario excludes the appearance of deregulated needles (Figs 2B, S7A).

For scenario 3, “over-regulation” by the small ruler is observed when [YscF]/[YscP] ≈ 1 (Fig 2C, S6B, D). As the measurement frequency decreases with lower values of [YscP], two distinct peaks do appear in correspondence, respectively of short and long needle distributions. For values of [YscF]/[YscP] above ~30, the computed nld is compatible with normal bimodal distribution (Table S9, Fig S5). Below this threshold the computed distributions are unlikely to be either normal or bimodal (Fig S7). The stopping rule is more restrictive than in scenario 2, allowing for growth interruption only when the needle length is equal (with a tolerance) to the passing-by ruler length. As [YscP] decreases the number of deregulated needles rapidly increases (Fig S7B) (see SI material for details). Thus, scenario 3, in contrast to scenario 2, features an increasing number of deregulated needles for low [YscP] (Fig 2E, S7). As an example, scenario 3 produces 29% deregulated needles when the ratio of [YscP]/[YscF] is 1/40, i.e., when there are less than 5 YscP per needle (Figs 2D, E and S7).

Diploid strains for short and long yscP alleles produce two distinct populations of regulated needles and no deregulated needles.

Three different types of genetic constructs were engineered. First, the *yscP*$_{388}$ allele was inserted on the 70-kb virulence plasmid by allelic replacement of the wt gene and the *yscP*$_{686}$ allele was introduced *in trans* on an expression vector, downstream from the strong pBAD promoter (Fig 3A). In *Y. enterocolitic*a E40, under the conditions used, this vector leads to a detectable expression in every bacterial cell (Fig S6). Both YscP proteins were produced and secreted by the diploid bacteria but the long variant was more abundantly secreted (Fig 4A). The needle length histogram revealed two peaks at 54 ± 6 and 98 ± 15 nm, similar to those obtained with haploid bacteria (50 ± 5 nm and 103 ± 12 nm)(Fig 4A).

In the second type of construct, the two alleles were placed on the same pDuet expression vector, each of them downstream from an individual T7 promoter (Fig 3B). As shown in Fig S7, *egfp* and *mCherry* cloned together on this vector were simultaneously expressed in every bacterium. In order to avoid any bias due to the respective position of the alleles on the pDuet, the two *yscP* alleles were cloned in

each position, generating two different expression plasmids (e.g., pLM18 and pM20, Fig 3B). The recombinant plasmids were introduced into the Δ*yscP* strain LJ4036 together with a plasmid encoding an inducible T7 polymerase. Synthesis of YscP was induced at the same time as type III secretion. Plasmid pLM20 seemed to drive more export of the long YscP than plasmid pLM18 (Fig 4B). For both constructs, the histograms of needle lengths revealed a clear peak of short needles (50 ± 8 nm and 48 ± 6 nm) similar to the needles produced by haploids (48 ± 6 nm and 50 ± 6 nm) besides a peak of longer needles (106 ± 12 and 99 ± 12 nm), also similar to the needles produced by the corresponding haploids (110 ± 10 and 107 ± 14 nm) (Fig 4B).

Finally, both alleles were fused in a single operon, downstream from the pBAD promoter (Fig 3C). There were again two populations of needles (50 ± 6 nm and 91 ± 13 nm) similar to those produced by the corresponding haploids (48 ± 5 nm and 103 ± 12 nm) (Fig 4C and Table S10).

Deregulated needles were never observed in eight different experiments with the four different constructs (Fig 4). The results were then pooled (1521 measurements) and found consistent with a bimodal normal distribution (EMA analysis in Tables S10, S11). As shown in Fig 5, two distinct peaks account for short and long needle populations and are clearly consistent with the predicted distributions found for scenario 1 and 3 (Fig 2A, E). However, scenario 3 is inconsistent with the experimental results since it predicts a significant percentage of deregulated needle (Fig 2E) whereas none was experimentally observed. The experimental data closely match the predicted distribution of scenario 1.

The proportion between the number of long and short needles reflects the proportions of long and short YscP molecules.

With all three different constructs, the proportion of long needles was always smaller than that of short needles as seen in the proof of principle experiment where equal numbers of bacteria producing either short or long molecules were mixed (Table S3). This probably results from the same bias. However, for LJ4036 (pLM20) secreting more of the long YscP version than LJ4036 (pML18), the proportion of long

needles was higher (~ 40% versus ~ 30%, Fig 4 and Table S10) than for LJ4036 (pML18). This data suggests that there is a correlation between the amount of needles of one type and the amount of ruler of that type that is secreted.

DISCUSSION

In this work, we measured the needles assembled by *Y. enterocolitica* bacteria producing simultaneously a short and a long version of the ruler protein. We ensured that both proteins were synthesised in every bacterium and readily exported. The experiment was done with three different kind of genetic constructs in order to exclude any bias due to a preferred transcription or translation of one allele versus the other. The three different *Y. enterocolitica* diploid bacteria produced a mixture of short and long needles. The length of the short and long needles corresponded exactly to the length of the needles produced when only one type of ruler was produced. The interpretation of these data is that only one molecule of ruler determines the length of one needle. Indeed, if more than one ruler were involved, depending on the exact mechanism, mathematical modeling predicts the appearance of intermediate sized or deregulated needles. In addition, with one genetic construct, we observed that more export of the long ruler correlated with more long needles. These two types of observations reinforce the molecular ruler model, based on the correlation between the needle length and the length of the control protein (Journet *et al*., 2003; Wagner *et al*., 2009).

The present conclusion that only one ruler determines the length of one needle may seem to be at odds with our previous observations that over-expression of YscP improves the needle length control (Agrain *et a*l., 2005b; Sorg *et al*., 2007). However, these observations were made, with systems in which export of YscP was reduced, either because one export signal was missing (Agrain *et al*., 2005b) or because YscU was mutated (Sorg *et al*., 2007). In these systems, over-expression of YscP only restored export of YscP to wt levels.

However, two aspects of the model remain to be investigated. First, the N-terminus of YscP, which is most likely exported first (Agrain *et al*., 2005b), needs to interact with the growing end of the needle. In good agreement with this prediction,

the N-terminus of the flagellum hook-length control protein FliK interacts with the hook cap protein, the protein located at the tip of the hook during elongation (Moriya *et al*., 2006). However, this observation cannot be simply extrapolated to the injectisome needle because no capping protein has been identified so far at the end of the growing needle. The mature needle terminates with a tip structure made of LcrV (Mueller *et al*., 2005) but the needle length is controlled in the absence of LcrV (Wagner *et al*., 2009), meaning that the length control protein must interact with a tip-less needle. The question of the ruler anchor is thus unanswered but one cannot exclude that YscP attaches to the needle end since it is detectable at the bacterial surface by immuno-gold labeling (Stainier *et al*., 2000).

MATERIAL AND METHODS

Bacterial strains, plasmids, oligonucleotides, and details of the mathematical modeling are described in the Supplementary Online Information. Induction of the *yop* regulon, Yop protein analysis and needle length measurement were as described in Wagner *et al*., 2009. Detached needles were measured.

ACKNOWLEDGEMENTS

We thank G Morson for assistance in EM. This work was supported by the Swiss National Science Foundation through grant 310000-113333/1 to GC and through the collaborative CRSII3_125110/1 Sinergia grant.

LITERATURE CITED

Agrain C, Callebaut I, Journet L, Sorg I, Paroz C, Mota LJ, Cornelis GR (2005a) Characterization of a Type III secretion substrate specificity switch (T3S4) domain in YscP from Yersinia enterocolitica. Molecular microbiology 56: 54-67

Agrain C, Sorg I, Paroz C, Cornelis GR (2005b) Secretion of YscP from Yersinia enterocolitica is essential to control the length of the injectisome needle but not to change the type III secretion substrate specificity. Molecular microbiology 57: 1415-1427

Botteaux A, Sani M, Kayath CA, Boekema EJ, Allaoui A (2008) Spa32 interaction with the inner-membrane Spa40 component of the type III secretion system of

Shigella flexneri is required for the control of the needle length by a molecular tape measure mechanism. Molecular microbiology 70: 1515-1528

Broz P, Mueller CA, Muller SA, Philippsen A, Sorg I, Engel A, Cornelis GR (2007) Function and molecular architecture of the Yersinia injectisome tip complex. Molecular microbiology 65: 1311-1320

Cornelis GR (2006) The type III secretion injectisome. Nat Rev Microbiol 4: 811-825

Ferris HU, Minamino T (2006) Flipping the switch: bringing order to flagellar assembly. Trends Microbiol 14: 519-526

Galan JE, Wolf-Watz H (2006) Protein delivery into eukaryotic cells by type III secretion machines. Nature 444: 567-573

Georgi B, Gesteira Costa I, Schliep A (2010) PyMix - The Python mixture package - a tool for clustering of heterogeneous biological data. BMC bioinformatics 11: 9

Goure J, Broz P, Attree O, Cornelis GR, Attree I (2005) Protective Anti-V Antibodies Inhibit Pseudomonas and Yersinia Translocon Assembly within Host Membranes. J Infect Dis 192: 218-225

Hirano T, Mizuno S, Aizawa S, Hughes KT (2009) Mutations in flk, flgG, flhA, and flhE that affect the flagellar type III secretion specificity switch in Salmonella enterica. Journal of bacteriology 191: 3938-3949

Hirano T, Yamaguchi S, Oosawa K, Aizawa S (1994) Roles of FliK and FlhB in determination of flagellar hook length in Salmonella typhimurium. Journal of bacteriology 176: 5439-5449

Hodgkinson JL, Horsley A, Stabat D, Simon M, Johnson S, da Fonseca PC, Morris EP, Wall JS, Lea SM, Blocker AJ (2009) Three-dimensional reconstruction of the Shigella T3SS transmembrane regions reveals 12-fold symmetry and novel features throughout. Nat Struct Mol Biol 16: 477-485

Journet L, Agrain C, Broz P, Cornelis GR (2003) The needle length of bacterial injectisomes is determined by a molecular ruler. Science 302: 1757-1760

Macnab RM (2003) How Bacteria Assemble Flagella. Annu Rev Microbiol 57: 77-100

Marlovits TC, Kubori T, Lara-Tejero M, Thomas D, Unger VM, Galan JE (2006) Assembly of the inner rod determines needle length in the type III secretion injectisome. Nature 441: 637-640

Minamino T, Gonzalez-Pedrajo B, Yamaguchi K, Aizawa SI, Macnab RM (1999) FliK, the protein responsible for flagellar hook length control in Salmonella, is exported during hook assembly. Molecular microbiology 34: 295-304.

Minamino T, Saijo-Hamano Y, Furukawa Y, Gonzalez-Pedrajo B, Macnab RM, Namba K (2004) Domain organization and function of Salmonella FliK, a flagellar hook-length control protein. Journal of molecular biology 341: 491-502

Moriya N, Minamino T, Hughes KT, Macnab RM, Namba K (2006) The type III flagellar export specificity switch is dependent on FliK ruler and a molecular clock. Journal of molecular biology 359: 466-477

Mueller CA, Broz P, Muller SA, Ringler P, Erne-Brand F, Sorg I, Kuhn M, Engel A, Cornelis GR (2005) The V-antigen of Yersinia forms a distinct structure at the tip of injectisome needles. Science 310: 674-676

Shibata S, Takahashi N, Chevance FF, Karlinsey JE, Hughes KT, Aizawa S (2007) FliK regulates flagellar hook length as an internal ruler. Molecular microbiology 64: 1404-1415

Sorg I, Wagner S, Amstutz M, Muller SA, Broz P, Lussi Y, Engel A, Cornelis GR (2007) YscU recognizes translocators as export substrates of the Yersinia injectisome. The EMBO journal 26: 3015-3024

Stainier I, Bleves S, Josenhans C, Karmani L, Kerbourch C, Lambermont I, Totemeyer S, Boyd A, Cornelis GR (2000) YscP, a Yersinia protein required for Yop secretion that is surface exposed, and released in low Ca2+. Molecular microbiology 37: 1005-1018.

Wagner S, Sorg I, Degiacomi M, Journet L, Dal Peraro M, Cornelis GR (2009) The helical content of the YscP molecular ruler determines the length of the Yersinia injectisome. Molecular microbiology 71: 692-701

Yip CK, Strynadka NC (2006) New structural insights into the bacterial type III secretion system. Trends Biochem Sci 31: 223-230

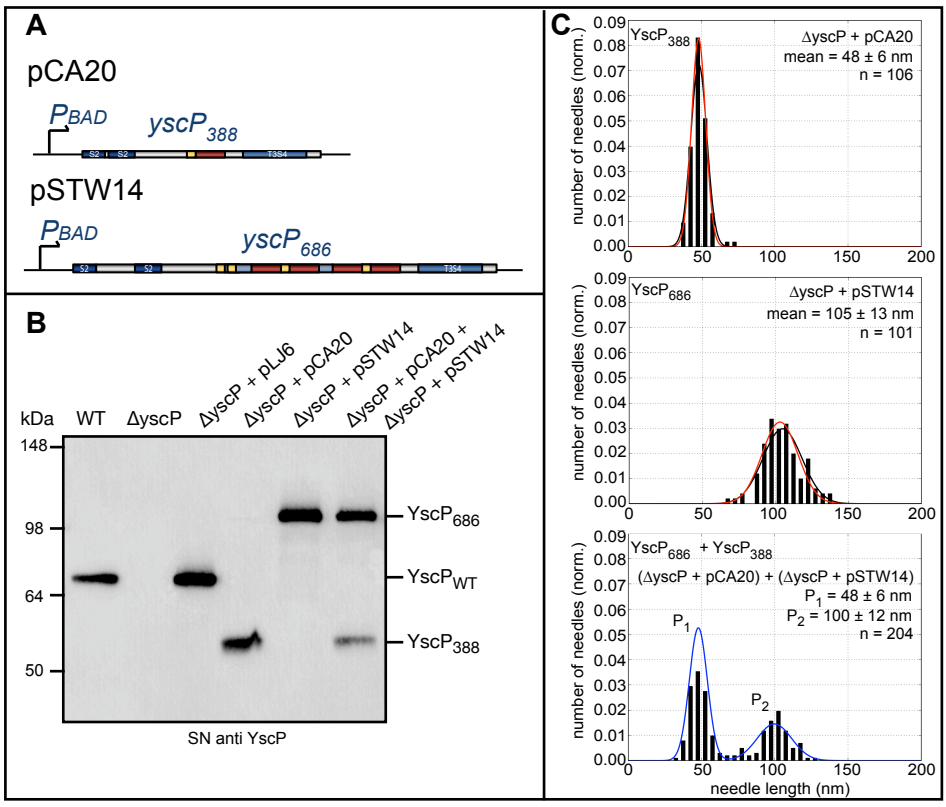

Figure 1

Selection and analysis of the alleles used in this study.

Schematic representation of two *yscP* genes (*yscP*$_{388}$ and *yscP*$_{686}$) cloned downstream from the pBAD promoter in pCA20 and pSTW14, respectively (A). Export of YscP by *Y. enterocolitica* E40 wt and LJ4036 (called *ΔyscP*) over-expressing YscP wt (from pLJ6), YscP$_{388}$ (from pCA20) or YscP$_{686}$ (from pSTW14) and a 1:1 mixture of bacteria over-expressing YscP$_{388}$ and YscP$_{686}$. Supernatant fractions (SN) were analyzed by immunoblotting using anti-YscP polyclonal antibodies (B). Histogram representation of the needle length distribution normalised to unity; a Gaussian function of experimental mean and st. dev. (black line) and the best fitting Gaussian (red line) are reported for haploids; a double Gaussian function obtained by EMA is reported for mixed samples, n, number of measured needles (C).

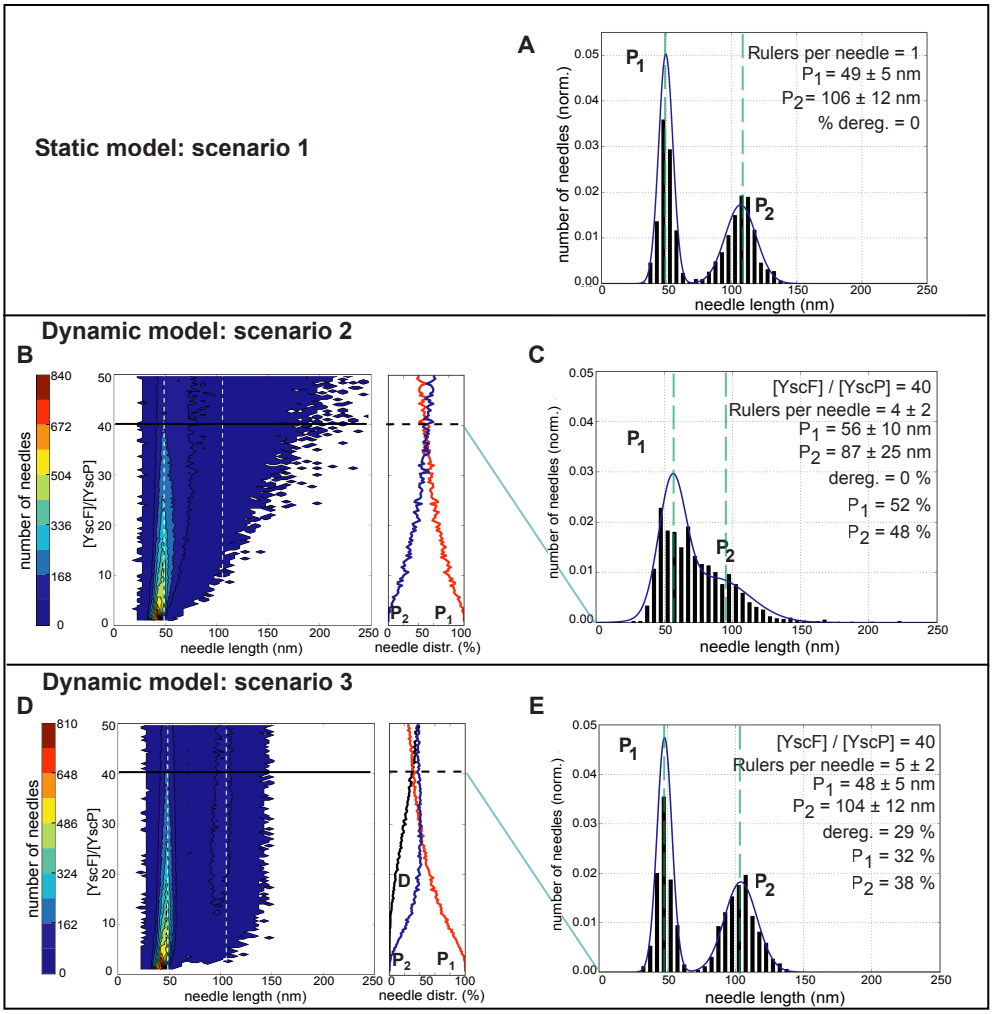

Figure 2

Nld predicted for the static and dynamic models.

Histogram representation of the normalized (area below the curve equated to 1) needle length distribution (nld) computed for the scenario 1 (A). Needle populations obtained for scenario 2 (B) and 3 (D), with the nld calculated at different values of [YscF]/[YscP] and reported as a not-normalized heat map representing the number of needles (see also Fig S6). Needle distribution among the short (red line), long (blue line) and deregulated (black line) species computed for scenario 2 and 3 are reported in the right-handed insets. Histogram representation for the nld obtained at significant value of [YscF]/[YscP]= 40 for scenario 2 (C) and 3 (E) are reported along with their bimodal normal distribution fitting as obtained by EMA analysis. Green dotted lines placed at the centre of each peak identify the mean value of each population belonging to the overall bimodal distribution.

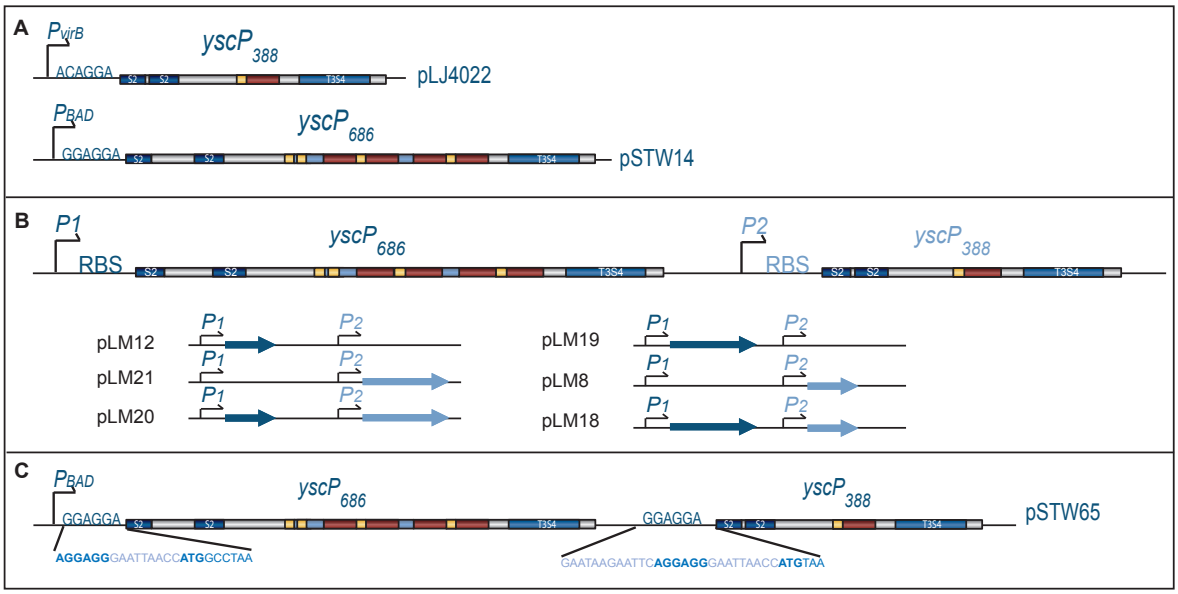

Figure 3

The various genetic constructs expressing *yscP*$_{388}$ and *yscP*$_{686}$.

pLJ4022 is the 70-kb virulence plasmid where *yscP*$_{388}$ replaces the wt allele, downstream from its natural promoter. pSTW14 encodes YscP$_{686}$ from the pBAD promoter (A). The six derivatives of pCDFDuet (four haploids and two diploids) are shown in panel B. In pSTW65, the two alleles are cloned as one operon downstream of the pBAD promoter (C).

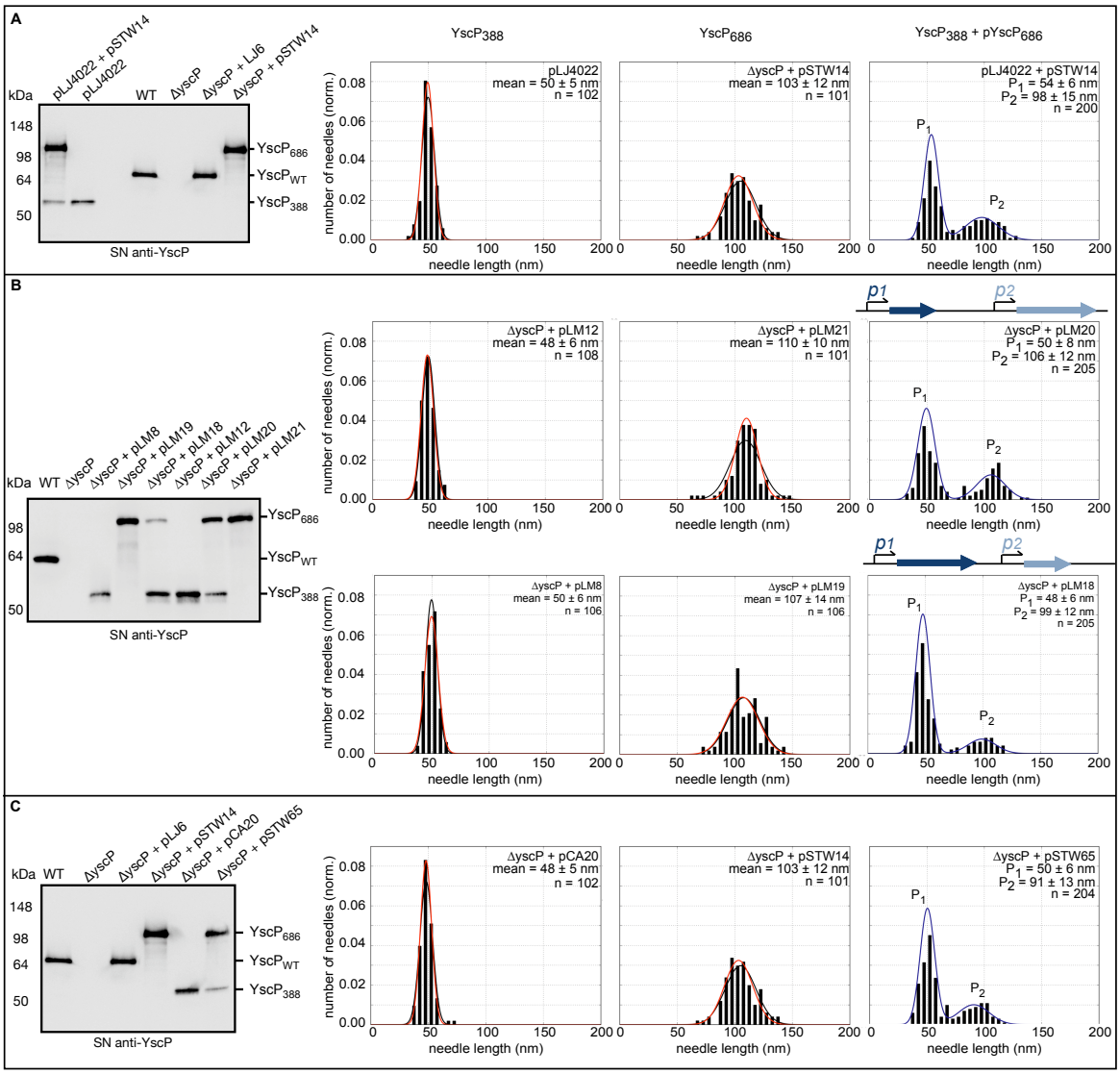

Figure 4

Experimental nld in bacteria expressing *yscP388*, yscP686 or both.

On the left, supernatant (SN) fractions were analyzed by immunoblotting using anti-YscP antibodies. On the right, nld of the needles from diploid and the corresponding haploid bacteria. Panels A, B and C show the data for the genetic constructs shown in panels A, B and C from Fig 3, respectively. The histogram representation is normalised to unity. A Gaussian function of experimental mean and st. dev. (black line) and the best fitting Gaussian (red line) are reported for haploids; a double Gaussian function obtained by EMA is reported for diploid samples. n, number of measured needles; p, Promoter; P, Peak.

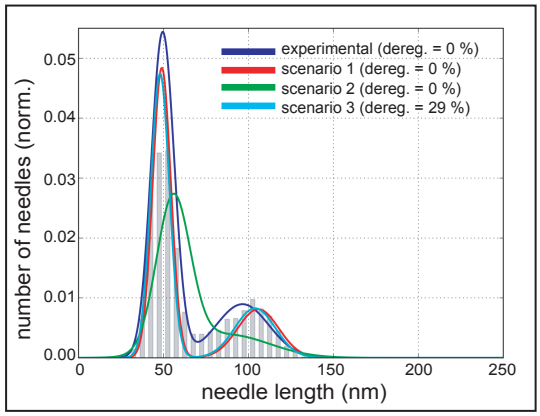

Figure 5

Experimental nld compared to predicted nld according to the different scenarios. Histogram representation of the nld obtained with the four different diploid constructs (histogram binning size = 5 nm) (A). The normalized experimental nld is fitted by a bimodal normal distribution as obtained by the EMA analysis (blue line), and superimposed to the bimodal normal distributions obtained for the different three computed scenarios. Bimodal normal distribution fits are here weighted to match the experimental ratio found between long and short needle populations in a mixture of cultures producing short and long needles. (see Table S11).

Supplementary Figure S1

Expression of the egfp gene cloned downstream from the pBAD promoter in Y. enterocolitica E40.

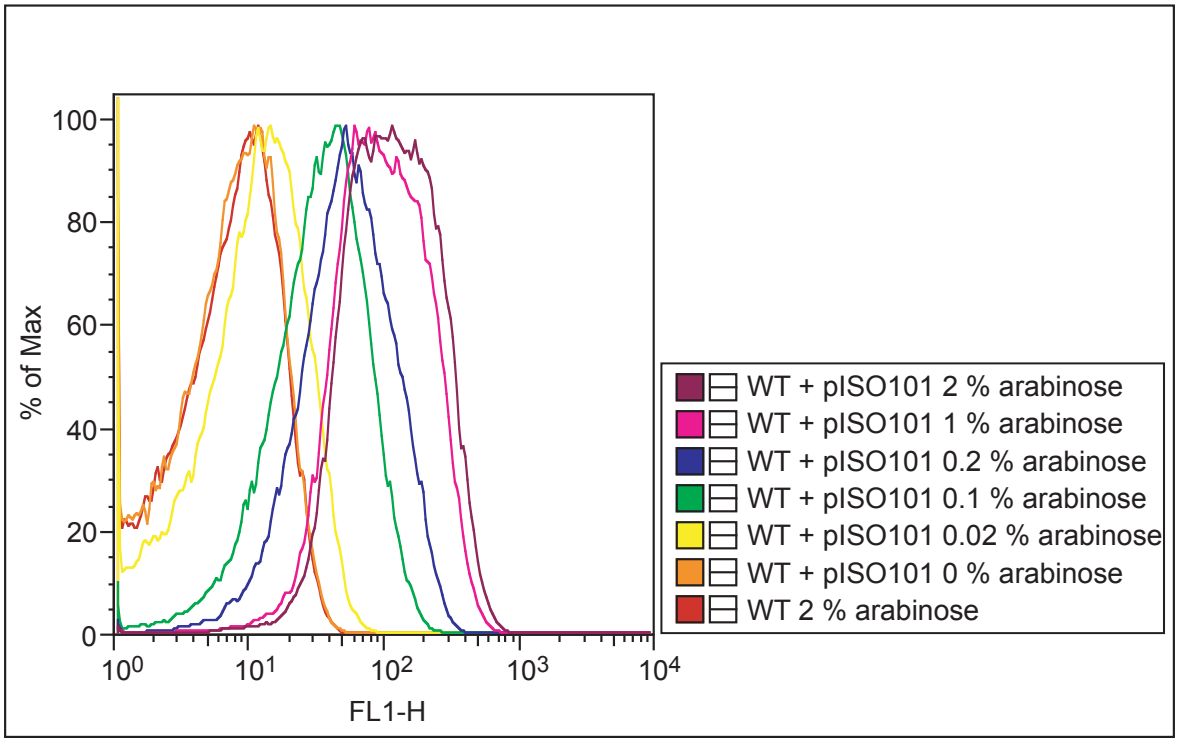

Y. enterocolitica strains were inoculated to an $O.D._{600}$ of 0.1 and cultivated in brain-heart infusion (BHI; Remel) supplemented with 35 µg/mL nalidixic acid, 4 mg/mL glycerol, 20 mM $MgCl_2$ and 20 mM sodium oxalate (BHI-Ox) 2 h at RT, then shifted to 37 °C and incubated for 4 h. Ampicillin was used at a concentration of 200 µg/mL to select for the expression plasmids. Expression of EGFP was induced by adding indicated amounts of arabinose to the culture just before the shift to 37 °C, and again 2 h later. EGFP expression was analyzed by fluorescence-activated cell sorter (FACS) analysis. After incubation at 37 °C for 4 h, 1 mL of bacterial cultures were centrifuged for 1 min at 20817 g and bacterial pellets were resuspended and adjusted do an $O.D._{600}$ of 0.2 in 1 mL PBS, prior to FACS analysis. FL1-H, Intensity of fluorescence; % of Max, % of bacteria.

Supplementary Figure S2

Expression of *egfp* and *mCherry* cloned in the two expression loci of pDuet in *Y. enterocolitica* E40.

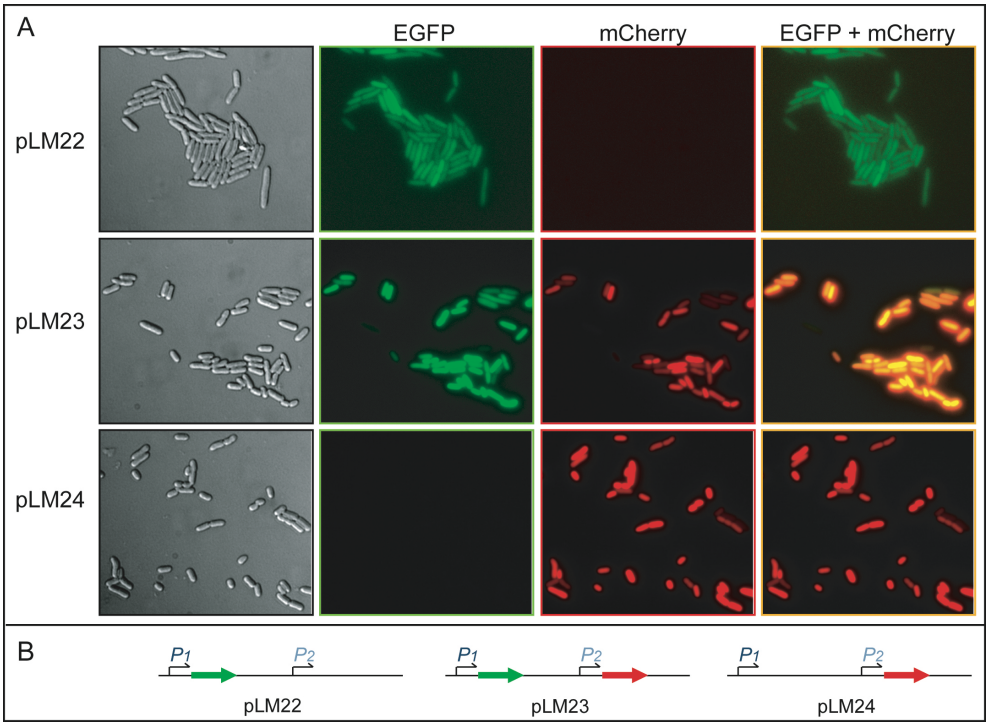

Y. enterocolitica strains were inoculated to an $O.D._{600}$ of 0.1 and grown in brain-heart infusion (Remel) supplemented with 35 µg/mL nalidixic acid, 200 µg/mL Ampicillin, 50 µg/mL Streptomycin, 4 mg/mL gycerol, 20 mM $MgCl_2$ and 5 mM $CaCL_2$ for 2 h at RT. Expression of the T7 polymerase was then induced with 0.1% arabinose. Ten minutes later, expression of EGFP and mCherry was induced with 800 µM IPTG at RT for 3 h. For fluorescence imaging, cells were placed on a microscope slide layered with a pad of 2% agarose dissolved in water. A Deltavision Spectris optical sectioning microscope (Applied Precision, Washington, United States) equipped with an UPlanSApo 100x/1.40 oil objective (Olympus, Japan) and a coolSNAP HQ CCD camera (Photometrics, AZ, United States) was used to take differential interference contrast (DIC) and fluorescence photomicrographs. FITC filter sets (Ex 490/20 nm, Em 528/38 nm) and Rhodamine filter sets (Ex 555/28 nm, EM 617/73 nm) were used for EGFP and mCherry respectively. Exposure times were 0.15 s for DIC and and 1.0 s for fluorescence frames. Per image a Z-stack containing 20 frames per wavelength with a spacing of 150 nm was acquired. Images at the median of the cell were chosen and processed with softWoRx v3.3.6 (Applied Precision, WA) and ImageJ (National Institute of Health, USA) software.

Supplementary Figure S3

Histogram representation of the (normalized on the right) nld obtained upon expression of the two rulers

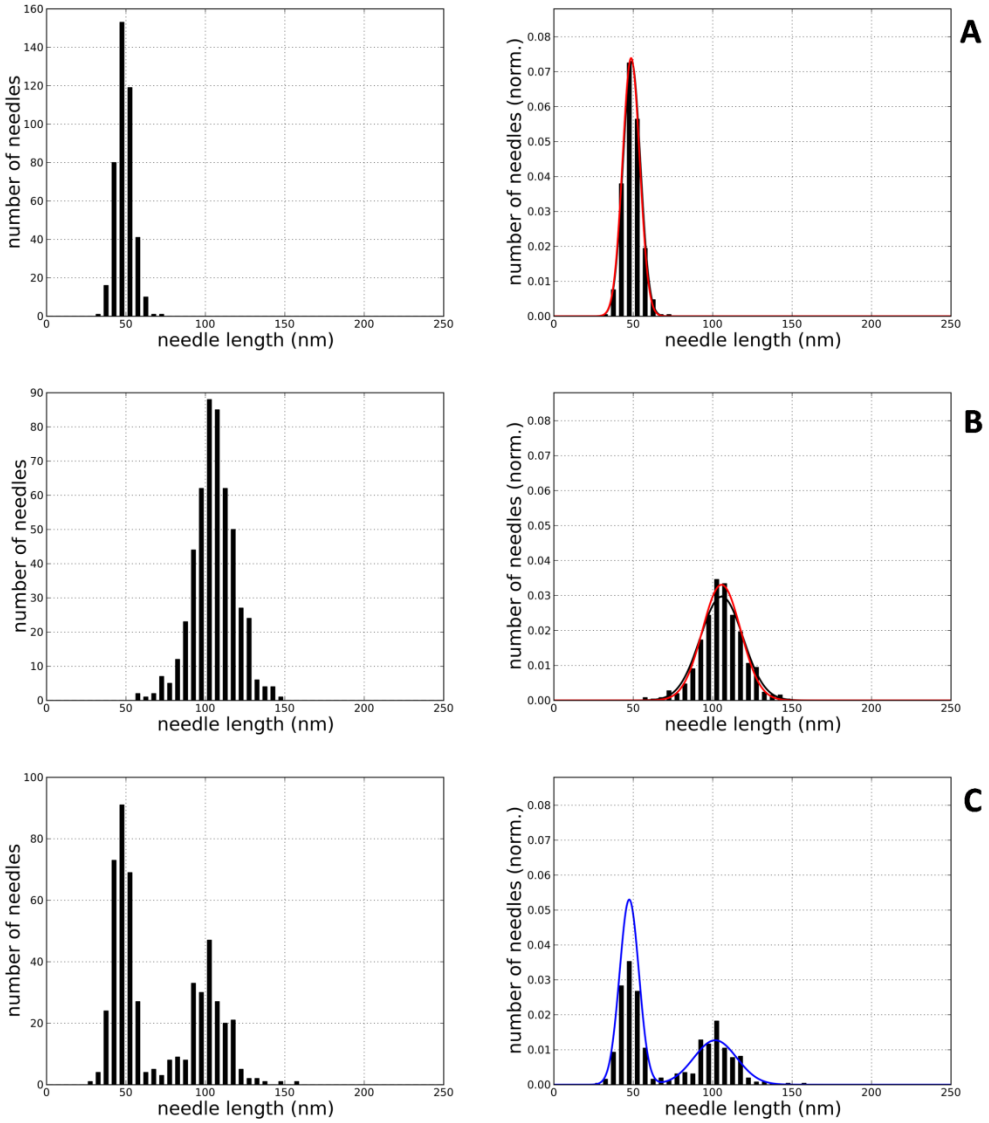

Histogram representation of the (normalized on the right) nld obtained upon expression of the two rulers (histogram binning size = 5 nm). A) Short ruler: YscP$_{388}$. B) Long ruler: YscP$_{686}$. C) Sample created by mixing organisms containing both the short and the long ruler. The black line in A and B represents a Gaussian function plotted using the experimental mean and standard deviation as centre and width, respectively. The red line in A and B represents a Gaussian whose centre and widths have been optimized to match the experimental nld. The blue line in C is a “double Gaussian” plotted using the parameters obtained by applying the EMA on the experimental nld. (left side: non-normalized; right side: normalized)

Supplementary Figure S4

Histogram representation for the needle length distribution computed for the "dynamic model" (Scenario 2)

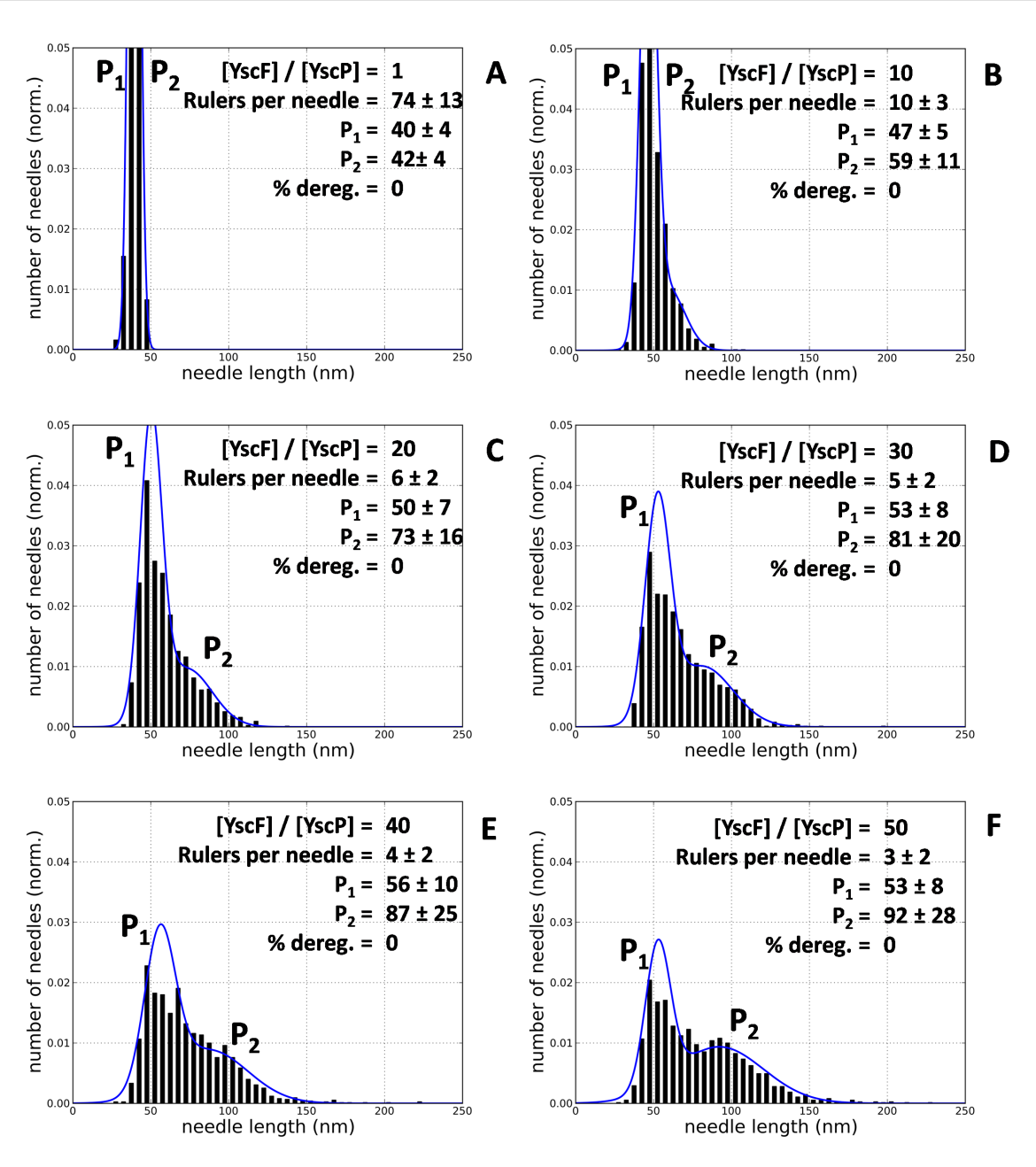

Histogram representation for the needle length distribution computed for the "dynamic model" (Scenario 2) at selected values of [YscF]/[YscP]. The blue line is a "double Gaussian" function plotted using the parameters obtained by applying the EMA on the calculated nld. The values reported are not normalized.

Supplementary Figure S5

Histogram representation for the needle length distribution computed for the "dynamic model" (Scenario 3)

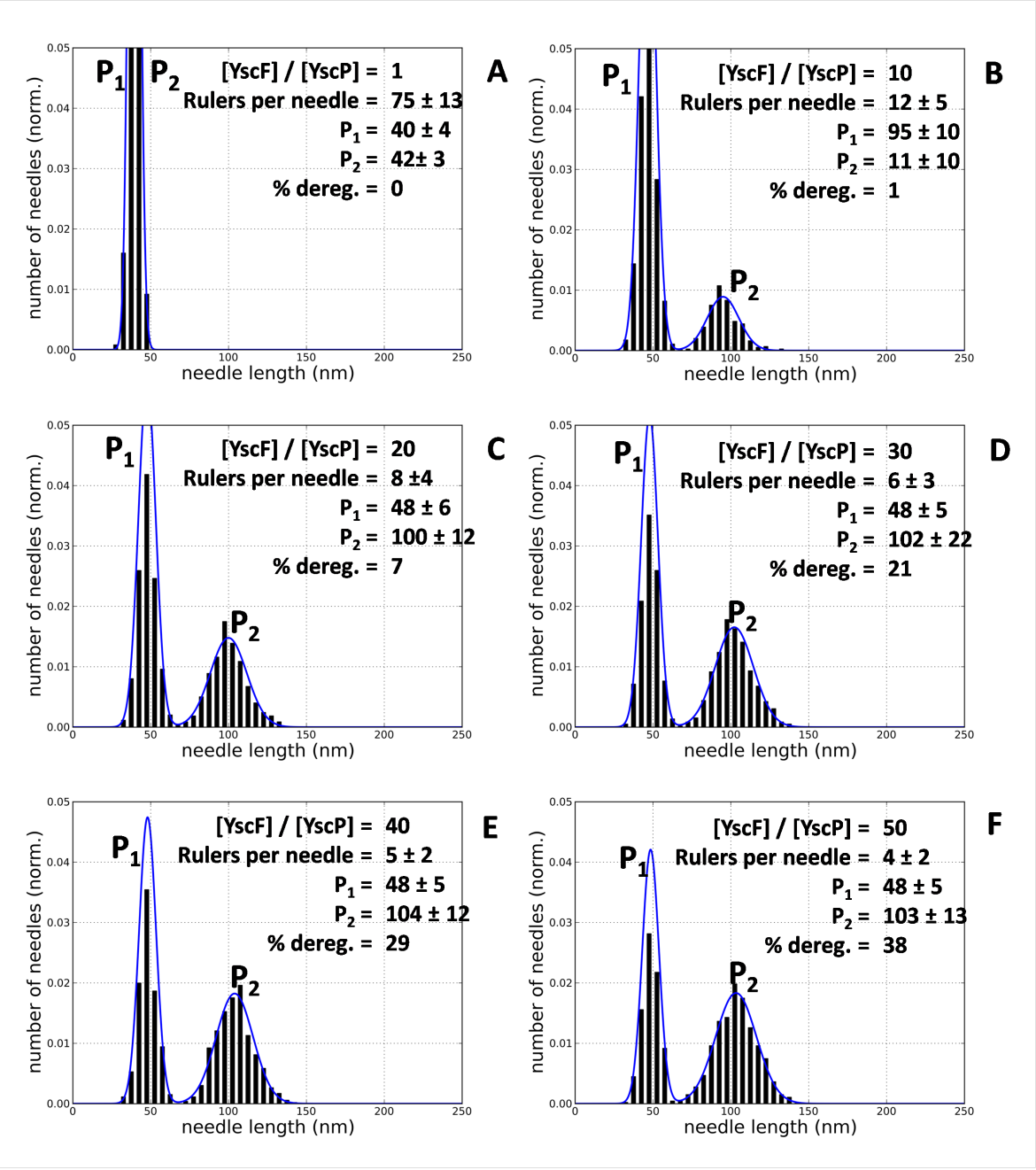

Histogram representation for the needle length distribution computed for the "dynamic model" (Scenario 3) at selected values of [YscF]/[YscP]. The blue line is a "double Gaussian" function plotted using the parameters obtained by applying the EMA on the calculated nld. The values reported are not normalized.

Supplementary Figure S6

Needle population computed for the 2 scenarios of the dynamic model

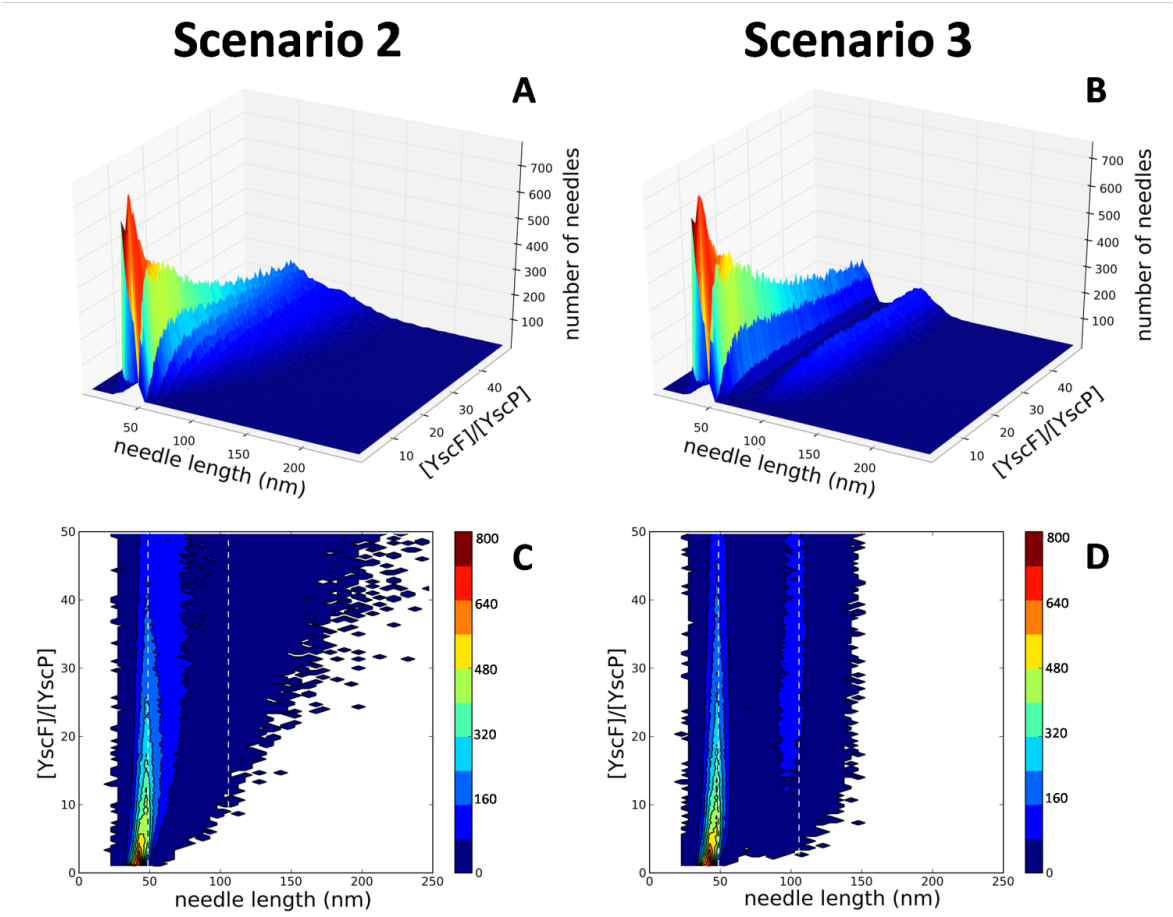

Needle population computed for Scenario 2 (A) and 3 (B) at different values of 1 / [YscP]. Bidimensional projections on the XY plane are reported (C and D) in the same color scale. The values reported are not normalized.

Supplementary Figure S7

Selected parameters computed for the Scenarios 2 and 3.

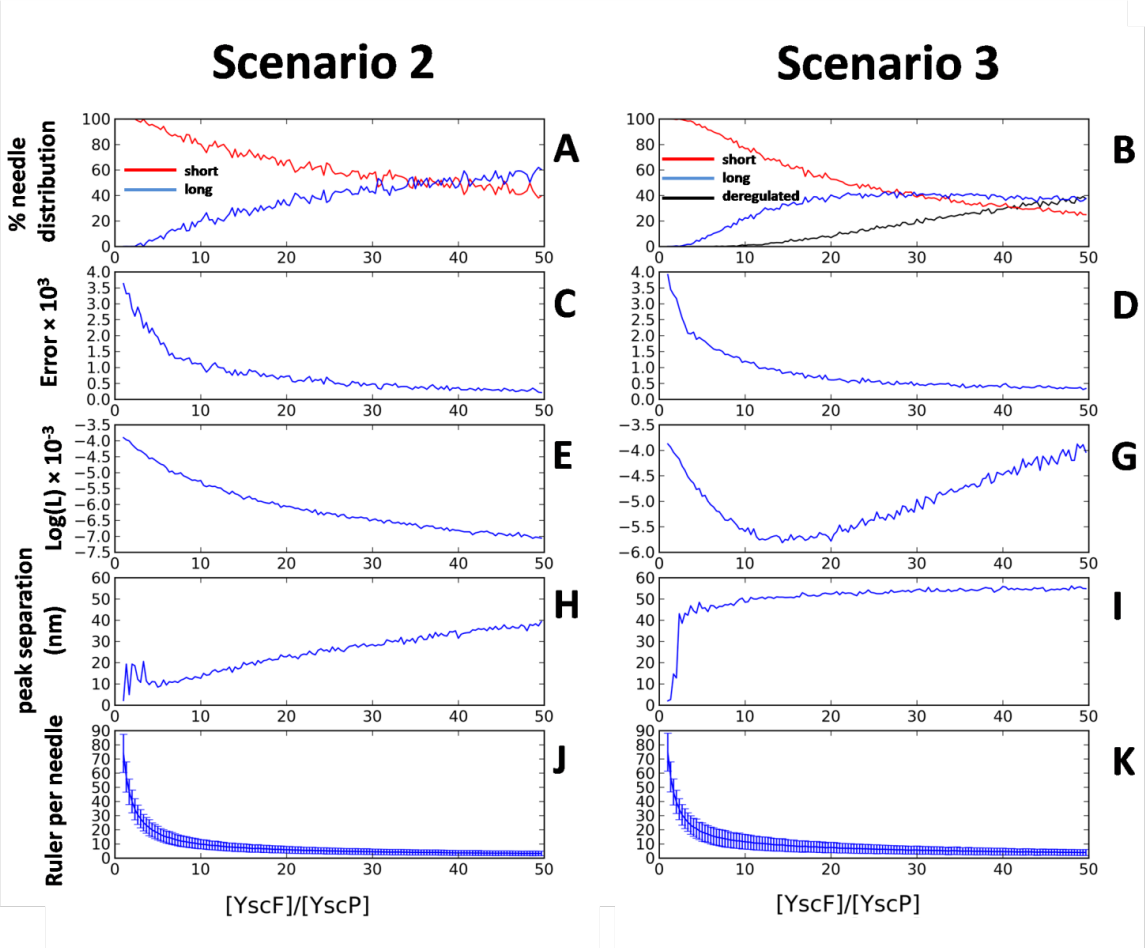

Selected parameters computed for the Scenarios 2 and 3. A) Needle distribution among the short (red), long (blue) and deregulated (black) species; B) Error from fitting the computed nld with the G2 functions obtained by the EMA; C) logarithm of the likelihood computed by the EMA; D) Distance between the peaks representing the population of short and long needles, computed as the difference between μ_1 and μ_2; E) average number of rulers secreted during the growth of a needle, with standard deviation reported as bars.

SUPPLEMENTARY INFORMATION

Supplementary Material and Methods

Bacterial strains and plasmids

This work was done with *Y.enterocolitica* E40 (Sory *et al*., 1995). Bacterial plasmids and genetic constructions are listed in Table S1. Plasmids were generated using either Pfu turbo polymerase (Stratagene) or Vent DNA polymerase (New England Biolabs). The oligonucleotides used for genetic constructions are listed in Table S2. All constructs were confirmed by sequencing using a 3100-Avant genetic analyzer (ABI Prism).

Induction of injectisome assembly and analysis of YscP proteins

Y. enterocolitica E40 bacteria were grown in liquid brain-heart infusion (BHI; Remel) medium. Induction of the *yop* regulon was done as described in ref (Sorg *et al*., 2007). Yop proteins from the supernatant were analyzed by SDS-PAGE. For detection of YscP in total cells, $1.6x10^7$ bacteria were loaded per lane. For YscP detection in supernatants, the supernatants from $1.6x10^8$ bacteria were loaded per lane. Immunoblotting was done using a polyclonal rabbit anti-YscP antibody (1:3000; MIPA57) as described in ref (Sorg *et al*., 2007). Expression of the different *yscP* genes cloned downstream from the pBAD promoter was induced by adding 0.2% arabinose to the culture just before the shift to 37 °C, and again 2 h later. Ampicillin was used at a concentration of 200 µg/mL to select for the expression plasmids and instead of glucose, glycerol was used as carbon source at a final concentration of 4 mg/mL. Expression of the *yscP* genes cloned downstream from the T7lac promoter was induced by adding 800 µM IPTG to the culture just before the shift to 37 °C. Expression of the T7 RNA polymerase gene cloned downstream of the pBAD promoter was induced by adding 0.1% arabinose to the culture 10 min before the shift to 37 °C. Streptomycin at a concentration of 50 µg/mL was used to select for the expression plasmids. Expression of the T7 RNA polymerase gene cloned downstream of the pBAD promoter was induced by adding 0.1% arabinose to the culture 10 min before the shift to 37 °C.

Needle length measurement

Visualization of needle-like structures was done by transmission electron microscopy as described in Hoiczyk & Blobel, 2001and Sorg *et al*., 2007. Detached needles were measured.

Mathematical analysis

The needle length distribution (nld) of needles produced by haploid bacteria is Gaussian

$YscP_{388}$ and $YscP_{680}$ were chosen as, respectively, short and long ruler. The nld of each (Tables S3, S4) was recorded and reported in Figure S3A,B in histogram representation, with a bin size of 5 nm. By visual inspection both distribution appeared to be Gaussian-shaped. To give a quantitative measure of the distribution 'normality' two approaches have been adopted: a) the mean and standard deviation of the two samples have been used, respectively, as the centre (μ) and width (σ) of a Gaussian function (Equation 1); b) for each distribution a value for μ, σ were obtained by fitting a Gaussian function on the experimental nld. To compare a continuous Gaussian function to a discrete distribution a simple strategy was devised: the number of needles in the i^{th} bin (height of the i^{th} histogram), indicated as H_i in Equation S2, is compared with the value the Gaussian function assumes in correspondence of the middle point of the i^{th} bin, indicated a $G(x_i)$ in Equation S2. The computed value of the error E was used to quantify the agreement of the experimental discrete length distribution with Gaussian functions. For both the short and long ruler the nld was in good agreement with the experimentally derived (black line, Figure S3A,B) and with the optimized Gaussian (red line, Figure S3A,B), as confirmed by: a) similar values of the computed errors E, b) mean and standard deviation of the samples compare fairly good with, respectively, centre (μ) and width (σ) of the optimized Gaussian functions.

$$G(x) = \frac{1}{\sigma\sqrt{2\pi}} e^{-\left(\frac{(\mu - x)^2}{2\sigma^2}\right)}$$

Equation S1

$$E = \sum_{i=1}^{n} (G(x_i) - H_i)^2$$

Equation S2

The nld of needles produced by a 1/1 mixture of cultures of haploid bacteria is Gaussian

As explained in the main text, to test whether the two kinds of needle could be discriminated, bacteria producing either $YscP_{388}$ or $YscP_{686}$ were mixed and the length of the expressed needles measured. The histogram nld, reported in Figure S3C, revealed two distinct peaks compatible with a bimodal distribution. Since a bimodal distribution can be expressed, if the constituting peaks are far apart, as a mixture of two unimodal distributions, a "double-Gaussian" function (G2, see Equation S3) wasn used to fit the experimental nld. Since a standard parameter fitting of the G2 function failed, due to the simultaneous presence of parameters within and outside the exponential part of G2, a more robust and sophisticated procedure, based on the "Expectation-Maximization" Algorithm (EMA), was employed to determine the centre and the width of each of the two constituting Gaussian functions and their respective weight (parameters c1 and c2 in Equation S3). Moreover this approach yielded a quantitative esteem for the likelihood relating the experimental distribution and the best parameters of the proposed Gaussian mixture model. By applying the EMA procedure to the experimental nld, the two peaks were placed at 47.5 ± 6.1 nm and 101.6 ± 13.5 nm, respectively (Table S5), in good agreement with the values found for the un-mixed haploid nld (see Figure S3 and Tables S1-3 for comparison).

$$G2(x) = c_1 \frac{1}{\sigma_1\sqrt{2\pi}} e^{-\left(\frac{(\mu_1 - x)^2}{2\sigma_1^2}\right)} + c_2 \frac{1}{\sigma_2\sqrt{2\pi}} e^{-\left(\frac{(\mu_2 - x)^2}{2\sigma_2^2}\right)}, (c_1 + c_2 = 1)$$

Equation S3

As explained in the main text, when equal amount of bacteria were mixed, about 60% of the measured needles were of the small type (Table S6). This has been attributed to a systematic error of the measure. The nld recorded for a set of needle belonging to each sample was processed by using the EMA; the optimized Gaussian mixture ($G2_{opt}$) of each set was used to separate the measured needles in two groups according to their length. A clustering tool based on EMA Gaussian mixtures was employed to assign the needles either to the "short" or to the "long" group.
It should be noted that neither for the separately measured haploids nor for their mixture were "unregulated" needles observed.

Relation between needle length and number of needle subunits

On the basis of the "static" and "dynamic" models for needle length regulation, an algorithm was assembled to generate needle length distributions according to the assumptions associated to the proposed models. The reliability of the various models was assessed by comparing the computed length distributions with the ones experimentally measured for partially diploids organism.

The devised algorithm makes use of the experimental nld of short and long needles expressed in haploid organisms. It is assumed than the $YscP_{388}$ ruler generates a population (P_1) of needles with mean M_1 = 49.0 nm and standard deviation SD_1=5.5 nm (Table S3), while the $YscP_{686}$ ruler yields a population (P_2) of needles with mean M_2 = 105.7 nm and standard deviation SD_2 = 13.4 nm (Table S4).

The approximate length of one needle subunit (L0 = 6.3 nm) and the unitary contribution of each subunit (L= 0.45 nm) to the overall needle length were calculated on an atomistic structural model of Y. enterocolitica T3SS needle, as built by homology modeling from the data available for Shighella (Deane et al, 2006). According to this model the needle features a helicoidal arrangement, each turn being formed by about 6 subunits, each one shifted with respect to the previous one by L (along the growth axis); for a needle composed by n subunits the total length is thus given by Equation S4.

$$L_{tot} = L_0 + (n-1)L$$

Equation S4

Stochastic method:

Mathematical algorithm for the static model (Scenario 1)

According to the static model the length of each needle is regulated by a single ruler molecule fastened to the cytoplasmic side of the basal body with the T3S4 domain and hooked to the growing end of the needle by the S1/S2 domains. The ruler is eventually released and the T3SS machinery stops exporting needle subunits (YscF protein) thus terminating needle growth. In this model the length of each needle is directly determined by the length of the ruler protein, to which both the mean and the standard deviation of the overall needle population are directly related.

In an organism endowed by a duplicate set for yscP gene (partial diploid), two variant of the YscP protein ($YscP_{388}$, $YscP_{686}$) of different length were expressed.

There is competition between the two rulers in negotiating their access to the basal body as to exert their function. The probability for one ruler to enter the basal body instead of the

other is a function of their relative expression levels, diffusion constants, export apparatus association and recognition coefficients, and other unknown factors. The "ruler effective concentration", [$YscP_{388}$] and [$YscP_{686}$], can be thus defined as a global parameter counting in, for each ruler, all known and unknown factors, including their actual molar concentration in the cytoplasm.

In the static model there is no competition between the needle subunits and the ruler proteins to access the basal body entrance, since the YscF proteins are exported while the YscP is stably positioned as described above. This implies that the YscF proteins are capable of passing through the channel constituted by the hollows in both the basal body and growing needle. Since this channel accommodates the (partially extended) YscP protein, for the needle subunits to pass a partial unfolding of either or both YscF and YscP protein could be required.

In the mathematical representation of the static model, the "ruler effective concentrations" [$YscP_{388}$] and [$YscP_{686}$] were given a statistical interpretation, their ratio R_{SL} (Equation S5) being considered as the bias favoring one ruler over the other in entering the export apparatus and exerting a measuring function.

The algorithm for generating the static model nld on the basis of these assumptions is given in Scheme S1:

$$R_{SL} = [YscP_{388}] / [YscP_{686}] \qquad \text{Equation S5}$$

Scheme S1. Algorithm employed to obtain a nld according to the assumptions contained in the static model (Scenario 1).

1) Input the sample size N, representing the number of needles to account for, and the value of the R_{SL} parameter.
2) Repeat N times:
  2.1) Choose which ruler does access the export apparatus, determining the length of the i^{th} needle; the random choice is biased by the given value of R_{SL}, actually favoring one ruler with respect to the other.
    2.1.1) If the short ruler $YscP_{388}$ is picked up, the length of the i^{th} needle is randomly chosen from a length population normally distributed around M_1 with a standard deviation SD_1 (from the experimental distribution obtained for short rulers in haploids).
    2.1.2) If the Long ruler $YscP_{686}$ is picked up the length of the i^{th} needle is randomly chosen from a length population normally distributed around M_2 with a standard deviation SD_2 (from the experimental distribution obtained for long rulers in haploids).
  2.2) Record the length of the i^{th} needle.
3) The resulting nld is plotted in the histogram representation (bin size = 5 nm) and then analyzed with the EMA to find the best parameter of the Gaussian mixture model G2 (Equation S4)

By running the algorithm with N = 1500 (and R_{SL} =1 (stating for and unbiased probability favoring neither the short nor the long ruler) a nld clearly featuring two peaks were obtained (Figure 2A in the main text). The EMA analysis of the obtained needle length population yielded the optimized variables for a Gaussian mixture model of the type G2 (Table S7) consistent with a neat bimodal normal distribution with unimodal components clearly matching the experimental distribution observed for the two kinds of haploids organisms.
A cluster analysis of the length population showed an equal amount of needle belonging to the two peaks.

Mathematical algorithm for the dynamic model: Scenarios 2 and 3

The difference between the static and dynamic model for needle length regulation is in the number of ruler molecules employed (and thus secreted) during the growth of each needle. While in the static model a single ruler molecule is associated to the basal body and to the

needle during the whole growing phase, in the dynamic model, an indeterminate number of rulers pass through the needle, until a last one causes the substrate specificity switch and thus growth stop. Two different scenarios can be envisaged depending on the conditions required for the switch signaling to take place:

Scenario 2. The actual needle length Ln is greater (within a tolerance) than the length of the passing ruler Lr; Ln ≥ Lr

Scenario 3. The actual needle length Ln exactly matches (within a tolerance) the length of the passing ruler Lr; Ln ≈ Lr

As in the static model, in both scenarios of the dynamic model there is a competition between the two kinds of rulers in accessing the export apparatus to exert the regulatory function. Two global parameters, [$YscP_{388}$] and [$YscP_{686}$], and their ratio R_{SL} can be defined for the dynamic model as described above for the static one.

Since in the dynamic model, during needle growth, more than one ruler molecule is required to enter the basal body and get secreted, a certain degree of competition could be envisioned between needle subunits and ruler proteins in gaining access to the export apparatus. The average frequency of ruler admittance can be thus related to the ratio between the “needle subunit effective concentration” [YscF] and the overall “ruler effective concentration” [YscP] (Equations S6, S7).

$$R_{NR} = [YscF]/[YscP] = 1 / R_{NR} \qquad \text{Equation S7}$$

The algorithm for generating the dynamic model nld on the basis of these assumptions is given in Scheme S2.

Scheme S2. Algorithm employed to obtain a nld according to the assumptions contained in the dynamic model (Scenarios 2 and 3).

1) Input the sample size N, representing the number of needles to account for, the value of the R_{SL} and R_{RN} parameters, the stopping rule (Scenario 2 or 3).
2) Repeat N times:
  2.1) The actual needle length Ln is set to L_0 (unitary length of the needle subunit): $Ln = L_0$.
  2.2) Choose whether a ruler or a needle subunit enters: the R_{RN} parameter is used to bias the random choice.
    2.2.1) If a needle subunit enters, the actual needle length Ln is increased by L (the unitary contribution of a needle subunit): Ln = Ln+L.
    2.2.2) If a ruler enters a choice is made between $YscP_{388}$ and $YscP_{686}$: the R_{SL} parameter is used to bias the random choice.
      2.2.2.1) If the short ruler $YscP_{388}$ is picked up, the ruler length Lr is randomly chosen from a length population normally distributed around M_1 with a standard deviation SD_1 (from the experimental distribution obtained for short rulers in haploids).
      2.2.2.2) If the long ruler $YscP_{686}$ is picked up the ruler length Lr is randomly chosen from a length population normally distributed around M_2 with a standard deviation SD_2 (from the experimental distribution obtained for short rulers in haploids).
    2.2.3) Defining the stopping criterion:
      2.2.3.1) If simulating Scenario 2: stop = YES if $Ln \geq Lr$
      2.2.3.2) If simulating Scenario 3: stop = YES if $Ln \approx Lr$
    2.2.4) Decide whether stop or not the growth process:
    2.2.4.1) If stop ≠ YES, the growing process continues: go to point **2.2**.
    2.2.4.2) If stop = YES, the growing process stops: go to point **2.1**.
  2.3) Record the length of the i^{th} needle and the number of rulers passed through the needle during its growth.
3) The resulting nld is plotted in the histogram representation (bin size = 5 nm) and then analyzed with the EMA to find the best parameter of the Gaussian mixture model G2 (Equation S4)

Since there is no experimental evidence about the ruler frequency acceptance, the procedure described in Scheme 2 was repeated, for each of the two scenarios, setting different values of the [YscP] parameter, thus obtaining 3D graphs by stacking together the histogram representation obtained at point 3 of the algorithm (in Figures S4, S5 selected histogram representation are reported, while in Figure S6 the 3D graphs and their 2D projection are given). To achieve a better understanding of the phenomenon the obtained values were plotted with respect [YscF]/[YscP]. The use of the reciprocal of the "effective ruler concentration" helped defining the lower boundary of the problem. Values of [YscF]/[YscP] smaller than 1 implying the ruler being secreted with a greater frequency than the needle subunits themselves and resulting in a massive waste were not considered. For values of [YscF]/[YscP] near 1 the system is "over-regulated", since the length of the needle is "measured" by rulers with almost the same frequency as it is incremented by needle subunits. An increasing value of [YscF]/[YscP] indicates a lower access frequency for the rulers, implying less frequent "measurements" of the needle length.

Scenario 2. When the "effective concentration" of rulers is similar to that of needle subunits ([YscF]/[YscP] ≈ 1) the system is "over-regulated" by the smaller ruler which is able to meet the stopping criterion (actual needle length greater than the ruler length) before the longer one. This is evident in Figures S3A,C where a single peak (corresponding to the smaller needles) is present for low Y values.

As the value of [YscF]/[YscP] increases the “measurement” frequency decreases, resulting in a broadening of the peak, also due to the more evident contributions to the nld by the long ruler.

For no value of [YscF]/[YscP] within the considered range two distinct peaks were observed, as confirmed by the EMA analysis (Figure S7), accounting for a Gaussian mixture composed by two Gaussian functions whose centre is never further apart than 35 nm, well below the coalescence limit. The EMA analysis provides parameter values allowing for the G2 function to fit the nld with increasing success (decreasing error, Figure S7) for higher Y values but the computed likelihood decreases rapidly, indicating that the distribution fitted by the G2 function is neither bimodal nor normal. This is more evident by observing the nld computed for six representative values of [YscF]/[YscP](see Figure S4) and their respective Gaussian parameters, as computed by EMA (see Table S8).

Scenario 3. As seen for Scenario 2 when the effective ruler concentration is higher ([YscF]/[YscP]≈ 1) the system is “over-regulated” by the smaller ruler, and a single peak (corresponding to the smaller needles) is seen for low Y values (Figures S6B,D). As the value of [YscF]/[YscP] increases and the “measurement” frequency decreases, two distinct peaks appeared in correspondence of the small and long needle, respectively. The EMA analysis provided insight to the nature of the obtained nld along the considered [YscP] range. For values of [YscF]/[YscP] above 40 the computed nld is clearly compatible with normal bimodal distribution, as confirmed by high likelihood and good fitting of the G2 function (small error). Below this threshold the computed distributions are unlikely to be either normal or bimodal. This was more evident by observing the nld computed for six representative values of [YscF]/[YscP] (see Figure S5) and their respective Gaussian parameters, as computed by EMA (see Table S9).

Scenario 3, in contrast with Scenario 2, features an increasing number of “deregulated” needles for high Y values (low [YscP]). According to the employed algorithm, a needle was defined “deregulated” when its length exceeded 250 nm and its growth becomes unlikely to be interrupted. For Scenario 2, since the stopping rule imposes a stop when the needle length is greater than the passing by ruler, even needles allowed to grow over the threshold limit of 250 nm by a low “measurement” frequency (low [YscP], high Y) could be stopped as soon as a ruler is allowed to enter the needle; thus the stopping probability is never null. In Scenario 3 the stopping rule is more restrictive, allowing for growth interruption only when the needle length is equal, within an arbitrary tolerance, to the passing-by ruler’s length To be consistent with the method employed to choose the ruler length (point 2.2.2 of the algorithm reported in Scheme S2) the tolerance varies for each of the two rulers as a Gaussian function whose center and spread match the mean and the standard deviation of experimental distributions obtained for the two rulers in haploids (see Section S2). For this reason the probability of a needle to be stopped in its growth when its length exceeds the value of $M_2 + 3 \times SD_2$ is almost null. As the [YscP] decreases (high Y values) the number of “deregulated” needles rapidly increases for Scenario 3, while for Scenario 2 an increasing number of simply exceedingly long needles are observed.

Statistical analysis of the experimental data obtained with diploid bacteria

The diploid nld was recorded for 8 different samples, obtaining for each one a set of rulers that was separately investigated by using the EMA method. The G2 parameters obtained for each set and for the overall ensemble are reported in Table S10. In each case the experimental nld is normal and bimodal, composed by two unimodal distribution closely resembling in both centre and spread the experimental distributions obtained for the two haploid organisms. A cluster analysis was made, based on the optimized Gaussian mixtures from EMA. The results of this analysis were employed to quantitatively classify the needles in two groups corresponding to the short and long species, respectively. It resulted that short

needle were predominant over the longer, the population of the former ones being about 60% of the total (Table S11). This result was consistent with those observed for mixture of haploids, and could be similarly attributed to a systematic error of the measure (see above).

Computational details

The algorithms described in the text were implemented using the “Python” programming language (van Rossum G. et al, 2001). The “matplotlib” graphics environment (van Rossum G et al, 2001) was used to generate histogram and line plots (Hunter J.D., 2007). The Gaussian mixture models were obtained by means of the “Python Mixture Model” implemented in the “PyMix” package (Georgi B. et al, 2010).

The “PyMix” package features an efficient version of the “Expectation-Maximization” Algorithm (EMA), an iterative method often used in statistics for finding maximum likelihood estimates of parameters in probabilistic models. This method consists in two steps iterated until convergence: 1) Expectation step, consisting in computing the expectation of the likelihood (often in logarithmic form) of the given distribution for some variables; 2) Maximization step, which optimize the parameters as to maximize the likelihood predicted at the previous step. In this context the term “likelihood” is not synonymous for “probability”: whereas the latter allows predicting unknown outcomes (probability distributions) from known parameters, the former is used to estimate unknown parameters on the basis of known outcomes (given distributions). In the present case the EMA was employed to find the best parameters of a Gaussian mixture model used to represent a bimodal normal distribution. The Gaussian mixture model with optimized parameters was then used to perform a cluster analysis on the given population.

Supplementary references

Agrain C, Callebaut I, Journet L, Sorg I, Paroz C, Mota LJ, Cornelis GR (2005) Characterization of a Type III secretion substrate specificity switch (T3S4) domain in YscP from Yersinia enterocolitica. Molecular microbiology 56: 54-67

Hoiczyk E, Blobel G (2001) Polymerization of a single protein of the pathogen Yersinia enterocolitica into needles punctures eukaryotic cells. Proceedings of the National Academy of Sciences of the United States of America 98: 4669-4674.

Journet L, Agrain C, Broz P, Cornelis GR (2003) The needle length of bacterial injectisomes is determined by a molecular ruler. Science 302: 1757-1760

Mota LJ, Cornelis GR (2005) The bacterial injection kit: type III secretion systems. Ann Med 37: 234-249

Sorg I, Wagner S, Amstutz M, Muller SA, Broz P, Lussi Y, Engel A, Cornelis GR (2007) YscU recognizes translocators as export substrates of the Yersinia injectisome. The EMBO journal 26: 3015-3024

Sory MP, Boland A, Lambermont I, Cornelis GR (1995) Identification of the YopE and YopH domains required for secretion and internalization into the cytosol of macrophages, using the cyaA gene fusion approach. Proceedings of the National Academy of Sciences of the United States of America 92: 11998-12002.

Tabor S, Richardson CC (1985) A bacteriophage T7 RNA polymerase/promoter system for controlled exclusive expression of specific genes. Proceedings of the National Academy of Sciences of the United States of America 82: 1074-1078

van Rossum G, Drake FL. (2001) Python Reference Manual, PythonLabs, Virginia, USA, 2001. Available at http://www.python.org. (Last visited: 2010/01/15)

Hunter JD. (2007) Matplotlib: A 2D Graphics Environment. Vol. 9, pp. 90-95.

Georgi B, Gesteira Costa I, Schliep A PyMix (2010) The Python mixture package - a tool for clustering of heterogeneous biological data. BMC Bioinformatics 11(1): 9

Supplementary tables

Table S1. Plasmids

Plasmid	encoded Protein	vector	Genotype or Description	Source or Reference
pYV plasmids				
pYV40		pYV	Wild-type virulence plasmid from strain *Y. enterocolitica* E40	(Sory *et al*., 1995)
pLJ4036		pYV	pYV40 Δ*yscP* (deleted from start to stop)	(Agrain *et al*., 2005))
pLJ4022		pYV	pYV40 $YscP_{\Delta 46\text{-}96+\Delta 222\text{-}306}$	(Mota & Cornelis, 2005)
Expression plasmids				
pBADMycHisA		pBAD		Invitrogen
pCDFDuet-1		pDuet		Novagen
pEGFP-1			EGFP	BD Biosciences Clontech
pCA20	$YscP_{388}$	pBAD	pBADMycHisA-$yscP_{\Delta 46\text{-}96+\Delta 222\text{-}306}$	(Journet *et al*., 2003)
pCA23	$YscP_{site\ I}$	pBAD	Introduction of a NotI and a XbaI site between codons 49 and 50 of $yscP_{WT}$ in pLJ6. All the *yscP* variants described in this paper were engineered from this gene.	(Journet *et al*., 2003)
pGP1-2	T7 RNA polymerase	pBR322	pBR322-T7 RNA polymerase	(Tabor & Richardson, 1985)
pLJ6	$YscP_{WT}$	pBAD	pBADMycHisA-*yscP* This yscP gene originates from strain W22703 and differs slightly from the ortholog in strain E40.	(Journet *et al*., 2003)
pLM7	$YscP_{WT}$	pDuet	$yscP_{WT}$ was amplified from pLJ6 using oligos 5201 and 5202 and ligated into MCS2 of pCDFDuet-1 using restriction sites NdeI/XhoI	This study
pLM8	$YscP_{388}$	pDuet	$yscP_{\Delta 46\text{-}96+\Delta 222\text{-}306}$ from pLM6 was ligated into MCS2 of pCDFDuet-1 using restriction sites NdeI/XhoI	This study
pLM12	$YscP_{388}$	pDuet	$yscP_{\Delta 46\text{-}96+\Delta 222\text{-}306}$ from pCA20 was ligated into MCS1 of pCDFDuet-1 using restriction sites NcoI/EcoRI	This study
pLM17	T7 RNA polymerase	pDuet	T7 RNA polymerase gene was amplified from pGP1-2 using oligos 5306 and 5307 and ligated into pBADMycHisA using restriction sites NcoI/EcoRI	This study
pLM18	$YscP_{686}$ and $YscP_{388}$	pDuet	$yscP_{siteIII\Omega YscP241\text{-}374}$ from pSTW14 was ligated into MCS1 of pLM8 using restriction sites NcoI/EcoRI	This study

Plasmid	encoded Protein	vector	Genotype or Description	Source or Reference
pLM19	$YscP_{686}$	pDuet	*yscP*$_{siteIII\Omega YscP241-374}$ from pSTW14 was ligated into MCS1 of pCDFDuet-1 using restriction sites NcoI/EcoRI	This study
pLM20	$YscP_{388}$ and $YscP_{686}$	pDuet	*yscP*$_{siteIII\Omega YscP241-374}$ from pLM21 was ligated into MCS2 of pLM12 using restriction sites NdeI/XhoI	This study
pLM21	$YscP_{686}$	pDuet	*yscP*$_{siteIII\Omega YscP241-374}$ was amplified from pSTW14 using oligos 5201 and 5202 and ligated into MCS2 of pCDFDuet-1 using restriction sites NdeI/XhoI	This study
pLM22	EGFP	pDuet	*egfp* was amplified from pEGFP-1 using oligos 3989 and 3992 and ligated into MCS1 of pCDFDuet-1 using restriction sites NcoI/EcoRI	This study
pLM23	EGFP and mCherry	pDuet	*mCherry* was amplified from pCHYC-2 using oligos 5437 and 5444 and ligated into MCS2 of pLM22 using restriction sites NdeI/XhoI	This study
pLM24	mCherry	pDuet	*mCherry* from pLM23 was ligated into MCS2 of pCDFDuet-1 using restriction sites NdeI/XhoI	This study
pSTW4	$YscP_{sites\ I + III}$	pBAD	Introduction of a ClaI and a SalI site between codons 250 and 251 of *yscP* from pCA23 by overlapping PCR using primer pairs 3344 and 4405 (introducing both sites) and 4402 (introducing both sites) and 3345.	This study
pSTW14	$YscP_{686}$	pBAD	Duplication of codons 214 to 374 from *yscP* (amplified with oligos 4407 and 4408) from pSTW4 (between codons 250 and 251)	This study
pSTW65	$YscP_{686}$ + $YscP_{388}$	pBAD	*yscP*$_{\Delta 46-96+\Delta 222-306}$ was amplified from pCA20 using oligos 5320 and 5321 and ligated into pSTW14 using restriction sites EcoRI/SalI	This study

Table S2. Oligonucleotides used in this study

Number	Sequence	Restriction site
3344	GATCCCATGGCCAATAAAATCACCACTCGT	NcoI
3345	GATCGAATTCTTATTCTTCAGCCTCCCACTC	EcoRI
3989	GATCCATGGTGAGCAAGGGCG	NcoI
3992	GATCGAATTCTTACTTGTACAGCTCGTCCATG	EcoRI
4402	GCAATCGATGCGACTAGTAGATGGTGTGCTACTCCTGTG GCT	ClaI-SpeI
4405	TCTACTAGTCGCATCGATTGCTACCAAATGATCATTCGGT GT	ClaI-SpeI
4407	CCATCGATGATAGCAGGCAAAAACGCCTTGCA	ClaI
4408	GGACTAGTTTCGCGCGGAAGTAACAGTTCTTC	SpeI
5201	GGAATTCCATATGGCCAATAAAATCACCACTCGT	NdeI
5202	CCGCTCGAGTCATTCTTCAGCCTCCCA	XhoI
5306	CATGCCATGGATGAACACGATT	NcoI
5307	GGAATTCTTACGCGAACGCGA	EcoRI
5320	GATCGAATTCAGGAGGAATTAACCATGAATAAAATCACCA CTCGTTCCCCATTAG	EcoRI
5321	ACGCGTCGACTTATTCTTCAGCCTCCCACTC	SalI
5437	CCGCTCGAGCTACTTGTACAGCTCGTC	XhoI
5444	GGAATTCCATATGGTGAGCAAGGGCGAGGAG	NdeI

Table S3. Experimental needle length distribution for organisms expressing the $YscP_{388}$ ruler.

$YscP_{388}$	Sample size	mean	St. dev	Err	μ_1	σ_1	Err
Sample 1	106	48.2	5.5	1.7e-04	48.0	4.8	3.2e-05
Sample 2	106	49.7	5.1	4.5e-04	49.7	5.8	3.3e-04
Sample 3	108	48.4	5.5	2.0e-04	47.5	5.5	6.4e-05
Sample 4	102	49.8	5.5	3.8e-04	49.5	5.0	3.0e-04
Total	**422**	**49.0**	**5.5**	**2.8e-05**	**48.7**	**5.4**	**7.0e-06**

Table S4. Experimental needle length distribution for organisms expressing the $YscP_{686}$ ruler.

$YscP_{686}$	Sample size	mean	St. dev	Err	μ_2	σ_2	Err
Sample 1	101	105.0	13.4	3.0e-04	103.3	12.3	2.5e-04
Sample 2	101	109.3	13.3	5.2e-04	110.1	9.7	2.0e-04
Sample 3	106	107.7	13.9	6.8e-04	106.7	13.8	6.7e-04
Sample 4	100	105.1	12.7	3.1e-04	104.6	11.4	2.8e-04
Sample 5	101	101.2	12.4	2.8e-04	103.3	10.9	1.7e-04
Total	509	105.7	13.4	8.4e-05	105.6	12.1	5.0e-05

Table S5. Gaussian mixture parameters for the needle population in a 1/1 mixture of cultures of haploid bacteria.

$YscP_{388}$ + $YscP_{686}$	Sample size	μ_1	σ_1	μ_2	σ_2	err
Sample 1	204	47.8	6.1	99.7	11.8	6.4e-04
Sample 2	208	45.6	5.5	101.6	12.0	7.7e-04
Sample 3	104	50.8	5.3	104.7	18.2	9.5e-04
Total	516	47.5	6.1	101.6	13.5	6.3e-04

Table S6. Percentages of long and short needles computed by EMA in a 1/1 mixture of cultures of haploid bacteria.

$YscP_{388}$ + $YscP_{686}$	Calculated (EMA) %		
	Sample size	Short	Long
Sample 1	204	57.4	42.6
Sample 2	208	57.7	42.3
Sample 3	105	54.8	45.2
Total	516	57.0	43.0

Table S7. Gaussian mixture parameters for the needle population obtained for Scenario 1.

	P_1		P_2		EMA		% dereg.
# of rulers per needle	μ_1	σ_1	μ_2	σ_1	Error	log(L)	
1	49.03	5.33	105.80	12.10		-6291.3	0.0

Table S8. Gaussian mixture parameters for the needle population obtained for Scenario 2 at different values of [YscF]/[YscP].

	P1		P2		Rulers per needle		EMA	
[YscF]/[YscP]	μ_1	σ_1	μ_2	σ_1	mean	st. dev.	Error	log(L)
1	39.49	3.26	41.73	3.51	73.96	13.44	3.63E-03	-3902.9
10	46.66	5.04	59.32	10.88	9.79	3.30	1.13E-03	-5246.9
20	50.15	6.96	72.95	16.34	5.91	2.37	7.28E-04	-6064.5
30	52.60	8.01	81.11	19.76	4.51	1.93	4.85E-04	-6479.4
40	55.79	9.89	87.28	24.90	3.70	1.73	3.73E-04	-6810.9
50	52.79	8.04	92.16	28.31	3.32	1.59	2.13E-04	-7054.7

Table S9. Gaussian mixture parameters for the needle population obtained for Scenario 3 at different values of [YscF]/[YscP].

	P_1		P_2		Rulers per needle		EMA		% dereg.
[YscF]/[YscP]	μ_1	σ_1	μ_2	σ_1	mean	st. dev.	Error	log(L)	
1	39.54	3.20	41.57	3.22	74.83	13.37	3.9E-03	-3874.31	0
10	46.51	5.23	94.98	10.14	11.57	5.21	1.2E-04	-5592.6	0.73
20	47.70	5.58	100.01	11.72	7.52	3.73	6.1E-04	-5781.0	6.93
30	47.82	5.38	102.22	12.23	5.67	2.87	5.0E-04	-4962.4	21.40
40	48.03	5.44	103.92	11.88	4.62	2.42	4.6E-04	-4482.7	29.27
50	48.47	5.35	103.34	13.09	3.97	2.08	3.4E-04	-4036.4	37.47

Table S10. Data of the individual experiments with diploid bacteria

	Sample size	μ_1	σ_1	μ_2	σ_2	err
Sample 1.1	200	53.8	6.2	97.8	14.5	6.3e-04
Sample 1.2	200	50.4	5.8	95.0	15.8	5.6e-04
Sample 2.1	205	49.5	7.5	105.8	12.3	6.9e-04
Sample 2.2	201	48.7	6.2	99.6	15.3	1.3e-03
Sample 3.1	205	47.8	6.3	99.2	12.0	1.1e-03
Sample 3.2	202	45.8	5.2	84.9	17.9	1.2e-03
Sample 4.1	204	50.3	6.3	90.5	13.7	8.2e-04
Sample 4.2	104	52.9	8.5	100.2	16.3	1.0e-03
total	1521	49.6	6.7	96.5	15.7	6.9e-04

Table S11. Percentages of long and short needles computed by EMA.

	Calculated (EMA) %	
	Short	Long
Sample 1.1	59.0	41.0
Sample 1.2	54.5	45.5
Sample 2.1	61.5	38.5
Sample 2.2	60.7	39.3
Sample 3.1	78.0	22.0
Sample 3.2	68.3	31.7
Sample 4.1	66.7	33.3
Sample 4.2	87.5	12.5
total	65.7	34.3

The role of YscU in needle length control and substrate specificity switching

YscU recognizes translocators as export substrates of the *Yersinia* injectisome

Isabel Sorg[1], Stefanie Wagner[1], Marlise Amstutz[1], Shirley A Müller[1,2], Petr Broz[1], Yvonne Lussi[1], Andreas Engel[1,2] and Guy R Cornelis[1,*]

[1] Biozentrum der Universität Basel, Basel, Switzerland.

[2] ME Müller Institute for Structural Biology, Basel, Switzerlandand.

Author contributions: I contributed to this paper by engineering the pSTW plasmids and analyzing their phenotype. I further contributed to the analysis of needle length of all strains presented in this paper.

YscU is an essential component of the export apparatus of the *Yersinia* injectisome. It consists of an N-terminal transmembrane domain and a long cytoplasmic C-terminal domain, which undergoes auto-cleavage at a NPTH site. Substitutions N263A and P264A prevented cleavage of YscU and abolished export of LcrV, YopB and YopD but not of Yop effectors. As a consequence, *yscU*$_{N263A}$ mutant bacteria made needles without the LcrV tip complex and they could not form translocation pores. The graft of the export signal of the effector YopE, at the N-terminus of LcrV, restored LcrV export and assembly of the tip complex. Thus, YscU cleavage is required to acquire the conformation allowing recognition of translocators, which represent an individual category of substrates in the hierarchy of export. In addition, *yscU*$_{N263A}$ mutant bacteria exported reduced amounts of the YscP ruler and made longer needles. Increasing YscP export resulted in needles with normal size, depending on the length of the ruler. Hence, the effect of the *yscU*$_{N263A}$ mutation on needle length was the consequence of a reduced YscP export.

Reprinted by permission from Macmillan Publishers Ltd: *The EMBO Journal* (I. Sorg, S. Wagner, M. Amstutz, S. Müller, P. Broz, Y. Lussi, A. Engel and G. Cornelis 2007, *EMBO Journal* **26**, 3015–3024) ©2007

The EMBO Journal (2007) 26, 3015–3024 | © 2007 European Molecular Biology Organization | All Rights Reserved 0261-4189/07
www.embojournal.org

THE
EMBO
JOURNAL

YscU recognizes translocators as export substrates of the *Yersinia* injectisome

Isabel Sorg[1], Stefanie Wagner[1], Marlise Amstutz[1], Shirley A Müller[1,2], Petr Broz[1], Yvonne Lussi[1], Andreas Engel[1,2] and Guy R Cornelis[1,*]

[1]Biozentrum der Universität Basel, Basel, Switzerland and [2]ME Müller Institute for Structural Biology, Basel, Switzerland

YscU is an essential component of the export apparatus of the *Yersinia* injectisome. It consists of an N-terminal transmembrane domain and a long cytoplasmic C-terminal domain, which undergoes auto-cleavage at a NPTH site. Substitutions N263A and P264A prevented cleavage of YscU and abolished export of LcrV, YopB and YopD but not of Yop effectors. As a consequence, *yscU*$_{N263A}$ mutant bacteria made needles without the LcrV tip complex and they could not form translocation pores. The graft of the export signal of the effector YopE, at the N-terminus of LcrV, restored LcrV export and assembly of the tip complex. Thus, YscU cleavage is required to acquire the conformation allowing recognition of translocators, which represent an individual category of substrates in the hierarchy of export. In addition, *yscU*$_{N263A}$ mutant bacteria exported reduced amounts of the YscP ruler and made longer needles. Increasing YscP export resulted in needles with normal size, depending on the length of the ruler. Hence, the effect of the *yscU*$_{N263A}$ mutation on needle length was the consequence of a reduced YscP export.

The EMBO Journal (2007) **26,** 3015–3024. doi:10.1038/sj.emboj.7601731; Published online 17 May 2007
Subject Categories: microbiology & pathogens
Keywords: effectors; targeting; translocation; type III secretion; Yops

Introduction

The injectisome allows pathogenic or symbiotic bacteria to inject effector proteins across eukaryotic cell membranes, a process called type III secretion (T3S). It is evolutionary related to the bacterial flagellum (reviewed by Macnab (2003)). Both structures share a similar basal body consisting of several rings embedded in the two bacterial membranes connected by a central rod (Blocker *et al*, 1999, 2001; Marlovits *et al*, 2004; Morita-Ishihara *et al*, 2006). Depending on the family of injectisomes, a hollow stiff needle (Kubori *et al*, 1998, 2000; Blocker *et al*, 1999, 2001; Hoiczyk and Blobel, 2001), a filament (Knutton *et al*, 1998; Daniell *et al*, 2001; Crepin *et al*, 2005) or a pilus (Van Gijsegem *et al*, 2000) terminate the structure. The length of the needle is genetically determined (Magdalena *et al*, 2002; Tamano *et al*, 2002; Journet *et al*, 2003).

The proximal rings are thought to contain the T3S export apparatus, made of a number of integral membrane proteins and soluble components (reviewed by Tampakaki *et al* (2004); Cornelis (2006); Galan and Wolf-Watz (2006)). In the *Yersinia* Ysc injectisome, a *ca* 60-nm long stiff hollow needle, assembled from the 9-kDa protein YscF, projects from the basal body into the exterior milieu (Hoiczyk and Blobel, 2001). The needle terminates in a tip structure (the tip complex) made of the protein LcrV (Mueller *et al*, 2005). Upon contact with a eukaryotic cell membrane, the injectisome translocates a set of proteins called Yops (reviewed by Mota and Cornelis (2005)). These include the translocators (YopB and YopD) that form a pore in the target membrane and the effectors that traffic through this pore. The tip complex is thought to act as a scaffold for the folding and assembly of YopB and YopD into a functional pore (Goure *et al*, 2005).

During morphogenesis, the components of the transmembrane rings are handled by the Sec machinery, while those of the rod and the needle are sequentially exported by the T3S apparatus itself (Sukhan *et al*, 2001), traveling through the growing structure and polymerizing at its distal end (Li *et al*, 2002). There is no clear hierarchy in the synthesis of the components. Thus, the export apparatus is expected to switch its substrate specificity over time from early to late substrates, so that needle subunits (early substrates) are exported before LcrV and before the Yops (late substrates). This substrate specificity switch presumably leads to the arrest of needle growth, which determines the needle length. Hence, it is only triggered when the needle has reached its genetically defined length. The trigger is provided by YscP, another early substrate of the export apparatus. The N-terminal sequence of YscP is thought to act as a molecular ruler (Journet *et al*, 2003), while the C-terminal domain triggers the substrate specificity switch (Agrain *et al*, 2005a).

Mutations affecting FliK, the flagellar YscP homolog, lead to extra-long hooks (called polyhooks) but no filament and hence bacteria are not motile (Hirano *et al*, 1994). Motile revertants appear as consequence of extragenic suppressive mutations in the integral membrane protein FlhB, suggesting that FlhB is involved in specificity switching (Kutsukake *et al*, 1994; Williams *et al*, 1996). FlhB has a long C-terminal cytosolic domain, which undergoes an autoproteolytic cleavage between N269 and P270; however, the resulting subdomains remain tightly associated with each other (Minamino and Macnab, 2000; Fraser *et al*, 2003; Ferris *et al*, 2005). This cleavage is abolished by the mutation N269A and cells producing FlhB$_{N269A}$ assemble polyhook structures lacking filaments, leading to the proposal that cleavage and interaction of the two fragments generates conformational changes important for the specificity switching process (reviewed by Ferris and Minamino (2006)).

*Corresponding author. Biozentrum, Universität Basel, Infection Biology, Klingelbergstrasse 50-70, Basel, CH 4056, Switzerland.
Tel.: +41 61 267 21 10; Fax: +41 61 267 21 18;
E-mail: guy.cornelis@unibas.ch

Received: 28 March 2007; accepted: 27 April 2007; published online: 17 May 2007

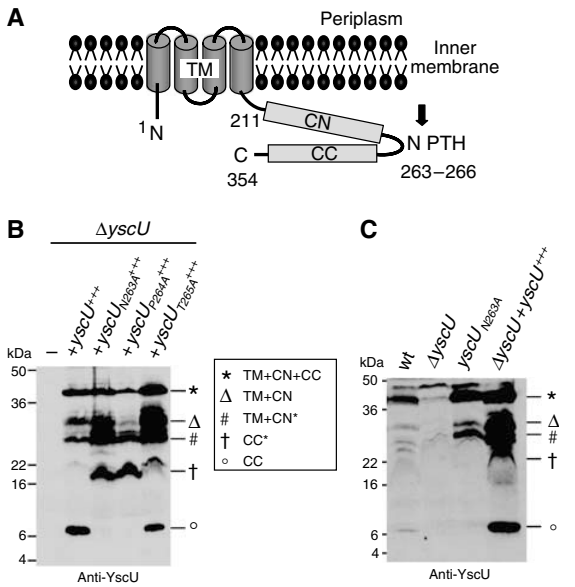

Figure 1 (**A**) Schematic representation of YscU based on studies by Allaoui *et al* (1994) and Lavander *et al* (2002). Letters indicate N-terminus (N), C-terminus (C), conserved NPTH motif (NPTH), transmembrane domain (TM, residues 1–210), N-terminal half of the cytoplasmic domain (CN, residues 211–263) and the C-terminal half of the cytoplasmic domain (CC, residues 264–354). Numbers indicate amino-acid positions in YscU from *Y. enterocolitica* W22703 (NCBI NC_002120). The black arrow represents the putative cleavage site at the NPTH motif. (**B**) Total membrane proteins of *Y. enterocolitica E40* Δ*yscU* mutant bacteria, complemented *in trans* with wt or mutated alleles under the arabinose inducible pBAD promoter, were purified after 4 h of induction of the *yop* regulon and analyzed by immunoblot with anti-YscU antibodies. The different forms of YscU are indicated as follows: YscU (star), $YscU_{TM+CN}$ (triangle), $YscU_{CC}$ (circle), $YscU_{TM+CN^*}$ (#) and $YscU_{CC^*}$ (cross). The latter two result from cleavage at the alternative site. (**C**) Total membrane proteins of the indicated *Y. enterocolitica* strains. Strains and plasmids used: wt (pYV40); Δ*yscU* (pLY4001); $yscU_{N263A}$, mutation inserted at the *yscU* locus (pISO4007); $yscU^{+++}$ (pLY7); $yscU_{N263A}{}^{+++}$ (pSTW7); $yscU_{P264A}{}^{+++}$ (pSTW8); $yscU_{T265A}{}^{+++}$ (pSTW9).

The FlhB homolog in the *Yersinia* injectisome is YscU, a 354-residue polypeptide with four transmembrane helices and a long cytoplasmic tail (Allaoui *et al*, 1994) (Figure 1A). Like FlhB, YscU undergoes autoproteolytic cleavage before P264, generating a 10-kDa C-terminal fragment (Lavander *et al*, 2002). $YscU_{N263A}$ is not cleaved at this site, but nevertheless retains the capacity to secrete Yops (Lavander *et al*, 2002).

The position of LcrV, at the tip of the needle, implies that LcrV is exported immediately after YscF but before the Yops. Thus, the hierarchy must consist of at least three categories of substrates and not two as in the flagellum; however, to date there are no genetic data to support this assumption. In this paper, we show that $YscU_{N263A}$ is impaired in the export of the translocators LcrV, YopB and YopD but not in the export of the effector Yops. Accordingly, cells with $YscU_{N263A}$ produce needles without tip complexes and this effect can be assigned to a lack of LcrV recognition. Thus, YscU is specifically involved in substrate recognition and has to be cleaved to acquire the conformation required for translocator recognition. This is the first genetic evidence that translocators represent an individual category of substrates in the hierarchy of export. Accordingly, the translocators, and not the Yop effectors, occupy the same rank as flagellin in the assembly of the flagellum.

Results

Mutation of residue N263 or P264 changes the autocleavage properties of YscU

To analyze the phenotype of a non-cleavable YscU mutant, we generated different point mutations in the NPTH motif of YscU and overexpressed the resulting $yscU_{N263A}$, $yscU_{P264A}$ and $yscU_{T265A}$ genes *in trans* in *Y. enterocolitica* Δ*yscU* mutant bacteria. The $yscU_{wt}$ gene and the mutated alleles were overexpressed from the pBAD promoter only at the end of the logarithmic growth phase when synthesis of the T3S system was induced by shifting to 37°C. In those conditions, we did not observe any clear toxicity of either the $YscU_{wt}$ or the mutated YscU, as reported by others (Lavander *et al*, 2002). This discrepancy presumably results from differences in the experimental conditions used in the two reports. It is indeed likely that early overexpression of an integral membrane protein is toxic.

We then analyzed YscU in membranes purified from the different *Y. enterocolitica* strains incubated in secretion permissive conditions by immunoblotting with anti-YscU antibodies (Figure 1B). In strains expressing *yscU* or $yscU_{T265A}$, an YscU fragment of about 10 kDa was clearly detectable. This could be assigned to the C-terminal part (CC) after cleavage at or around the NPTH motif. In contrast no 10-kDa fragment was present in bacteria expressing $yscU_{N263A}$ or $yscU_{P264A}$. Here, a protein fragment of about 16 kDa (indicated as CC*), probably resulting from cleavage at an alternative site, was observed, as already shown for an $yscU_{\Delta NPTH}$ mutant from *Y. pseudotuberculosis* (Lavander *et al*, 2002). This 16-kDa fragment was also present in lower amounts in membranes of strains expressing $yscU_{wt}$ or $yscU_{T265A}$. The 24-kDa N-terminal part (TM + CN*) remaining after cleavage at this alternative site was detected in all YscU expressing strains. The cleavage at or around the NPTH motif, which results in the C-terminal 10-kDa (CC) fragment described above, would leave a 30-kDa N-terminal fragment (TM + CN). This 30-kDa fragment was not only found in strains overexpressing $yscU_{wt}$ or $yscU_{T265A}$ that contained the small 10-kDa fragment, but also in samples from bacteria overexpressing $yscU_{N263A}$ or $yscU_{P264A}$, where we did not observe the 10-kDa fragment. Furthermore, uncleaved $YscU_{wt}$ (TM + CN + CC) could be detected in all bacterial samples expressing *yscU*, demonstrating that cleavage was never complete. The data presented in Figure 1 are representative of a number of highly reproducible experiments.

Up to now, due to detection problems the cleavage of YscU and its flagellar homolog FlhB has only been demonstrated after overexpression of the protein (above and Minamino and Macnab, 2000; Lavander *et al*, 2002). We also analyzed the cleavage of wild-type (wt) amounts of $YscU_{wt}$. As shown in Figure 1C, the 10-kDa (CC) and the 30-kDa (TM + CN) fragments of $YscU_{wt}$ could be detected in purified membranes. In addition, we observed cleavage at the alternative site, resulting in the 24-kDa (TM + CN*) and the 16-kDa (CC*) fragments, as shown for overproduced $YscU_{wt}$ (Figure 1B, lane 2 and Figure 1C, lane 4). We then analyzed

a mutant expressing $yscU_{N263A}$ from its native promoter on the virulence plasmid of *Y. enterocolitica*. In agreement with the data obtained after overproduction of $YscU_{N263A}$, a 30-kDa protein was present in the membranes from $yscU_{N263A}$ mutant bacteria, suggesting cleavage at or around the NPTH motif, but again no 10-kDa fragment co-purified. In addition, the 24-kDa signal corresponding to the N-terminal part after cleavage at the alternative site was present. Importantly, the uncleaved YscU protein was always detected at 40 kDa (TM + CN + CC), demonstrating that even when expressed at natural levels, YscU cleavage was not complete. These data thus confirm the data obtained with the over-expressed protein presented above. Together, they suggest that YscU is cleaved at least at two different sites. Although the 10-kDa fragment only co-purifies with the remaining N-terminal part in strains producing $YscU_{wt}$ or $YscU_{T265A}$, it does not formally rule out that the first cleavage occurs in $YscU_{N263A}$ or $YscU_{P264A}$, because the sequence alteration could prevent the binding of the cleaved 10-kDa fragment. In contrast, the C-terminal 16-kDa fragment produced by the cleavage at the alternative site co-purifies with its N-terminal half, even in strains producing $YscU_{N263A}$ or $YscU_{P264A}$. Although the data are not quantitative, they show that a preferred point of cleavage exists, which depends on the protein examined.

$yscU_{N263A}$ and $yscU_{P264A}$ mutants export effector Yops but no translocators

Next we tested whether export of Yop proteins was affected in the different *yscU* mutants. To do this, the *yop* regulon was induced in the different *Y. enterocolitica* strains and the culture supernatants were analyzed by SDS–PAGE and Coomassie staining. In agreement with previously reported data, no Yops were secreted by Δ*yscP* and Δ*yscU* mutant bacteria (Allaoui *et al*, 1994; Stainier *et al*, 2000), and the $yscU_{T265A}$ mutant showed the same pattern of exported proteins as the wt (Figure 2A). In contrast, the $yscU_{N263A}$ and $yscU_{P264A}$ mutant bacteria did not export translocators (Figure 2A). The defect in translocator export was not due to overexpression of $yscU_{N263A}$, since expression of $yscU_{N263A}$ from its native promoter had the same effect (Figure 2A). Analysis of YopE and LcrV in culture supernatants by immunoblotting confirmed this result (Figure 2B). The intrabacterial levels of YopE and LcrV were comparable in wt and $yscU_{N263A}$ mutant bacteria. Whereas the export of YopE in $yscU_{N263A}$ mutant bacteria was only slightly decreased compared to the wt, no exported LcrV could be detected (Figure 2B). To check whether overexpression of *lcrV* in an $yscU_{N263A}$ mutant background could overcome the lack of export, as previously shown for export compromised *yscP* mutants (Agrain *et al*, 2005b), *lcrV* was overexpressed from the pBAD promoter by adding varying concentrations of L-arabinose (Figure 2C). Only on maximal *lcrV* overexpression with 0.5% L-arabinose a faint LcrV band could be observed in the supernatant fraction of $yscU_{N263A}$ mutant bacteria (Figure 2C). Overexpression of *lcrV* in wt *Yersinia* did not change the export level, possibly because the export capacity of the wt was already saturated.

The $yscU_{N263A}$ mutant does not assemble a tip complex and fails to induce lysis in red blood cells

The fact that the $yscU_{N263A}$ mutant did not export the translocators LcrV, YopB and YopD suggests that this mutant may not be able to form the translocation pore. Formation of the translocation pore can be studied by infection of red blood cells (RBCs), which undergo hemolysis (Hakansson *et al*, 1996). Since *Y. enterocolitica* bacteria do not adhere to RBCs, a Δ*yopN* mutant that secretes Yops in a contact-independent manner has been used previously (Marenne *et al*, 2003).

Therefore, a Δ$yopNyscU_{N263A}$ mutant was generated. As expected from the Δ*yopN* deletion, secretion of Yops by the Δ$yopNyscU_{N263A}$ mutant was independent of the presence of calcium, whereas secretion of Yops by the $yscU_{N263A}$ mutant and wt bacteria was calcium dependent (data not shown). The pattern of proteins secreted by the Δ$yopNyscU_{N263A}$ mutant was identical to that of proteins secreted by the $yscU_{N263A}$ mutant, except that YopN was missing (Figure 3B). We analyzed the capacity of the Δ$yopNyscU_{N263A}$ mutant to

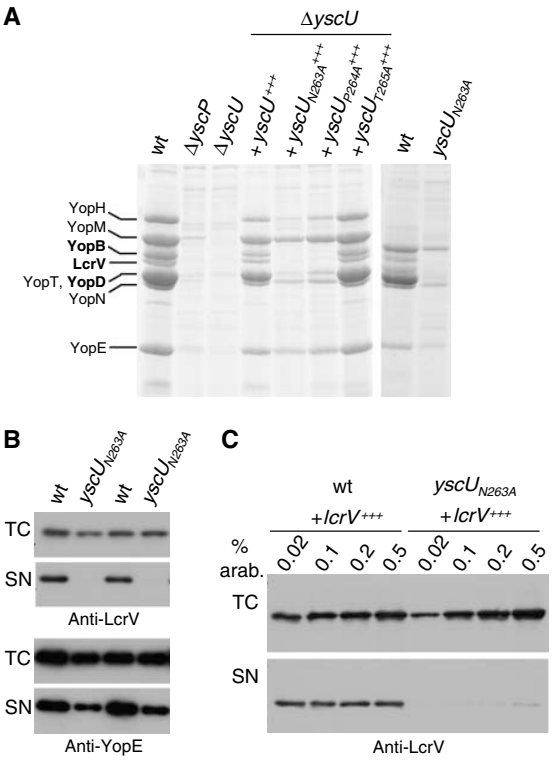

Figure 2 Analysis of the Yop proteins secreted by different *yscU* mutants. (**A**) Coomassie-stained 12% SDS–PAGE of Yops secreted by wt, Δ*yscP*, Δ*yscU* mutant bacteria, Δ*yscU* mutant bacteria over-expressing mutated *yscU* alleles *in trans* from the pBAD promoter, or bacteria carrying the $yscU_{N263A}$ allele at the *yscU* locus (natural *yscU* promoter). (**B**) Expression and export of LcrV and YopE in *Y. enterocolitica* E40 wt and $yscU_{N263A}$ mutant bacteria. Total cell (TC) and supernatant fractions (SN) were analyzed by immunoblotting using anti-LcrV or anti-YopE antibodies. Shown are samples from two independent experiments. (**C**) Expression and export of LcrV after overexpression of *lcrV in trans* from the pBAD promoter in *Y. enterocolitica* wt and $yscU_{N263A}$ mutant bacteria. L-arabinose concentrations ranging from 0.02 to 0.5% were used to induce LcrV synthesis when bacteria were shifted to 37°C and again 2 h later. TC and SN were analyzed by immunoblotting using anti-LcrV antibodies. Strains and plasmids used: wt (pYV40); Δ*yscP* (pLJ4036); Δ*yscU* (pLY4001); $yscU^{+++}$ (pLY7); $yscU_{N263A}^{+++}$ (pSTW7); $yscU_{P264A}^{+++}$ (pSTW8); $yscU_{T265A}^{+++}$ (pSTW9); $yscU_{N263A}$ (pISO4007); $lcrV^{+++}$ (pPB42).

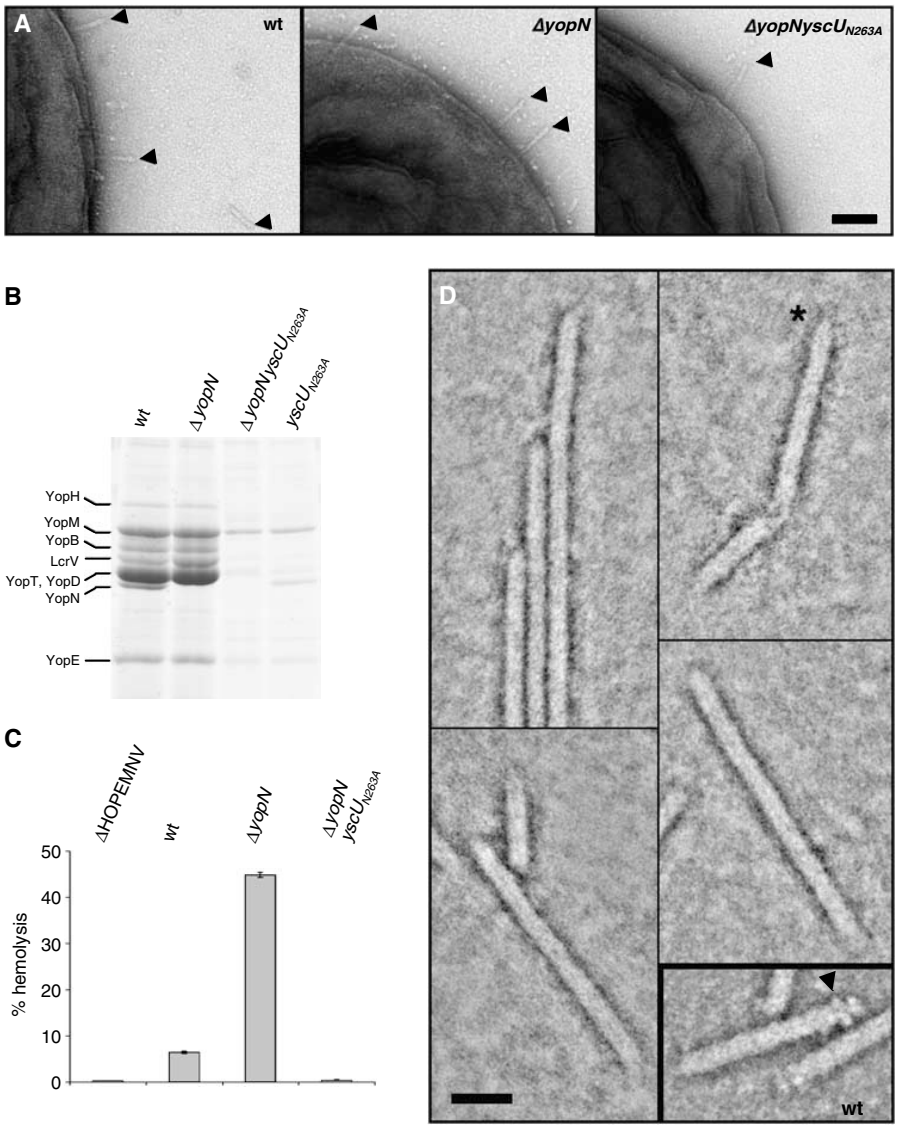

Figure 3 The *yscU$_{N263A}$* mutant does not induce hemolysis in RBC due to a missing tip complex. (**A**) Transmission electron micrographs of *Y. enterocolitica* E40 WT, Δ*yopN* and Δ*yopNyscU$_{N263A}$* bacteria negatively stained with 2% uranyl acetate. Scale bar, 100 nm. Needles are indicated by arrowheads. (**B**) Yops secreted by *Y. enterocolitica* wt, Δ*yopN, yscU*$_{N263A}$ and Δ*yopNyscU$_{N263A}$* bacteria. Coomassie-stained 12% SDS–PAGE. The position of YopN is indicated on the left. (**C**) Percentage lysis of RBCs after 1 h of contact with the indicated *Y. enterocolitica* strains. (**D**) STEM dark-field image of *Y. enterocolitica yscU$_{N263A}$* needles. Protein is displayed in bright shades. Inset: wt needles similarly imaged. The *yscU$_{N263A}$* mutant needles had rather pointed ends (asterisk); the tip complexes so characteristic of wt needles (arrowhead) were not detected. Scale bar, 20 nm. Strains: wt (pYV40); Δ*yopN* (pIM41); Δ*yopNyscU$_{N263A}$* (pISO4010); *yscU$_{N263A}$* (pISO4007); ΔHOPEMNV (pMN4002).

induce lysis in RBCs. In agreement with the loss of translocator export, lytic activity was neither observed for the Δ*yopNyscU$_{N263A}$* mutant nor for the negative control ΔHOPEMNV mutant lacking LcrV (Figure 3C). Like for wt, and Δ*yopN* mutant bacteria, needles could be observed on the surface of Δ*yopNyscU$_{N263A}$* mutant bacteria (Figure 3A). The needles from *yscU$_{N263A}$* mutant bacteria were purified and analyzed by scanning transmission electron microscopy (STEM) (Figure 3D). Out of 51 needles analyzed, none had a tip and 16 had a clear pointed end (Figure 3D), as previously reported for the *lcrV* mutant (Mueller *et al*, 2005). These data confirm the defect in the export of LcrV.

The impaired export of LcrV is due to a lack of recognition by the YscU$_{N263A}$ protein

There might be at least two reasons why LcrV is not exported in the *yscU$_{N263A}$* mutant; either LcrV is not recognized by the YscU$_{N263A}$ protein or the YscU$_{N263A}$ protein has an altered conformation, which blocks the export channel for some substrates. To investigate if the channel is still permissive for LcrV, we fused the export signal of the effector YopE to the N-terminus of LcrV and analyzed the export of the hybrid protein in the *yscU$_{N263A}$* mutant. As shown in Figure 4A, a protein of the expected size was detected by Coomassie-stained SDS–PAGE of the supernatant fraction. The identity

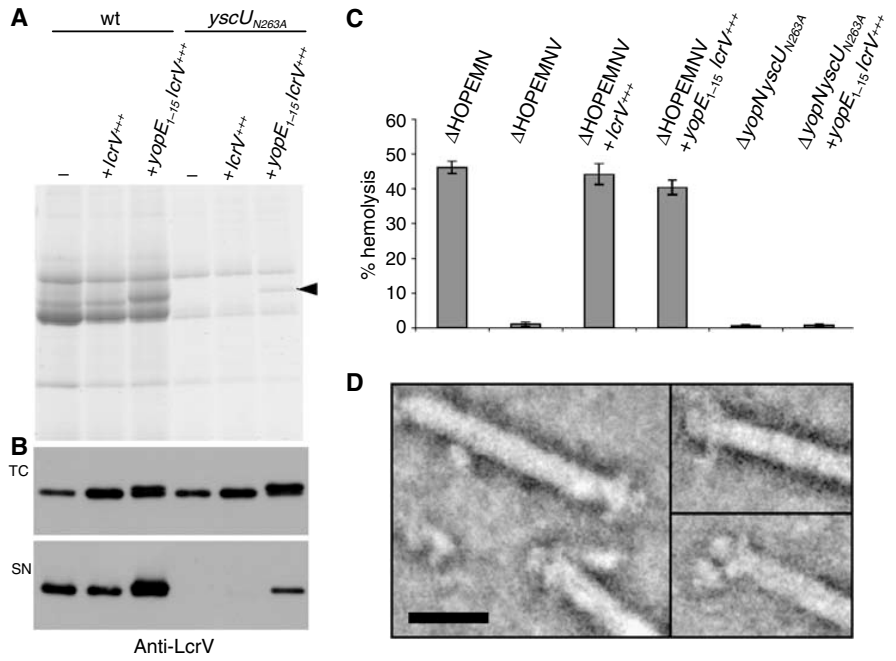

Figure 4 $YopE_{1-15}LcrV$ is exported by *Y. enterocolitica* $yscU_{N263A}$ mutant bacteria and forms a tip complex. (**A**) Yops secreted by *Y. enterocolitica* E40 wt (pYV40) and *Y. enterocolitica* E40 $yscU_{N263A}$ (pISO4007) mutant bacteria overexpressing *lcrV* (pPB42) or $yopE_{1-15}lcrV$ (pISOA132) *in trans* from the pBAD promoter. The position of the $YopE_{1-15}LcrV$ protein is indicated by the arrowhead. (**B**) Total cell (TC) and supernatant fractions (SN) of the same cultures as in (A) were analyzed by immunoblot with anti-LcrV antibodies. (**C**) Lysis of RBCs after 1 h of contact with the indicated *Y. enterocolitica* E40 strains. (**D**) STEM images of needles isolated from *Yersinia* $yscU_{N263A}$ expressing $YopE_{1-15}LcrV$ from the pBAD promoter. Protein is displayed in bright shades. Scale bar, 20 nm. Strains and plasmids: wt (pYV40); $yscU_{N263A}$ (pISO4007); ΔHOPEMN (pIM417); ΔHOPEMNV (pMN4002); Δ$yopNyscU_{N263A}$ (pISO4010); $lcrV^{+++}$ (pPB42); $yopE_{1-15}lcrV^{+++}$ (pISOA132).

of the protein was confirmed by immunoblot using anti-LcrV antibodies (Figure 4B). In contrast to the YopE-hybrid protein, LcrV alone was not exported in the $yscU_{N263A}$ mutant. These data suggest that the loss of LcrV export in the $yscU_{N263A}$ mutant is not due to changes of the channel properties, but rather due to a defect in recognition of LcrV as export substrate. We then wondered whether the $YopE_{1-15}LcrV$ hybrid protein would be functional in the $yscU_{N263A}$ mutant, that is, whether this protein would be able to form a functional tip complex. We first investigated the functionality of the hybrid protein in an *lcrV* mutant (here ΔHOPEMNV), by testing its ability to induce lysis of RBCs. The multi-effector mutant ΔHOPEMN was used as positive control and induced 46% hemolysis, whereas the *lcrV* mutant ΔHOPEMNV only led to 1% hemolysis (Figure 4C). Overexpression of either *lcrV* or $yopE_{1-15}lcrV$ in *lcrV* mutant bacteria could restore hemolysis up to wt level, indicating that the hybrid protein was functional (Figure 4C). As expected, expression of $yopE_{1-15}lcrV$ in the Δ$yopNyscU_{N263A}$ mutant could not restore the lytic activity, because not only LcrV but also the two other translocators YopB and YopD were not exported by this mutant (Figure 4C). When purified needles of an $yscU_{N263A}$ mutant expressing $yopE_{1-15}lcrV$ were analyzed using STEM, tip complexes were detected on 43 out of 76 analyzed needles (Figure 4D). This shows that LcrV export by $yscU_{N263A}$ mutant bacteria could be restored by using the export signal of YopE. Furthermore, the $yopE_{1-15}lcrV$ fusion resulted in a functional protein that was able to form a tip complex. From these data we cannot say that not all the needles have a tip, because we can never exclude that some needles analyzed broke during purification.

Needles of Yersinia $yscU_{N263A}$ and $yscU_{P264A}$ mutants are longer and less regulated

Next, we were interested in whether the different *yscU* mutations described above would affect the length of the injectisome needle. Therefore, needles from *Y. enterocolitica* Δ*yscU* bacteria overexpressing *yscU*, $yscU_{N263A}$, $yscU_{P264A}$ or $yscU_{T265A}$ were measured. Needles of $yscU_{T265A}$ mutant bacteria had wt length ($yscU_{wt}$: median 61 ± 15 nm; $yscU_{T265A}$: median 63 ± 15 nm), whereas needles from bacteria overexpressing $yscU_{N263A}$ or $yscU_{P264A}$ were longer and less controlled than the wt ($yscU_{N263A}$: median 107 ± 51 nm; $yscU_{P264A}$: median 119 ± 53 nm) (Supplementary Figure S1). These data reflect the differences that we reported above for the cleavage of YscU and the export of the translocators.

Needle length in a $yscU_{N263A}$ mutant is still controlled by YscP

To analyze whether YscP still exerts its ruler function in a $yscU_{N263A}$ mutant, we combined *yscP* alleles of different sizes with the $yscU_{N263A}$ allele. As shown before (Journet *et al*, 2003; Mota *et al*, 2005), $yscU_{wt}$ bacteria producing the 388-amino acid ruler $YscP_{388}$ made shorter needles (49 ± 7 nm), whereas bacteria producing the 680-amino acid ruler $yscP_{680}$ made longer needles (149 ± 45 nm) than $yscU_{wt}$ bacteria endowed with the wt ruler $yscP_{515}$ (67 ± 11 nm) (Figure 5A, histograms I–III).

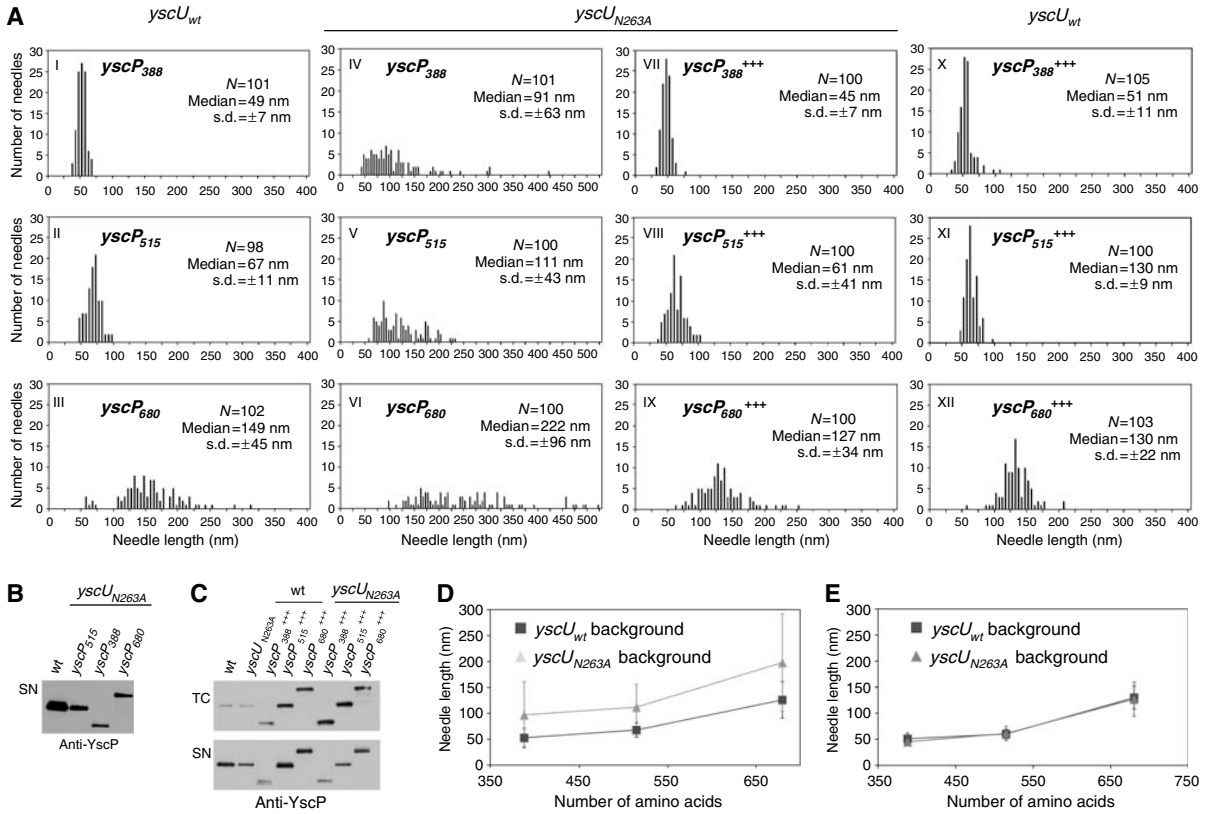

Figure 5 (**A**) Histograms showing the length of needles from *Y. enterocolitica* E40 $yscU_{wt}$ and E40 $yscU_{N263A}$ mutant bacteria expressing three different YscP proteins either from their native promoter (histograms I–VI) or additionally *in trans* from the pBAD promoter (histograms VII–XII). Overexpression of *yscP in trans* from the pBAD promoter was induced with 0.1% L-arabinose. N, number of needles measured; s.d., standard deviation. (**B**) The supernatant (SN) of culture of *Y. enterocolitica* E40 strains expressing the three indicated *yscP* alleles from their native promoter in an $yscU_{N263A}$ mutant background were analyzed by immunoblot with anti-YscP antibodies. (**C**) Total cell (TC) and supernatant fractions (SN) of *Y. enterocolitica* $yscU_{wt}$ and $yscU_{N263A}$ mutant bacteria expressing the indicated *yscP* alleles from their native promoter and additionally *in trans* from the pBAD promoter. Overexpression of *yscP* alleles from the pBAD promoter was induced with 0.1% L-arabinose. Samples were analyzed by immunoblotting using anti-YscP antibodies. (**D**) Plot of the needle length versus the number of residues in YscP for *Y. enterocolitica* strains expressing different *yscP* alleles from their native promoter in either $yscU_{wt}$ or $yscU_{N263A}$ mutant bacteria. The medians and s.d.s of histograms I–VI that are given in (A) are shown. (**E**) Plot of the needle length versus the number of residues in YscP for *Y. enterocolitica* $yscU_{wt}$ and $yscU_{N263A}$ mutant bacteria expressing indicated *yscP* alleles from their native promoter and additionally *in trans* from the pBAD promoter, which was induced with 0.1% L-arabinose. The medians and s.d.s of histograms VII–XII that are given in (A) are shown. Strains and plasmids used: wt (pYV40); $yscP_{388}$ (pLJ4022); $yscP_{515}$ (pYV40); $yscP_{680}$ (pLJM4001); $yscU_{N263A}yscP_{388}$ (pISO4011); $yscU_{N263A}yscP_{515}$ (pISO4007); $yscU_{N263A}yscP_{680}$ (pISO4012); $yscU_{N263A}$ and $yscP_{388}^{+++}$ (pISO4011 + pCA20); $yscU_{N263A}$ and $yscP_{515}^{+++}$ (pISO4007 + pLJ6); $yscU_{N263A}$ and $yscP_{680}^{+++}$ (pISO4012 + pLJ19); $yscU_{wt}$ and $yscP_{388}^{+++}$ (pLJ4022 + pCA20); $yscU_{wt}$ and $yscP_{515}^{+++}$ (pYV40 + pLJ6); $yscU_{wt}$ and $yscP_{680}^{+++}$ (pLJM4001 + pLJ19).

$yscU_{N263A}$ mutant bacteria producing the different YscP proteins made longer needles than $yscU_{wt}$ bacteria. Length still correlated with the number of residues of YscP, but the control was not as tight, as shown by the larger standard deviations ($yscU_{N263A}yscP_{388}$: 91 nm ± 63 nm; $yscU_{N263A}yscP_{515}$: 111 ± 43 nm; $yscU_{N263}$ $yscP_{680}$: 222 ± 96 nm) (Figure 5A, histograms IV–VI). By plotting the medians of needle length against the number of amino acids in YscP, we obtained parallel slopes for the $yscU_{wt}$ and the $yscU_{N263A}$ mutant (Figure 5D). In addition to these changes in needle length, $yscU_{N263A}$ mutant bacteria exported less YscP than wt bacteria (Figure 5B and C). The increase in needle length as well as the decrease in length control could be due to this decrease in YscP export, as shown previously (Agrain *et al*, 2005b). We therefore tested whether an increase in YscP production would compensate the defects in length control. Therefore, $yscP_{388}$, $yscP_{515}$ and $yscP_{680}$ were overexpressed from the pBAD promoter in $yscU_{N263A}$ mutant bacteria harboring the corresponding *yscP* allele on the virulence plasmid. Overproduction of the different YscP proteins increased their export to wt level, as shown by immunoblot analysis of the total cell and supernatant fractions using anti-YscP antibodies (Figure 5C). Increased production of $YscP_{388}$, $YscP_{515}$ and $YscP_{680}$ in $yscU_{N263A}$ mutant bacteria (Figure 5A, histograms VII–IX) led to needles that were comparable to those of the corresponding $yscU_{wt}$ strains (Figure 5A, histograms X–XII). Although $yscU_{N263A}$ mutant bacteria overexpressing *yscP* had needles of the expected length (Figure 5A, histogram VIII), they still did not export translocators (Supplementary Figure S2).

The plot in Figure 5E shows that overexpression of YscP can indeed restore needle length control in the $yscU_{N263A}$

mutant to wt level. This showed that the defect in needle length control of the $yscU_{N263A}$ mutant was rather due to a failure in YscP export than to a failure of the substrate specificity switch.

Discussion

The fact that the injectisome exports its own distal components, before it exports the effectors, implies that the T3S apparatus can recognize and sequentially export different categories of substrates. To achieve this, it is believed to switch its substrate specificity when assembly is completed.

To better understand this sequential export process, we introduced mutations into the NPTH cleavage site of YscU and analyzed the phenotypes. At variance with previous reports on FlhB (Minamino and Macnab, 2000) and YscU (Lavander *et al*, 2002), we not only analyzed the phenotype after overexpression of cloned *yscU* alleles, but also after replacement of the *yscU* alleles on the pYV plasmid, ensuring physiological expression levels. To detect minute protein quantities, we probed the proteins with an anti-YscU antiserum rather than an antibody directed against the C-terminus or a C-terminal His-tag. Our results confirmed that the 40-kDa YscU is naturally cleaved into a TM + CN 30-kDa fragment and a 10-kDa CC fragment, as shown previously for FlhB (Minamino and Macnab, 2000) and for YscU from *Y. pseudotuberculosis* (Lavander *et al*, 2002). In good agreement with the estimated stoichiometry of two FlhB molecules per flagellum (Zhu *et al*, 2002), unless overexpressed, the CC product from YscU could only be detected after enrichment by purification of the membrane fraction from *Y. enterocolitica*. Surprisingly, the cleavage of YscU was never complete, even at physiological expression levels, although bacteria were harvested at a stage where all the needles analyzed had their normal length and tip complex. No CC fragment was detected for the mutant proteins $YscU_{N269A}$ and $YscU_{P264A}$, as shown before by Lavander *et al* (2003) using C-terminal tagged YscU. As pointed out by these authors, this suggests that cleavage did not occur. However, since a band corresponding to the size of the TM + CN fragment was still observed, we cannot formally rule out that cleavage was prevented. We observed an alternative cleavage site in the $YscU_{N269A}$ and $YscU_{P264A}$ mutant proteins, yielding a *ca* 24-kDa (TM + CN*) and a *ca* 16-kDa (CC*) fragment. This alternative cleavage of YscU is reminiscent of the alternative cleavage observed in $FlhB_{N269A}$ and $FlhB_{P270A}$, but was not reported for YscU from *Y. pseudotuberculosis*. Surprisingly, we detected the TM + CN* fragment in extracts from bacteria producing $YscU_{wt}$, suggesting that even $YscU_{wt}$ could be partially cleaved at this alternative cleavage site.

The $yscU_{N263A}$ mutant bacteria assembled injectisome needles, but their length seemed to be poorly controlled and the median length was 111 nm rather than the 67 nm found for wt bacteria. When this $yscU_{N263A}$ allele was combined with a longer (680 codons) and a shorter (388 codons) allele of *yscP*, the median needle lengths were 222 nm and 91 nm, respectively, indicating that needle length was still dependent on the length of the YscP ruler, although the standard deviation was much larger. In addition to this loose length control, the $yscU_{N263A}$ bacteria released less YscP into the culture supernatant than wt bacteria do, although the intra-bacterial amount of protein was unchanged. We tried to overcome the poor export efficiency of YscP by overexpressing the gene downstream from the pBAD promoter. As expected from the previous work of Agrain *et al* (2005b), overexpression of the three different *yscP* alleles indeed led to the export of more YscP proteins, and also to a better control of needle length. The latter was in fact as good as in $yscU_{wt}$ bacteria. Hence, we conclude that the $yscU_{N263A}$ mutation reduces the efficacy of the T3S system to export YscP, which, indirectly, leads to a less stringent control of needle length. We also conclude that the $yscU_{N263A}$ mutation does not affect the capacity of the T3S export apparatus to switch off the export of the YscF needle subunits when the needle reaches its genetically defined length.

These data demonstrate that the cleavage at the NPTH motif is not required to switch off needle subunit export. Even more, they confirm that the same variants of YscU and YscP can give rise to two different needle lengths, depending on the amount of YscP exported. To us, this rules out the hypothesis that YscU could play a role as a timer to determine needle length, as was proposed for the flagellar hook length control (Moriya *et al*, 2006).

$yscU_{N263A}$ mutant bacteria also released slightly less effector Yops than wt bacteria, but the export of effectors was still significant. This observation shows that the export machine is still capable of switching on the export of Yops. Hence, the $yscU_{N263A}$ mutation does not affect the substrate specificity switching from early (YscF, YscP) to late (Yops) substrates. This interpretation agrees with the observations reported by Lavander *et al* (2002) that mutation $yscU_{N263A}$ does not affect Yop secretion in *Y. pseudotuberculosis*. However, it may seem at odds with the observation that mutation $flhB_{N269A}$ prevents export of flagellin, and with the interpretation that it inhibits the substrate specificity switch.

The most intriguing phenotype of the $yscU_{N263A}$ mutation was the deficiency in export of the translocators LcrV, YopB and YopD. In good agreement with the fact that LcrV was not exported, needles produced by the mutant bacteria had no tip complex.

A deficiency in translocator export is not completely unprecedented. The *invE* mutant of *Salmonella enterica* showed reduced secretion of the translocators SipB, SipC and SipD, while the export of other T3S effectors was increased (Kubori and Galan, 2002). Beside these observations and the fact that InvE is not required for the assembly of the needle complex, nothing is known about the actual function of InvE and its putative homologs. Mutants *sepL* and *sepD*, mutants of enteropathogenic and enterohemorrhagic *Escherichia coli*, as well as of *Citrobacter rodentium*, have a similar phenotype; translocator secretion is completely abolished, while the export of effector proteins is increased (Deng *et al*, 2005). It was suggested that SepL and SepD are not only necessary for efficient translocator secretion but also control a switch from translocator to effector secretion by sensing certain environmental signals such as low calcium (Deng *et al*, 2005). A *yscW* (called earlier *virG*) mutant of *Y. enterocolitica* also shows a decrease in the amounts of secreted proteins, especially of the translocators YopB, YopD and LcrV (Allaoui *et al*, 1995). YscW is the pilot protein of the secretin YscC (Burghout *et al*, 2004) and hence its absence probably modifies the channel properties.

Here, the failure to export LcrV and to assemble the needle tip could be circumvented by the N-terminal addition of the

YopE export signal to LcrV. This indicates that the failure to export LcrV was not due to a change in the channel conformation, making it unsuitable for protein export, but rather to a failure in substrate recognition. This implies that the translocators have a specific type of export signal and a status distinct from the effectors regarding export. This makes sense, since they need to be exported before the effectors (Cornelis and Wolf-Watz, 1997). We already know that LcrV is exported before the Yops, since it forms the tip complex, even in the absence of Yop secretion (Mueller *et al*, 2005). However, no mutation specifically affecting export of the effectors has been described before. Surprisingly, while considerable effort was made to unravel the export signal of YopE (Michiels and Cornelis, 1991; Sory *et al*, 1995; Anderson and Schneewind, 1997), YopH (Michiels and Cornelis, 1991; Sory *et al*, 1995), YopN (Anderson and Schneewind, 1997) and YopQ (Michiels and Cornelis, 1991; Anderson and Schneewind, 1999) in *Yersinia*, little has been done to decipher the signal of translocators. It is known that LcrV can be exported even with an N-terminal His-tag, and that both the N- and C-termini of LcrV are required for its export (Fields *et al*, 1999). This can be taken as a hint that the signals are different for effectors and translocators, although more work is needed to characterize the export signals of the translocators and hence to understand the hierarchy of assembly. The export signal of YscP, an early substrate, was recently characterized and turned out to be totally different from the known export signal of effectors (Agrain *et al*, 2005b).

As mentioned above, the phenotype of the $yscU_{N263A}$ mutation may appear, at first sight, to be different from the phenotype of the $flhB_{N269A}$ mutation, in the sense that $YscU_{N263A}$ allows Yop (late substrate) export, while $FlhB_{N269A}$ does not allow flagellin export. However, the two observations can easily be reconciled, given the additional observation that $YscU_{N263A}$ prevents export of the translocators. Keeping in mind that there are two hierarchy classes in the assembly of the flagellum (hook/rod and filament) and three hierarchy classes in the operation of the injectisome (needle, translocators, effectors), both mutants are simply deficient in the export of the second hierarchy class.

Finally, our results confirm that YscU, and especially the structure of the CC fragment, plays a critical role in substrate recognition. They also show that the translocators are specifically recognized by YscU and thus, the injectisome has at least three classes of substrates. However, they do not provide any evidence that cleavage of the CC fragment is involved in the substrate specificity switch.

Materials and methods

Bacterial strains, plasmids and genetic constructions are listed in Supplementary Table 1.

Alleles to be inserted in the pYV plasmids were subcloned into the pKNG101 suicide vector and the allelic exchange was selected by plating diploid bacteria on sucrose (Kaniga *et al*, 1991).

E. coli Top10 was used for plasmid purification and cloning. *E. coli* BL21 Rosetta was used for protein expression. Bacteria were routinely grown on Luria–Bertani agar plates and in liquid Luria–Bertani medium. Ampicillin was used at a concentration of 200 μg/ml to select for expression vectors.

Plasmids were generated using either *Pfu* turbo polymerase (Stratagene) or Vent DNA polymerase (New England Biolabs). The oligonucleotides used for genetic constructions are listed in Supplementary Table 2. All constructs were confirmed by sequencing using a 3100-Avant genetic analyzer (ABI Prism).

Yop secretion

Induction of the *yop* regulon was described by Cornelis *et al* (1987). Expression of the different genes cloned downstream from the pBAD promoter was routinely induced by adding 0.2% L-arabinose to the culture just before the shift to 37°C, and again 2 h later. The carbon source was glycerol (4 mg/ml) when expressing genes from the pBAD promoter, and glucose (4 mg/ml) in the other case. Total cell and supernatant fractions were separated by centrifugation at 20 800 *g* for 10 min at 4°C. The cell pellet was taken as total cell fraction. Proteins in the supernatant were precipitated with trichloroacetic acid 10% (w/v) final for 1 h at 4°C.

Secreted proteins were analyzed by Coomassie-stained 12% SDS–PAGE; in each case, proteins secreted by 3×10^8 bacteria were loaded per lane. For detection of YscP in total cells, 1.6×10^8 bacteria were loaded per lane. For YscP detection in supernatants, the supernatants from 2.5×10^7 bacteria were loaded per lane. For analysis of LcrV and YopE, 2.5×10^7 bacteria and the supernatants from 2×10^7 bacteria were loaded per lane on a 12% SDS–PAGE. Immunoblotting was carried out using rabbit polyclonal antibodies against LcrV (MIPA220; 1:2000) and YscP (MIPA57; 1:3000), or rat polyclonal antibodies against YopE (MIPA94; 1:10000). Detection was performed with the respective secondary antibodies conjugated to horseradish peroxidase (1:5000; Dako), before development with supersignal chemiluminescent substrate (Pierce).

Electron microscopy

Needles at the cell surface of bacteria were visualized by transmission electron microscopy, as described by Hoiczyk and Blobel (2001) and Agrain *et al* (2005b). After 4 h of induction of the *yop* regulon at 37°C, bacteria were harvested at 2000 *g* and resuspended gently in 20 mM Tris–HCl, pH 7.5. Droplets were applied for 1 min to freshly glow-discharged, formvar-carbon-coated grids, and negatively stained with 2% (w/v) uranyl acetate. Bacteria were visualized in a Philips CM100 electron microscope at a nominal magnification of × 20 000 and an acceleration voltage of 80 kV. Sizes were measured with the 'Soft imaging system' software (Hamburg, Germany).

Needle purification

Needles were purified from *Y. enterocolitica* cultures incubated under secretion permissive conditions. Bacteria from 300 ml culture were harvested by centrifugation (10 min at 5700 *g*) and washed once with 20 mM Tris–HCl, pH 7.5 (1/30 of initial culture volume). The washing supernatant was passed through a 0.45 μm mesh filter (cellulose acetate membrane) and then centrifuged for 30 min at 20 000 *g*. The resulting pellet was resuspended in 20 mM Tris–HCl, pH 7.5 (1/3000 of initial culture volume) and analyzed by electron microscopy (Mueller *et al*, 2005).

STEM

The purified needles were diluted with buffer (20 mM Tris–HCl, pH 7.5), as required, adsorbed to thin carbon film, washed with four droplets of quartz double-distilled water and stained with 2% (w/v) sodium phosphotungstate. Digital dark-field images were generated using a Vacuum Generators HB5 STEM interfaced to a modular computer system (Tietz Video and Image Processing Systems GmbH, D-8035 Gauting). The microscope was operated at 100 kV and a nominal magnification of × 500 000, using doses that ranged between 4400 and 13 500 electrons/nm^2.

Hemolysis

Hemolytic assays were carried out as described by Goure *et al* (2005).

Purification of total membrane proteins

To purify total cell membranes, *Yersinia* bacteria were cultivated in secretion permissive conditions (BHI-Ox), as described before. Bacteria from 200 ml culture were harvested by centrifugation (20 min/5000 *g*/4°C) and washed once with phosphate-buffered saline (PBS). After resuspending the cells in 5 ml buffer I (50 mM Hepes pH 7.6, 500 mM potassium acetate, 5 mM magnesium acetate) containing the protease inhibitor cocktail complete Mini (Roche), 0.7 mg/ml lysozyme was added, followed by a 30-min incubation at 4°C. Then cells were lysed by sonication on ice. After removal of unbroken cells by low-speed centrifugation (30 min/6000 *g*/4°C), the supernatant was passed through a 0.45 μm mesh filter (cellulose acetate membrane) and centrifuged at high speed

(2 h/150 000 *g*/4°C). The pellet containing the total cell membranes was resuspended in 400 µl buffer I. Lipids were extracted with 400 µl *n*-hexan for 30 min/4°C on a rotating wheel. After isolation of the lower hydrophilic phase, proteins were precipitated by addition of four volumes acetone (1 h/4°C), centrifuged (10 min/20−800 *g*/4°C) and resuspended in 160 µl buffer II (7 M urea, 2 M thiourea, 2% CHAPS), and supplemented with 40 µl 5 × SDS loading buffer (5 × SDS loading buffer: 225 mM Tris–HCl, pH 6.8, 5% SDS, 50% glycerol, 50 mM DTT, bromophenol blue). Samples were separated on a 15% SDS–PAGE, transferred onto nitrocellulose membrane and analyzed by immunoblotting with anti-YscU antibodies.

YscU antibodies

To produce polyclonal anti-YscU antibodies (MIPA 221), $YscU_{211-354}$ was expressed from the pBAD promoter with a C-terminal His-tag, using plasmid pLY1. A soluble His-protein was produced in *E. coli* Top10 and purified on chelating sepharose beads (Amersham Biosciences). A rabbit was immunized by four injections with a total of 1 mg of $YscU_{211-354}$ (CER, Marloie, Belgium). For immunoblot analysis, anti-YscU antibodies were used at a dilution of 1:1000.

Supplementary data

Supplementary data are available at *The EMBO Journal* Online (http://www.embojournal.org).

Acknowledgements

We thank Laure Journet for plasmid pLJ14, Gianni Morson for assistance with the TEM and Philippe Ringler for the STEM microscopy. This work was supported by the Swiss National Science Foundation (grant 32-65393.01 to GC and grant 3100A-108299 to AE) and the Maurice E Müller Foundation of Switzerland).

References

Agrain C, Callebaut I, Journet L, Sorg I, Paroz C, Mota LJ, Cornelis GR (2005a) Characterization of a type III secretion substrate specificity switch (T3S4) domain in YscP from *Yersinia enterocolitica*. *Mol Microbiol* **56:** 54–67

Agrain C, Sorg I, Paroz C, Cornelis GR (2005b) Secretion of YscP from *Yersinia enterocolitica* is essential to control the length of the injectisome needle but not to change the type III secretion substrate specificity. *Mol Microbiol* **57:** 1415–1427

Allaoui A, Scheen R, Lambert de Rouvroit C, Cornelis GR (1995) VirG, a *Yersinia enterocolitica* lipoprotein involved in Ca^{2+} dependency, is related to exsB of *Pseudomonas aeruginosa*. *J Bacteriol* **177:** 4230–4237

Allaoui A, Woestyn S, Sluiters C, Cornelis GR (1994) YscU, a *Yersinia enterocolitica* inner membrane protein involved in Yop secretion. *J Bacteriol* **176:** 4534–4542

Anderson DM, Schneewind O (1997) A mRNA signal for the type III secretion of Yop proteins by *Yersinia enterocolitica*. *Science* **278:** 1140–1143

Anderson DM, Schneewind O (1999) *Yersinia enterocolitica* type III secretion: an mRNA signal that couples translation and secretion of YopQ. *Mol Microbiol* **31:** 1139–1148

Blocker A, Gounon P, Larquet E, Niebuhr K, Cabiaux V, Parsot C, Sansonetti P (1999) The tripartite type III secreton of *Shigella flexneri* inserts IpaB and IpaC into host membranes. *J Cell Biol* **147:** 683–693

Blocker A, Jouihri N, Larquet E, Gounon P, Ebel F, Parsot C, Sansonetti P, Allaoui A (2001) Structure and composition of the *Shigella flexneri* 'needle complex', a part of its type III secreton. *Mol Microbiol* **39:** 652–663

Burghout P, Beckers F, de Wit E, van Boxtel R, Cornelis GR, Tommassen J, Koster M (2004) Role of the pilot protein YscW in the biogenesis of the YscC secretin in *Yersinia enterocolitica*. *J Bacteriol* **186:** 5366–5375

Cornelis G, Vanootegem JC, Sluiters C (1987) Transcription of the yop regulon from *Y. enterocolitica* requires trans acting pYV and chromosomal genes. *Microb Pathog* **2:** 367–379

Cornelis GR (2006) The type III secretion injectisome. *Nat Rev Microbiol* **4:** 811–825

Cornelis GR, Wolf-Watz H (1997) The *Yersinia* Yop virulon: a bacterial system for subverting eukaryotic cells. *Mol Microbiol* **23:** 861–867

Crepin VF, Shaw R, Abe CM, Knutton S, Frankel G (2005) Polarity of enteropathogenic *Escherichia coli* EspA filament assembly and protein secretion. *J Bacteriol* **187:** 2881–2889

Daniell SJ, Takahashi N, Wilson R, Friedberg D, Rosenshine I, Booy FP, Shaw RK, Knutton S, Frankel G, Aizawa S (2001) The filamentous type III secretion translocon of enteropathogenic *Escherichia coli*. *Cell Microbiol* **3:** 865–871

Deng W, Li Y, Hardwidge PR, Frey EA, Pfuetzner RA, Lee S, Gruenheid S, Strynakda NC, Puente JL, Finlay BB (2005) Regulation of type III secretion hierarchy of translocators and effectors in attaching and effacing bacterial pathogens. *Infect Immun* **73:** 2135–2146

Ferris HU, Furukawa Y, Minamino T, Kroetz MB, Kihara M, Namba K, Macnab RM (2005) FlhB regulates ordered export of flagellar components via autocleavage mechanism. *J Biol Chem* **280:** 41236–41242

Ferris HU, Minamino T (2006) Flipping the switch: bringing order to flagellar assembly. *Trends Microbiol* **14:** 519–526

Fields KA, Nilles ML, Cowan C, Straley SC (1999) Virulence role of V antigen of *Yersinia pestis* at the bacterial surface. *Infect Immun* **67:** 5395–5408

Fraser GM, Gonzalez-Pedrajo B, Tame JR, Macnab RM (2003) Interactions of FliJ with the *Salmonella* type III flagellar export apparatus. *J Bacteriol* **185:** 5546–5554

Galan JE, Wolf-Watz H (2006) Protein delivery into eukaryotic cells by type III secretion machines. *Nature* **444:** 567–573

Goure J, Broz P, Attree O, Cornelis GR, Attree I (2005) Protective anti-v antibodies inhibit *Pseudomonas* and *Yersinia* translocon assembly within host membranes. *J Infect Dis* **192:** 218–225

Hakansson S, Schesser K, Persson C, Galyov EE, Rosqvist R, Homble F, Wolf-Watz H (1996) The YopB protein of *Yersinia pseudotuberculosis* is essential for the translocation of Yop effector proteins across the target cell plasma membrane and displays a contact-dependent membrane disrupting activity. *EMBO J* **15:** 5812–5823

Hirano T, Yamaguchi S, Oosawa K, Aizawa S (1994) Roles of FliK and FlhB in determination of flagellar hook length in *Salmonella typhimurium*. *J Bacteriol* **176:** 5439–5449

Hoiczyk E, Blobel G (2001) Polymerization of a single protein of the pathogen *Yersinia enterocolitica* into needles punctures eukaryotic cells. *Proc Natl Acad Sci USA* **98:** 4669–4674

Journet L, Agrain C, Broz P, Cornelis GR (2003) The needle length of bacterial injectisomes is determined by a molecular ruler. *Science* **302:** 1757–1760

Kaniga K, Delor I, Cornelis GR (1991) A wide-host-range suicide vector for improving reverse genetics in Gram-negative bacteria: inactivation of the blaA gene of *Yersinia enterocolitica*. *Gene* **109:** 137–141

Knutton S, Rosenshine I, Pallen MJ, Nisan I, Neves BC, Bain C, Wolff C, Dougan G, Frankel G (1998) A novel EspA-associated surface organelle of enteropathogenic *Escherichia coli* involved in protein translocation into epithelial cells. *EMBO J* **17:** 2166–2176

Kubori T, Galan JE (2002) *Salmonella* type III secretion-associated protein InvE controls translocation of effector proteins into host cells. *J Bacteriol* **184:** 4699–4708

Kubori T, Matsushima Y, Nakamura D, Uralil J, Lara-Tejero M, Sukhan A, Galan JE, Aizawa SI (1998) Supramolecular structure of the *Salmonella typhimurium* type III protein secretion system. *Science* **280:** 602–605

Kubori T, Sukhan A, Aizawa SI, Galan JE (2000) Molecular characterization and assembly of the needle complex of the *Salmonella typhimurium* type III protein secretion system. *Proc Natl Acad Sci USA* **97:** 10225–10230

Kutsukake K, Minamino T, Yokoseki T (1994) Isolation and characterization of FliK-independent flagellation mutants from *Salmonella typhimurium*. *J Bacteriol* **176:** 7625–7629

Lavander M, Sundberg L, Edqvist PJ, Lloyd SA, Wolf-Watz H, Forsberg A (2002) Proteolytic cleavage of the FlhB homologue

YscU of *Yersinia pseudotuberculosis* is essential for bacterial survival but not for type III secretion. *J Bacteriol* **184:** 4500–4509

Lavander M, Sundberg L, Edqvist PJ, Lloyd SA, Wolf-Watz H, Forsberg A (2003) Characterisation of the type III secretion protein YscU in *Yersinia pseudotuberculosis*. YscU cleavage—dispensable for TTSS but essential for survival. *Adv Exp Med Biol* **529:** 109–112

Li CM, Brown I, Mansfield J, Stevens C, Boureau T, Romantschuk M, Taira S (2002) The Hrp pilus of *Pseudomonas syringae* elongates from its tip and acts as a conduit for translocation of the effector protein HrpZ. *EMBO J* **21:** 1909–1915

Macnab RM (2003) How bacteria assemble flagella. *Annu Rev Microbiol* **57:** 77–100

Magdalena J, Hachani A, Chamekh M, Jouihri N, Gounon P, Blocker A, Allaoui A (2002) Spa32 regulates a switch in substrate specificity of the type III secreton of *Shigella flexneri* from needle components to Ipa proteins. *J Bacteriol* **184:** 3433–3441

Marenne MN, Journet L, Mota LJ, Cornelis GR (2003) Genetic analysis of the formation of the Ysc–Yop translocation pore in macrophages by *Yersinia enterocolitica*: role of LcrV, yscF and YopN. *Microb Pathogen* **35:** 243–258

Marlovits TC, Kubori T, Sukhan A, Thomas DR, Galan JE, Unger VM (2004) Structural insights into the assembly of the type iii secretion needle complex. *Science* **306:** 1040–1042

Michiels T, Cornelis GR (1991) Secretion of hybrid proteins by the *Yersinia* Yop export system. *J Bacteriol* **173:** 1677–1685

Minamino T, Macnab RM (2000) Domain structure of *Salmonella* FlhB, a flagellar export component responsible for substrate specificity switching. *J Bacteriol* **182:** 4906–4914

Morita-Ishihara T, Ogawa M, Sagara H, Yoshida M, Katayama E, Sasakawa C (2006) *Shigella* Spa33 is an essential C-ring component of type III secretion machinery. *J Biol Chem* **281:** 599–607

Moriya N, Minamino T, Hughes KT, Macnab RM, Namba K (2006) The type III flagellar export specificity switch is dependent on FliK ruler and a molecular clock. *J Mol Biol* **359:** 466–477

Mota LJ, Cornelis GR (2005) The bacterial injection kit: type III secretion systems. *Ann Med* **37:** 234–249

Mota LJ, Journet L, Sorg I, Agrain C, Cornelis GR (2005) Bacterial injectisomes: needle length does matter. *Science* **307:** 1278

Mueller CA, Broz P, Muller SA, Ringler P, Erne-Brand F, Sorg I, Kuhn M, Engel A, Cornelis GR (2005) The V-antigen of *Yersinia* forms a distinct structure at the tip of injectisome needles. *Science* **310:** 674–676

Sory MP, Boland A, Lambermont I, Cornelis GR (1995) Identification of the YopE and YopH domains required for secretion and internalization into the cytosol of macrophages, using the cyaA gene fusion approach. *Proc Natl Acad Sci USA* **92:** 11998–12002

Stainier I, Bleves S, Josenhans C, Karmani L, Kerbourch C, Lambermont I, Totemeyer S, Boyd A, Cornelis GR (2000) YscP, a *Yersinia* protein required for Yop secretion that is surface exposed, and released in low Ca^{2+}. *Mol Microbiol* **37:** 1005–1018

Sukhan A, Kubori T, Wilson J, Galan JE (2001) Genetic analysis of assembly of the *Salmonella enterica* serovar *Typhimurium* type III secretion-associated needle complex. *J Bacteriol* **183:** 1159–1167

Tamano K, Katayama E, Toyotome T, Sasakawa C (2002) *Shigella* Spa32 is an essential secretory protein for functional type III secretion machinery and uniformity of its needle length. *J Bacteriol* **184:** 1244–1252

Tampakaki AP, Fadouloglou VE, Gazi AD, Panopoulos NJ, Kokkinidis M (2004) Conserved features of type III secretion. *Cell Microbiol* **6:** 805–816

Van Gijsegem F, Vasse J, Camus JC, Marenda M, Boucher C (2000) *Ralstonia solanacearum* produces hrp-dependent pili that are required for PopA secretion but not for attachment of bacteria to plant cells. *Mol Microbiol* **36:** 249–260

Williams AW, Yamaguchi S, Togashi F, Aizawa SI, Kawagishi I, Macnab RM (1996) Mutations in fliK and flhB affecting flagellar hook and filament assembly in *Salmonella typhimurium*. *J Bacteriol* **178:** 2960–2970

Zhu K, Gonzalez-Pedrajo B, Macnab RM (2002) Interactions among membrane and soluble components of the flagellar export apparatus of *Salmonella*. *Biochemistry* **41:** 9516–9524

Supplementary data 1

Needles of *Y. enterocolitica* $yscU_{N263A}$ and $yscU_{P264A}$ mutants are longer and less regulated

To analyze the influence of mutations in the NPTH motif of YscU on needle length, $yscU_{wt}$, $yscU_{N263A}$, $yscU_{P264A}$, or $yscU_{T265A}$ were overexpressed from the pBAD promoter in *Y. enterocolitica* E40 Δ*yscU* mutant bacteria. Needles were analyzed after 4 hour induction of the *yop* regulon at 37 °C. The pBAD promoter was induced by adding 0.2 % L-arabinose to the culture just before the shift to 37 °C, and again 2 hours later. Bacteria were harvested at 2000 *g* and resuspended gently in 20 mM Tris-HCl, pH 7.5. Droplets were applied for 1 minute to freshly glow-discharged, formvar-carbon coated grids, and negatively stained with 2 % (w/v) uranyl acetate. Bacteria were visualized in a Philips CM100 transmission electron microscope at a nominal magnification of 20 000x and an acceleration voltage of 80 kV. Sizes were measured with the 'Soft imaging system' software (Hamburg, Germany).

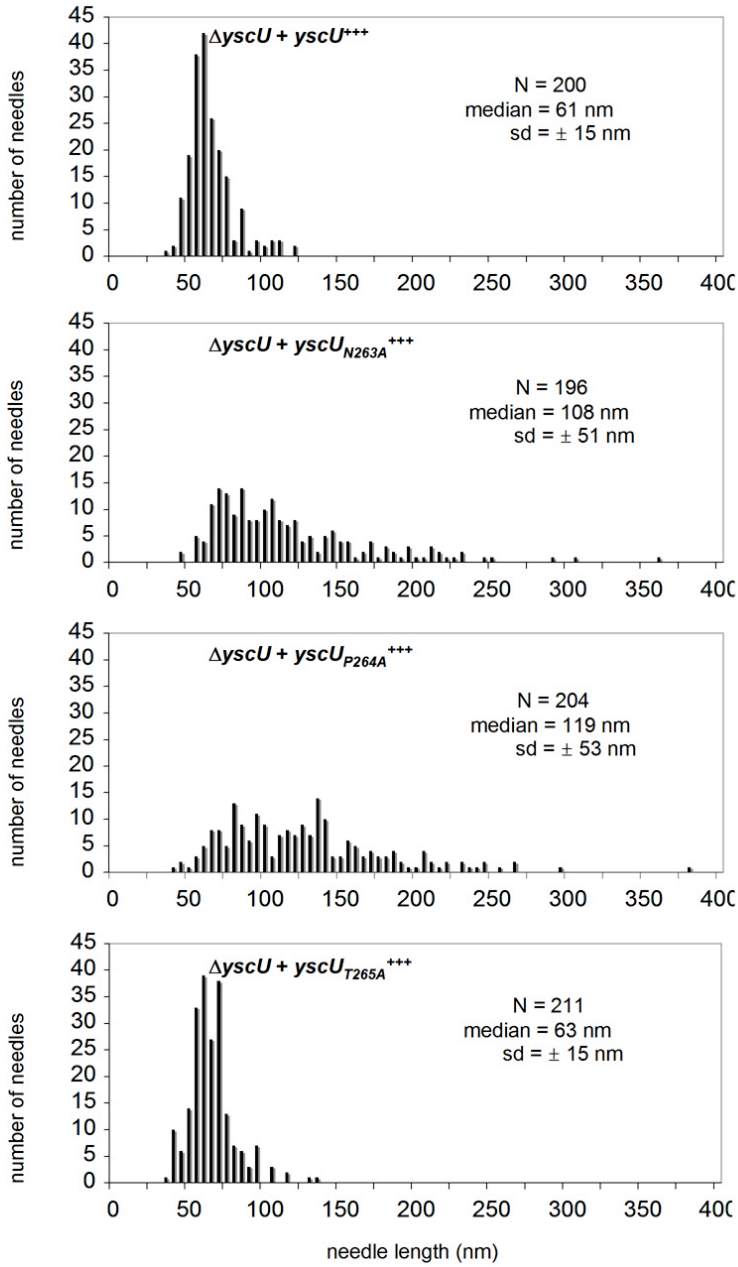

Legend to Figure S1

Histograms showing the needle length of *Y. enterocolitica* E40 Δ*yscU* mutant bacteria (pLY4001) overexpressing *yscU* (pLY7), $yscU_{N263A}$ (pSTW7), $yscU_{P264A}$ (pSTW8), or $yscU_{T265A}$ (pSTW9). N, number of measured needles; sd, standard deviation.

Supplementary data 2

Overexpression of *yscP* in the *Y. enterocolitica* $yscU_{N263A}$ mutant background does not restore translocator export

Needles of *Y. enterocolitica* $yscU_{N263A}$ mutant bacteria were longer and less regulated than needles from wildtype bacteria. The same was true for $yscU_{N263A}$ mutant bacteria producing a shorter ($YscP_{388}$) or a longer ($YscP_{680}$) version of the molecular ruler YscP. Although $yscP_{388}$ led to shorter and $yscP_{680}$ to longer needles than the wildtype $yscP_{515}$ ruler, needles were longer and less regulated than needles from the corresponding *yscU* wildtype strain. Overexpression of different yscP alleles in $yscU_{N263A}$ mutant bacteria led to needles that were comparable to those of the corresponding *yscU* wildtype strains. Although $yscU_{N263A}$ mutant bacteria overexpressing *yscP* had needles with the expected length, they still did not export the translocators YopB, YopD, and LcrV (Figure S2).

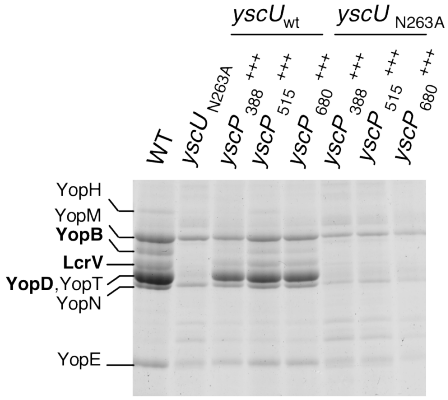

Legend to Figure S2

Coomassie-stained 12 % SDS-PAGE showing the Yops secreted by *Yersinia* $yscU_{wt}$ and $yscU_{N263A}$ mutant bacteria producing the indicated YscP proteins from their native promoter and additionally from the pBAD promoter. Overexpression of YscP proteins from the pBAD promoter was induced with 0.1 % L-arabinose. *Yersinia* wildtype (WT) $yscU_{N263A}$ mutant strains were used as controls. The secreted Yops are indicated on the side. Yop translocators are shown in bold and Yop effectors in regular letters.

Table I: Plasmids used in this work

Plasmids	Current strain designation	Genotype and derivation	References
pYV plasmids			
pYV40	WT	pYV plasmid from *Y. enterocolitica* E40	Sory et al, 1995
pYVe22703	pYVe22703	pYV plasmid from *Y. enterocolitica* W227 serotype O:9	Cornelis et al, 1987
pLJ4036	Δ*yscP*	pYV40 Δ*yscP*; complete deletion of *yscP* from start to stop	Agrain et al, 2005
pIM417	ΔHOPEMN	pYV40 $yopE_{21}$, $yopH_{\Delta 1\text{-}352}$, $yopO_{\Delta 65\text{-}558}$, $yopP_{23}$, $yopM_{23}$, $yopN_{45}$	Neyt & Cornelis, 1999
pMN4002	ΔHOPEMNV	pYV40 $yopE_{21}$, $yopH_{\Delta 1\text{-}352}$, $yopO_{\Delta 65\text{-}558}$, $yopP_{23}$, $yopM_{23}$, $yopN_{45}$, $lcrV_{\Delta 6\text{-}319}$	Marenne et al, 2003
pIM41	Δ*yopN*	pYV40 $yopN_{45}$; deletion of *yopN* after condon 45	Boland et al, 1996
pLJ4022	$yscP_{388}$	pYV40 $yscP_{388}$; deletion of codons 46 to 96 and 222 to 306 of YscP	Mota et al, 2005
pLJM4001	$yscP_{680}$	pYV40 $yscP_{680}$; duplication of codons 222 to 381 from YscP and insertion between codons 49/50	Mota et al, 2005
pLY4001	Δ*yscU*	pYV40 Δ*yscU;* deletion of yscU codons 1-354 using mutator pLY16	this study
pISO4007	$yscU_{N263A}$	pYV40 $yscU_{N263A}$; introduction of mutation N263A into *yscU* by allelic exchange using mutator pISO108	this study
pISO4010	Δ*yopN*$yscU_{N263A}$	pYV40 $yopN_{45}$, $yscU_{N263A}$; $yopN_{45}$ was introduced into pISO4007 using mutator pIM150	this study
pISO4011	$yscP_{388}yscU_{N263A}$	pYV40 $yscP_{388}$, $yscU_{N263A}$; $yscP_{388}$ was introduced into pISO4007 using mutator pLJ22	this study
pISO4012	$yscP_{680}yscU_{N263A}$	pYV40 $yscP_{680}$, $yscU_{N263A}$; $yscP_{680}$ was introduced into pISO4007 using mutator pLJM29	this study
Expression plasmids			
pBADMycHisA			Invitrogen
pLJ6	$yscP_{515}{}^{+++}$	pBAD::*yscP*; complete *yscP* gene	Journet et al, 2003
pCA20	$yscP_{388}{}^{+++}$	pBAD:: $yscP_{388}$; deletion of codons 46 to 96 and 222 to 306 of YscP	Journet et al, 2003
pLJ19	$yscP_{680}{}^{+++}$	pBAD:: $yscP_{680}$; duplication of codons 222 to 381 from YscP and insertion between codons 49/50	Journet et al, 2003
pPB42	$lcrV^{+++}$	pBAD:: *lcrV*; *lcrV* was amplified with oligos 3806 and 3807 from pMN12 and cloned into the *NcoI* / *EcoRI* sites of pBADmycHisA	this study

pISOA132	*yopE*$_{1-15}$*lcrV*$^{+++}$	pBAD:: *yopE*$_{1-15}$*lcrV*; *lcrV* was amplified with oligos 4578 and 4461 from pMN12 and cloned into the *NcoI* / *PstI* sites of pBADmycHisA	this study
pLY1	*yscU*$_{211-354}$*his*	pBAD:: *yscU*$_{211-354}$*his*$_6$; codons 211-354 of *yscU* were amplified from pYVe22703 using oligos 3705 and 3707 and cloned into the *NcoI* / *EcoRI* sites of pBADmycHisA	this study
pLY7	*yscU*$^{+++}$	pBAD:: *yscU*; *yscU* was amplified from pYVe22703 using oligos 3704 and 3724 and cloned into the *NcoI* / *EcoRI* sites of pBADmycHisA	this study
pSTW7	*yscU*$_{N263A}$$^{+++}$	pBAD:: *yscU*$_{N263A}$; mutation N263A was introduced into pLY7 by site directed mutagenesis using oligos 3725 and 3726	this study
pSTW8	*yscU*$_{P264A}$$^{+++}$	pBAD:: *yscU*$_{P264A}$; mutation P264A was introduced into pLY7 by site directed mutagenesis using oligos 3727 and 3728	this study
pSTW9	*yscU*$_{T265A}$$^{+++}$	pBAD:: *yscU*$_{T265A}$; mutation T265A was introduced into pLY7 by site directed mutagenesis using oligos 3729 and 3730	this study
pMN12		pBBR1-MCS2::P*yopElcrV*$^{+}$	Marenne et al, 2003

Suicide plasmid			
pKNG101		*Ori*$_{R6K}$ *sac*BR^{+} *ori*T$_{RK2}$ *str*AB^{+}	Kaniga et al, 1991
Mutator plasmids			
pIM150	mutator *yopN*$_{45}$	pKNG101::*yopN*$_{45}$$^{+}$; mutator to delete *yopN* after codon 45	Boland et al, 1996
pLJ22	mutator *yscP*$_{388}$	pKNG101::*yscP*$_{388}$$^{+}$; mutator to delete codons 46 to 96 and 222 to 306 of *yscP*	Mota et al, 2005
pLJM29	mutator *yscP*$_{680}$	pKNG101::*yscP*$_{680}$$^{+}$; mutator to insert codons 222 to 381 of *yscP* between codons 49/50 of *yscP*	Mota et al, 2005
pLY16	mutator *yscU*	pKNG101::*yscU*$^{+}$; flanking regions of *yscU* bp 29112 -29896 and 30959 – 31561 were amplified by overlapping PCR from the pYVe22703 plasmid using oligos 3780, 3968, 3781, 3967 and cloned into the *SalI* / *XbaI* sites of pKNG101	this study
pISO108	mutator *yscU*$_{N263A}$	pKNG101::*yscU*$_{N263A}$$^{+}$; the region encoding amino acids 172-354 of YscU was amplified from pSTW7 using oligos 4141 and 3877 and cloned into the *SalI* / *XbaI* sites of pKNG101	this study

References:

Agrain C, Callebaut I, Journet L, Sorg I, Paroz C, Mota LJ, Cornelis GR (2005) Characterization of a Type III secretion substrate specificity switch (T3S4) domain in YscP from Yersinia enterocolitica. *Mol Microbiol* **56:** 54-67

Boland A, Sory MP, Iriarte M, Kerbourch C, Wattiau P, Cornelis GR (1996) Status of YopM and YopN in the Yersinia Yop virulon: YopM of Y.enterocolitica is internalized inside the cytosol of PU5-1.8 macrophages by the YopB, D, N delivery apparatus. *Embo J* **15:** 5191-5201.

Cornelis G, Vanootegem JC, Sluiters C (1987) Transcription of the yop regulon from Y. enterocolitica requires trans acting pYV and chromosomal genes. *Microb Pathog* **2:** 367-379.

Journet L, Agrain C, Broz P, Cornelis GR (2003) The needle length of bacterial injectisomes is determined by a molecular ruler. *Science* **302:** 1757-1760

Kaniga K, Delor I, Cornelis GR (1991) A wide-host-range suicide vector for improving reverse genetics in gram-negative bacteria: inactivation of the blaA gene of Yersinia enterocolitica. *Gene* **109:** 137-141

Marenne MN, Journet L, Mota LJ, Cornelis GR (2003) Genetic Analysis of the formation of the Ysc-Yop translocation pore in macrophages by Yersinia enterocolitica: role of LcrV, yscF and YopN. *Microb Pathogen* **35:** 243-258

Mota LJ, Cornelis GR (2005) The bacterial injection kit: type III secretion systems. *Ann Med* **37:** 234-249

Neyt C, Cornelis GR (1999) Insertion of a Yop translocation pore into the macrophage plasma membrane by Yersinia enterocolitica: requirement for translocators YopB and YopD, but not LcrG. *Mol Microbiol* **33:** 971-981.

Sory MP, Boland A, Lambermont I, Cornelis GR (1995) Identification of the YopE and YopH domains required for secretion and internalization into the cytosol of macrophages, using the cyaA gene fusion approach. *Proc Natl Acad Sci U S A* **92:** 11998-12002.

Table II: Oligonucleotides used for the genetic constructions

No.	Sequence	Restriction site
3704	gatcgaattcttataacatttcggaatg	*EcoRI*
3705	gatcccatggccaaggaacttaaaatgagc	*NcoI*
3707	gatcgaattcggtaacatttcggaatgctg	*EcoRI*
3806	atcatgccatggcaattagagcctacgaacaaaacc	*NcoI*
3807	ccgggcgaattcttacctcgtgtcatctagcag	*EcoRI*
3967	gatccctgttttggagaagtaataggctgcaatgtaactaggaat	-
3968	cctagttacattgcagcctattacttctccaaaacagggatc	-
3724	gatcccatggccagcggagaaaagacagag	*NcoI*
3725	tcatcagtggtggtagctgctccgacccatattgctatt	-
3726	aatagcaatatgggtcggagcagctaccaccactgatga	-
3727	tcagtggtggtagctaatgcgacccatattgctattggt	-
3728	accaatagcaatatgggtcgcattagctaccagcactga	-
3729	gtggtggtagctaatccggcccatattgctattggtatt	-
3730	aataccaatagcaatatgggccggattagctaccaccac	-
3780	gatcgtcgacatgatagcggatttaatccaaagacca	*SalI*
3781	gatctctagaggcgcaccccactaatagaaaagaaat	*XbaI*
3877	ctagtctagattataacatttcggaatgctgatt	*XbaI*
4141	acgcgtcgacgtggaattgaatgtattacccc	*SalI*
4578	gatcccatggccaaaatatcatcatttatttctacatcactgcccctgccggcaattagagcctacgaacaaaaccc	*NcoI*

Structure of the Type III secretion recognition protein YscU from *Y. enterocolitica*

Ulrich Wiesand[1], Isabel Sorg[2], Marlise Amstutz[2], Stefanie Wagner[2],

Joop van den Heuvel[1], Thorsten Lührs[1], Guy R. Cornelis[2] and Dirk W. Heinz[1]*

[1] Division of Structural Biology, Helmholtz Centre for Infection Research (HZI), Braunschweig, Germany.

[2] Biozentrum der Universität Basel, Basel, Switzerland.

Author contributions: I contributed to this paper by engineering the pSTW plasmids, analyzing the needle length and export levels of YscP of all YscU mutants presented in this paper.

The inner-membrane protein YscU has an important role during the assembly of the *Yersinia enterocolitica* type III secretion injectisome. Its cytoplasmic domain ($YscU^C$) recognizes translocators as individual substrates in the export hierarchy. Activation of YscU entails auto-cleavage at a conserved NPTH motif. Modification of this motif markedly changes the properties of YscU, including translocator export cessation and production of longer injectisome needles. We determined the crystal structures of the uncleaved variants N263A and N263D of $YscU^C$ at 2.05 Å and 1.55 Å resolution, respectively. The globular domain is found to consist of a central, mixed β-sheet surrounded by α-helices. The NPTH motif forms a type II β-turn connecting two β-strands. NMR analysis of cleaved and uncleaved $YscU^C$ indicates that the global structure of the protein is retained in cleaved $YscU^C$. The structure of $YscU^C$ variant N263D reveals that wild type $YscU^C$ is poised for cleavage due to an optimal reaction geometry for nucleophilic attack of the scissile bond by the side chain of Asn263. *In vivo* analysis of N263Q and H266A/R314A YscU variants showed a phenotype that combines the absence of translocator secretion with normal needle-length control. Comparing the structure of YscU to those of related proteins reveals that the linker domain between the N-terminal transmembrane domain and the auto-cleavage domain can switch from an extended to a largely α-helical conformation, allowing for optimal positioning of the auto-cleavage domain during injectisome assembly.

doi:10.1016/j.jmb.2008.10.034 J. Mol. Biol. (2009) 385, 854–866

JMB

Available online at www.sciencedirect.com

ScienceDirect

ELSEVIER

Structure of the Type III Secretion Recognition Protein YscU from *Yersinia enterocolitica*

Ulrich Wiesand[1], Isabel Sorg[2], Marlise Amstutz[2], Stefanie Wagner[2], Joop van den Heuvel[1], Thorsten Lührs[1], Guy R. Cornelis[2] and Dirk W. Heinz[1]*

[1]*Division of Structural Biology, Helmholtz Centre for Infection Research (HZI), Inhoffenstrasse 7, 38124 Braunschweig, Germany*

[2]*Division of Molecular Microbiology, Biozentrum, University of Basel, Klingelbergstrasse 50/70, CH-4056 Basel, Switzerland*

Received 24 July 2008; received in revised form 6 October 2008; accepted 8 October 2008
Available online 19 October 2008

Edited by R. Huber

The inner-membrane protein YscU has an important role during the assembly of the *Yersinia enterocolitica* type III secretion injectisome. Its cytoplasmic domain ($YscU^C$) recognizes translocators as individual substrates in the export hierarchy. Activation of YscU entails autocleavage at a conserved NPTH motif. Modification of this motif markedly changes the properties of YscU, including translocator export cessation and production of longer injectisome needles. We determined the crystal structures of the uncleaved variants N263A and N263D of $YscU^C$ at 2.05 Å and 1.55 Å resolution, respectively. The globular domain is found to consist of a central, mixed β-sheet surrounded by α-helices. The NPTH motif forms a type II β-turn connecting two β-strands. NMR analysis of cleaved and uncleaved $YscU^C$ indicates that the global structure of the protein is retained in cleaved $YscU^C$. The structure of $YscU^C$ variant N263D reveals that wild type $YscU^C$ is poised for cleavage due to an optimal reaction geometry for nucleophilic attack of the scissile bond by the side chain of Asn263. *In vivo* analysis of N263Q and H266A/R314A YscU variants showed a phenotype that combines the absence of translocator secretion with normal needle-length control. Comparing the structure of YscU to those of related proteins reveals that the linker domain between the N-terminal transmembrane domain and the autocleavage domain can switch from an extended to a largely α-helical conformation, allowing for optimal positioning of the autocleavage domain during injectisome assembly.

Keywords: auto-proteolysis; crystal structure; type III secretion system; Yersinia

Introduction

The enteric pathogen *Yersinia enterocolitica* uses a sophisticated injection machinery called an injectisome to translocate effector proteins across eukaryotic cell membranes by type III secretion (T3S). This supramolecular structure, found in many Gram-negative pathogenic or symbiotic bacteria, including *Salmonella* spp., *Shigella* spp. and enteropathogenic *Escherichia coli*, is evolutionarily related to the bacterial flagellum.[1] A basal body consisting of several rings connected by a central rod spans the two bacterial membranes in both structures.[2–5] The basal body bears an extracellular structure referred to as needle,[2,3,6–8] pilus[9] or filament,[10–12] depending on the family of injectisomes. Upon contact with the eukaryotic host cell, a set of effector proteins that subvert host cellular functions to the pathogen`s benefit is translocated into the eukaryotic cytoplasm.[13,14]

The rotationally symmetric basal body of the T3S system (T3SS) actively exports the components of the extracellular needle structure.[3,4,15,16] The length of the *Yersinia* injectisome needle, assembled from the 9 kDa protein YscF, differs from species to species. In *Yersinia enterocolitica,* the needle length of ~60 nm correlates with the length of the "molecular ruler" protein YscP.[17] A needle tip complex, made of the

*Corresponding author. E-mail address: Dirk.Heinz@helmholtz-hzi.de.

Abbreviations used: $YscU^C$, C-terminal domain of YscU comprising amino acids 211–354; T3SS, type III secretion system.

protein LcrV,[18] functions as a scaffold to assemble a pore in the target cell membrane consisting of YopB and YopD, through which T3SS effectors are translocated into the host cell.[19] Beside the "molecular ruler" model,[14] two other models for needle/hook length control, the cup model[20] and the molecular stopwatch mechanism,[21] are discussed. As a clear hierarchy in the synthesis of the needle components is not discernible, the T3SS presumably discriminates between substrate classes to assemble this complex molecular machine.[22] Needle assembly depends on the export of early substrates such as the needle subunit YscF and the molecular ruler YscP. Thereafter, the system switches its substrate specificity to intermediate (translocators) and late (effectors) export substrates. The substrate specificity switch is thought to involve at least two proteins, the molecular ruler YscP and the inner membrane protein YscU.[23,24]

In the 40 kDa membrane protein YscU, four N-terminal transmembrane helices are followed by a globular cytoplasmic domain ($YscU^C$).[25] The latter, which was originally found in the C-terminal cytoplasmic domain of the *Salmonella* flagellar YscU homolog, FlhB,[26] is cleaved autoproteolytically within a conserved NPTH sequence.[27] Autocleavage, however, is abrogated by substituting either asparagine or proline by alanine.[27] Bacterial mutants carrying these substitutions no longer export translocator proteins (YopB, YopD and LcrV), whereas export of effector proteins is not affected.[22] Cleaved YscU thus appears to discriminate between translocator and effector proteins. The mutant $yscU_{N263A}$, furthermore, secretes less YscP and makes longer needles.[22]

Here, we report the crystal structures of the non-cleavable $YscU^C_{N263A}$ and $YscU^C_{N263D}$ variants from *Yersinia enterocolitica* and compare them to the related structures of EscU, SpaS[28] and Spa40.[29] Based on the structural information, additional $YscU^C$ mutants were designed to elucidate their *in vitro* autocleavage behaviour and the nature of the resulting *in vivo* phenotypes.

Results

Crystal structures of $YscU^C$ N263A and N263D

The $YscU^C$ variants N263A and N263D readily yielded well-diffracting tetragonal crystals. Crystallization of cleaved, wild type $YscU^C$, by contrast, was not successful. The structure of $YscU^C$ N263A was solved using SeMet-based multiwavelength anomalous diffraction (MAD) phasing. Two (of four expected) selenium positions were sufficient to build an initial model, which was refined at a resolution of 2.05 Å (Table 1). The isomorphous structure of $YscU^C$ N263D was refined at a resolution of 1.55 Å (Table 1).

The globular domain of uncleaved $YscU^C$ (Fig. 1) consists of a central, five-stranded, mixed β-sheet (I–V), surrounded by four α-helices (1–4). α-Helix 3 is almost perpendicular to the strand orientation of the central β-sheet. The NPTH cleavage motif forms a type II β-turn connecting β-strands I and II, with position 263 located at the C-terminal end of β-strand I.

The globular autocleavage domain is preceded by an extended N-terminal loop containing a well defined α-helix (α0) comprising residues 231–246. This helix forms an antiparallel interaction with helix 4 of a symmetry-related $YscU^C$ monomer in the crystal.

Structural basis for autocleavage of YscU

Close inspection of the modified NPTH motif in the isosteric variant $YscU^C$ N263D (DPTH, Fig. 2a) shows that the main-chain carbonyl of Asp263 is tightly locked into position *via* hydrogen bonds to the backbone nitrogen atoms of His266 and Ile267. This structural stiffness is enhanced by the peptide bond of Pro264. All main-chain dihedral angles of the DPTH residues fall in the allowed regions of the Ramachandran plot, indicating no obvious conformational strain. A salt bridge with the guanidinium group of Arg314 positions the side chain of Asp263 above its main chain carbonyl group.

The ideal entry angle for a nucleophilic attack of a carbonyl group has been proposed to lie between 100° and 110°, and a distance between nucleophile and electrophile of <2.5 Å.[30,31] The corresponding angle of the $YscU^C$ N263D variant is 109° with an N–C distance of 2.8 Å. The β-amide nitrogen of Asn263 would therefore be positioned perfectly for a nucleophilic attack. Furthermore this geometric arrangement favours a stabilizing orbital overlap (Fig. 2b), where the anti-bonding σ*-molecular orbital (MO) of the $C\alpha_{Asn}$–N_{Asn} bond interferes with the nascent bonding σ-MO of the C(=O)-N bond in native YscU.

Cleavage does not affect the overall structure of wild type $YscU^C$

Recombinantly produced wild-type $YscU^C$ is readily cleaved into a ~6.3 kDa N-terminal (α-helices 0–1 and β-strand I) and a ~10.5 kDa C-terminal (α-helices 2–4 and β-strands II–V) fragment. The fragments remain tightly linked, however,[27] resulting in a single peak in gel-filtration chromatography (data not shown). Cleavage of the wild-type protein thus does not cause significant overall structural rearrangements compared to the uncleaved $YscU^C$ variants. This was confirmed by 2D NMR (^{15}N,^1H HMQC) spectroscopy by comparing ^{15}N-labelled wild type and N263A $YscU^C$ (Fig. 3). Overall, wild type $YscU^C$ shows a good dispersion of the signals, characteristic for a folded globular conformation. An equally good dispersion of the signals is observed for N263A $YscU^C$. The NMR spectra of wild type and N263A $YscU^C$ superimpose very well, with most peak positions being virtually identical and linewidths apparently unaffected. Cleaved and un-

Table 1. Data collection and refinement statistics

	SeMet-labelled YscU N263A				
	Peak	Inflection	High-energy remote	Low-energy remote	YscU N263D
A. *Data collection statistics*					
Beamline	DESY X12	DESY X12	DESY X12	DESY X12	ESRF ID29
Space group	$P4_32_12$	$P4_32_12$	$P4_32_12$	$P4_32_12$	$P4_32_12$
Unit cell dimensions					
a (Å)	66.2	66.2	66.2	66.3	66.5
c (Å)	68.1	68.1	68.1	68.8	68.1
Wavelength (Å)	0.97854	0.97893	0.95370	1.0000	0.9500
Resolution (Å)	30.0–2.33 (2.41–2.33)	40.0–2.33 (2.41–2.33)	40.0–2.33 (2.41–2.33)	30.0–2.0 (2.11–2.0)	10.0–1.55 (1.63–1.55)
Mosaicity (°)	0.80	0.98	0.89	0.95	0.24
Unique reflections	6910 (670)	6907 (663)	6920 (667)	10,836 (1517)	21,871 (3232)
Completeness (%)	100 (99.9)	100 (100)	100 (100)	100 (100)	96.7 (99.9)
Multiplicity	13.6 (12.0)	13.6 (12.6)	13.8 (13.3)	13.6 (13.6)	3.1 (3.1)
$I/\sigma I$	31.7 (8.2)	34.3 (8.8)	34.0 (9.5)	8.1 (2.2)	8.4 (4.8)
R_{merge} (%)	8.2 (31.5)	7.7 (29.8)	7.8 (31.0)	6.9 (35.2)	5.2 (15.1)
Wilson *B*-factor (Å^2)	39	39	38	25	19
Solvent content (%)	45	45	45	45	45
B. *Refinament statistics*					
R_{cryst} (%)				22.1	20.1
R_{free} (%)				25.3	22.5
Number of atoms					
Protein				1027	1104
Solvent				52	133
Cl^-				1	2
r.m.s.d. from ideal					
Bond lengths (Å)/				0.015	0.019
Bond angles (°)				1.756	1.698
Ramachandran plot regions					
Favoured (%)				95.3	96.4
Allowed (%)				4.7	3.6
Average *B*-factor					
Protein (Å^2)				29.9	20.3
Solvent (Å^2)				34.7	33.6
Cl^- (Å^2)				27.0	35.1

Values in parentheses refer to shell of highest resolution. R_{free} test set size for YscU N263A 5% and for YscU N263D 3%.

cleaved YscU thus share the same overall structure with minor, but physiologically highly relevant, changes in and close to the NPTH motif.

The role of conserved amino acids in YscU^C cleavage *in vitro*

Substituting the nucleophile Asn263 by alanine, aspartate and glutamine abolishes autocleavage of YscU. While Asn263 is thus essential for YscU autocleavage, the role of surrounding residues is less clear. A systematic mutational analysis of the NPTH motif reveals an active participation of Pro264 and His266 in YscU autocleavage (Fig. 4a and b), whereas Thr265 is not involved.[22] Substitution of Pro264 by alanine reduces cleavage of YscU^C significantly, whereas substitution by glycine prevents cleavage altogether. Variant H266A shows a partial cleavage of YscU^C. The structure of YscU^C shows that two arginine residues (Arg296 and 314) flank the NPTH motif. Of these, Arg314 is highly conserved, Arg296 less so. Substituting Arg314 by alanine correspondingly reduces cleavage partly, whereas cleavage of variant R296A is unaffected. Interestingly, cleavage is entirely abrogated in the double variant H266A/R314A, suggesting a synergistic involvement of these residues in the mechanism of cleavage.

Cleavage of some autocleavage-deficient YscU mutants is partially restored at high pH

Autocleavage of the slow-cleaving variant P270A of the flagellar protein FlhB^C (a homologue of YscU^C) has been reported to be pH-dependent.[32] YscU^C variants N263D, P264G, P264A and H266A/R314A were therefore analysed at pH 9, 10 and 11 (Fig. 4c). In variant N263D, no cleavage was observed at higher pH values, whereas P264G, P264A and H266A/R314A were partially cleaved only at elevated pH. These observations match the published data on FlhB P270A,[32] suggesting that the nucleophile Asn263 needs to be activated by deprotonation of its side chain amide group.

YscU mutants that are not cleaved *in vitro* do not export the translocator LcrV

Next, the export of the LcrV protein in the corresponding *Yersinia* mutant strains was investigated.

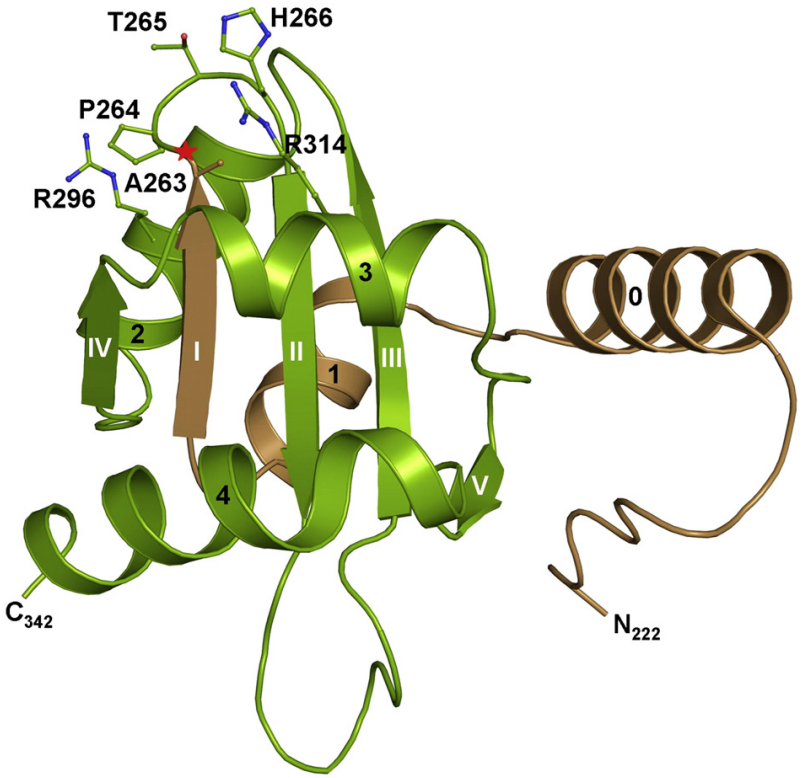

Fig. 1. Ribbon plot of the monomer of YscU^{C} N263A. The position of the mutation in the cleavage site is indicated by an asterisk (*). After cleavage YscU^{C} is divided into an N-terminal and a C-terminal half, shown in brown and green, respectively. The modified NPTH motif, as well as Arg314 and Arg296, are depicted as stick-and-ball models.

Secretion was not affected for wild type YscU, and the variants H266A, R314A and R296A, but is lost in variants N263A, N263D, N263Q, P264A, P264G, and H266A/R314A, as confirmed by an immunoblot of the supernatant (Fig. 5). The LcrV secretion pattern is in excellent agreement with the data described above for *in vitro* autocleavage.

The T3SS injectisome needle length is influenced strongly by YscU mutations

The influence of the YscU modifications on needle length was investigated by measuring needles from *Y. enterocolitica* Δ*yscU* mutant bacteria expressing the respective mutants *in trans*. Bacteria expressing wild type *yscU* produced regulated needles of 69±10 nm. Similar needle lengths were measured for the YscU variants H266A (67±9 nm), R314A (72±12 nm), and R296A (76±11 nm). In contrast, the length of needles in YscU variants N263A (125±40 nm), N263D (143±51 nm), P264A (112±42 nm), and P264G (114±30 nm) was longer and less regulated. Interestingly, YscU variants N263Q (80±16 nm) and H266A/R314A (77±15 nm) were regulated with a length distribution slightly larger than that of wild type YscU (Fig. 6).

Discussion

YscU is poised for autocatalytic cleavage

To elucidate the structural basis of YscU^{C} autocleavage, the crystal structures of YscU^{C} variants N263A and N263D were determined at high resolution. Additional single-residue YscU^{C} variants within the NPTH motif or its immediate vicinity were investigated with respect to their participation in cleavage and needle-length control.

The crystal structure of non-cleaving YscU^{C} variant N263D (the asparagine nucleophile is replaced by the isosteric homologue aspartate) suggests that the side chain of Asn263 is positioned ideally for a nucleophilic attack and subsequent cleavage of wild-type YscU^{C}. In N263D, the attack on its own carbonyl is prevented by the insufficient nucleophilicity of the Asp263 carboxylate, despite its equivalent positioning. In N263Q, the nucleophilicity should be similar to that of asparagine. However, the longer, and hence more flexible, side chain disfavours the formation of a lactam ring in this variant, preventing cleavage of YscU^{C}.

YscU^{C} autocleavage is crucially dependent on the positioning of the attacked carbonyl group of

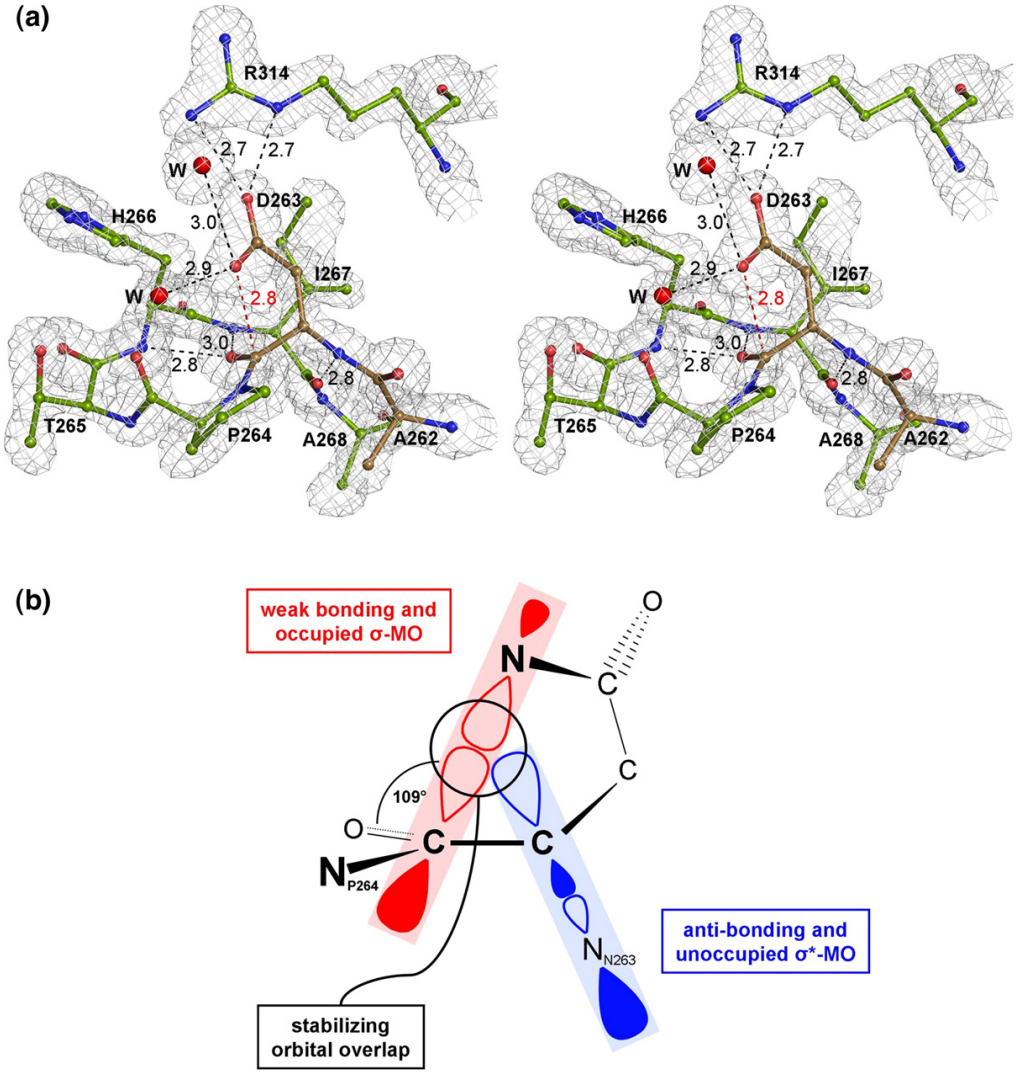

Fig. 2. (a) Detailed stereoview of the modified NPTH motif of YscU^{C} N263D. The C-terminal and N-terminal halves are shown in brown and green, respectively. The isosteric Asp263 is positioned optimally (109°) for a nucleophilic attack, as indicated by the broken red line. Hydrogen bonds are indicated by broken black lines. The ($2F_O - F_C$,α_C) electron density map of the cleavage site is depicted at a contour level of 1.5 σ. (b) Orbital model illustrating the stabilizing orbital overlap. The anti-bonding σ*-molecular orbital (MO) of the Cα−N bond in Asn263 (blue) interferes with the nascent bonding σ-MO of the C(═O)-N-bond (red).

Asn263, which is part of the peptide bond to Pro264. Increased flexibility of the main chain correspondingly disfavours cleavage in the variants P264A and P264G. As indicated above, cleavage is less efficient in variants H266A and R314A, but abrogated entirely in H266A/R314A. Raising the pH increases cleavage, implicating both His266 and Arg314 in efficient autocleavage. By means of a hydrogen bond, Arg314 presumably serves to optimally position the side chain of Asn263 allowing nucleophilic attack to occur at an angle of 109°. The role of His266 is, however, less clear. It may potentially mediate the abstraction of a proton from Asn263 either directly or by deprotonating an intermediate water molecule. A similar phenomenon has been proposed for a histidine residue during autosplicing of the DnaB mini-intein.[33] Thr265, the only imperfectly conserved amino acid of the NPTH motif, does not appear to be involved directly in the cleavage reaction.[22,28] A preference for β-branched amino acids indicates a role in stabilizing the type II turn.[34]

Our results are supported by similar structural and functional data reported recently for the YscU homologues EscU from enteropatogenic *E. coli*, SpaS from *Salmonella typhimurium*[28] and Spa40 from

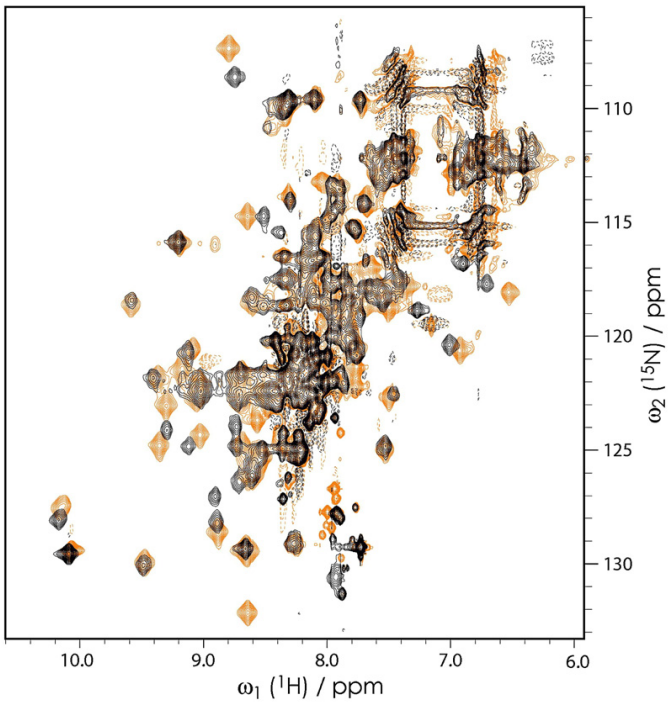

Fig. 3. The $^{15}N,^{1}H$ HMQC NMR spectra of $YscU^{C}$. The contour lines of wild type $YscU^{C}$ are orange, and those of $YscU^{C}$ N263A are black.

Shigella flexneri.[29] The crystal structures of the cleaved wild type EscU as well as a number of EscU variants were determined and correlated with *in vivo* cleavage experiments of full-length EscU (variants). Wild type EscU, SpaS and Spa40 reveal unchanged tertiary structures of nicked proteins, concurring with our conclusion based on NMR-analysis of $YscU^{C}$ wild type and mutant.

The only major differences concern $YscU^{C}$ variants H266A and R314A and their homologous variants *in vivo* in full-length EscU. Both $YscU^{C}$ variants show partial autocleavage *in vitro* and a wild type-like secretion of LcrV *in vivo*. EscU variant H265A is found be fully autocleaved but secretion of T3S substrates is lost.[28] EscU variant R313A, by contrast, remains uncleaved but again T3S substrates secretion is lost.[28] A third EscU variant, R133T, is fully cleaved but retains normal effector secretion.[28] Thus, despite a high level of structural conservation between YscU and EscU, some differences between the *Yersina* and EPEC T3SS may exist. The *in vitro* cleavage data on $YscU^{C}$ His266 variants would presumably implicate His265 in EscU in the asparagine-driven autocleavage reaction.

We propose the following autocleavage reaction mechanism (Fig. 7). (i) The unique reaction geometry of YscU and its homologues is a prerequiste for the nucleophilic attack. The β-amide nitrogen, activated through proton abstraction by His266 or an intermediate water molecule, is optimally positioned to attack the electrophilic carbonyl carbon at an angle of 109° (108° in EscU). (ii) The tetrahedral reaction intermediate is stabilized by hydrogen bonds to the backbone amides of His266 and Ile267. (iii) Protein cleavage gives rise to a labile succinimide, which is rapidly hydrolysed to yield a new C-terminal asparagine or iso-asparagine.

The structure of $YscU^{C}$ also explains phenotypes of previously reported YscU variants. The strongly reduced export of the presumed inner rod protein YscI (in an *yscPyscU* mutant background) in the YscU variant Y317D implicates Tyr317 in interacting directly with YscI.[35] Structurally, this strictly conserved residue is fully exposed at the surface of α-helix 3. Presumably, the introduction of a negative charge prevents interaction with YscI explaining the observed phenotype.[28] The YscU variant G270N has been reported to cause the complete loss of T3S and YscU autocleavage.[36] Gly270, in the middle in β-strand II, is fully buried in the hydrophobic core of the domain. Replacing this by the significantly bulkier asparagine presumably prevents correct protein folding, resulting in the loss of this protein and nonfunctional T3SS.

Needle length in a non-cleavable YscU mutant is controlled even without YscP over-expression

In vivo analyses reveal a new phenotype for the YscU variants N263Q and H266A/R314A. These variants do not undergo autocleavage *in vitro*. Corresponding bacterial mutants do not secrete the translocator LcrV. Their needles are, however, of normal size, although significantly less YscP is secreted compared to wild type bacteria (data not shown). In the YscU N263A mutant, wild type needle length could be restored only by YscP over-expression implying that YscU autocleavage inhibition diminishes YscP

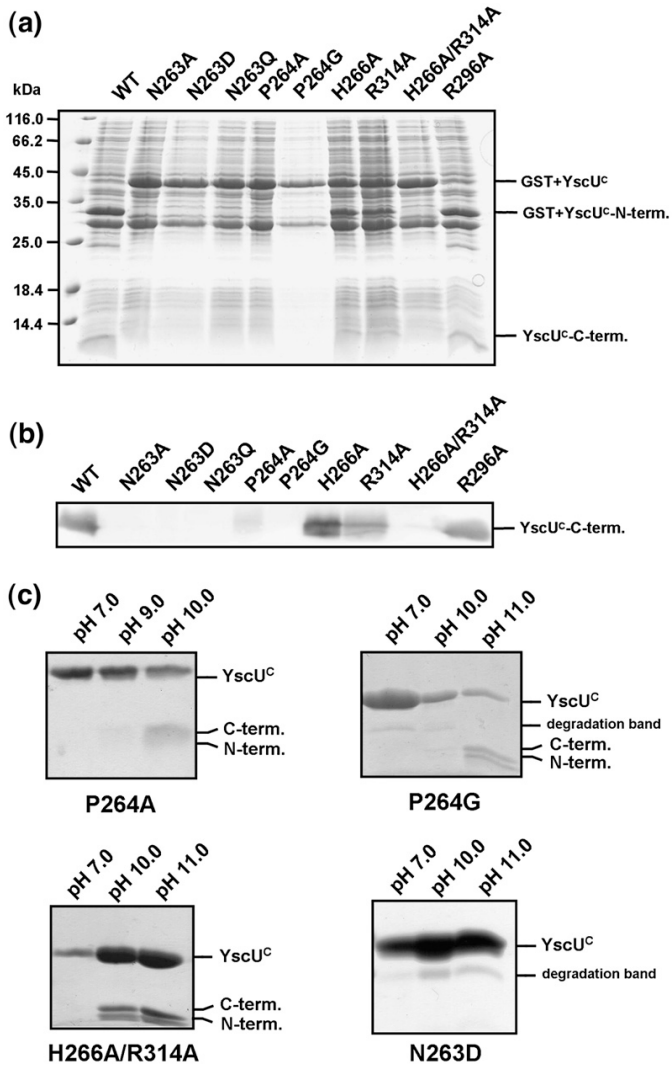

Fig. 4. Cleveage behaviour of different YscU^C variants expressed in *E. coli*. (a) Coomassie brilliant blue-stained SDS/15% PAGE analysis of cells producing various YscU^C variants. (b) Over-expressed cells analysed by immunoblotting using an anti-YscU^C antibody. (c) The pH-dependent cleavage of YscU^C-variants. SDS-PAGE analysis of purified YscU^C-variants incubated at different pH values.

secretion losing control over needle length.[22] The phenotype observed here for the variants N263Q and H266A/R314A demonstrates that the inhibition of the autocleavage may indeed affect the secretion of YscP and LcrV without relinquishing control over needle length. The fact that different phenotypes are observed for N263A and N263Q despite involving the same residue, may indicate that small amounts of YscP are sufficient to determine needle length but that a defined conformation of YscU is also required.

The flexible linker region is composed of two hinged α-helices

A structural superposition of uncleaved YscU^C variant N263A with EscU^C (rmsd 1.3 Å for 94 common Cα atoms), SpaS form *Salmonella typhimurium* (rmsd 1.0 Å for 80 Cα atoms), and Spa40 from *Shigella flexneri* (rmsd 1.0 Å for 82 Cα atoms) reveal virtually identical folds for the cytoplasmic core region and

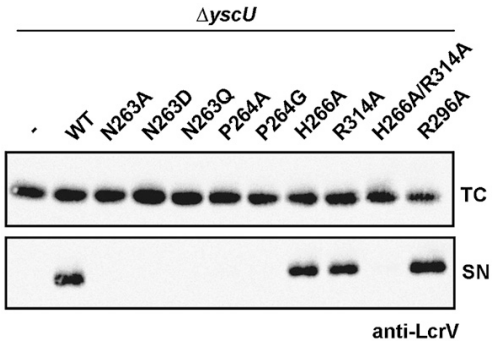

Fig. 5. Analysis of LcrV secretion by different *yscU* mutants. Total cell (TC) and supernatant (SN) fractions of corresponding *in trans* complemented *Yersinia* Δ*yscU* mutant bacteria analysed by immunoblot with anti-LcrV antibodies.

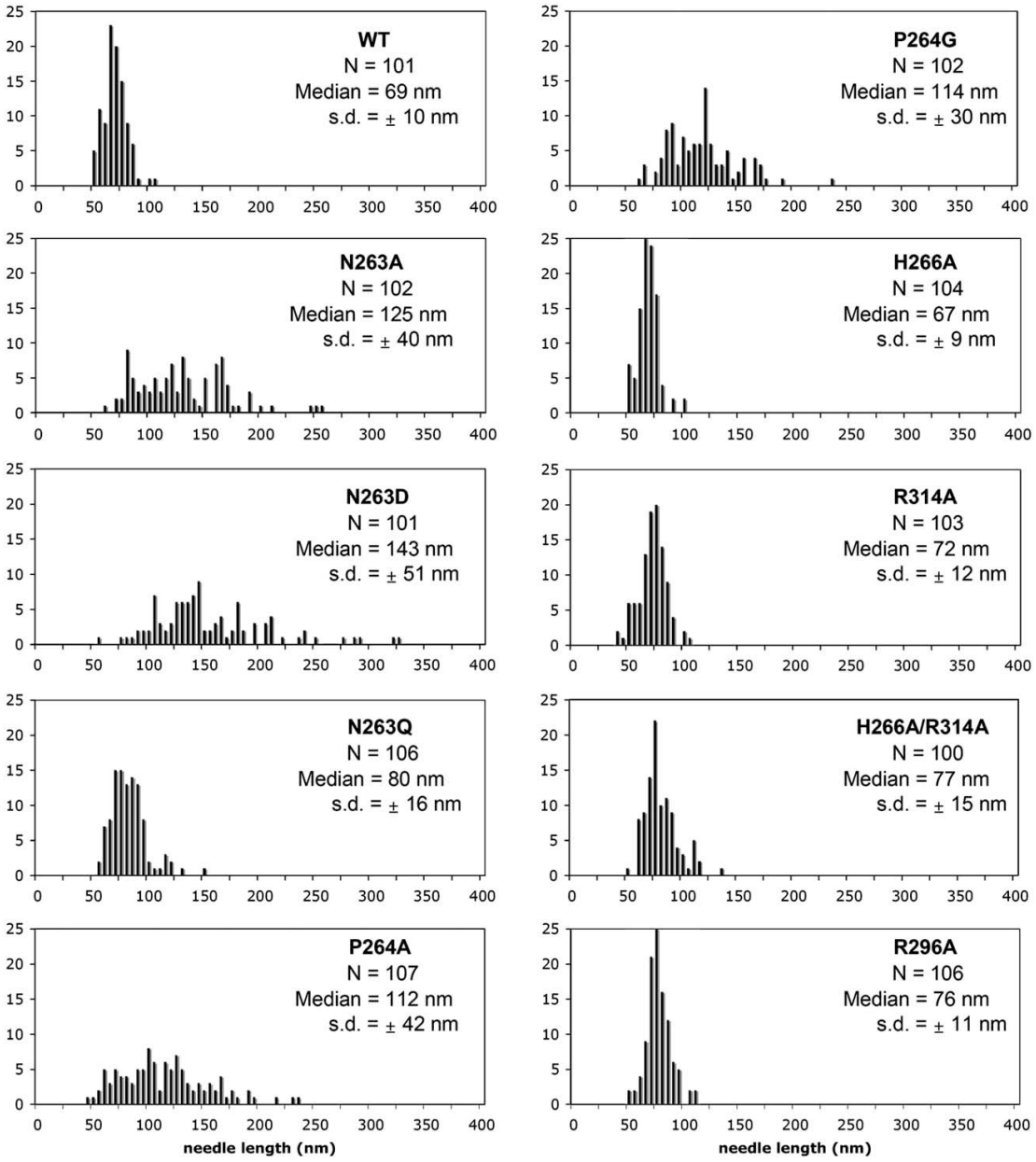

Fig. 6. Needle length measurements of *yscU* mutant bacteria expressing the corresponding yscU alleles *in trans* from the pBAD promoter. The median, the standard deviation (sd), and the number of needles measured (*N*) are indicated.

the NPTH motifs (Fig. 8b), despite a low level of overall sequence identity (Fig. 8a).

An obvious difference between $YscU^C$ and its homologues $EscU^C$, $SpaS^C$ and $Spa40^C$ involves the proposed flexible linker (211–248) connecting the globular autocleavage domain to the N-terminal membrane-spanning four-helix bundle (Fig. 8b). In $YscU^C$, amino acids 232–244 form a well-defined α-helix, which is not observed in the homologous structures. In the crystal structure of $YscU^C$, α-helix α0 is involved in a crystal contact to α-helix α4 of the next monomer. One of the crystal forms of $EscU^C$ reveals a further α-helix (α-1) N-terminal of α0.[28] The presence of α-helix α0 confirms earlier predictions of the secondary structure for the flagellar protein FlhB.[37]

The linker region is essential for T3S.[28] Corresponding deletions 232–236, 234–245 and 230–245 in

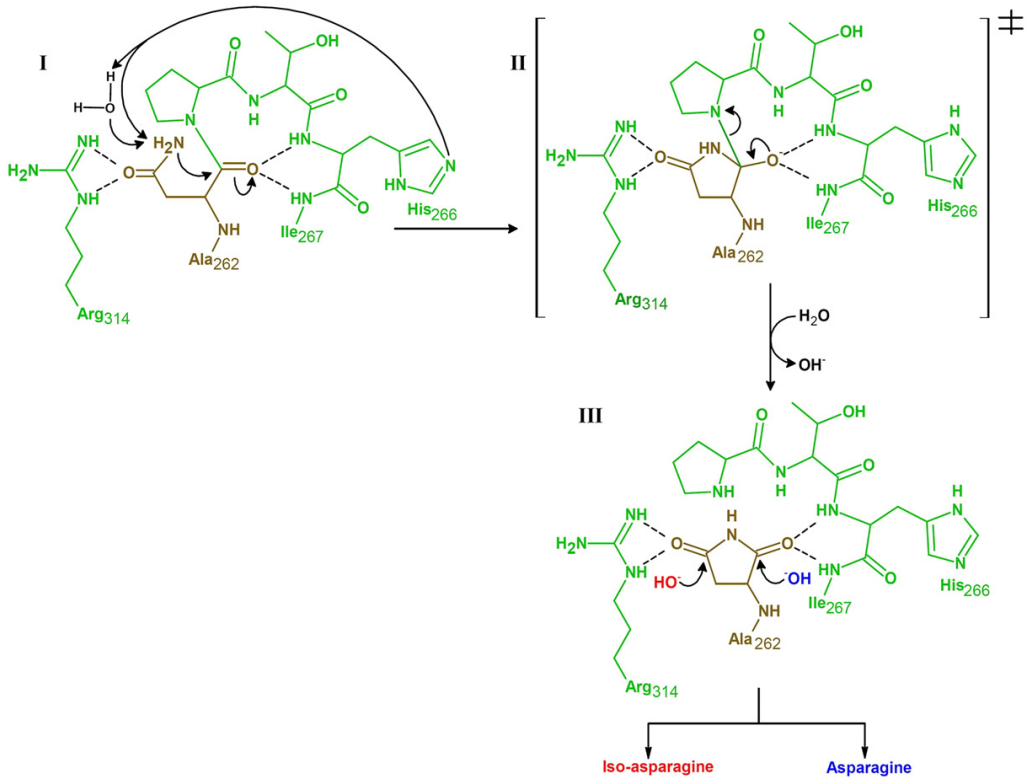

Fig. 7. Structure-based model of succinimide-mediated cleavage of YscU. (I) His266 (or a His266-activated water molecule) abstracts a proton from the β-amide nitrogen of Asn263. The latter makes a nucleophilic attack on the Asn263 carbonyl, resulting in the rate-limiting tetrahedral intermediate (II). Cleavage of the peptide bond yields a labile C-terminal succinimide (III), which is hydrolysed to asparagine or iso-asparagine.

EscU and the point mutation G235P (S236P in YscU) abolish the export of T3S substrates, despite autocleavage of EscU being detectable. Similar results have been obtained for the FlhB protein.[37] Mapping these mutations onto the structure of YscU^C indicates that each would delete or kink α-helix α0, which presumably functions as a spacer element, separating the globular autocleavage domain from the inner membrane. Additionally, the helix could be involved in direct or indirect binding of other components.

Amino acids such as Gly229 and Gly248 in EscU are assumed to provide flexibility to the linker region.[28] Substituting conserved Gly229 by proline in EscU (G230 in YscU and located N-terminal of α-helix α0) decrease the export of T3S substrates dramatically. An equivalent substitution in Gly247 (G248P in YscU and located C-terminal of α0) also reduces the export of T3S substrates. Combining the structural information on YscU^C and EscU^C with the *in vivo* data suggests that YscU-like proteins are composed of three units (Fig. 9): A membrane-spanning N-terminal domain and a C-terminal, cytoplasmic, globular, autocleavage domain bridged by a flexible linker region that can switch from an extended to a partially α-helical conformation. This adaptable architecture of the linker allows for sufficient conformational freedom to enable interactions of the autocleavage domain with other components of the T3SS during T3SS assembly.

Materials and Methods

YscU *in vivo* experiments

Bacterial strains, plasmids and genetic constructions are given in Supplementary Data Table 1. *E. coli* Top10 was used for plasmid purification and cloning. Bacteria were grown routinely on Luria-Bertani (LB) agar plates and in liquid LB medium. Ampicillin was used at concentrations of 200 μg/ml.

Plasmids were generated using either the *Pfu* turbo polymerase (Stratagene) or Vent DNA polymerase (New England, Biolabs). Oligonucleotides for genetic constructs are given in Supplementary Data Table 2. All constructs were confirmed by sequencing using a 3100-Avant genetic analyser (ABI Prism).

LcrV secretion and immunoblotting

Induction of the *yop* regulon was as described by Cornelis et al.[38] Expression of the different genes cloned downstream of the pBAD promoter was induced routinely by adding 0.2% l-arabinose to the culture before the shift to

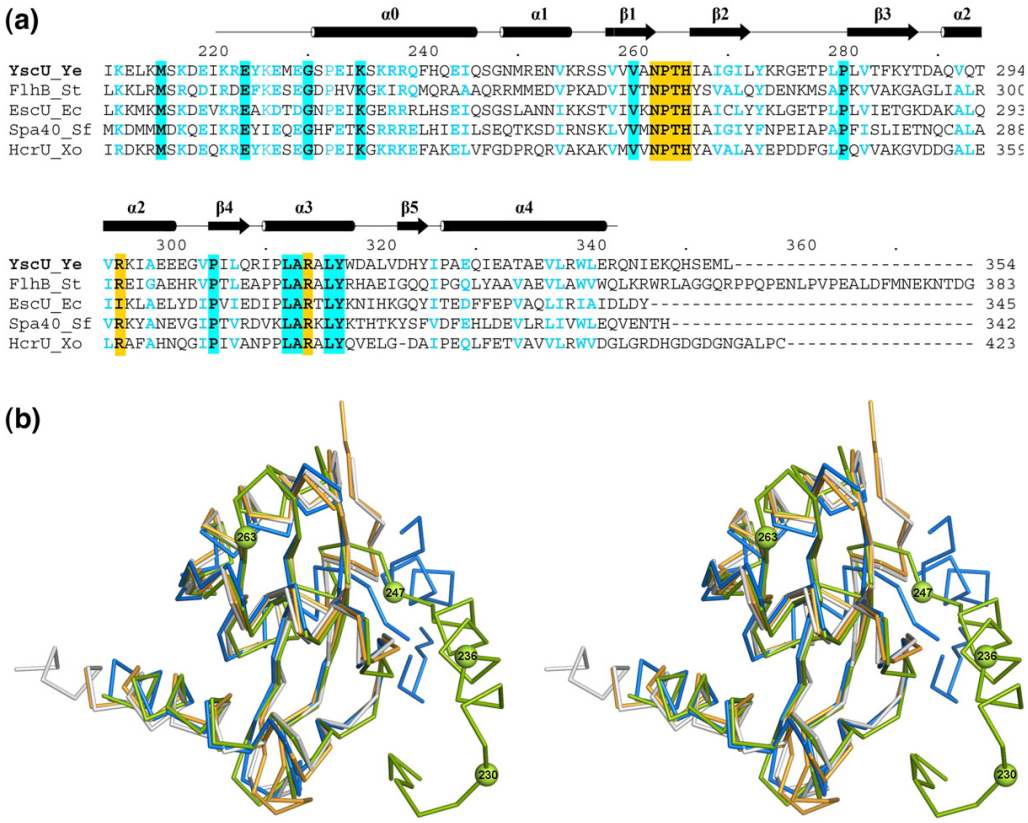

Fig. 8. (a) Structure-based sequence alignment of YscU^C from *Y. enterocolitica* (Swiss-Prot. accession number Q56844) with FlhB^C from *S. typhimurium* (P40727), EscU^C from *E. coli* (Q7DB59), SpaS^C from *S. typhimurium* (P40702), Spa40^C from *S. flexneri* (Q6XVW1) and HcrU^C from *X. oryzae* (Q5H6T1). The secondary structures are from YscU^C N263D. Conserved amino acids are marked in bold letters on coloured backgrounds. Substituted residues in this study are indicated by a yellow background. Less well conserved amino acids are in bold and coloured blue. (b) A stereoview of the YscU^C variant N263D (green) superimposed on its wild type homologues EscU^C (blue), SpaSC (grey) and Spa40^C (orange). Important positions are marked by a green sphere.

37 °C, and again 2 h later. Glycerol (4 mg/ml) was added as a carbon source when expressing genes from the pBAD promoter. Total cell and supernatant fractions were separated by centrifugation at 20,800*g* for 10 min at 4 °C. The cell pellet was taken as the total cell fraction. Proteins in the supernatant were precipitated with 10% (w/v) trichloroacetic acid (final concentration) for 1 h at 4 °C.

Supernatant (SN) and total cell (TC) fractions were separated by SDS/12% PAGE. In each case, proteins secreted (SN) or produced (TC) by 2.5×10^7 bacteria were loaded in each lane. Immunoblotting was done using rabbit polyclonal antibodies against LcrV (MIPA220; 1:2000). Detection was done with the respective secondary antibodies conjugated to horseradish peroxidase (1:5000; Dako), before development with supersignal chemiluminescent substrate (Pierce).

Electron microscopy

Needles were visualized by transmission electron microscopy as described.[8,23] After induction of the *yop* regulon at 37 °C for 4 h bacteria were harvested by centrifugation at 2000*g* and suspended gently in 20 mM Tris–HCl, pH 7.5. Droplets were applied for 1 min to freshly glow-discharged, formvar-carbon coated grids, and negatively stained with 2% (w/v) uranyl acetate. Bacteria were visualized in a Philips CM100 transmission electron microscope at a nominal magnification of 20,000× and an acceleration voltage of 80 kV. Sizes were measured with Soft imaging system software (Hamburg, Germany).

Expression and purification of YscU^C

The cytoplasmic domain of YscU^C was expressed in *E. coli* Tuner (DE3) cells using vector pGEX-6P-1 (GE Healthcare). A single colony was used to inoculate a preculture of 20 mL of L-B medium with 100 μg/mL of ampicillin. The cells were grown at 37 °C to an A_{600} of 0.6. A 10 mL preculture was transferred in 1 L of Terrific Broth (100 μg/mL of ampicillin), grown at 37 °C to an A_{600} of 0.6, supplemented with 0.2 mM isopropyl thiogalactopyranoside, incubated for 16 h, and then harvested by centrifugation.

Harvested cells were resuspended in PBS, containing 2 μL of Benzonase (250 U/mL, Novagen) and one tablet of Complete Mini Protease Inhibitor (Roche). Cells were lysed by French press and centrifuged. The supernant was incubated with glutathione Sepharose (GS, GE Healthcare)

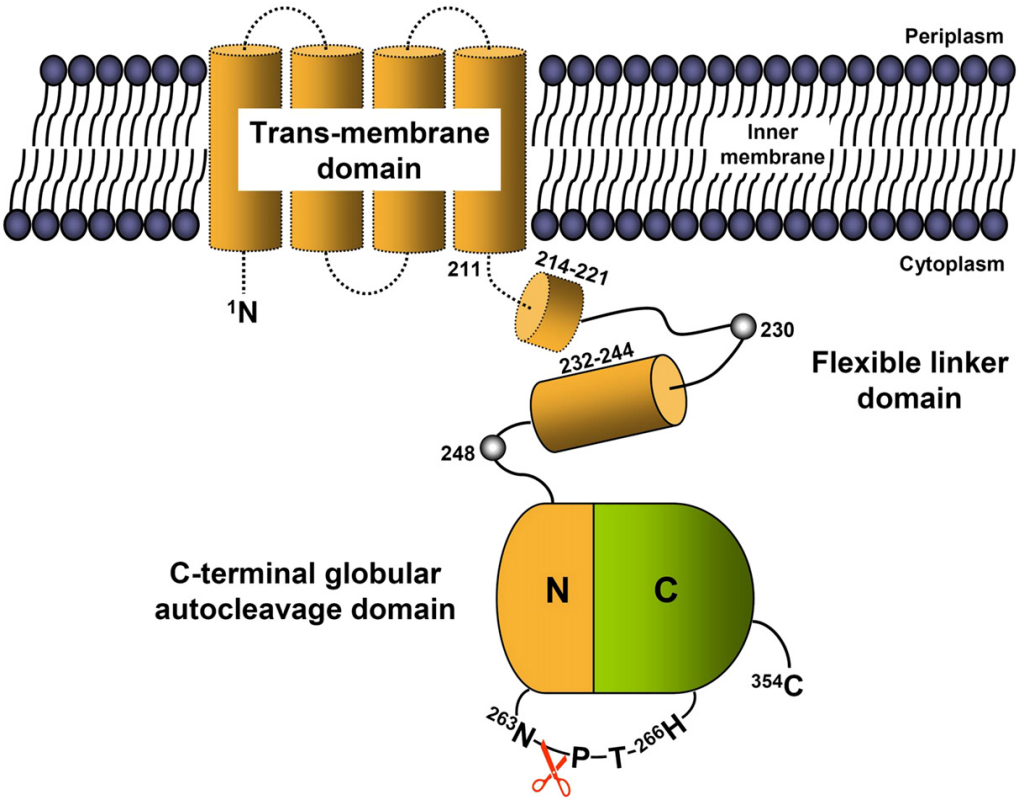

Fig. 9. Model of the tripartite domain arrangement of YscU. The N-terminal, membrane-spanning domain is followed by a flexible linker region and a globular autocleavage domain.

for 4 h at 4 °C. Unbound protein was washed three times from the GS column with protease buffer (50 mM Trizma base, pH 7.5, 150 mM NaCl, 1 mM DTT, 1 mM EDTA). A 75 μL sample of PreScission Protease (GE Healthcare) in 10 mL of protease buffer was incubated with loaded GS overnight at 4 °C. The protein was eluted four times with protease buffer and dialysed against buffer A (20 mM Hepes, pH 7.0, 100 mM NaCl). The protein solution was applied to a cation-exchange column (MonoS, GE Healthcare) equilibrated with buffer A and eluted with a 0.1 M – 1 M NaCl gradient in buffer A. The $YscU^C$-containing fractions were identified by SDS-PAGE, concentrated to 5 – 15 mg/mL and further purified using a gel permeation column (Superdex S75 16/60, GE Healthcare) equilibrated with 20 mM Hepes, pH 7.0, 150 mM NaCl. l-Selenomethionine (SeMet)-labelled and ^{15}N-labelled $YscU^C$ N263A, as well as ^{15}N-labelled $YscU^C$ wild type were produced as described.[39] $YscU^C$ mutations were introduced using the QuikChange kit (Stratagene) and verified by DNA sequencing (GATC, Konstanz, Germany). $YscU^C$ variants were purified as described above.

Preparation of pH-dependent cleavage

The different $YscU^C$ variants were expressed and purified as described above. P264A was dialysed against 25 mM Ches buffer (pH 7.0, 9.0 and 10.0), 100 mM NaCl for 3 h at room temperature. P624G, H266A/R314A and N263D were dialysed against 25 mM Caps (pH 7.0, 10.0 and 11.0) buffer, 100 mM NaCl for 4 h at room temperature. Afterwards, the solution of protein P264G was stored for 48 h and H266A/R314A and N263D were stored for 24 h at 4 °C. Cleaved proteins were submitted to SDS/15% PAGE and stained with Coomassie brilliant blue.

Crystallization and structure determination

$YscU^C$ N263A and its SeMet-labelled derivative were crystallised using the hanging drop method using 3 μL of a 8 mg/mL protein solution mixed with 3 μL of reservoir buffer (1.6 M $(NH_4)_2SO_4$, 0.2 M NaCl, 0.1 M Hepes, pH 7.5) in the droplet. Crystals grew within ~4 days at 20 °C to sizes of up to 180 μm × 180 μm × 120 μm. Crystals were transferred in cryo buffer containing reservoir buffer with 16% (v/v) glycerol as a cryoprotectant and flash-frozen at 100 K in liquid nitrogen. Four multiwavelength anomalous diffraction (MAD) data sets of SeMet-labelled $YscU^C$ N263A were collected at beamline X12 at the EMBL Outstation (Hamburg, Germany), and processed with the HKL2000[40] and MOSFLM.[41] Localization of two selenium sites, which were used for phasing and the generation of a partial model, was done with AUTORICKSHAW.[42] Manual model building was carried out using COOT[43] and refinement was completed using REFMAC5.[44]

The X-ray data set of $YscU^C$ N263D was collected at ESRF beamline ID29 (Grenoble, France), processed with MOSFLM[41] and scaled with SCALA.[45] Using REFMAC5[46] and SeMet-labelled $YscU^C$ N263A as a phasing model, the

structure was solved by difference Fourier and further refined with COOT[43] and REFMAC5.[44]

The validation of both structures was done with MOLPROBITY.[47] Data collection and refinement statistics are given in Table 1. Figures were prepared using PyMOL†.

NMR analysis

For NMR spectroscopy, we used a 12 mg/mL solution of uniformly ^{15}N-labelled YscU^{C} in a mixed solvent of 95% (v/v) H_2O, 5% (v/v) ^2H_2O and a 10 mg/mL solution of YscU^{C} N263A in the same solvent. The NMR samples contained 50 mM NaCl, 3 mM KCl, 12 mM Na_2HPO_4 and 2 mM KH_2PO_4 at pH 6.8. The Bruker Advance III 600 spectrometer used for this study was equipped with a 5 mm *Z*-axis gradient triple-resonance cryo-probehead. The 2D [^{15}N,^{1}H] correlation spectra were recorded at ω_1 = 2100 Hz and ω_1 = 8400 Hz. The maximal evolution times were t_{1max} = 60 ms and t_{2max} = 240 ms and the time domain data size was 256 × 2048. Programs PROSA[48] and CARA[49] were used for data processing and spectral analysis, respectively.

Protein Data bank accession codes

The coordinates have been deposited in the Protein Data bank (PDB) under accession code 2v5g and 2w0r.

Acknowledgements

We thank Hauke Pagel for his support during the initial stage of protein preparation. We are grateful to Dr Manfred Weiss (DESY/ EMBL, beamline X12), the team of ESRF-ID29, for helping during data collection and processing. We are grateful to Dr Victor Wray and Dr Wolf-Dieter Schubert for critical comments on the manuscript. D.W.H. acknowledges support by the Fonds der Chemischen Industrie. This work was supported by the Swiss National Science Foundation (grant 310000 – 113333/1 to GRC).

Supplementary Data

Supplementary data associated with this article can be found, in the online version, at doi:10.1016/j.jmb.2008.10.034

References

1. Macnab, R. M. (2003). How bacteria assemble flagella. *Annu. Rev. Microbiol.* **57**, 77–100.
2. Blocker, A., Gounon, P., Larquet, E., Niebuhr, K., Cabiaux, V., Parsot, C. & Sansonetti, P. (1999). The tripartite type III secreton of *Shigella flexneri* inserts IpaB and IpaC into host membranes. *J. Cell Biol.* **147**, 683–693.
3. Blocker, A., Jouihri, N., Larquet, E., Gounon, P., Ebel, F., Parsot, C. *et al.* (2001). Structure and composition of the *Shigella flexneri* "needle complex", a part of its type III secreton. *Mol. Microbiol.* **39**, 652–663.
4. Marlovits, T. C., Kubori, T., Sukhan, A., Thomas, D. R., Galan, J. E. & Unger, V. M. (2004). Structural insights into the assembly of the type III secretion needle complex. *Science*, **306**, 1040–1042.
5. Morita-Ishihara, T., Ogawa, M., Sagara, H., Yoshida, M., Katayama, E. & Sasakawa, C. (2006). *Shigella* Spa33 is an essential C-ring component of type III secretion machinery. *J. Biol. Chem.* **281**, 599–607.
6. Kubori, T., Matsushima, Y., Nakamura, D., Uralil, J., Lara-Tejero, M., Sukhan, A. *et al.* (1998). Supramolecular structure of the *Salmonella typhimurium* type III protein secretion system. *Science*, **280**, 602–605.
7. Kubori, T. & Galan, J. E. (2002). *Salmonella* type III secretion-associated protein InvE controls translocation of effector proteins into host cells. *J. Bacteriol.* **184**, 4699–4708.
8. Hoiczyk, E. & Blobel, G. (2001). Polymerization of a single protein of the pathogen *Yersinia enterocolitica* into needles punctures eukaryotic cells. *Proc. Natl Acad. Sci. USA*, **98**, 4669–4674.
9. Van Gijsegem, F., Vasse, J., Camus, J. C., Marenda, M. & Boucher, C. (2000). *Ralstonia solanacearum* produces hrp-dependent pili that are required for PopA secretion but not for attachment of bacteria to plant cells. *Mol. Microbiol.* **36**, 249–260.
10. Knutton, S., Rosenshine, I., Pallen, M. J., Nisan, I., Neves, B. C., Bain, C. *et al.* (1998). A novel EspA-associated surface organelle of enteropathogenic *Escherichia coli* involved in protein translocation into epithelial cells. *EMBO J.* **17**, 2166–2176.
11. Daniell, S. J., Takahashi, N., Wilson, R., Friedberg, D., Rosenshine, I., Booy, F. P. *et al.* (2001). The filamentous type III secretion translocon of enteropathogenic *Escherichia coli*. *Cell. Microbiol.* **3**, 865–871.
12. Crepin, V. F., Shaw, R., Abe, C. M., Knutton, S. & Frankel, G. (2005). Polarity of enteropathogenic *Escherichia coli* EspA filament assembly and protein secretion. *J. Bacteriol.* **187**, 2881–2889.
13. Mota, L. J. & Cornelis, G. R. (2005). The bacterial injection kit: type III secretion systems. *Ann. Med.* **37**, 234–249.
14. Cornelis, G. R. (2006). The type III secretion injectisome. *Nat. Rev., Microbiol.* **4**, 811–825.
15. Michiels, T. & Cornelis, G. R. (1991). Secretion of hybrid proteins by the *Yersinia* Yop export system. *J. Bacteriol.* **173**, 1677–1685.
16. Galan, J. E. & Wolf-Watz, H. (2006). Protein delivery into eukaryotic cells by type III secretion machines. *Nature*, **444**, 567–573.
17. Journet, L., Agrain, C., Broz, P. & Cornelis, G. R. (2003). The needle length of bacterial injectisomes is determined by a molecular ruler. *Science*, **302**, 1757–1760.
18. Mueller, C. A., Broz, P., Muller, S. A., Ringler, P., Erne-Brand, F., Sorg, I. *et al.* (2005). The V-antigen of *Yersinia* forms a distinct structure at the tip of injectisome needles. *Science*, **310**, 674–676.
19. Goure, J., Broz, P., Attree, O., Cornelis, G. R. & Attree, I. (2005). Protective anti-V antibodies inhibit Pseudomonas and *Yersinia* translocon assembly within host membranes. *J. Infect. Dis.* **192**, 218–225.
20. Makishima, S., Komoriya, K., Yamaguchi, S. & Aizawa, S. I. (2001). Length of the flagellar hook and the capacity of the type III export apparatus. *Science*, **291**, 2411–2413.
21. Marlovits, T. C., Kubori, T., Lara-Tejero, M., Thomas, D., Unger, V. M. & Galan, J. E. (2006). Assembly of the inner rod determines needle length in the type III secretion injectisome. *Nature*, **441**, 637640.

† http://pymol.org

22. Sorg, I., Wagner, S., Amstutz, M., Muller, S. A., Broz, P., Lussi, Y. *et al.* (2007). YscU recognizes translocators as export substrates of the *Yersinia* injectisome. *EMBO J.* **26**, 3015–3024.
23. Agrain, C., Callebaut, I., Journet, L., Sorg, I., Paroz, C., Mota, L. J. & Cornelis, G. R. (2005). Characterization of a Type III secretion substrate specificity switch (T3S4) domain in YscP from *Yersinia enterocolitica*. *Mol. Microbiol.* **56**, 54–67.
24. Agrain, C., Sorg, I., Paroz, C. & Cornelis, G. R. (2005). Secretion of YscP from *Yersinia enterocolitica* is essential to control the length of the injectisome needle but not to change the type III secretion substrate specificity. *Mol. Microbiol.* **57**, 1415–1427.
25. Allaoui, A., Woestyn, S., Sluiters, C. & Cornelis, G. R. (1994). YscU, a *Yersinia enterocolitica* inner membrane protein involved in Yop secretion. *J. Bacteriol.* **176**, 4534–4542.
26. Minamino, T. & Macnab, R. M. (2000). Domain structure of *Salmonella* FlhB, a flagellar export component responsible for substrate specificity switching. *J. Bacteriol.* **182**, 4906–4914.
27. Lavander, M., Sundberg, L., Edqvist, P. J., Lloyd, S. A., Wolf-Watz, H. & Forsberg, A. (2002). Proteolytic cleavage of the FlhB homologue YscU of *Yersinia pseudotuberculosis* is essential for bacterial survival but not for type III secretion. *J. Bacteriol.* **184**, 4500–4509.
28. Zarivach, R., Deng, W., Vuckovic, M., Felise, H. B., Nguyen, H. V., Miller, S. I. *et al.* (2008). Structural analysis of the essential self-cleaving type III secretion proteins EscU and SpaS. *Nature*, **453**, 124–127.
29. Deane, J. E., Graham, S. C., Mitchell, E. P., Flot, D., Johnson, S. & Lea, S. M. (2008). Crystal structure of Spa40, the specificity switch for the *Shigella flexneri* type III secretion system. *Mol. Microbiol.* **69**, 267–276.
30. Bürgi, H. B., Dunitz, J. D. & Shefter, E. (1973). Geometrical reaction coordinates. II. Nucleophilic addition to a carbonyl group. *J. Am. Chem. Soc.* **95**, 5065–5067.
31. Bürgi, H. B., Dunitz, J. D., Lehn, J. M. & Wipff, G. (1974). Stereochemistry of reaction paths at carbonyl centres. *Tetrahedron*, **30**, 1563–1572.
32. Ferris, H. U., Furukawa, Y., Minamino, T., Kroetz, M. B., Kihara, M., Namba, K. & Macnab, R. M. (2005). FlhB regulates ordered export of flagellar components via autocleavage mechanism. *J. Biol. Chem.* **280**, 41236–41242.
33. Ding, Y., Xu, M. Q., Ghosh, I., Chen, X., Ferrandon, S., Lesage, G. & Rao, Z. (2003). Crystal structure of a mini-intein reveals a conserved catalytic module involved in side chain cyclization of asparagine during protein splicing. *J. Biol. Chem.* **278**, 39133–39142.
34. Gunasekaran, K., Ramakrishnan, C. & Balaram, P. (1997). Beta-hairpins in proteins revisited: lessons for de novo design. *Protein Eng.* **10**, 1131–1141.
35. Wood, S. E., Jin, J. & Lloyd, S. A. (2008). YscP and YscU switch the substrate specificity of the *Yersinia* type III secretion system by regulating export of the inner rod protein YscI. *J. Bacteriol.* **190**, 4252–4262.
36. Riordan, K. E. & Schneewind, O. (2008). YscU cleavage and the assembly of *Yersinia* type III secretion machine complexes. *Mol. Microbiol.* **68**, 1485–1501.
37. Fraser, G. M., Hirano, T., Ferris, H. U., Devgan, L. L., Kihara, M. & Macnab, R. M. (2003). Substrate specificity of type III flagellar protein export in *Salmonella* is controlled by subdomain interactions in FlhB. *Mol. Microbiol.* **48**, 1043–1057.
38. Cornelis, G., Vanootegem, J. C. & Sluiters, C. (1987). Transcription of the yop regulon from *Y. enterocolitica* requires trans acting pYV and chromosomal genes. *Microb. Pathog.* **2**, 367–379.
39. Guerrero, S. A., Hecht, H. J., Hofmann, B., Biebl, H. & Singh, M. (2001). Production of selenomethionine-labelled proteins using simplified culture conditions and generally applicable host/vector systems. *Appl. Microbiol. Biotechnol.* **56**, 718–723.
40. Otwinowski, Z. M. & Minor, W. (1997). Processing of X-ray diffraction data collected in oscillation mode. *Methods Enzymol.* **276**, 307–326.
41. Leslie, A. G. (2006). The integration of macromolecular diffraction data. *Acta Crystallogr., D Biol. Crystallogr.* **62**, 48–57.
42. Panjikar, S., Parthasarathy, V., Lamzin, V. S., Weiss, M. S. & Tucker, P. A. (2005). Auto-Rickshaw: an automated crystal structure determination platform as an efficient tool for the validation of an X-ray diffraction experiment. *Acta Crystallogr. D*, **61**, 449–457.
43. Emsley, P. & Cowtan, K. (2004). Coot: model-building tools for molecular graphics. *Acta Crystallogr. D*, **60**, 2126–2132.
44. Murshudov, G. N., Vagin, A. A. & Dodson, E. J. (1997). Refinement of macromolecular structures by the maximum-likelihood method. *Acta Crystallogr. D*, **53**, 240–255.
45. Evans, P. (2006). Scaling and assessment of data quality. *Acta Crystallogr. D*, **62**, 72–82.
46. McCoy, A. J., Grosse-Kunstleve, R. W., Storoni, L. C. & Read, R. J. (2005). Likelihood-enhanced fast translation functions. *Acta Crystallogr. D*, **61**, 458–464.
47. Davis, I. W., Leaver-Fay, A., Chen, V. B., Block, J. N., Kapral, G. J., Wang, X. *et al.* (2007). MolProbity: all-atom contacts and structure validation for proteins and nucleic acids. *Nucleic Acids Res.* **35**, W375–W383.
48. Guntert, P., Dotsch, V., Wider, G. & Wuthrich, K. (1992). Processing of multidimensional Nmr data with the new software Prosa. *J. Biomol. NMR*, **2**, 619–629.
49. Keller, R. (2004). Optimizing the process of NMR spectrum analysis and computer aided resonance assignment. ETH, Zürich.

Plasmids	Current strain designation	Genotype and derivation	References
pYV plasmids			
pYV40	WT	pYV plasmid from *Y. enterocolitica* E40	Sory et al, 1995
pYVe22703	pYVe22703	pYV plasmid from *Y. enterocolitica* W227 serotype O:9	Cornelis et al, 1987
pLY4001	Δ*yscU*	pYV40 Δ*yscU;* deletion of yscU codons 1-354	Sorg et al., 2007
Expression plasmids			
pBADMycHisA			Invitrogen
pLY7	$yscU^{+++}$	pBAD:: *yscU*; *yscU* was amplified from pYVe22703 using oligos 3704 and 3724 and cloned into the *NcoI* / *EcoRI* sites of pBADmycHisA	Sorg et al., 2007
pSTW7	$yscU_{N263A}{}^{+++}$	pBAD:: $yscU_{N263A}$; mutation N263A was introduced into pLY7 by site directed mutagenesis using oligos 3725 and 3726	Sorg et al., 2007
pISO153	$yscU_{R314A}{}^{+++}$	pBAD:: $yscU_{R314A}$; mutation R314A was introduced into pLY7 by site directed mutagenesis using oligos 4842 and 4843	this study
pISO166	$yscU_{N263D}{}^{+++}$	pBAD:: $yscU_{N263D}$; mutation N263D was introduced into pLY7 by overlapping PCR using oligos 3724/4955 and 4954/3704	this study
pISO167	$yscU_{N263Q}{}^{+++}$	pBAD:: $yscU_{N263Q}$; mutation N263Q was introduced into pLY7 by overlapping PCR using oligos 3724/4957 and 4956/3704	this study
pISO168	$yscU_{H266A}{}^{+++}$	pBAD:: $yscU_{H266A}$; mutation H266A was introduced into pLY7 by overlapping PCR using oligos 3724/4959 and 4958/3704	this study
pISO169	$yscU_{H266A/R314A}{}^{+++}$	pBAD:: $yscU_{H266A/R314A}$; mutation H266A was introduced into pISO153 by overlapping PCR using oligos 3724/4959 and 4958/3704	this study
pISOA174	$yscU_{P264G}{}^{+++}$	pBAD:: $yscU_{P264G}$; mutation P264G was introduced into pLY7 by site directed mutagenesis using oligos 5031 and 5032	this study
pISOA175	$yscU_{R296A}{}^{+++}$	pBAD:: $yscU_{R296A}$; mutation R296A was introduced into pLY7 by site directed mutagenesis using oligos 5033 and 5034	this study

Supplement 1: Plasmids

[1]Sory MP, Boland A, Lambermont I, Cornelis GR (1995) Identification of the YopE and YopH domains required for secretion and internalization into the cytosol of macrophages, using the cyaA gene fusion approach. *Proc Natl Acad SciU S A* **92:** 11998-12002.
[2]Cornelis G, Vanootegem JC, Sluiters C (1987) Transcription of the yop regulon from *Y. enterocolitica* requires trans acting pYV and chromosomal genes. *Microb Pathog* **2:** 367-379.
[3]Sorg, I., Wagner, S., Amstutz, M., Muller, S. A., Broz, P., Lussi, Y., Engel, A. & Cornelis, G. R. (2007). YscU
recognizes translocators as export substrates of the Yersinia injectisome. *Embo J* **26**, 3015-24.

Supplement 2 Oligonucleotides used for the genetic constructions

No.	Sequence	Restriction site
3704	gatcgaattcttataacatttcggaatg	*EcoRI*
3724	gatcccatggccagcggagaaaagacagag	*NcoI*
4842	atcccattagccgctgctctttattgg	
4843	ccaataaagagcagcggctaatgggat	
4956	gtggtggtagctcagccgacccatattg	
4957	caatatgggtcggctgagctaccaccac	
4958	gctaatccgaccgctattgctattgg	
4959	ccaatagcaatagcggtcggattagc	
5031	gctcatcagtggtggtagctaatgggacccatattgctattggtattctttataagc	
5032	gcttataaagaataccaatagcaatatgggtcccattagctaccaccactgatgagc	
5033	cgatgcccaagttcagactgtggccaaaatagcagaagaagaagg	
5034	ccttcttcttctgctattttggccacagtctgaacttgggcatcg	

Discussion

Length control of the injectisome needle is a crucial step in the assembly of a functional secretion machinery. Different models have been postulated to explain the control mechanism. However, the exact mechanism still remains unclear and the aim of this thesis was to refine the model of length control of the type III secretion injectisome needle.

The protein YscP of *Y. enterocolitica* has two repeated segments [125] within the second ruler region and a high proline content. Sequence comparison of different YscP proteins revealed that the percentage of proline residues and the content of predicted α-helices varies [157]. By proline substitutions and molecular dynamics calculations it could be shown, that not only the number of residues of YscP but also its helical content correlates with needle length [157]. These new data support the molecular ruler model as published by Journet *et al*. [53] which was evocative of the molecular ruler proteins controlling the length of bacteriophage tails [66, 67, 73]. Confirming a direct correlation between the length of the ruler protein and the length of the injectisome needle contradicts the 'inner rod model' which was proposed for length regulation in *Salmonella* [123]. Here, InvJ, the YscP homolog, is proposed to stabilize the socket structure and not to act as a molecular ruler, tape measure, or molecular timer. In this model a direct correlation between needle and InvJ length would not be necessary.

The ruler model in its original form suggests that one molecule of YscP determines the length of one injectisome needle. This implies that YscP and the needle subunit YscF travel inside the growing needle at the same time. Modeling a partially helical YscP protein showed only a partial occupation of the needle channel [157] and thus renders the above assumption possible. However, more than one molecule of YscP could be involved in needle length control. In a dynamic ruler model, YscP and YscF would be exported alternately. In this model YscP could only switch substrate specificity, when the needle has the right length for YscP to be in the right position to switch. In order to distinguish between the two possible models, the number of YscP molecules needed for needle length determination was investigated (Wagner *et al*., submitted). By a genetic approach, two different variants of YscP - a long and a short one - were expressed in one bacterium. These bacteria

exported both variants and analyzing needle length revealed two distinct needle populations (one population of short needles and a second population of long needles). The experimentally obtained needle length distribution was analyzed mathematically and compared to the distributions predicted by mathematical modeling of the various possible scenarios. The experimental data are compatible with the single ruler model and not with the scenarios involving more than one ruler per needle These data suggest that one needle is controlled by only one molecule of YscP, as proposed by the ruler model in its original form (Wagner *et al*., submitted; [53]). This fact is moreover supported by the observations published, by Agrain *et al*. [126] and Wiesand *et al*. [158], that very small amounts of YscP are sufficient to control needle length. In addition, a correlation between the number of needles of a given length and the amount of secreted YscP of that length was observed. This emphasizes the observation that YscP needs to be secreted to fulfill its function. These data contradict the interpretation by Shibata *et al*. [113], who proposes that FliK acts as an internal ruler without being secreted. As mentioned before, the data published by Aizawa and coworkers [113] are, however, not conclusive.

Another question was to understand whether YscP determines the needle length by acting as a molecular ruler or rather as a timer. In the first case, the sequence length of YscP determines needle length, whereas in the second case the time of YscP secretion would determine needle length. For *Shigella* and *Salmonella*, over-expression of the needle subunit (MxiH or PrgI, respectively) leads to elongated needles [31, 123]. These results favour the timer model, when over-expression results in an enhanced/faster export of the needle subunit. In *Y. enterocolitica* elongated needles were only observed upon over-expression of the entire operon *yscEFGHI* (Isabel Sorg, unpublished data, see pages 136-137). To test the timer model, the effect of decreased expression of YscEFGHI was subsequently tested. Decreased expression of YscEFGHI led to very low amounts of needles which were of wild type length (pages 136-137). These results do not support a molecular timer model. The elongated needle length observed while over-expressing YscEFGHI might result from a delayed switching process, due to an increased export rate of the small Ysc proteins.

Assuming the ruler model as proposed by Journet *et al*. [53] is correct, YscP must interact with other proteins in order to fulfill its function. These proteins are most likely located at the base of the basal body and at the tip of the growing needle. Since a *ΔlcrV* mutant strain assembles wild type needles [157] the tip forming protein LcrV can be excluded as binding partner. Several small Ysc proteins (YscI, YscH, YscX and YscO) are secreted as early substrates but the function of these proteins is unknown. Another possible mechanism: YscP forms an umbrella-like structure at the tip of the growing needle which serves as a cap or anchor to sense the distal needle end. For this, an additional binding partner (besides YscF) at the distal needle end would not be necessary. Polymerization of the needle could be the driving force for export of YscP in this model of needle length control. A binding partner at the base of the basal body, however, remains a prerequisite to switch substrate specificity. In the flagellum, FliK was inferred to interact with the soluble carboxy-terminal domain of FlhB (FlhBc) [116]. This interaction plays a crucial role in the switch from hook to filament secretion in the flagellum system. Botteaux *et al*. [132] showed by immuno-precipitation experiments that Spa32, the *Shigella flexneri* homolog of YscP, interacts with Spa40 the homolog of YscU. These data together with the results by Sorg *et al*. [130] show a role for YscU in substrate recognition, suggest an interaction between YscP and YscU in *Y. enterocolitica*. In this thesis, two different experiments to test for interactions between YscU and YscP were done which could later be useful for identification of other binding partners of YscP. The $YscP_{\Delta tail}$ ($YscP_{\Delta 500\text{-}515}$) mutant was included in this study as a control which is not exported by the type III secretion machinery (pages 138-141). The YscP tail might be important for correct recognition of YscP or for correct interaction with its binding partner(s) to switch substrate specificity as suggested for FliK [109]. Preliminary results could not confirm a binding between YscP and YscU, but further investigation is necessary.

The injectisome exports its own distal components before it exports the effectors, which implies that the type III secretion apparatus can recognize and sequentially export different categories of substrates. For this purpose, the apparatus is believed to switch its substrate specificity after completed assembly. Encouraged

by the results for the flagellum where FliK and FlhB are both involved in the substrate specificity switch [105, 116], the role of YscU was investigated in more detail.

For a detailed understanding of this sequential export process, mutations were introduced in the NPTH cleavage site of YscU. In contrast to previous reports on FlhB [116] and YscU [129], the phenotypes resulting from over-expression of cloned *yscU* alleles, and from replacement of the *yscU* alleles on the pYV plasmid to ensure physiological expression levels were analyzed. The results confirmed a cleavage of the 40-kDa YscU into a 30-kDa TM + CN fragment and a 10-kDa CC fragment, as shown previously for FlhB [116] and for YscU from *Y. pseudotuberculosis* [129]. A CC fragment was not detected for the mutant proteins $YscU_{N269A}$ and $YscU_{P264A}$, confirming the results by Lavander *et al.* [159] using C-terminal tagged YscU. The $yscU_{N263A}$ mutant bacteria assembled injectisome needles, but their length was poorly controlled and the median length was almost double the size (111 nm) than for wild type bacteria (67 nm). When the $yscU_{N263A}$ allele was combined with a longer (680 codons) and a shorter (388 codons) allele of *yscP*, the median needle lengths were 222 nm and 91 nm, respectively, indicating that needle length was still dependent on the length of the YscP ruler, although the standard deviation was much larger. In addition to this loose length control, the $yscU_{N263A}$ bacteria released less YscP into the culture supernatant than wild type bacteria. The intrabacterial amount of the protein, however, was unchanged. To overcome the poor export efficiency of YscP, the gene was over-expressed downstream from the pBAD promoter. As expected from previous work by Agrain *et al.* [126], over-expression of the three different *yscP* alleles led to a higher export of YscP proteins and to a better control of needle length. The latter was as good as in *yscU*wt bacteria. Hence, it can be concluded that the $yscU_{N263A}$ mutation reduces the efficacy of the type III secretion system to export or recognize YscP, which indirectly leads to a less stringent control of needle length. Furthermore, the $yscU_{N263A}$ mutation does not affect the capacity of the type III secretion export apparatus to switch off the export of the YscF needle subunits when the needle reaches its genetically defined length. Thus, cleavage at the NPTH motif is not required to switch off needle subunit export. The same variants of YscU and YscP can give rise to two different needle lengths,

depending on the amount of YscP exported. This excludes YscU playing a role as a timer to determine needle length, as proposed for the flagellar hook length control [118].

yscU$_{N263A}$ mutant bacteria were able to release effector Yops, to a slightly lower extent than wt bacteria. Hence, the *yscU*$_{N263A}$ mutation does not affect the substrate specificity switching from early (YscF, YscP) to late (Yops) substrates. The most intriguing phenotype of the *yscU*$_{N263A}$ mutation was the deficiency in export of the translocators LcrV, YopB and YopD. Our results [130] confirmed that YscU plays a critical role in substrate recognition, particularly the structure of the CC fragment. Furthermore, the translocators are specifically recognized by YscU. Thus, the injectisome has at least three classes of substrates. However, evidence for a specific role of the cleavage of the CC fragment in the substrate specificity switch was not found.

The crystal structures of the cytoplasmic domain of YscU (YscU$_C$) variants N263A and N263D were determined at high resolution [158]. Additional single-residue YscU$_C$ variants in the NPTH motif or its immediate vicinity were investigated with respect to their participation in cleavage and needle-length control. The observed phenotype of variants N263Q and H266A/R314A demonstrates that inhibition of auto-cleavage of yscU affects secretion of YscP and LcrV without relinquishing control over needle length. Different phenotypes are observed for N263A and N263Q, indicating that small amounts of YscP are sufficient to determine needle length when YscU is in the correct conformation. This is supporting the ‘one ruler per needle’ model as described above. Preliminary experiments of *yscU*$_{N263Q}$ under physiological conditions (under its native promoter) showed the needle of the new mutant to be shorter than needles from the cleavage site mutant (81±26 nm *versus* 111±43 nm; [130]) but length regulation was not as tight as in wild type bacteria (67±10 nm; pages 134-135). Combining the structural information on YscU$_C$ and EscU$_C$ [158, 160] with the *in vivo* data suggests that YscU-like proteins are composed of three units: a membrane-spanning N-terminal domain and a C-terminal, cytoplasmic, globular, auto-cleavage domain bridged by a flexible linker region that can switch from an extended to a partially α-helical conformation. This

adaptable architecture of the linker gives sufficient conformational freedom to enable interactions of the auto-cleavage domain with other components of the type III secretion system during its assembly.

Based on these results a refined model for length control of the injectisome needle in *Yersinia* can be proposed. The data presented in this thesis suggest that YscP acts as a molecular ruler. One molecule of YscP would measure the length of the growing needle. Whether YscP is anchored at both ends and stretches or whether it is exported during this process (co-translationally or with the help of a chaperone) still remains unclear. Hints for the latter possibility are the direct correlation between the partially folded YscP and the injectisome length. Moreover, the observation that YscP is insoluble and the predicted secondary structure suggest either co-translational export or a need for a chaperone. Since no polymerization cap has been identified and the *ΔlcrV* strain assembles needles of wild type length [157], the N-terminal part of YscP is believed to be outside the needle channel with a certain structure replacing the cap. During needle growth YscP is pulled out of the bacterium. Once the C-terminal domain of YscP (T3S4 domain) is in the right position to interact with its binding partner at the basal body, substrate specificity switches and consequently terminates needle growth. Whether this binding partner is YscU or another member of the export machinery needs further investigation. Furthermore, it remains unclear whether YscP and the needle subunit YscF are exported *via* the same channel in the export machinery, or if different members of the export machinery recognize different substrate classes. Solving the composition and exact function of the export apparatus will help to understand the missing details in needle length control.

For *Shigella*, a similar model for needle length control was suggested [132]. Replacing *spa32* by *Y. enterocolitica yscP* led to needles of controlled length, but longer than in the wild type *Shigella* strain [132]. This fits with the molecular ruler hypothesis: Spa32 consists of 292 residues resulting in needles of 45 +/- 7 nm length, compared to YscP which consists of 515 residues and determines needle length at 65 +/- 10 nm in *Yersinia* and 54 +/- 13 nm in *Shigella* [132]. In contrast, the inner rod model was suggested [123] for needle length control in *Salmonella*

proposing a different function for InvJ, the YscP homolog in *Salmonella*. The data reported in this thesis, especially the direct correlation between YscP length and needle length, can exclude this model of length control for *Yersinia*.

Appendix

Additional results

Insertions in the central part of YscP lead to longer needles

In a previous work, insertions were made between the two export signals at residues 49 and 50 of YscP (site I, Figure A1 A), and an increase in needle length was observed [53]. No insertion was made between residues 137 and 405. The ruler hypothesis predicts that insertions of the same polypeptide at different sites of YscP would lead to the same needle length. To test this, restriction sites were engineered (after codons 186 (site II), 250 (site III) or 390 (site IV)) and either the ruler region of YscP encoding residues 214-374 was duplicated by insertion or the ruler region of its flagellum homolog FliK (amino acids (aa) 151-270) was inserted in either of these three sites (Figure A1 A). Although the extra region was inserted at three different sites, the two sets of recombinant proteins had the same number of residues (i.e., 686 or 645). The inserted domains were the same as the ones inserted earlier after codon 49 [53]. The eight different recombinant genes, expressed downstream from the pBAD promoter were introduced into *yscP* knockout bacteria and needles were measured. As predicted from the ruler hypothesis, needles from clones with insertions at sites I, II or III had the same median length (105 or 106 nm for YscP insertions and 93 or 94 for FliK insertions, Figure A1) and a similar small standard deviation indicating a functional length control. Moreover, YscP mutants with insertions from the FliK protein were able to control needle length to the same degree as YscP mutants with YscP insertions. These data strengthen the ruler model.

In contrast, the clones with the insert at position 390 (site IV) resulted in needles with variable length. This suggests that the insert altered the functionality of YscP presumably due to the close vicinity of the T3S4 domain (aa 405-500; Figure A1 B).

To verify whether the value of 105 nm correlates with the length values determined by other YscP variants, wild type (wt) needles (YscP = 515 aa) and needles assembled by bacteria endowed with the double deletion mutant pCA20 ($YscP_{388}$ = 388 aa) were measured. An extra-long variant of YscP was engineered by

inserting residues 151-270 of FliK, into site III and the YscP repeat (residues 214-374) into site I (805 aa in total). As shown in Figure A1 C, there was a good linear correlation between needle length and the number of residues in YscP, with an increment of 2.1 Å per residue (Figure A1 C).

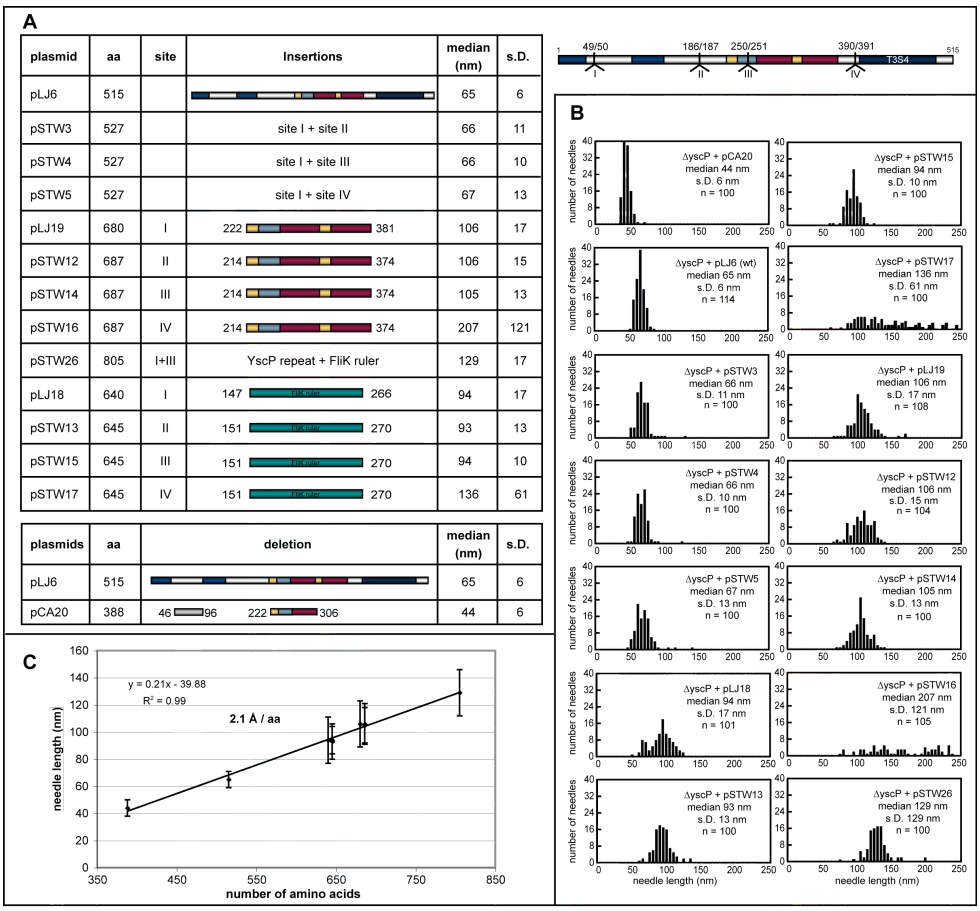

Figure A1

Effect of insertions and deletions within YscP on the needle length.

A. Schematic representation of YscP showing the four engineered restriction sites for insertions. The table shows the inserted or deleted material, the site of insertion, the total number of residues in YscP and the length of the needles.

B. Histograms of length measurements. s.D., standard deviation; n, number of measured needles

C. Correlation of needle length with the total number of residues in YscP. Note that some points are completely overlapping. The unregulated length of the needles controlled by the yscP variants encoded by pSTW16 and pSTW17 are not plotted.

The needle lengths of wt and previously published constructs (pLJ6, pLJ18, pLJ19, pCA20) were slightly different from the values published in a previous work [53] as a result of a better calibration of the microscope. Taken together, these data reinforce the observation that the length of the needle is a direct function of the number of residues in the central region of YscP (aa 36-380).

How many rulers are secreted by the *Yersinia* injectisome?

Insertion of Penicillin Binding Protein into the ruler domain

One attempt to address the question of how many YscP proteins are secreted per injectisome was the labelling of exported YscP with a radioactive marker. The advantage of this method lies in its accuracy due to the sensitivity of the quantification. A prerequisite is the constant labelling of that YscP with the same amount of radioactivity. Since it was shown that large insertions in YscP result in a functional protein ([53]; Figure A1), a hybrid consisting of YscP and a Penicillin Binding Protein (PBP) inserted into the ruler region should allow quantification of secreted YscP by tritium labelled Penicillin. PBP from *Streptomyces* K15 was inserted between export signals 1 and 2 of YscP into pCA23 using restriction sites NotI/XbaI (pSTW18) or into the repeat region of YscP using restriction sites ClaI/SpeI of pSTW4 (pSTW23).

The two YscP mutants were transformed into a *ΔyscP Y. enterocolitica* strain and tested for complementation concerning Yop secretion, YscP export and needle length control. Both mutants had wt levels of Yop secretion. However, the needle length was less controlled (standard deviation: ~ 30 nm) probably due to the weak export level of the fusion proteins. Thus, the YscP-PBP fusion proteins were not suitable to quantitatively study the amount of exported YscP per injectisome needle.

Quantification of secreted YscP and YscF

A second attempt to address the above question was the determination of the number of YscP molecules released in the culture supernatant by quantitative immunoblotting and the number of needles present at the surface of the bacteria. There are, however, three major caveats. First, only exported YscP and YscF molecules must be assayed to avoid overestimation due to the intrabacterial pool of non-exported proteins. This implies that needles need to be quantitatively shaved from the bacterial surface. Second, although the models imply that all YscF subunits polymerize after export, this has never been demonstrated experimentally. Third, it was reported that exported molecules of YscP remain attached at the bacterial surface [125]. Finally, it is unknown if there is unspecific excess export of YscP. This

attempt is therefore only able to show how many rulers are exported per injectisome needle, but not to answer the question of how many rulers are needed to determine the length of one needle.

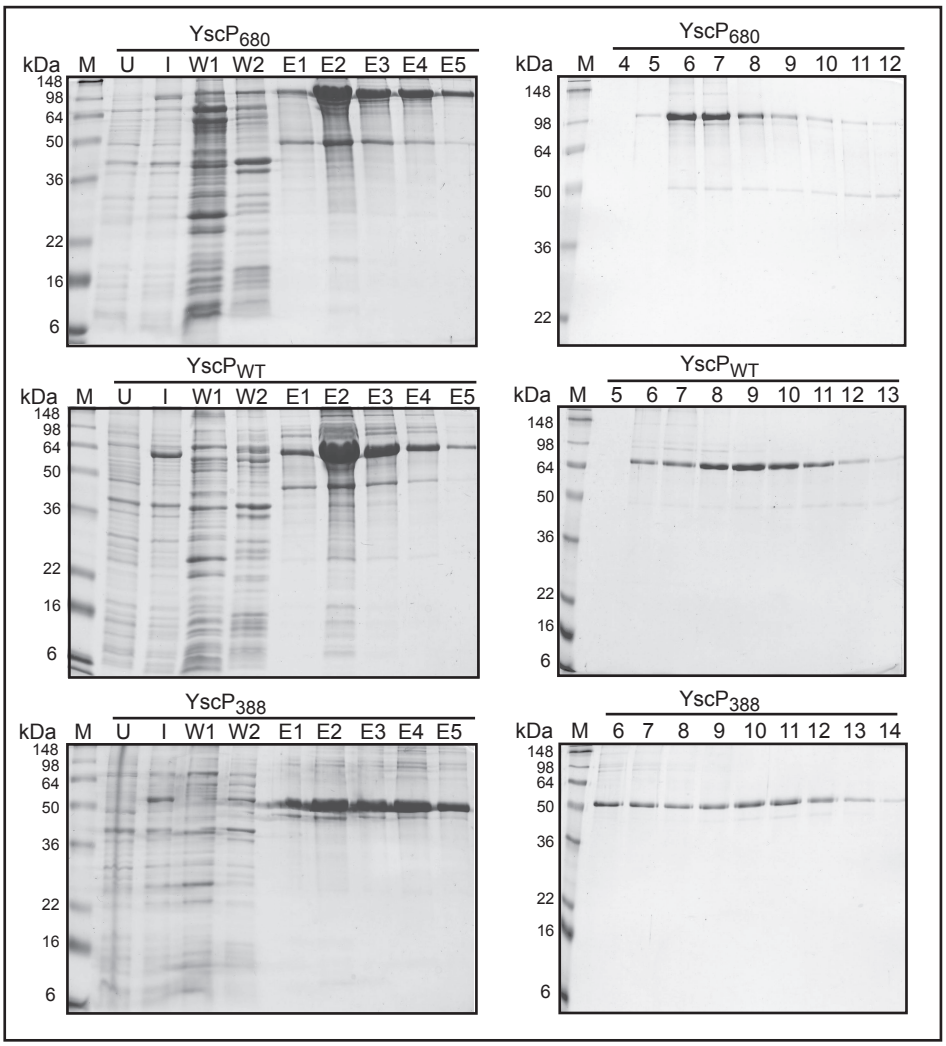

Figure A2

Purification of His_6-tagged YscP variants.
Purification of $YscP_{680}$ (pSTW29), YscP wt (pLJ14) and $YscP_{388}$ (pSTW28) from inclusion bodies under denaturing conditions using 8 M urea. The uninduced (U), induced (I), washing (W) and elution (E) fractions from the nickel-sepharose column were analyzed by SDS-PAGE (left panels). The elution fractions were subjected to a size exclusion column and elution fraction were analyzed by Coomassie-stained SDS-PAGE (right panels).

For the calculation of the ratio of secreted YscP per injectisome needle, the exact amounts of extracellular YscP and extracellular YscF must be quantified. The latter is needed for the calculation of the number of injectisome needles. Purified YscP and

YscF serve as protein standards for quantification of these proteins obtained from the culture supernatant.

$YscP_{388}$ (from pCA20), YscP wt (from pLJ6) and $YscP_{680}$ (from pLJ19) were cloned with a N-terminal His_6-tag downstream of the pBAD promoter (see Table I). Expression of the His_6-tagged proteins in *E. coli* Top10 strains was induced with 0.2% arabinose and bacteria were harvested after 4 hours at 37 °C. Insoluble YscP proteins (data not shown), were purified from inclusion bodies under denaturing conditions using 8 M urea (Figure A2, left panel). Elution fractions # 3 from wt YscP, # 3 from $YscP_{680}$ and # 4 from $YscP_{388}$ were applied to a size exclusion column (Figure A2, right panel). Concentrations from fractions 9 (YscP wt = 213.8 µg/mL), 10 ($YscP_{388}$ = 131.4 µg/mL) and 7 ($YscP_{680}$ = 260.6 µg/mL) were calculated using BSA as protein standard in a Bradford assay.

YscF was purified as GST-tagged fusion protein followed by cleavage of the GST-tag with thrombin (kindly provided by Isabel Sorg; data not shown). The concentration of purified YscF was determined by UV spectroscopy (1.40 mg/mL, data not shown).

Because of the attachment of YscP to the bacterial surface, the bacteria were "shaved" to solubilize YscP from the surface, and to break all the needles from the surface. The shearing was done mechanically by re-suspending the bacterial pellet 40 times in 100 µL buffer using a P-200 pipette. Tris-buffer was tested for shaving of the bacteria at varying pH (6-7), detergent concentrations (Nonidet P 40 substitute (NP 40): 0.01-1%) and salt concentrations (NaCl) under secreting and non-secreting conditions (Figure A3 A and B, respectively). As a control, the supernatant and shearing fractions were tested for cell lysis by immunoblotting using antibodies against the intracellular protein YscJ. As shown in Figure A3 A Tris-buffer containing 0.5% NP 40 at pH 7 (SN + Ca^{2+} sample 5) were optimal conditions for complete removal of the needles from the bacterial surface.

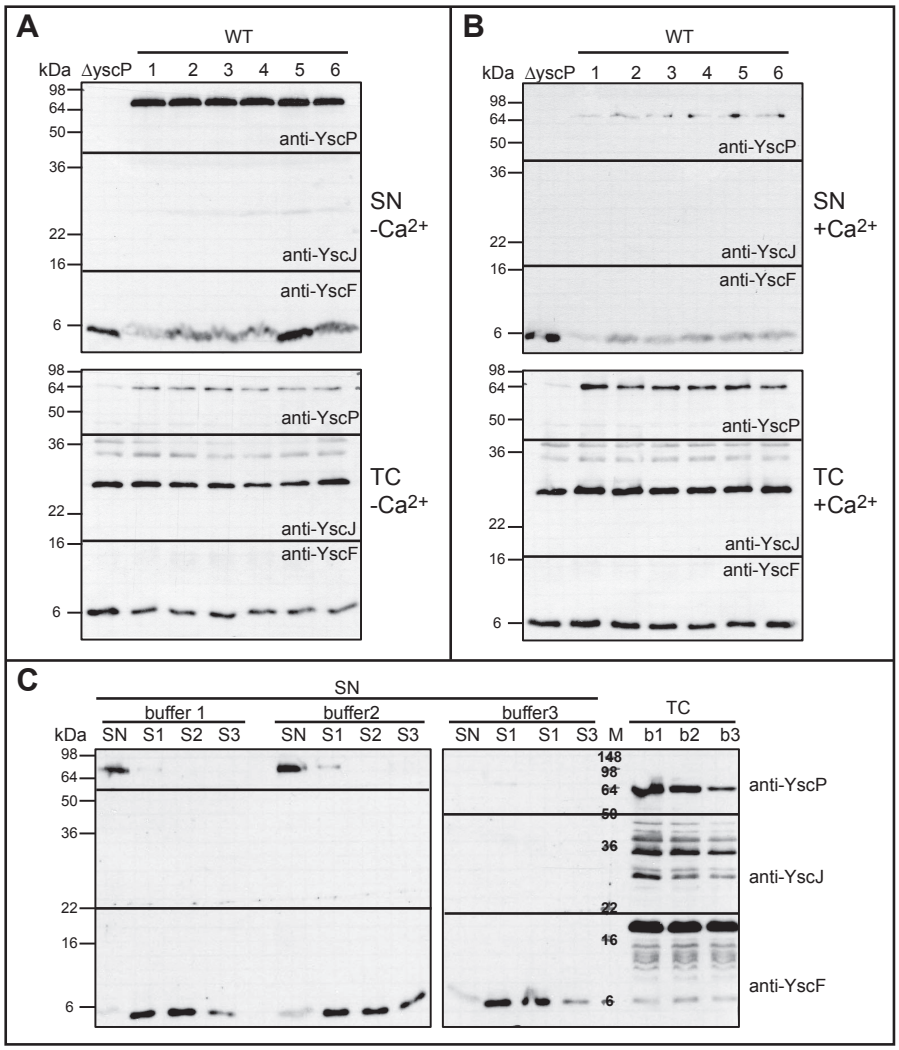

Figure A3

Shaving YscP and injectisome needles from the bacterial surface of *Y. enterocolitica*.

A. Supernatant fractions (SN) and total cell (TC) fractions of *Y. enterocolitica* E40 wt (pYV40) or *Y. enterocolitica* E40 *ΔyscP* (pLJ4036). Cultures were grown in secretion conditions (-Ca^{2+}). Bacterial pellets were treated like usual (see Method section) (1) or sheared mechanically using different buffers: Tris-HCl pH 7, 0.01% NP 40, 100 mM NaCl (2); Tris-HCl pH 6 (3); Tris-HCl pH 6, 1% NP 40 (4); Tris-HCl pH 7, 0.5% NP 40 (5); Tris-HCl pH 7, 1% NP 40 (6). Supernatant and shearing fractions were combined. Supernatant (SN) and total cell (TC) fractions were analyzed by immunoblot using anti-YscP, anti-YscJ and anti-YscF antibodies.

B. Supernatant fractions (SN) and total cell (TC) fractions of the same cultures as in (A). Cultures were grown in non-secretion conditions (+Ca^{2+}). Bacterial pellets were treated like described for (A). Supernatant (SN) and total cell (TC) fractions were analyzed by immunoblot using anti-YscP, anti-YscJ and anti-YscF antibodies.

C. Supernatant fractions (SN) and total cell (TC) fractions of *Y. enterocolitica* E40 wt (pYV40). Culture was grown in non-secretion conditions (+Ca^{2+}). Bacterial pellets were sheared mechanically using different buffers: Tris-HCl pH 7, 0.01% NP 40, 100 mM NaCl (buffer 1); Tris-HCl pH 7, 0.1% NP 40, 200 mM NaCl (buffer 2); Tris-HCl pH 6, 0.5% NP 40 (buffer 3). The shearing was done three times. Supernatant (SN), shearing (S) and total cell (TC) fractions were analyzed by immunoblot using anti-YscP, anti-YscJ and anti-YscF antibodies.

Under these conditions, partial lysis of the bacteria was observed by a faint band for the internal YscJ. Considering this control and the fact that the quantification experiment should be carried out in non-secreting conditions (only assembly of the type III secretion system), the best buffer to shave bacteria was Tris-buffer 2 containing 100 mM NaCl, and 0.01% NP 40 at pH 7 (Figure A3 B). To improve shaving, the number of shearing steps was increased to completely recover YscP and YscF from the bacterial surface.

As shown in Figure A3 C, after the third shearing step bands for YscF and YscP were still detected by immunoblotting, without observing cell lysis. In the experiment shown in Figure A3 C buffer 5 was further adjusted and the best result was obtained using a Tris-buffer with 200 mM NaCl, 0.1% NP 40 at pH 7 (Figure A3 C). In the fifth shearing supernatant fraction YscF and YscP could not be detected. However, a control to prove that all YscP and YscF was completely shaved from the bacterial surface is not available. The conditions used for the quantification experiment were therefore shearing the bacterial pellet five times in 100 µL of shearing buffer (200 mM NaCl, 0.1% NP 40, Tris-HCl pH 7) and combining the supernatant fraction with the five shearing fractions.

Y. enterocolitica wt, *Y. enterocolitica* LJ4022 ($YscP_{388}$) or *Y. enterocolitica* LJM4001 ($YscP_{680}$) were grown at room-temperature in BHI + Ca^{2+} and expression of the type III system was induced by a temperature shift to 37 °C. Bacteria were harvested 2 hours after the temperature shift and samples were prepared as described before. The samples and different amounts of purified YscF and YscP were subjected to a 15% SDS-PAGE and analyzed by immunoblotting using antibodies against YscF and YscP (Figure A4 A). Immunoblots were detected using films, scanned and analyzed using software GelEval 1.21b (demo version, FrogDance software), immunoblots obtained with the Fuji LAS 4000 imager were analyzed by Fujifilm Multi Gauge software. The calculation was performed according to:

*YscP/needle = (ng YscP * (molecules YscF/needle) * MW [YscF]) / (MW [YscP] * ng YscF)*

Several quantification assays were performed, but the resulting number of secreted YscP per injectisome needle differed with an average and standard deviation of 22±21 YscP per needle.

Considering the data obtained in Result Section “One ruler per needle”, this method proved unsuitable for determining the correct number of secreted YscP per needle.

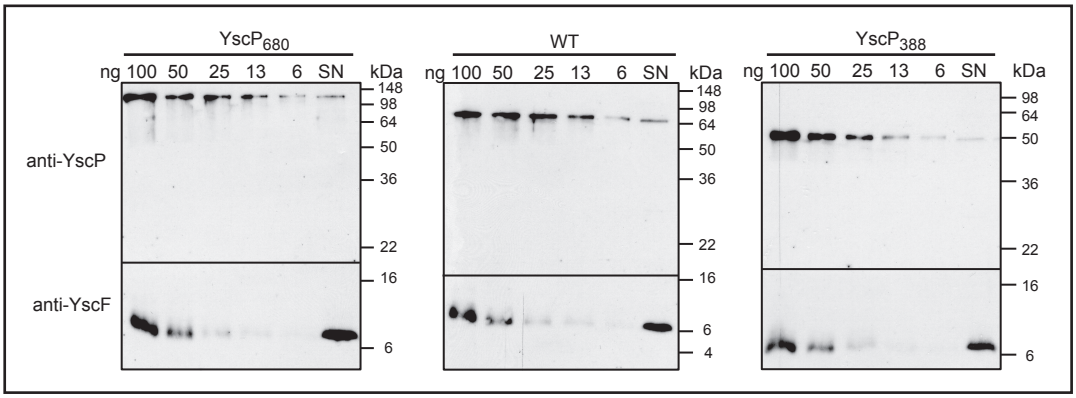

Figure A4

Quantitative immunoblot of detached YscP and injectisome needles.

Supernatant fractions (SN) of Y. enterocolitica E40 *yscP*$_{680}$ (pLJM4001), Y. enterocolitica E40 wt (pYV40) and Y. enterocolitica E40 *yscP*$_{388}$ (pLJ4022). Cultures were grown in non-secretion conditions (+Ca^{2+}). Bacterial pellets were sheared five times mechanically in shearing buffer (Tris-HCl pH 7, 0.1% NP 40, 200 mM NaCl). The shearing fraction were combined with the supernatant fraction. The supernatant (SN) fractions were analyzed by immunoblotting using anti-YscP and anti-YscF antibodies. Different amounts of purified YscF and YscP variants were used as protein standard.

$YscU_{N263Q}$

In our previous work, we could show that the transmembrane protein YscU is involved in substrate recognition and a cleavage site mutant $YscU_{N263A}$ is impaired in exporting translocators and secretion of YscP [130]. Due to the impaired secretion of YscP needle length regulation was diminished which could be rescued by over-expression of the molecular ruler YscP. In a further study the crystal structure of the cytoplasmic domain of YscU was deciphered and the auto-cleavage reaction was analyzed [158]. In this study several YscU point-mutations were engineered and a new phenotype was observed. The cleavage deficient mutant $YscU_{N263Q}$ expressed *in trans* in a *yscU* knockout strain could not secrete LcrV and moreover, YscP export was reduced. Nevertheless needles were regulated, but longer than wt needles. The cleavage of this mutant could not be analyzed *in vivo* and therefore the mutation was introduced in the wt bacteria using homologous recombination. As shown in Figure A5 A Yop secretion by $YscU_{N263Q}$ was similar to the secretion pattern of the cleavage site mutant $YscU_{N263A}$ (under physiological and over-expression conditions). Secretion of effector proteins was comparable to wt levels, whereas the translocators were missing. Cleavage of YscU was analyzed by immunoblotting, as shown in Figure A5 B. Since YscU is a transmembrane protein and is probably present in a very low copy number, it was not possible to detect YscU wt in its cleaved conformation. Only when expressed *in trans* a faint band of the non-cleaved YscU was visible probably due to over-expression of the protein. In contrast, for both YscU mutants ($YscU_{N263A}$ and $YscU_{N263Q}$) a band of the full-length protein was visible, even under physiological conditions (Figure A5 B). When YscU mutants were expressed *in trans* even the alternative cleaving products could be observed like published in Sorg *et al*., 2007. Both mutations showed the same pattern suggesting that also the $YscU_{N263Q}$ mutant was not cleaved *in vivo*. Furthermore, export levels of YscP and LcrV were analyzed by immunoblotting (Figure A5 B). Again, the $YscU_{N263Q}$ mutant showed the same phenotype as the cleavage site mutant $YscU_{N263A}$. Export of LcrV was diminished and secretion of YscP was reduced when mutants were expressed *in trans*, whereas similar levels of YscP were secreted when the mutants were expressed downstream of the native promoter. Needle length was analyzed as

shown in Figure A5 C. The median of needles did not differ (80 and 81 nm), independent of $YscU_{N263A}$ expressed *in trans* under the pBAD promoter or under its native promoter. The standard deviation was, however, higher when $YscU_{N263Q}$ was expressed under its native promoter.

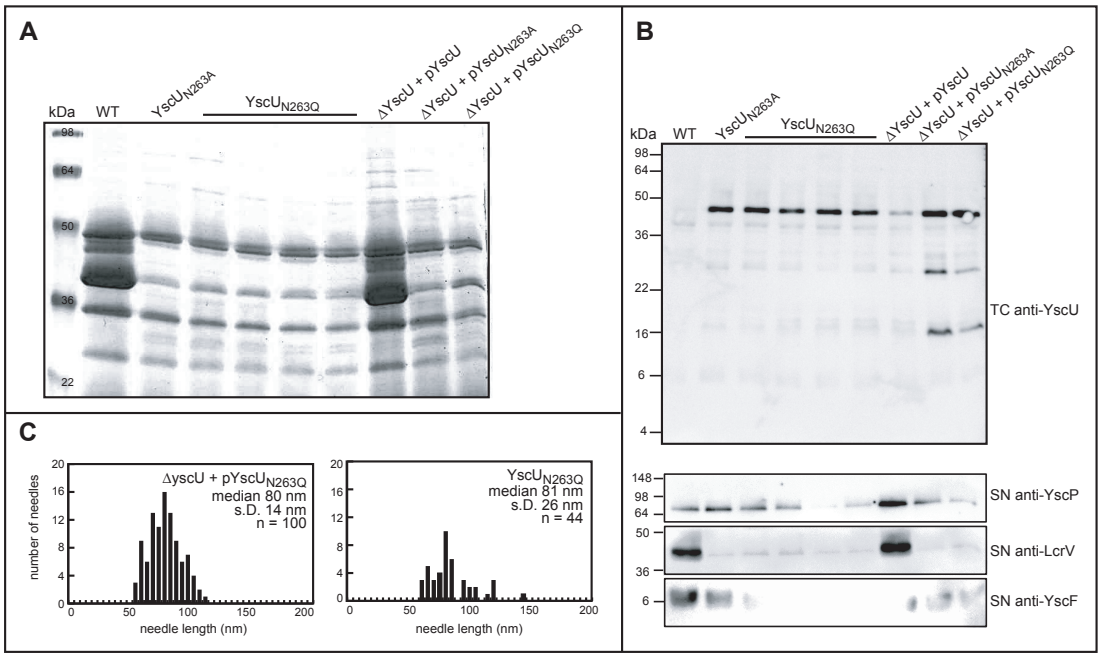

Figure A5

Analysis of a "new" phenotype observed for $YscU_{N263Q}$ over-expression.

A. Yops secreted by *Y. enterocolitica* E40 wt (pYV40), *Y. enterocolitica* E40 *yscU*$_{N263A}$ (pISO4007), *Y. enterocolitica* E40 *yscU*$_{N263Q}$ (pSTW4003), *Y. enterocolitica* E40 *ΔyscU* (pLY4001) and *Y. enterocolitica* E40 *ΔyscU* (pLY4001) mutant bacteria over-expressing YscU (pLY7), $YscU_{N263A}$ (pSTW7), or $YscU_{N263Q}$ (pISOA167) *in trans* from the pBAD promoter. Supernatant fractions (SN) were analyzed by SDS-PAGE.

B. Supernatant fractions (SN) and total cell (TC) fractions of the same cultures as in (A) were analyzed by immunoblot with anti-YscP, anti-LcrV and anti-YscF antibodies.

C. The histograms of needle length measurements of bacteria expressing $YscU_{N263Q}$. s.D., standard deviation; n, number of measured needles.

These preliminary data need to be confirmed. Nevertheless, it seems as if there is no difference between the cleavage site mutant $YscU_{N263A}$ and $YscU_{N263Q}$. Needle of the latter mutant are shorter than needles from the cleavage site mutant $YscU_{N263A}$ (125 nm; [130]) but regulation is not very tight when compared to wt (67 +/- 10 nm).

YscP - molecular ruler or molecular timer?

In previous work we were able to show a direct correlation between the length of YscP and the needle length [53, 157]. There are at least two possible explanations for these results. Either YscP acts as a molecular ruler where YscP would be secreted and partially fold during needle assembly. When the C-terminal domain of YscP gets in contact with the export apparatus, the T3S4 domain would be in the right position to switch substrate specificity and thereby stop needle elongation. Or YscP acts as a molecular timer and it is the time YscP needs to be exported which determines the needle length. In *Shigella* and *Salmonella,* over-expression of the needle subunit (MxiH or PrgI, respectively) leads to elongated needles [31, 123]. These results are in favour of the timer model, if over-expression would result in enhanced/faster export of the needle subunit. However, over-expression of the needle subunit YscF alone did not give elongated injectisome needles in *Y. enterocolitica*, whereas over-expression of the needle subunit YscF together with its chaperones YscE and YscG, and two other small secreted proteins in this operon (YscI and YscH) led to elongated needle length (Isabel Sorg, unpublished data). To test if the timer model applies to YscP, over-expression and decreased expression of YscEFGHI was investigated. A plasmid carrying *yscEFGHI* downstream of the pBAD promoter was transformed into *Y. enterocolitica* E40 wt or a *ΔyscEFGHI* strain. For over-expression of YscEFGHI, expression was induced using 0.5% arabinose in the wt background (Figure A6). For decreased expression levels of YscEFGHI, the plasmid was induced with 0-0.2% arabinose in the *ΔyscEFGHI* strain. Inducing the expression of YscEFGHI with 0.2% arabinose gave levels of YscF and YscI as in wt bacteria (data not shown). Therefore needles were analyzed using only 0.1% arabinose, and induction was done either once at the temperature shift to 37 °C or twice at the temperature shift and 2 hours after growing bacteria at 37 °C (standard condition). As shown in Figure A6 B export of YscP and export of YscI were decreased when the expression of YscEFGHI was induced at low levels, compared to the wt. In comparison, expression levels of YscP were similar in all strains (Figure A6 B). Only a faint band of YscF was detectable in the total cell (TC) fractions when the expression of YscEFGHI was induced at low levels, compared to the wt.

Analysis of needle length confirmed that over-expression of YscEFGHI leads to elongated needles (data not shown). However, with decreased expression of YscEFGHI only few needles of wt length were observed. These results exclude YscP being a molecular timer as described before. The elongated needle length observed upon over-expressing YscEFGHI might result from a delayed export stop of early substrates, due to the massive over-expression of the small Yscs.

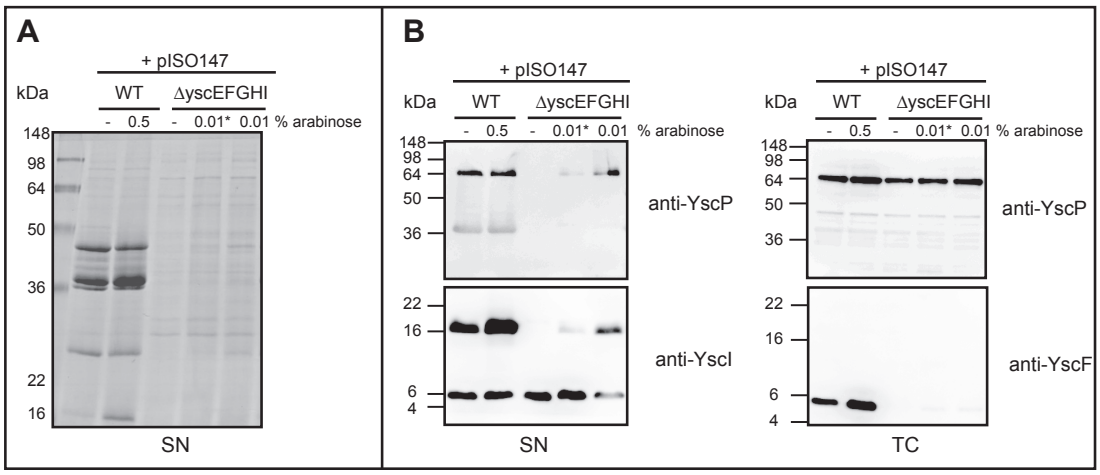

Figure A6

Over-expression of YscEFGHI does influence needle length control.

A. Yops secreted by *Y. enterocolitica* E40 wt (pYV40), *Y. enterocolitica* E40 wt (pYV40) bacteria over-expressing YscEFGHI (pISO147) *in trans* from the pBAD promoter, *Y. enterocolitica* E40 *ΔyscEFGHI* (pISO4017) and *Y. enterocolitica* E40 *ΔyscEFGHI* (pISO4017) mutant bacteria over-expressing YscEFGHI (pISO147) *in trans* from the pBAD promoter. The amount of arabinose used for protein expression is indicated. Arabinose was only added once (at the temperature shift), when indicated with an asterisk (*). Supernatant fractions (SN) were analyzed by SDS-PAGE.

B. Supernatant fractions (SN) and total cell (TC) fractions of the same cultures as in (A) were analyzed by immunoblot with anti-YscP, anti-YscF, and anti-YscI antibodies. The amount of arabinose used for protein expression is indicated. Arabinose was only added once (at the temperature shift), when indicated with an asterisk (*).

The [tāl] **of YscP**

Agrain *et al.* showed that YscP has a tail (aa 500-515) which is conserved in the YscP family and predicted to form a α-helix [110]. A $YscP_{\Delta 501\text{-}515}$ mutant (over-expressed from pLJC12) was shown to complement the *ΔyscP* strain for Yop secretion [110]. YscP export has not been shown and needle length analysis revealed that needles are regulated but with a high standard deviation (45±44 nm, [110]). Moreover, needles from these mutants were shorter than expected for a 15 amino acid deletion. It must be noted that the needle length values for wt and other constructs measured in this study were slightly different from the values published previously [53] as a result of a better calibration of the microscope.

Since all the results published so far resulted from an over-expression of the $YscP_{\Delta 501\text{-}515}$ mutant *in trans*, the deletion was introduced into the wt allele of YscP on the pYV plasmid. A stop codon was introduced after amino acid 499 using homologous recombination to obtain the mutant $YscP_{\Delta Tail}$ (Δ500-515). The phenotype resulting from this mutation, was compared to the phenotype observed from the over-expression of this mutant downstream of the pBAD promoter. As shown in Figure A7 A the pattern of Yop secretion was different under physiological conditions. Over-expression of $YscP_{\Delta 501\text{-}515}$ resulted in a complete complementation of a *ΔyscP* strain (concerning Yop secretion) as it was shown for wt YscP. In contrast, when $YscP_{\Delta 500\text{-}515}$ was expressed under its native promoter only effector Yops were secreted but not the translocators (Figure A7 A). This secretion pattern reminded of the phenotype described for the YscU cleavage site mutant $YscU_{N263A}$ (Results chapter; [130]) which suggested a role for YscU in substrate recognition. Immunoblotting using antibodies against YopB, YopD (data not shown) and LcrV (Figure A7 B) revealed a dramatically reduced export of the translocators compared to the wt. Moreover and most strikingly, secretion of YscP was also impaired when $YscP_{\Delta 500\text{-}515}$ was expressed under its native promoter, but not when over-expressed *in trans* (Figure A7 B). Analyzing needle length control showed regulated needles, though not to wt level, with a median and standard deviation of 70 ± 36 nm (wt: 66 ± 7 nm, Figure A7 C) when $YscP_{\Delta 501\text{-}515}$ is over-expressed. In contrast, expression of

YscP$_{\Delta 500\text{-}515}$ downstream of its native promoter resulted in uncontrolled needle length, however needles where not longer than ~ 300 nm.

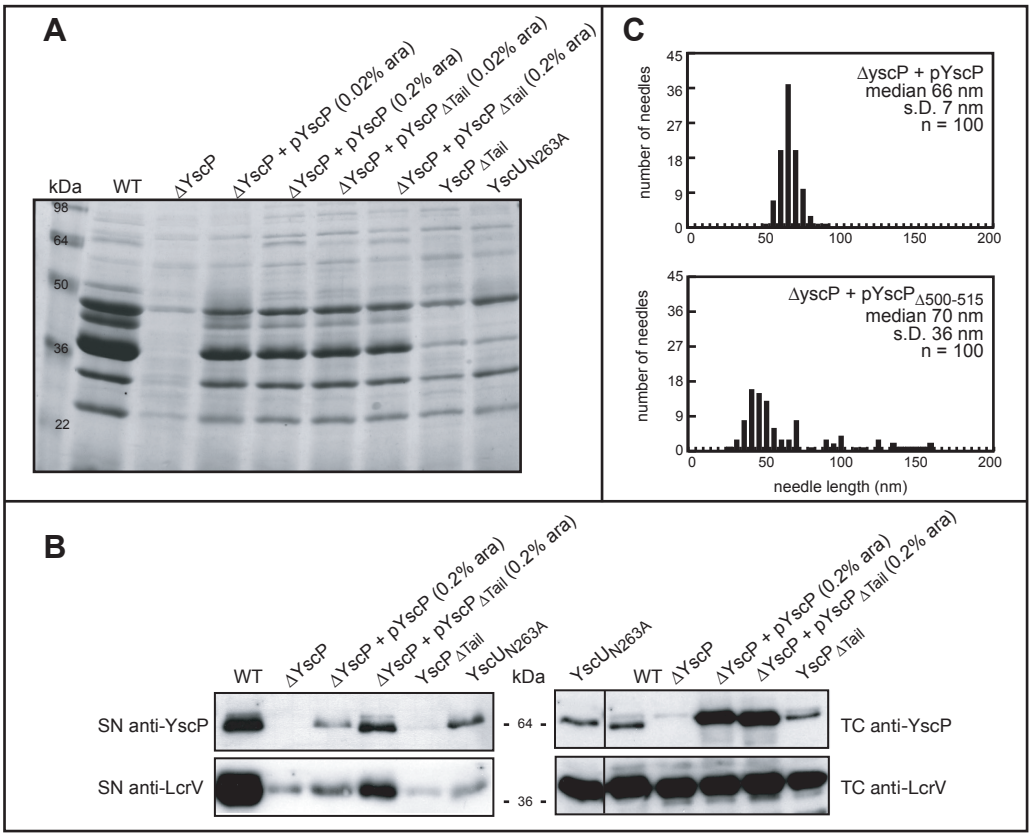

Figure A7

Effect of deleting the tail of YscP on the needle length and substrate switching.

A. Yops secreted by *Y. enterocolitica* E40 wt (pYV40), *Y. enterocolitica* E40 *ΔyscP* (pLJ4036), *Y. enterocolitica* E40 *yscP$_{\Delta tail}$* (pSTW4002), *Y. enterocolitica* E40 *yscU$_{N263A}$* (pISO4007) and *Y. enterocolitica* E40 *ΔyscP* (pLJ4036) mutant bacteria over-expressing YscP (pLJ6) or YscP$_{\Delta tail}$ (pLJC12) *in trans* from the pBAD promoter. The amount of arabinose used for protein expression is indicated.

B. Supernatant fractions (SN) and total cell (TC) fractions of the same cultures as in (A) were analyzed by immunoblot with anti-YscP and anti-LcrV antibodies.

C. The histograms of length measurements. s.D., standard deviation; n, number of measured needles.

To investigate whether the YscP$_{\Delta 500\text{-}515}$ mutant bacteria were able to switch substrate specificity from early substrates (e.g., YscF) to intermediate substrates (translocators) a YopE-LcrV fusion [130] was used as reporter construct (Figure A8). The export signal of the effector YopE was fused to the N-terminus of LcrV [130] and export of the hybrid was analyzed in YscP$_{\Delta 500\text{-}515}$ and in YscU$_{N263A}$ mutant bacteria. As shown in Figure A8 a protein of the expected size was detected by Coomassie-stained

SDS-PAGE of the supernatant fractions. The identity of the protein was confirmed by immunoblotting using anti-LcrV antibodies (Figure A8). In contrast to the YopE-hybrid protein, LcrV alone was not exported in the YscP$_{\Delta 500\text{-}515}$ and the YscU$_{N263A}$ mutants (Figure A8). These data suggest that the loss of LcrV export is due to a defect in recognition of LcrV as export substrate.

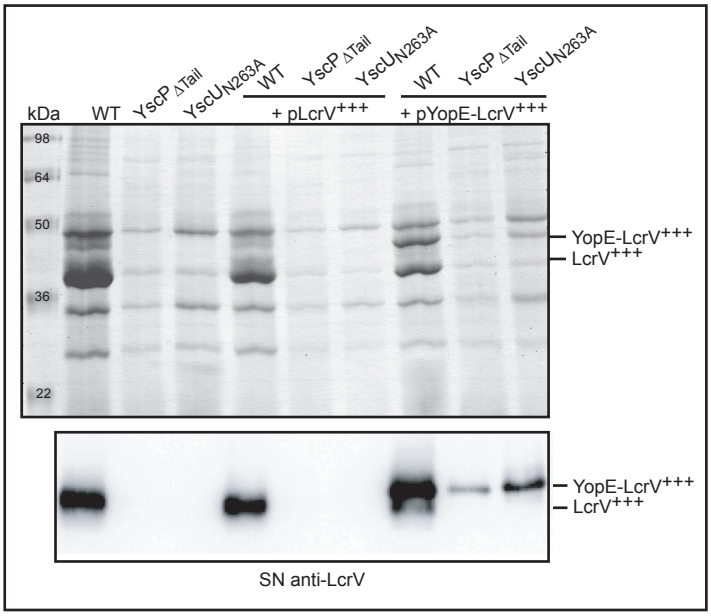

Figure A8
YopE$_{1\text{-}15}$LcrV is exported by *Y. enterocolitica yscU$_{N263A}$* and *yscP$_{\Delta 500\text{-}515}$* mutant bacteria.
Yops secreted by *Y. enterocolitica* E40 wt (pYV40), *Y. enterocolitica* E40 *yscU$_{N263A}$* (pISO4007) and *Y. enterocolitica* E40 *yscP$_{\Delta 500\text{-}515}$* (pSTW4002) mutant bacteria over-expressing LcrV (pPB42) or YopE$_{1\text{-}15}$LcrV (pISOA132) *in trans* from the pBAD promoter. The position of the YopE$_{1\text{-}15}$LcrV and LcrV proteins are indicated. Supernatant fractions (SN) were analyzed by immunoblot with anti-LcrV antibodies (lower blot).

To test if over-expression of the tail peptide could rescue the phenotype observed for the YscP$_{\Delta 500\text{-}515}$ mutant, the tail of YscP, *yscP$_{497\text{-}515}$* or *his$_6$-yscP$_{497\text{-}515}$* was cloned downstream of the pBAD promoter and expressed *in trans* in the *Y. enterocolitica* E40 wt strain. An effect on expression and secretion level of YscP was not observed by immunoblotting with anti-YscP antibodies (Figure A9 A).

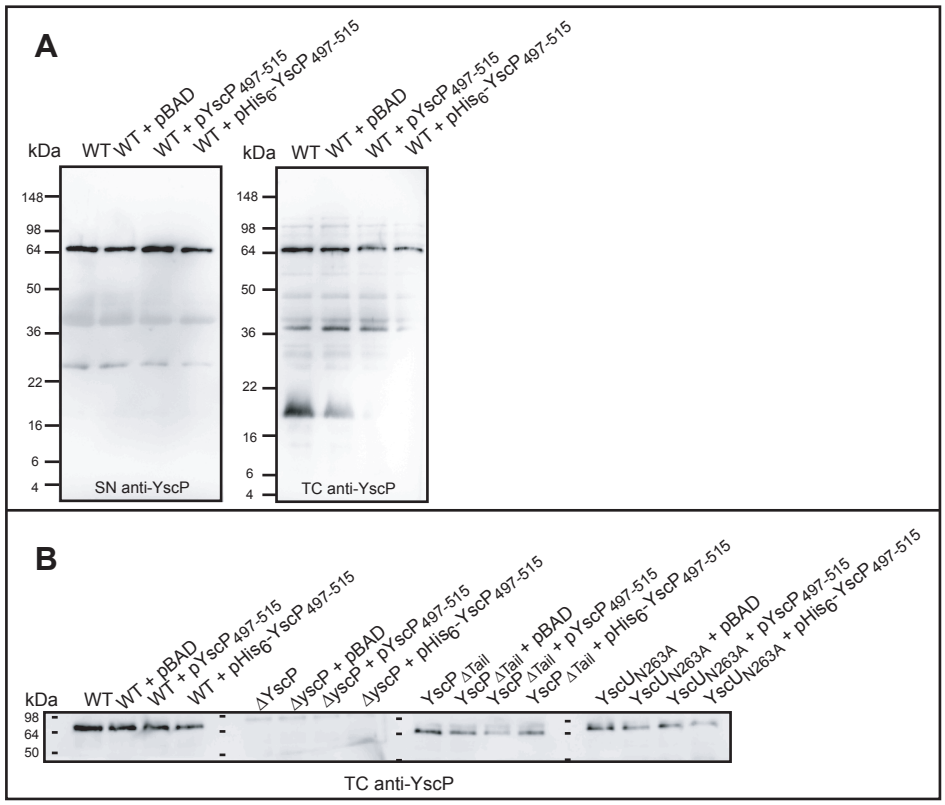

Figure A9

Effect of over-expression of the YscP tail peptide in different backgrounds.

A. Supernatant fractions (SN) and total cell (TC) fractions of *Y. enterocolitica* E40 wt (pYV40), *Y. enterocolitica* E40 wt (pYV40) bacteria over-expressing YscP$_{497-515}$ (pSTW49) or His$_6$-YscP$_{497-515}$ (pSTW50) *in trans* from the pBAD promoter or *Y. enterocolitica* E40 wt (pYV40) transformed with an empty pBAD vector. Supernatant (SN) and total cell (TC) fractions were analyzed by immunoblot using anti-YscP antibodies.

B. Total cell (TC) fractions of *Y. enterocolitica* E40 wt (pYV40), *Y. enterocolitica* E40 wt (pYV40) bacteria over-expressing YscP$_{497-515}$ (pSTW49) or His$_6$-YscP$_{497-515}$ (pSTW50) *in trans* from the pBAD promoter or *Y. enterocolitica* E40 wt (pYV40) transformed with an empty pBAD vector; *Y. enterocolitica* E40 *ΔyscP* (pLJ4036), *Y. enterocolitica* E40 *ΔyscP* (pLJ4036) bacteria over-expressing YscP$_{497-515}$ (pSTW49) or His$_6$-YscP$_{497-515}$ (pSTW50) *in trans* from the pBAD promoter or *Y. enterocolitica* E40 *ΔyscP* (pLJ4036) transformed with an empty pBAD vector; *Y. enterocolitica* E40 *yscP$_{Δtail}$* (pSTW4002), *Y. enterocolitica* E40 *yscP$_{Δtail}$* (pSTW4002) bacteria over-expressing YscP$_{497-515}$ (pSTW49) or His$_6$-YscP$_{497-515}$ (pSTW50) *in trans* from the pBAD promoter or *Y. enterocolitica* E40 *yscP$_{Δtail}$* (pSTW4002) transformed with an empty pBAD vector; *Y. enterocolitica* E40 *yscU$_{N263A}$* (pISO4007), *Y. enterocolitica* E40 *yscU$_{N263A}$* (pISO4007) bacteria over-expressing YscP$_{497-515}$ (pSTW49) or His$_6$-YscP$_{497-515}$ (pSTW50) *in trans* from the pBAD promoter or *Y. enterocolitica* E40 *yscU$_{N263A}$* (pISO4007) transformed with an empty pBAD vector. Total cell (TC) fractions were analyzed by immunoblot with anti-YscP antibodies.

However, expression of the tail peptide YscP$_{497-515}$ could not be detected, neither by immunoblotting, nor by a silver-stained SDS-PAGE (data not shown). This is most likely due to the very small size of the peptide (19 aa). Expression of YscP$_{497-515}$ or His$_6$-YscP$_{497-515}$ in the *ΔyscP* strain, the *yscP$_{Δ500-515}$* or the *yscU$_{N263A}$* mutants did

also not lead to an effect on expression or export level of YscP wt (Figure A9 B, data not shown).

Since the mutant $YscP_{497\text{-}515}$ can not be exported by the type III secretion machinery when expressed under its native promoter, the YscP tail might either be important for the correct recognition of YscP or for the correct interaction with its binding partner to switch substrate specificity as suggested for FliK and FlhB [109]. Therefore, the $YscP_{\Delta 500\text{-}515}$ ($YscP_{\Delta 500\text{-}515}$) mutant was included in the interactions studies with YscU as described below.

Interactions (and) partners

YscI - polymerization-cap or rod?

YscI is a 12.7 kDa protein which is exported by the type III secretion system of *Yersinia*. YscI is needed for needle assembly and is secreted in amounts proportional to YscF ([161], Group Cornelis unpublished data). The homolog protein in *Salmonella typhimurium* is PrgJ, which is proposed to form the inner rod of the basal body [37]. In *Shigella* it is still under debate, whether the PrgJ homolog MxiI is the inner rod protein [162] or forming a cap-like structure on top of the needle [30]. MxiI is supposed to be the functional homolog of FlgD the flagellar hook cap protein [100].

Wood *et al*. [161] propose YscI to be the inner rod protein based on a sequence alignment (with YscF and YscI family members) and suggest that the formation of the inner rod is critical for substrate specificity switching and that YscU and YscP use their effects on substrate export by controlling the secretion of YscI. This model is based on the finding that certain point mutations in YscI secrete Yops but show a severe defect in needle formation. In the absence of YscP these mutants are able to assemble needles, but are unable to secrete Yops. Wood *et al*. [161] also show that YscI export is increased in a *yscP* knockout strain but that mutations in the cytoplasmic domain of YscU can rescue this phenotype.

Since Wood *et al*. [161] did not analyze needle formation in the YscI mutants by electron microscopy, we decided to engineer two of the published mutants and analyze needle formation and length. $YscI_{Q84A}$ and $YscI_{L96A}$ were engineered by site directed mutagenesis and expressed *in trans* under the pBAD promoter in a *ΔyscI* strain. As shown in Figure A10 A, YscI wt expressed *in trans* was able to complement the Δ*yscI* strain concerning Yop secretion (Figure A10 A), export of YscP, LcrV and YscI (Figure A10 B) and needle length control (Figure A10 C). In contrast, both YscI mutants only partially complemented the deletion mutant for Yop secretion. Export of effector Yops was comparable to wt levels, whereas secretion of translocators was dramatically decreased (Figure A10 A). Secretion of YscP and LcrV was not detectable by immunoblotting (Figure A10 B) in both mutants, whereas export of YscI was reduced in $YscI_{Q84A}$ but not in $YscI_{L96A}$. Length measurement of the injectisome needle showed that the $YscI_{Q84A}$ mutant assembled needles which

were controlled, but with a higher median and a slightly increased standard deviation (Figure A10 C). This might be due to the decreased export of YscP.

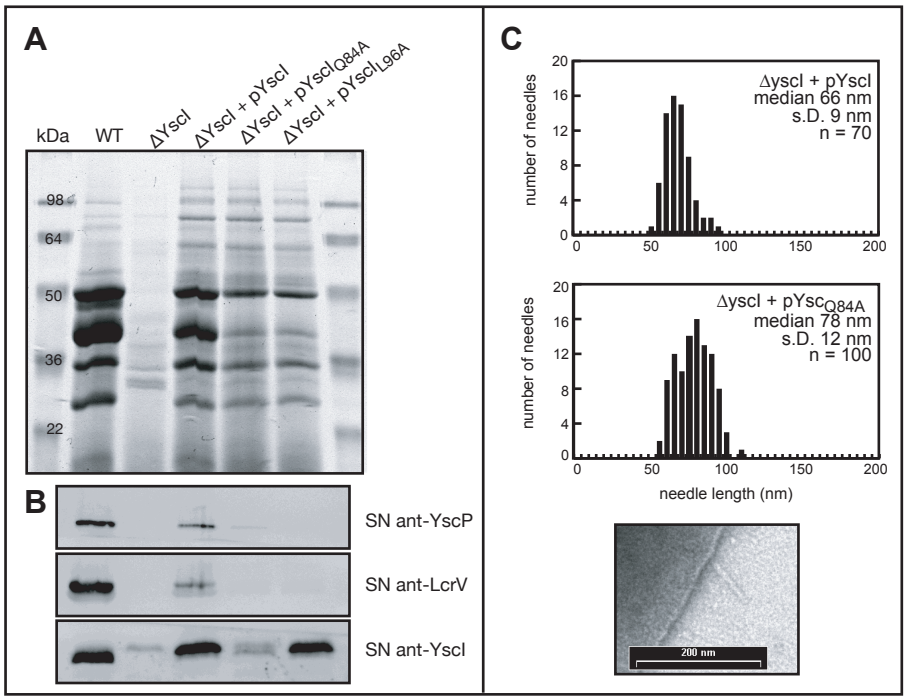

Figure A10

YscI$_{Q84A}$ and YscI$_{L96A}$ mutant proteins are not exported but do not inhibit needle length control.

A. Yops secreted by *Y. enterocolitica* E40 wt (pYV40), *Y. enterocolitica* E40 *ΔyscI* (pKEM4001) and *Y. enterocolitica* E40 *ΔyscI* (pKEM4001) mutant bacteria over-expressing YscI (pKEM4), YscI$_{Q84A}$ (pSTW55), or YscI$_{L96A}$ (pSTW56) *in trans* from the pBAD promoter. Supernatant fractions (SN) were analyzed by SDS-PAGE.

B. Supernatant fractions (SN) of the same cultures as in (A) were analyzed by immunoblot with anti-YscP, anti-LcrV and anti-YscI antibodies.

C. The histograms of length measurements and transmission electron micrograph. s.D., standard deviation; n, number of measured needles.

In contrast to Wood *et al*. [161], in our hands both mutants were able to assemble injectisome needles, but were impaired in the secretion of translocators. Moreover, YscI$_{Q84A}$ secretion was dramatically reduced while needles were still assembled. In a *ΔyscI* strain no needle formation was observed.

To analyze needle formation in a *ΔyscP* background, a yscI/yscP double knockout strain was engineered using allelic exchange to delete *yscP* in the *ΔyscI* strain. As shown in Figure A11 A, no Yop secretion was observed when YscP is deleted. Immunoblotting revealed that YscI wt as well as the two YscI mutants were expressed in a *ΔyscP* background (Figure A11 B) whereas only YscI$_{Q84A}$ was not

secreted into the culture supernatant (Figure A11 B). LcrV export was completely diminished in the absence of YscP and YscF was only detectable in the supernatant of YscI wt and $YscI_{L96A}$ bacteria, suggesting that these two strains are able to assemble needles, whereas $YscI_{Q84A}$ is impaired in needle formation (Figure A11 B). The absence of needles in the $YscI_{Q84A}$ strain was confirmed by electron microscopy. The double deletion *ΔyscI/ΔyscP* complemented with either YscI wt or $YscI_{L96A}$ resulted in extra-long needles like observed in a *ΔyscP* strain [53].

Taking together, these results show that $YscI_{Q84A}$ with reduced export can assemble needles in the presence of YscP, but not in its absence.

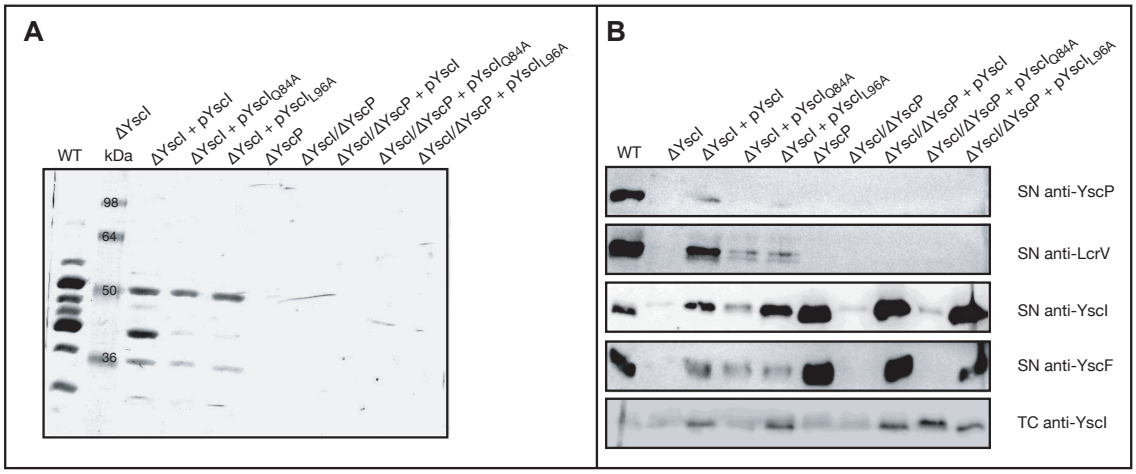

Figure A11

The $YscI_{Q84A}$ mutant is not able to assemble needles in a *ΔyscP* background.

A. Yops secreted by *Y. enterocolitica* E40 wt (pYV40), *Y. enterocolitica* E40 *ΔyscI* (pKEM4001), *Y. enterocolitica* E40 *ΔyscI* (pKEM4001) mutant bacteria over-expressing YscI (pKEM4), $YscI_{Q84A}$ (pSTW55), or $YscI_{L96A}$ (pSTW56) *in trans* from the pBAD promoter, *Y. enterocolitica* E40 *ΔyscP* (pLJ4036), *Y. enterocolitica* E40 *ΔyscI/ΔyscP* (pSTW4005) and *Y. enterocolitica* E40 *ΔyscI/ΔyscP* (pSTW4005) mutant bacteria over-expressing YscI (pKEM4), $YscI_{Q84A}$ (pSTW55), or $YscI_{L96A}$ (pSTW56) *in trans* from the pBAD promoter. Supernatant fractions (SN) were analyzed by SDS-PAGE.

B. Supernatant fractions (SN) and total cell (TC) fractions of the same cultures as in (A) were analyzed by immunoblot with anti-YscP, anti-LcrV, anti-YscF, and anti-YscI antibodies.

Interaction studies

Assuming the ruler model as proposed by Journet *et al*. [53] is correct, YscP would have to interact with other proteins in order to fulfill its function. These proteins are most likely located at the base of the basal body and at the tip of the growing needle. Since a *ΔlcrV* mutant does assemble wt needles [157] the tip forming protein LcrV can be excluded as binding partner. However, several small Ysc proteins (YscI, YscH, YscX and YscO) are secreted as early substrates but to date none of these proteins has a function assigned. Another possibility is that YscP might form an umbrella like structure at the tip of the growing needle which would serve as a polymerization cap or anchor to sense the distal needle end. In this model a binding partner at the distal needle end would not be needed. Polymerization of the needle could be the driving force to export YscP in this model of needle length control. Despite that, a binding partner at the base of the basal body remains a prerequisite to switch substrate specificity. In the flagellum, FliK was inferred to interact with the soluble carboxyl-terminal domain of FlhB (FlhBc) [116]. This interaction plays a crucial role in the switch from hook to filament secretion in the flagellum system. Botteaux *et al*. [132] showed for *Shigella flexneri* by pull down experiments that the YscP homolog Spa32 interacts with the YscU homolog Spa 40. These data together with the results by Sorg *et al*. [130] showing a role for YscU in substrate recognition, suggest that YscP and YscU do interact in *Y. enterocolitica*. This has never been shown experimentally.
Two different attempts were chosen to test interaction between YscU and YscP which could later serve for identification of other binding partners of YscP. The $YscP_{\Delta tail}$ ($YscP_{\Delta 500\text{-}515}$) mutant was included in this study since the mutant can not be exported by the type III secretion machinery, and the YscP tail might either be important for the correct recognition of YscP or for the correct interaction with its binding partner to switch substrate specificity as suggested for FliK [109].

Retardation column

First, a GST-tagged protein (YscU) immobilized to a matrix was incubated with either the supernatant fraction of a bacterial culture secreting YscP, or purified proteins (YscP or YscU). Retardation of the untagged protein would suggest that several

transient interactions take place and slow down the flow of the untagged protein [163]. So far, purification of YscP was only possible under denaturing conditions, in 8 M urea. Nevertheless, a GST-tagged YscP fusion leads to detectable amounts of soluble YscP after cleavage of the tag with PreScission protease. Since YscU (and its homologs) undergoes an autoproteolytic cleavage between N263 and P264 [116, 158, 160, 164, 165] the non cleavable mutant $YscU_{N263A}$ was chosen for these interaction studies.

When GST-$YscU_{211-354}$ (from pISO116) or GST-$YscU_{211-354,N263A}$ (from pISO117) was immobilized to glutathione sepharose beads and incubated with either supernatant from a *Y. enterocolitica* E40 wt strain or from a *ΔyscP* strain complemented with pLJC12 (secretion of $YscP_{\Delta tail}$, see A [tāl] of YscP) bands for YscP could not be detected by immunoblotting of the elution fraction (data not shown). This could be due to a low concentration of YscP in the supernatant fraction. Therefore the experiments were repeated with purified proteins, at higher concentrations and in absence of possible disturbing contaminants. Figure A12 shows an assay where GST-tagged YscP or $YscP_{\Delta tail}$ was immobilized to glutathione sepharose beads and incubated with purified $YscU_{211-354}$ or $YscU_{211-354,N263A}$. Figure A12 (right panel) shows the absence of detectable amounts of YscU by immunoblotting with anti-YscU antibodies for $YscU_{211-354}$. However, for the non cleavable $YscU_{211-354,N263A}$, bands for YscU were detected in the washing fractions and in the elution fractions (glutathione concentrations, 0-10 mM). $YscU_{211-354,N263A}$ was detected by immunoblotting when incubated with GST alone, but this background was negligible when compared to the intensity of the bands detected when GST-YscP wt was immobilized to the matrix (Figure A12). The bands detected for $YscU_{211-354,N263A}$ when $YscP_{\Delta tail}$ was immobilized to the beads were less intense than for GST-YscP (Figure A12). These results suggest that $YscP_{\Delta tail}$ has a defect in binding to $YscU_{N263A}$. However, these preliminary results need to be confirmed. Moreover, these data only suggest an impaired binding between $YscP_{\Delta tail}$ and $YscU_{N263A}$. A difference in binding between $YscP_{\Delta tail}$ and YscU compared to YscP and YscU remains to be demonstrated.

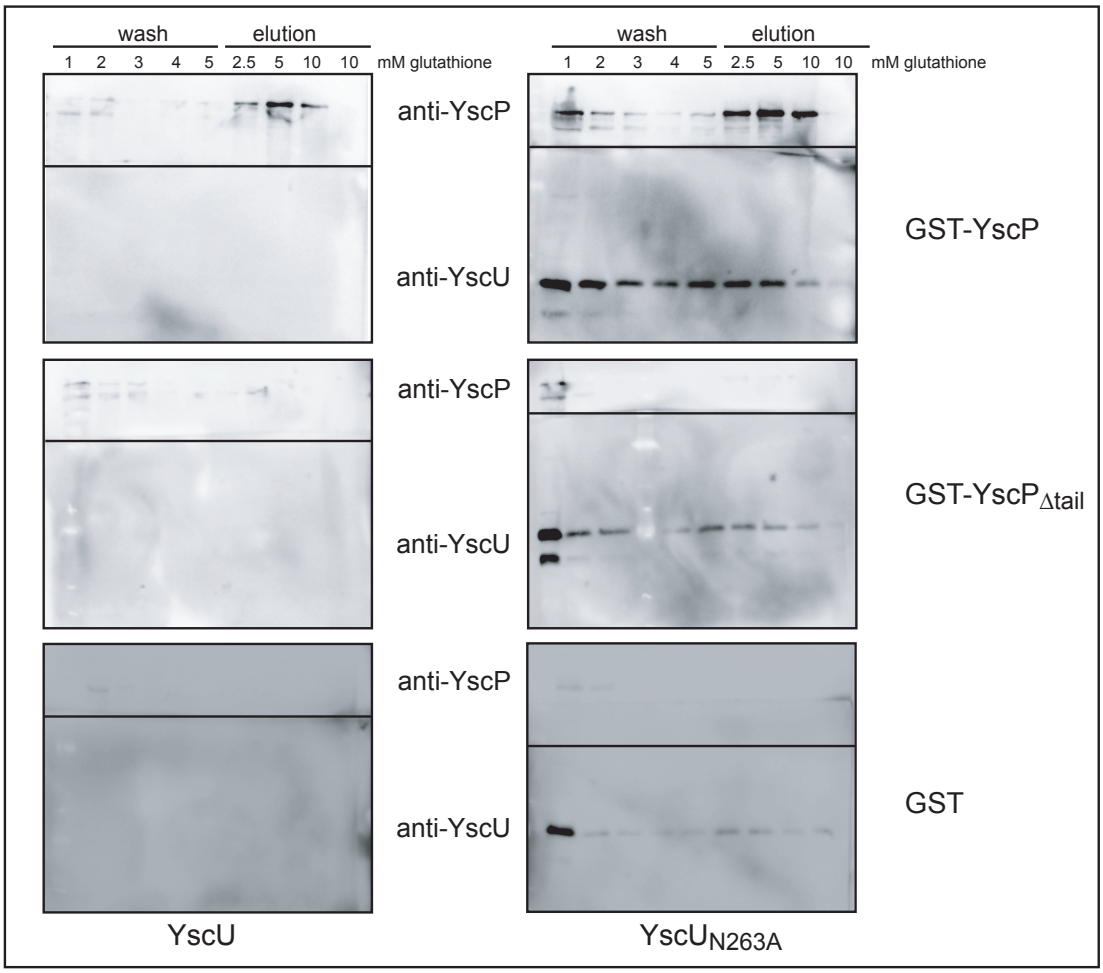

Figure A12

$YscU_{N263A}$ is retarded on a YscP-labelled column.
GST-tagged YscP (pSTW19), $YscP_{\Delta tail}$ (pSTW57) or GST (pGEX-6P-1) alone are immobilized to glutathione sepharose beads and incubated with either purified $YscU_{211-354}$ (pISO116) or purified $YscU_{211-354,N263A}$ (pISO117). Elution of GST-tagged proteins was carried out with 2.5-10 mM glutathione. Washing and elution fractions were analyzed by immunoblot with anti-YscP and anti-YscU antibodies.

FRET

For a second attempt to investigate binding between YscP and YscU, the FRET (Fluorescence Resonance Energy Transfer) technology was used. Here, a donor chromophore in its electronic excited state, transfers energy to an acceptor chromophore (in proximity, typically less than 10 nm) through non-radiative dipole–dipole coupling. FRET is a widely used method for reporting the interaction of macromolecules [166, 167]. To use FRET there are three prerequisites: first, there must be an acceptor and a donor probe, second, the emission spectrum of the

donor must overlap with the absorption spectrum of the acceptor and third, the distance between donor and acceptor should be less than ~ 7 nm (Förster, 1948).
Interactions between the soluble cytoplasmic domain of YscU (aa 211-354) and tail peptide of YscP (aa 497-515) were studied using Alexa Fluor 488 and Alexa Fluor 546 (Invitrogen) labelled proteins. These Alexa Fluor dyes selectively label proteins at cysteine residues. The cytoplasmic domain of YscU does not contain a cysteine residue, but a serine at position 351, close to the C-terminus (Figure A13 A) of the protein. The S351C mutation was tested *in vivo* to assure that this mutation does not interfere with the function of YscU. The *yscU*$_{N263A,S351C}$ and *yscU*$_{S351C}$ mutants were engineered by site-directed mutagenesis and cloned downstream of the pBAD promoter. YscU$_{S351C}$ and YscU$_{N263A,S351C}$ were expressed *in trans* in a *ΔyscU* strain to test these mutants for their ability to complement the knockout strain. The S351C mutation in YscU and YscU$_{N263A}$ complement the *ΔyscU* strain to the same level as the corresponding controls (YscU and YscU$_{N263A}$, respectively; Figure A13B). As shown in Figure A13 B wt Yop secretion was detected by Coomassie-stained SDS-PAGE of the supernatant fractions for the YscU$_{S351C}$ mutant. The secretion pattern for YscU$_{N263A,S351C}$ was similar to the pattern observed for the cleavage site mutant YscU$_{N263A}$ [130]. The export of YscP and LcrV were confirmed by immunoblotting using anti-YscP and anti-LcrV antibodies (Figure A13 B). Expression levels of YscU$_{S351C}$ and YscU$_{N263A,S351C}$ corresponded to the pattern observed for the controls (Figure A13 B). Therefore, the S351C mutation in YscU did not influence the function of YscU and can be used to label the cytoplasmic domain of YscU and YscU$_{N263A}$.
YscP harbours five cysteine residues. To assign a function to the YscP tail (described in a previous chapter), only the last 29 amino acids of YscP including one additional cystein, introduced at the C-terminus, were used for the interaction studies with YscU. This additional cysteine at the C-terminus of YscP was tested *in vivo* not to influence the function of YscP. Therefore a cysteine was added to the C-terminus of the full-length YscP (Figure A13 A) using site-directed mutagenesis and the resulting gene was cloned downstream of a pBAD promoter. Yop secretion was analyzed by Coomassie-stained SDS-PAGE of the supernatant fractions for the YscP$_{C516}$ mutant (Figure A13B). Export of YscP and LcrV was confirmed by immunoblotting with anti-

YscP and anti-LcrV antibodies (Figure A13 B). The expression level of $YscP_{C516}$ corresponded to the pattern observed for its corresponding control (YscP wt, Figure A13 B). The obtained results showed that the C516 mutation in YscP did not influence the function of YscP and therefore can be used to label the C-terminal peptide of YscP.

$YscU_{211\text{-}354,S351C}$ and $YscU_{211\text{-}354,N263A,S351C}$ were cloned downstream of a T7 promoter as fusion to a GST-tag harbouring a PreScission protease cleavage site (pGEX-6P-1) and the resulting proteins were purified (data not shown).

First attempts were carried out to label the synthetic C-terminal peptide of $YscP_{C516}$. However, due to the small size of the peptide (30 aa) it was so far not possible to purify the labelled peptide from excess dye (data not shown).

The protocol for labelling and purification of the synthetic $YscP_{C516}$ peptide and for the cytoplasmic domain of $YscU_{S351C}$ and $YscU_{N263A,S351C}$ need to be established in order to study interactions using FRET.

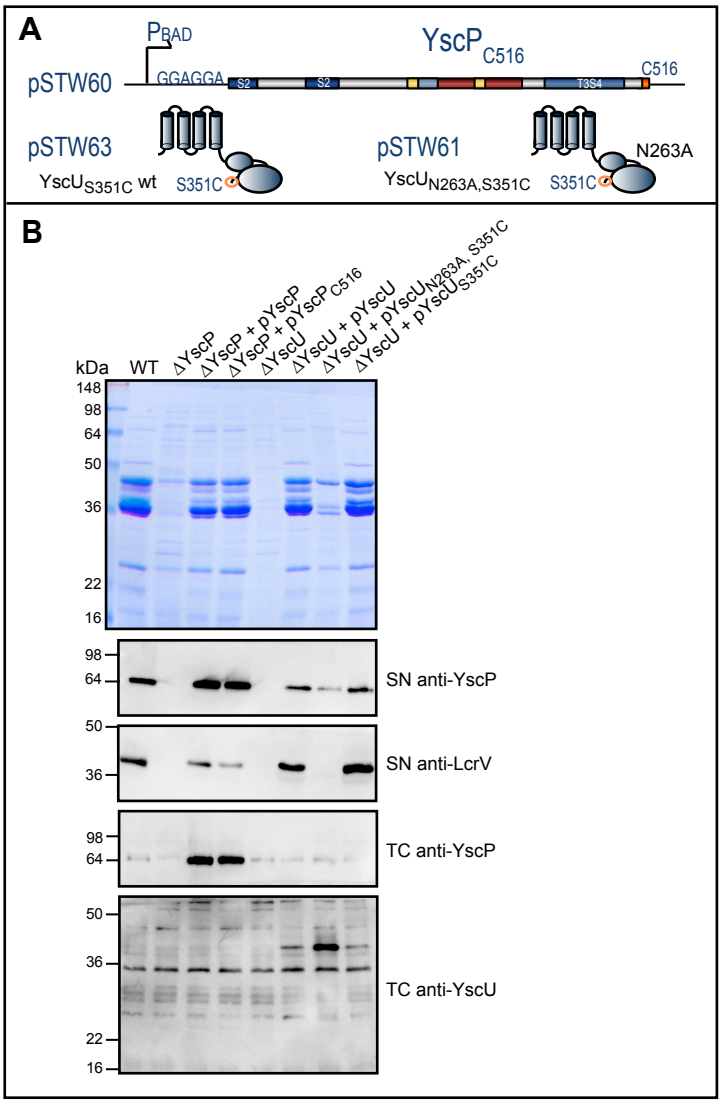

Figure A13

Cysteine mutations in the C-terminus of YscU, $YscU_{N263A}$ and YscP do not influence needle length control.

A. Schematic representation of the cysteine substitution in YscU (pSTW63) or $YscU_{N263A}$ (pSTW61) and the cysteine addition at the C-terminus of YscP (pSTW60).

B. Yops secreted by *Y. enterocolitica* E40 wt (pYV40), *Y. enterocolitica* E40 *ΔyscP* (pLJ4036), *Y. enterocolitica* E40 *ΔyscP* (pLJ4036) mutant bacteria over-expressing YscP (pLJ6) or $YscP_{C516}$ (pSTW60) *in trans* from the pBAD promoter, *Y. enterocolitica* E40 *ΔyscU* (pLY4001), *Y. enterocolitica* E40 *ΔyscU* (pLY4001) mutant bacteria over-expressing YscU (pLY7), $YscU_{S351C}$ (pSTW63) or $YscU_{N263A,S351C}$ (pSTW61) *in trans* from the pBAD promoter. Supernatant fractions (SN) and total cell (TC) fractions of the same cultures were analyzed by immunoblot with anti-YscP, anti-LcrV and anti-YscU antibodies.

Overlays

To further identify other binding partners of YscP, interactions between YscP and proteins secreted by the type III secretion machinery were analyzed by an overlay assay. A construct encoding the full-length *yscP* fused to a N-terminal GST-tag was generated and expressed in *E. coli* (see previous chapter). The supernatant fractions of *Y. enterocolitica* wt, were separated by SDS-PAGE and transferred to a nitrocellulose membrane. The membranes were incubated with the purified full-length YscP and as control without protein. An interaction between the full-length YscP and two proteins secreted by the *Yersinia* injectisome was detected (Figure A14). The two bands observed corresponded to the sizes of YopB or YopD and YopH. Since YopH is a late substrate, the interaction with YscP is most likely unspecific. In contrast, YopB and YopD are intermediate substrates and interaction was confirmed by using the supernatant fraction of a *ΔyopBD* strain where the major band disappeared (Figure A14). This knockout strain, however, assembles wt needles suggesting that also this interaction is likely to be unspecific. Other interactions were not detected, which does not exclude interactions undetectable in this experimental setup.

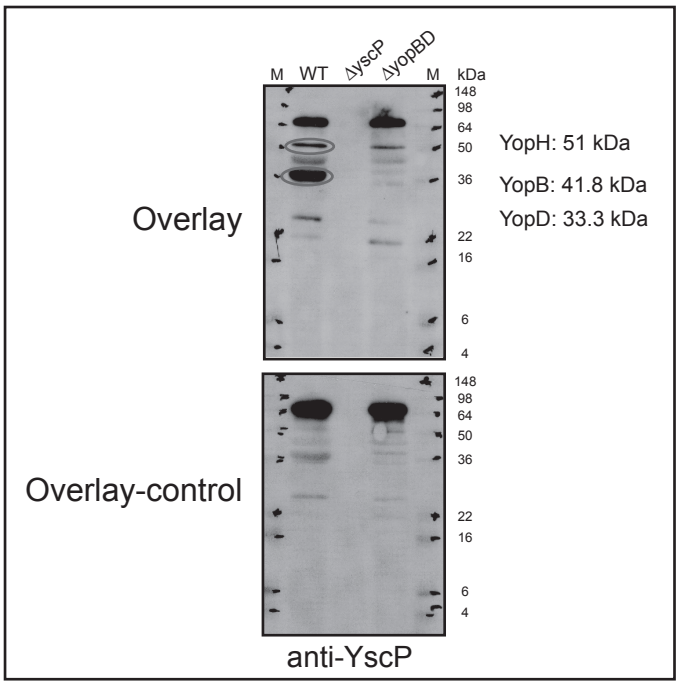

Figure A14
Overlay assay to identify binding partners of YscP.
Proteins secreted by *Y. enterocolitica* E40 wt (pYV40), *Y. enterocolitica* E40 *ΔyscP* (pLJ4036) and *Y. enterocolitica* E40 *ΔyopBD* (pISO4005) mutant bacteria were separated by SDS-PAGE and transferred to a nitrocellulose membrane. The membranes were subsequently used for overlay assays with either purified YscP as probe or without protein (indicated on the left). After incubation with or without protein (control), bound YscP was analyzed by immunoblotting using anti-YscP antibodies.

Structure/purification

In order to obtain a crystal structure of parts of the YscP protein, several YscP constructs were engineered as GST-fusions (GST-YscP$_{wt}$ (pSTW19), GST-YscP$_{367-515t}$ (pSTW20), GST-YscP$_{497-515}$ (pSTW51), GST-YscP$_{1-137}$ (pSTW53)), which were analyzed by the group of Dirk Heinz at the Helmholtz Insitute in Braunschweig, Germany.

However, so far non of the constructs which were soluble were able to crystallize.

Does YscP measure needle length inside or outside the needle?

YscP is proposed to be a molecular ruler, measuring the needle length while being stretched during needle assembly ([53, 157], previous chapter). To address the question whether it is inside or outside of the growing needle, two YscP mutants were engineered with a thrombin cleavage site (Figure A15 A). In presence of thrombin protease in the culture supernatant, YscP should be cleaved when it is outside of the bacterium (Figure A15 B). Cleavage of YscP while measuring the growing needle would most likely result in extra-long needles, since YscP would not be able to sense the tip of the growing needle (Figure A15 B). In contrast, when YscP is itself inside the channel of the growing needle it would be protected from the protease and length measurement should not be impaired (Figure A15 B). However, since a certain extent of YscP remains non-cleaved at the early time-point (Figure A15 D) even upon changing various conditions, a conclusion could not be drawn from these experiments. The non-cleaved amount of YscP might control needle growth or YscP acts outside the growing needle but is not accessible for the protease. Another attempt to address the question whether YscP is outside or inside the needle channel while measuring needle length is using proteinase K. These experiments are described in the Master Thesis of Lisa Metzger.

The thrombin cleavage site was introduced either between the two export signals of YscP (pSTW1) or after the second export signal (pSTW2) by site-directed mutagenesis. As shown in Figure A15 C, both constructs were cleaved by thrombin protease after a normal *in vitro* secretion experiment (see Methods, the medium was supplemented with 25 U/mL thrombin protease at the shift to 37 °C).

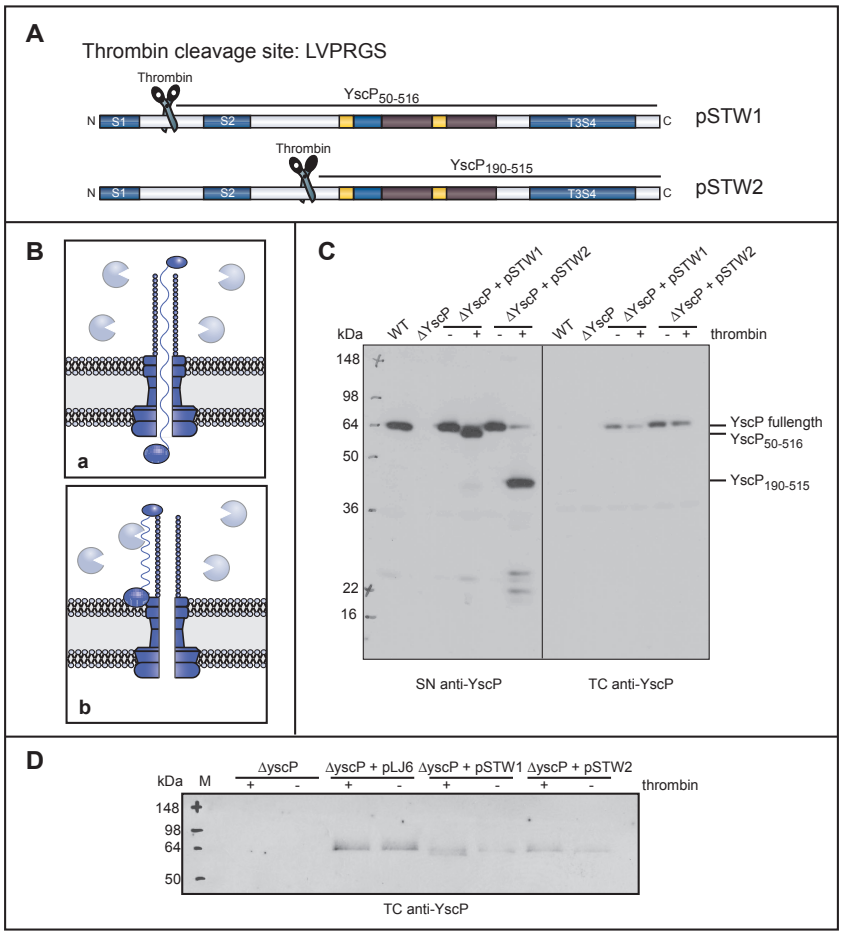

Figure A15

Thrombin protease cleaves $YscP_{\Omega TCS}$ but does not influence needle length control.

A. Schematic representation of YscP harbouring the thrombin cleavage site (TCS) either between export signal 1 and 2 (pSTW1) or after the second export signal (pSTW2).

B. Schematic representation of possible scenarios. YscP is inside the growing needle channel and protected from cleavage (a), or outside and accessible for the protease (b)

C. Supernatant fractions (SN) and total cell (TC) fractions of *Y. enterocolitica* E40 wt (pYV40), *Y. enterocolitica* E40 *ΔyscP* (pLJ4036) and *Y. enterocolitica* E40 *ΔyscP* (pLJ4036) bacteria over-expressing $YscP_{\Omega TCS1}$ (pSTW1) or $YscP_{\Omega TCS2}$ (pSTW2) *in trans* from the pBAD promoter. Thrombin protease was added to the culture supernatant at the temperature shift to 37 °C. Supernatant (SN) and total cell (TC) fractions were analyzed by immunoblot using anti-YscP antibodies.

D. Supernatant (SN) fractions of the same cultures as in (C) and *Y. enterocolitica* E40 *ΔyscP* (pLJ4036) bacteria over-expressing YscP (pLJ6) *in trans* from the pBAD promoter. Samples were taken 90 min after induction of the type III secretion system. Supernatant (SN) fractions were analyzed by immunoblot using anti-YscP antibodies.

Methods

Bacterial strains

The different strains used in this study are listed in Table I.

Construction of plasmids

Bacterial strains, plasmids and genetic constructions are listed in Table II. *E. coli* Top10 (Invitrogen), *E. coli* GM48 [168] or *E. coli* BW19610 [169] were used for plasmid purification and cloning. Bacteria were routinely grown on Lysogeny Broth (LB) agar plates and in liquid LB medium. Ampicillin was used at a concentration of 200 µg/mL to select for expression vectors. Plasmids were generated using either Pfu turbo polymerase (Stratagene) or Vent DNA polymerase (New England Biolabs). The oligonucleotides used for genetic constructions are listed in Table III. All constructs were confirmed by sequencing using a 3100-Avant genetic analyzer (ABI Prism).

Induction of the *yop* regulon and Yop protein analysis

Bacteria were routinely grown on LB agar plates and in liquid brain-heart infusion (BHI; Remel) medium. For the induction of the *yop* regulon, *Y. enterocolitica* strains were inoculated to an $O.D._{600}$ of 0.1 and cultivated in BHI medium supplemented with 35 µg/mL nalidixic acid, 4 mg/mL glucose, 20 mM $MgCl_2$ and 20 mM sodium oxalate (BHI-Ox) 2 h at RT, then shifted to 37 °C and incubated for 4 h.

Proteins from the supernatant were precipitated on ice for one hour with trichloroacetic acid 10% (w/v) final. Electrophoresis was carried out in 10%, 12%, or 15% (w/v) polyacrylamide gels in the presence of SDS (SDS-PAGE). Proteins secreted by $3.3x10^8$ bacteria were loaded per lane. For detection of YscP in total cells by immunoblotting, $1.6x10^7$ bacteria were loaded per lane. For YscP detection in supernatants by immunoblotting, the supernatants from $1.6x10^8$ bacteria were loaded per lane. After electrophoresis, proteins were stained with Coomassie brilliant blue (Pierce) or transferred by electroblotting to a nitrocellulose membrane (Hybond-C extra (Pierce); 25 V; 30-45 min). The membranes were then blocked with 5% (w/v) non-fat dried milk in PBS-T (PBS, 0.2% (v/v) Tween) for 45 min or over night at 4 °C.

Immunoblotting was carried out using a polyclonal rabbit anti-YscP antibody (1:3000; MIPA57; purified). Detection of immunoblots was performed with a secondary swine anti-rabbit antibody conjugated to horseradish peroxidase (1:5000; Dako) before development with supersignal chemiluminescent substrate (Pierce) or Amersham ECL PlusTM Western Blotting Detection System (GE Healthcare).

Expression of the different *yscP* genes cloned downstream from the pBAD promoter was routinely induced by adding 0.2% arabinose to the culture just before the shift to 37 °C, and again 2 h later. Ampicillin was used at a concentration of 200 µg/mL to select for the expression plasmids and instead of glucose, glycerol was used as carbon source at a final concentration of 4 mg/mL.

Needle length measurement

Visualization of needle-like structures at the cell surface of the bacteria was done by transmission electron microscopy as described in references [26, 130].

Purification of His_6-YscP from inclusion bodies

His_6-YscP variants were expressed in *E. coli* BL21 (DE3) Rosetta. At an $O.D._{600}$ of ~ 0.5, expression of recombinant N-terminal His-tagged *yscP* genes was induced by the addition of 0.2% L-arabinose. After 4 h of incubation at 37 °C, cells were harvested by centrifugation (3000 g / 4 °C / 10 min). The bacterial pellet was resuspended in 2 mL lysis buffer (10 mM Tris-HCl pH 8.0, 0.5 M NaCl, 1 mM PMSF, 5 mM DTT and 0.01% Nonidet P 40 substitute (Fluka, #74385; NP 40)). After sonication, the extract was treated with 5 U DNase I for 1 hour at 37 °C. Inclusion bodies (IB) were sedimented by centrifugation (18500 g / 30 min / 4 ºC). Pelleted inclusion bodies were washed twice with wash buffer A (10 mM Tris-HCl pH 8.0, 0.5 M NaCl, 1 mM PMSF and 0.1% NP 40), followed by spinning at 18500 g for 30 min at 4 ºC. The washed inclusion bodies were dissolved in 2 mL of IB lysis buffer (10 mM Tris-HCl pH 8.0, 100 mM NaH_2PO_4, 500 mM NaCl, 0.1% NP 40, 8 M urea) and left overnight at 4 ºC. Insoluble material was removed by centrifugation at 18500 g for 10 min.

The supernatant from 100 mL bacterial culture was incubated with 1 mL nickel-sepharose beads for 2 h at 4 ºC. The mixture was then poured on a BioRad column.

Bound proteins were washed with wash buffer B (2 x 10 mL: 10 mM Tris-HCl pH 8.0, 100 mM NaH_2PO_4, 500 mM NaCl, 0.1% NP 40, 8 M urea). To remove contaminants, the column was washed with an additional 20 mL of wash buffer supplemented with 10 mM imidazol. The His-tagged proteins were recovered from the column with elution buffer (5 x 1 mL: 10 mM Tris-HCl pH 8.0, 100 mM NaH_2PO_4, 500 mM NaCl, 0.01% NP 40, 250 mM imidazole and 8 M urea). Purity of the eluted protein fraction was analyzed by SDS-PAGE. Protein concentrations were determined using the Bradford-assay

Purification of GST-tagged proteins

GST-fusion proteins were expressed in *E. coli* BL21 (DE3) Rosetta. Bacteria were cultivated in 100-300 mL LB medium at 37 °C up to an $O.D._{600}$ of 0.6. Then, expression of the fusion protein was induced by addition of 0.2 mM IPTG and the cultures were grown for 4 h at 37 °C. After harvesting the bacteria, the cell pellet was resuspended in 1/20 volume phosphate buffered saline (PBS) containing protease inhibitors (Complete Mini, Roche). Cells were lyzed by sonication and unbroken cell debris was removed by centrifugation (15500 g / 30 min / 4 °C). The supernatant was incubated with 1/100 volume glutathione sepharose 4B (Amersham) (bed volume) for 2 h or overnight at 4 °C on a rotating wheel. The matrix was separated by centrifugation (500 g / 5 min / 4 °C) and washed three times with PBS containing protease inhibitors and once with cleavage buffer (50 mM Tris-HCl pH 7.5, 150 mM NaCl, 1 mM EDTA, 1mM DTT). GST-tagged proteins were eluted using PreScission protease (16 U/100 µL glutathione sepharose bed volume) in cleavage buffer for 3-5 h at 4 °C. Glutathione sepharose beads were washed twice with cleavage buffer to elute residual cleaved proteins. Purity of the eluted protein fraction was analyzed by SDS-PAGE. Protein concentrations were determined UV spectroscopy.

Overlay assay

Supernatant fractions of secreting bacteria were separated on a 15% SDS-PAGE, transferred to nitrocellulose membrane (Hybond-C extra; Pierce) and stained with Ponceau S solution to visualize the transferred proteins. The membranes were then blocked with 5% (w/v) non-fat dried milk in PBS-T (PBS, 0.2% (v/v) Tween) over night at 4 °C. After washing once with PBS-T, and once with binding buffer (PBS; 0.1% (w/

v) BSA; 0.1% (v/v) Tween), membranes were incubated 2 h at room temperature with or without purified YscP proteins in binding buffer (2 µg/mL protein final). The membranes were then washed for 1 h with PBS-T by changing the buffer several times. Bound YscP proteins were detected by immunoblotting using anti-YscP antibodies.

Purification of anti-YscP antibodies

The bacterial pellet of a 10 mL *Y. enterocolitica ΔyscP* overnight culture was resuspended in 3 mL PBS. Cells were lyzed by sonication and proteins were precipitated by addition of 4 volumes acetone at 0 °C and incubation for 1 h on ice. Precipitated proteins were pelleted (10600 g / 10 min / 4 °C) and washed with 10 mL acetone. The protein pellet was dried overnight and was then incubated with 1 mL anti-YscP antibodies (MIPA57) for 30 min on ice. Purified antibodies were separated from the protein pellet by centrifugation (10600 g / 10 min / 4 °C) and the supernatant was stored at - 20 °C.

Retardation column

GST-tagged YscP proteins, $YscP_{\Delta tail}$ proteins or GST alone were expressed in *E. coli* BL21 (DE3) Rosetta. Bacteria were cultivated in 100 mL LB medium at 37 °C up to an $O.D._{600}$ of 0.6. Then, expression of the fusion protein was induced by addition of 0.2 mM IPTG and the cultures were grown for 4 h at 37 °C. After harvesting the bacteria, the cell pellet was resuspended in 1/20 volume phosphate buffered saline (PBS) containing protease inhibitors (Complete Mini, Roche). The cells were lyzed by sonication and unbroken cell debris was removed by centrifugation (15500 g / 30 min / 4 °C). The supernatants were split into two samples with equal volume and incubated with either purified $YscU_{211-354}$ (from pISO116) or purified $YscU_{211-354,N263A}$ (from pISO117) for 2 h at room temperature on a rotating wheel. Afterwards, the supernatant mix was incubated with 1/100 volume glutathione sepharose 4B (Amersham) (bed volume) for 2 h at room temperature on a rotating wheel. The mixture was then poured on a BioRad column. Bound proteins were washed with PBS (5 x 1 mL). The GST-tagged proteins were recovered from the column with 1 x 1 mL of 2.5 mM glutathione in PBS, 1 x 1 mL 5 mM glutathione in PBS, and 2 x 1 mL 10 mM glutathione in PBS. Proteins from the collected flow-through, washing and

elution fractions were precipitated on ice (1 h) with trichloroacetic acid 10% (w/v) final. Dried protein pellets were resuspended in 100 µL SDS-sample buffer and analyzed by immunoblotting using anti-YscP and anti-YscU antibodies.

Bacterial Strains

Bacterial strain	Genotype or Description	Source or Reference
E. coli		
BL21 ROSETTA	F- *ompT hsdS*$_B$($r_B^-m_B^-$) *gal dcm lac*Y1 pRARE 6 (Cm^r)	Novagen
BW19610	DE3(*lac*)X74 *uidA*(ΔMlu1)::*pir-116 recA1 ΔphoA532* Δ(*phnC?DEFGHIJKLMNOP*)33-30	[169]
BW19612	DE3(*lac*)X74 *uidA*(ΔMlu1)::*pir+ recA1 ΔphoA532* Δ(*phnC?DEFGHIJKLMNOP*)33-30	[169]
GM48	F- *thr leu thi lacY galK galT ara fhuA tsx dam dcm glnV44*	[168]
SM10λ*pir*	*thi-1, thr, leu, tonA, lacY, supE, recA*::RP4-2-*tet::Mu1 kan* (Km^r)	[170]
Top10	F- *mcr*A Δ(*mrr-hsd*RMS-*mcr*BC) φ80*lac*ZΔM15 Δ*lac*X74 *rec*A1 *ara*D139 Δ(*ara leu*)7697 *gal*U *gal*K *rps*L (Sm^r) *end*A1 *nup*G	Invitrogen
Y. enterocolitica		
MRS40	Wild-type virulence plasmid pYV40	[171]
WAT9/88	Wild-type virulence plasmid pYVwat9/88	[157]
A11/86	Wild-type virulence plasmid pYVa11/86	[157]
WAT288	Wild-type virulence plasmid pYVwat288	[157]
A127/90	Wild-type virulence plasmid pYVa127/90	[157]
E40	Wild-type virulence plasmid pYV40	[157]
W22703	Wild-type virulence plasmid pYVe22703	[157]
IP17	Wild-type virulence plasmid pYVip17	[157]
MRS40 $YscU_{N263A}$	pISO4007 $YscU_{N263A}$	[130]
MRS40 ΔyscEFGHI	pISO4017 ΔyscEFGHI	Isabel Sorg, unpublished
MRS40 ΔyscI	pKEM4001 ΔyscI	Diepold *et al.* (in prep.)
MRS40 ΔyopBD	pISO4005 ΔyopBD	[47]
MRS40 ΔyscP	pLJ4036 ΔyscP (deleted from start to stop)	[110]
MRS40 $YscP_{Δ46-96+Δ222-306}$	pLJ4022 $YscP_{Δ46-96+Δ222-306}$	[32]
MRS40 $YscP_{sitelΩYscP222-381}$	pLJM4001 $YscP_{sitelΩYscP222-381}$	[32]
MRS40 ΔyscU	pLY4001 ΔyscU (deleted from start to stop)	[130]
MRS40 $YscP_{Δ500-515}$	pSTW4002 $YscP_{Δ500-515}$	This study

Bacterial strain	Genotype or Description	Source or Reference
MRS40 YscU$_{N263Q}$	pSTW4003 YscU$_{N263Q}$	This study
MRS40 ΔyscI/ΔyscP	pSTW4005 ΔyscI/ΔyscP	This study

Plasmids

Plasmid	encoded Protein	Genotype or Description	Source or Reference
pYV plasmids			
pYV40		Wild-type virulence plasmid from strain *Y. enterocolitica* E40	[171]
pYVe22703		Wild-type virulence plasmid from strain *Y. enterocolitica* W22703	[172]
pISO4005		pYV40 ΔyopBD	[47]
pISO4007		pYV40 YscU$_{N263A}$	[130]
pISO4017		pYV40 ΔyscEFGHI multiple knockout of yscE, yscF, yscG, yscH and yscI by allelic exchange using mutator pISOA171	Isabel Sorg, unpublished
pKEM4001		pYV40 ΔyscI	Diepold *et al.* (in prep.)
pLJ4036		pYV40 ΔyscP (deleted from start to stop)	[110]
pLJ4022		pYV40 YscP$_{Δ46-96+Δ222-306}$	[32]
pLJM4001		pYV40 YscP$_{siteIΩYscP222-381}$	[32]
pLY4001		pYV40 ΔyscU (deleted from start to stop)	[130]
pSTW4002		pYV40 YscP$_{Δ500-515}$ deletion of the YscP tail (aa 500-515) by allelic exchange using mutator pSTW33	This study
pSTW4003		pYV40 YscU$_{N263Q}$ introduction of pointmutation N263Q in YscU by allelic exchange using mutator pSTW54	This study
pSTW4005		pYV40 ΔyscI/ΔyscP double knockout of yscP and yscI by allelic exchange using mutator pLJ4036 on pKEM4001	This study
Suicide plasmid			

Plasmid	encoded Protein	Genotype or Description	Source or Reference
pKNG101		*Ori*$_{R6K}$ *sac*BR$^+$ *ori*T$_{RK2}$ *str*AB$^+$	[173]
Mutator plasmids			
pISOA171		pKNG101-ΔyscEFGHI$^+$ the flanking regions of yscE and yscI were amplified by overlapping PCR from pYVe22703 using primer pairs 4972/4973 and 4974/4975 and cloned into pKNG101 using restriction sites SalI/XbaI	Isabel Sorg, unpublished
pSTW31		pKNG101-yscP$_{805}^+$ the region encoding aa 1-805 of YscP$_{805}$ and flanking regions of YscO and YscQ were amplified from pYVe22703 using primer pairs 4719/4720 and 4723/4781 and from pSTW26 using primer pair 4721/4722 and cloned into pKNG101 using restriction sites SalI/ApaI	This study
pSTW34		pKNG101-yscP$_{\Delta 500-515}^+$ the region encoding aa 430-515 of YscP and aa 1-55 of YscQ was amplified from pYVe22703 introducing a stop codon after aa 499 of YscP by overlapping PCR using primer pairs 4397/4398 and 4399/4400 and cloned into pKNG101 using restriction sites SalI/XbaI	This study
pSTW54		pKNG101-yscU$_{N263Q}^+$ the region encoding aa 172-354 of YscU was amplified from pISO167 using oligos 4141 and 5161 and cloned into pKNG101 using restriction sites SalI/XbaI	This study
Expression plasmids			
pBADMycHisA			Invitrogen
pBluescript II KS (+)			Stratagene
pCDFDuet-1			Novagen
pEGFP-1		EGFP	BD Biosciences Clontech
pET28a-pbpK15		Penicillin Binding Protein (PBP) from *Streptomyces* K15	Ghuysen, J.
pCA20	YscP$_{\Delta 46-96+\Delta 222-306}$	pBADMycHisA-yscP$_{\Delta 46-96+\Delta 222-306}$	[53]

Plasmid	encoded Protein	Genotype or Description	Source or Reference
pCA23	$YscP_{site\ I}$	pBADMycHisA-$yscP_{siteI}$ Introduction of a NotI and a XbaI site between codons 49 and 50 of $yscP_{WT}$ in pLJ6.	[53]
pGEX-6P-1		N-terminal GST-tag with PreScission Protease cleavage site	Amersham
pGP1-2	T7 RNA polymerase	pBR322-T7 RNA polymerase	[174]
pISO116	GST-$YscU_{211-354}$	pGEX-6P-1-$yscU_{WT}$ $yscU_{211-354}$ was amplified from pYVe22703 using oligos 4337 and 4338 and cloned into pGEX-6P-1 using restriction sites BamHI/XhoI	Isabel Sorg, unpublished
pISO117	GST-$YscU_{211-354\ N263A}$	pGEX-6P-1-$yscU_{N263A}$ $yscU_{211-354}$ was amplified from pSTW7 using oligos 4337 and 4338 and cloned into pGEX-6P-1 using restriction sites BamHI/XhoI	Isabel Sorg, unpublished
pISOA132	$YopE_{1-15}$LcrV	pBADMycHisA-$yopE_{1-15}$lcrV	[130]
pISO147	YscEFGHI	pBADMycHisA-yscEFGHI yscEFGHI was amplified from pYVe22703 using oligos 3410 and 3522 and cloned into pBADMycHisA using restriction sites NcoI/HindIII	Isabel Sorg, unpublished
pISO167	$YscU_{N263Q}$	pBADMycHisA-$yscU_{N263Q}$	[158]
pKEM4	YscI	pBADMycHisA-$yscI_{WT}$ $yscI_{WT}$ was amplified from pYVe22703 using oligos 3521 and 3523 and cloned into pBADMycHisA using restriction sites NcoI/EcoRI	Kerstin Maylandt, unpublished
pLJ6	$YscP_{WT}$	pBADMycHisA-$yscP_{WT}$ This yscP gene originates from strain W22703 and differs slightly from the ortholog in strain E40. All the yscP variants described in this paper were engineered from this gene.	[53]
pLJC12	$YscP_{\Delta 501-515}$	pBADMycHisA-$yscP_{\Delta 501-515}$	[110]
pLJ14	His_6-$YscP_{WT}$	pBADMycHisA-his_6-$yscP_{WT}$ $yscP_{WT}$ was amplified from pYVe22703 using oligos 3081 (carrying N-terminal His_6-tag) and 3345 and cloned into pBADMycHisA using restriction sites NcoI/EcoRI	Laure Journet, unpublished
pLJ18	$YscP_{siteI\Omega FliK147-266}$	pBADMycHisA-$yscP_{siteI\Omega FliK147-266}$	[53]

Plasmid	encoded Protein	Genotype or Description	Source or Reference
pLJ19	$YscP_{sitelΩYscP222-381}$	pBADMycHisA-$yscP_{sitelΩYscP222-381}$	[53]
pLY7	$YscU_{WT}$	pBADMycHisA-$yscU_{WT}$	[130]
pPB42	$LcrV_{WT}$	pBADMycHisA-$lcrV_{WT}$	[130]
pSTW1	$YscP_{thrombin\ cleavage\ site\ aa46-51}$	pBADMycHisA-$yscP_{thrombin\ cleavage\ site\ aa46-51}$ Introduction of Thrombin cleavage site (aa 46-51) by inverted PCR using oligos 3973 and 3974. Template plasmid pLJ6 was digested with DpnI.	This study
pSTW2	$YscP_{thrombin\ cleavage\ site\ aa186-191}$	pBADMycHisA-$yscP_{thrombin\ cleavage\ site\ aa186-191}$ Introduction of Thrombin cleavage site (aa 46-51) by invert PCR using oligos 3975 and 3976. Template plasmid pLJ6 was digested with DpnI.	This study
pSTW3	$YscP_{sites\ I + II}$	pBADMycHisA-$yscP_{sites\ I + II}$ Introduction of a ClaI and a SalI site between codons 186 and 187 of yscP from pCA23 by overlapping PCR using primer pairs 3344/4404 (introducing both sites) and 4401/3345 (introducing both sites) and cloned into pBADMycHisA using restriction sites NcoI/EcoRI	This study
pSTW4	$YscP_{sites\ I + III}$	pBADMycHisA-$yscP_{sites\ I + III}$ Introduction of a ClaI and a SalI site between codons 250 and 251 of yscP from pCA23 by overlapping PCR using primer pairs 3344/4405 (introducing both sites) and 4402/3345 (introducing both sites) and cloned into pBADMycHisA using restriction sites NcoI/EcoRI	This study
pSTW5	$YscP_{sites\ I + IV}$	pBADMycHisA-$yscP_{sites\ I + IV}$ Introduction of a ClaI and a SalI site between codons 390 and 391 of yscP from pCA23 by overlapping PCR using primer pairs 3344/4406 (introducing both sites) and 4403/3345 (introducing both sites) and cloned into pBADMycHisA using restriction sites NcoI/EcoRI	This study
pSTW7	$YscU_{N263A}$	pBADMycHisA-$yscU_{N263}$	[130]

Plasmid	encoded Protein	Genotype or Description	Source or Reference
pSTW8	YscU$_{P264A}$	pBADMycHisA-yscU$_{P264A}$	[130]
pSTW9	YscU$_{T265A}$	pBADMycHisA-yscU$_{T265A}$	[130]
pSTW10	YscU$_{\Delta NPTH}$	pBADMycHisA-yscU$_{\Delta NPTH}$ Deletion of cleavage site NPTH by overlapping PCR using primer pairs 3724/4216 and 4217/3704 on pLY7. Ligation into pBADMycHisA using restriction sites NcoI/EcoRI	This study
pSTW11	YscU$_{\Delta 264-354}$	pBADMycHisA-yscU$_{\Delta 264-354}$ Deletion of aa 264-354 using oligos 3724 and 4218 on pLY7. Ligation into pBADMycHisA using restriction sites NcoI/EcoRI	This study
pSTW12	YscP$_{siteII\Omega YscP241-374}$	pBADMycHisA-yscP$_{siteII\Omega YscP241-374}$ Duplication of codons 214 to 374 from yscP (amplified with oligos 4407 and 4408) from pSTW3 (between codons 186 and 187)	This study
pSTW13	YscP$_{siteII\Omega FliK151-270}$	pBADMycHisA-yscP$_{siteII\Omega FliK151-270}$ Insertion of codons 151 to 270 from fliK of Salmonella typhimurium (amplified with oligos 4412 and 4413) into yscP from pSTW3 (between codons 186 and 187)	This study
pSTW14	YscP$_{siteIII\Omega YscP241-374}$	pBADMycHisA-yscP$_{siteIII\Omega YscP241-374}$ Duplication of codons 214 to 374 from yscP (amplified with oligos 4407 and 4408) from pSTW4 (between codons 250 and 251)	This study
pSTW15	YscP$_{siteIII\Omega FliK151-270}$	pBADMycHisA-yscP$_{siteIII\Omega FliK151-270}$ Insertion of codons 151 to 270 from fliK of Salmonella typhimurium (amplified with oligos 4412 and 4413) into yscP from pSTW4 (between aa 250 and 251)	This study
pSTW16	YscP$_{siteIV\Omega YscP241-374}$	pBADMycHisA-yscP$_{siteIV\Omega YscP241-374}$ Duplication of codons 214 to 374 from yscP$_{WT}$ (amplified with oligos 4407 and 4408) from pSTW5 (between codons 390 and 391)	This study
pSTW17	YscP$_{siteIV\Omega 151-270}$	pBADMycHisA-yscP$_{siteIV\Omega 151-270}$ Insertion of codons 151 to 270 from fliK of Salmonella typhimurium (amplified with oligos 4412 and 4413) into yscP from pSTW5 (between codons 390 and 391)	This study

Plasmid	encoded Protein	Genotype or Description	Source or Reference
pSTW18	YscP$_{siteIΩPBP}$	pBADMycHisA-yscP$_{siteIΩPBP}$ PBP K15 was amplified from pET28a-pbpK15 using oligos 4432 and 4433 and cloned into pCA23 using restriction sites XbaI/NotI	This study
pSTW19	GST-YscP$_{WT}$	pGEX-6P-1-gst-yscP$_{WT}$ yscP$_{WT}$ was amplified from pLJ6 using oligos 4409 and 4428 and cloned into pGEX-6P-1 using restriction sites BamHI/XhoI	This study
pSTW20	GST-YscP$_{367-515}$	pGEX-6P-1-gst-yscP$_{367-515}$ yscP$_{367-515}$ was amplified from pLJ6 using oligos 4409 and 4429 and cloned into pGEX-6P-1 using restriction sites BamHI/XhoI	This study
pSTW21	His$_6$-YscP$_{400-515}$	pBADMycHisA-his$_6$-yscP$_{400-515}$ yscP$_{400-515}$ was amplified from pLJ6 using oligos 4448 and 3345 and cloned into pBADMycHisA using restriction sites NcoI/EcoRI	This study
pSTW22	His$_6$-YscP$_{1-399}$	pBADMycHisA-his$_6$-yscP$_{1-399}$ yscP$_{1-399}$ was amplified from pLJ6 using oligos 3081 and 4443 and cloned into pBADMycHisA using restriction sites NcoI/EcoRI	This study
pSTW23	YscP$_{siteIIIΩPBP}$	pBADMycHisA-yscP$_{siteIIIΩPBP}$ PBP K15 was amplified from pET28a-pbpK15 using oligos 4628 and 4629 and cloned into pSTW4 using restriction sites ClaI/SpeI	This study
pSTW26	YscP$_{siteIΩYscP222-381 +siteIIIΩFliK151-270}$	pBADMycHisA-yscP$_{siteIΩYscP222-381 +siteIIIΩFliK151-270}$ Duplication of codons 222 to 381 from yscP (from pLJ19) into site I of pSTW15.	This study
pSTW28	His$_6$-YscP$_{Δ46-96+Δ222-306}$	pBADMycHisA-his$_6$-yscP$_{Δ46-96+Δ222-306}$ yscP$_{Δ46-96+Δ222-306}$ was amplified from pCA20 using oligos 3081 and 3345 and cloned into pBADMycHisA using restriction sites NcoI/EcoRI	This study
pSTW29	His$_6$-YscP$_{siteIΩYscP222-381}$	pBADMycHisA-his$_6$-yscP$_{siteIΩYscP222-381}$ yscP$_{siteIΩYscP222-381}$ was amplified from pLJ19 using oligos 3081 and 3345 and cloned into pBADMycHisA using restriction sites NcoI/EcoRI	This study

Plasmid	encoded Protein	Genotype or Description	Source or Reference
pSTW32	His_6-$YscP_{siteIΩYscP222-381\ +siteIIIΩFliK151-270}$	pBADMycHisA-his_6-$yscP_{siteIΩYscP222-381\ +siteIIIΩFliK151-270}$ $yscP_{siteIΩYscP222-381\ +siteIIIΩFliK151-270}$ was amplified from pSTW26 using oligos 3081 and 3345 and cloned into pBADMycHisA using restriction sites NcoI/EcoRI	This study
pSTW33	$YscP_{Δ500-515}$	pBluescriptIIKS(+)-$yscP_{Δ500-515}$ (mutator)	This study
pSTW35	$YscP_{P237A,\ P238A}$	pBADMycHisA-$yscP_{P237A,\ P238A}$	[157]
pSTW36	$YscP_{P237A,\ P238A,\ P244A,P256A}$	pBADMycHisA-$yscP_{P237A,\ P238A,\ P244A,P256A}$	[157]
pSTWIS37	$YscP_{Q212P,\ Q217P}$	pBADMycHisA-$yscP_{Q212P,\ Q217P}$ Mutations Q212P, Q217P were introduced into pLJ6 by overlapping PCR using oligo pairs 3344/4948 and 4947/3345. Ligation into pBADMycHisA using restriction sites NcoI/EcoRI	This study
pSTWIS38	$YscP_{L268P,L303P}$	pBADMycHisA-$yscP_{L268P,L303P}$	[157]
pSTWIS39	$YscP_{L268P,\ E277P,\ L283P,\ L303P}$	pBADMycHisA-$yscP_{L268P,\ E277P,\ L283P,\ L303P}$	[157]
pSTW40	$YscP_{E375P,\ E379P}$	pBADMycHisA-$yscP_{E375P,\ E379P}$ Mutations E375P, E379P were introduced into pLJ6 by overlapping PCR using oligo pairs 3344/4963 and 4962/3345. Ligation into pBADMycHisA using restriction sites NcoI/EcoRI	This study
pSTW41	$YscP_{Q212P,\ Q217P,\ L268P,\ L303P}$	pBADMycHisA-$yscP_{Q212P,\ Q217P,\ L268P,\ L303P}$	[157]
pSTW42	$YscP_{Q212P,\ Q217P,\ L268P,\ E277P,\ L283P,\ L303P}$	pBADMycHisA-$yscP_{Q212P,\ Q217P,\ L268P,\ E277P,\ L283P,\ L303P}$	[157]
pSTW43	$YscP_{Q212P,\ Q217P,\ E375P,\ E379P}$	pBADMycHisA-$yscP_{Q212P,\ Q217P,\ E375P,\ E379P}$	[157]
pSTW44	$YscP_{E145P,\ E151P,\ L162P,\ Q165P}$	pBADMycHisA-$yscP_{E145P,\ E151P,\ L162P,\ Q165P}$	[157]

Plasmid	encoded Protein	Genotype or Description	Source or Reference
pSTW45	YscP$_{L303P}$	pBADMycHisA-yscP$_{L303P}$ Mutation L303P was introduced into pLJ6 by overlapping PCR using oligo pairs 3344/4952 and 4951/3345. Ligation into pBADMycHisA using restriction sites NcoI/EcoRI (happend by mistake; was planned to carry 4 mutations)	This study
pSTW46	YscP$_{Q212G, Q217G, E375G,E379G}$	pBADMycHisA-yscP$_{Q212G, Q217G, E375G,E379G}$	[157]
pSTW47	YscP$_{Q212P, Q217P, L268P, E277P, L283P, L303P, E375P, E379P}$	pBADMycHisA-yscP$_{Q212P, Q217P, L268P, E277P, L283P, L303P, E375P, E379P}$	[157]
pSTW48	YscP$_{P174A, P181A, P185A, P188A, P237A, P238A, P244A, P256A}$	pBADMycHisA-yscP$_{P174A, P181A, P185A, P188A, P237A, P238A, P244A, P256A}$	[157]
pSTW49	YscP$_{497-515}$	pBADMycHisA-yscP$_{497-515}$ Alignment of oligos 4883 and 4884 and ligation into pBADMycHisA using restriction sites NcoI/EcoRI	This study
pSTW50	His$_6$-YscP$_{497-515}$	pBADMycHisA-yscP$_{497-515}$ Alignment of oligos 4879 and 4880 and ligation into pBADMycHisA using restriction sites NcoI/EcoRI	This study
pSTW51	GST-YscP$_{497-515}$	pGEX-6P-1-yscP$_{497-515}$ Alignment of oligos 4881 and 4882 and ligation into pGEX-6P-1 using restriction sites BamHI/XhoI	This study
pSTW52	YscP$_{P174A, P181A, P185A, P188A, P237A, P238A}$	pBADMycHisA-yscP$_{P174A, P181A, P185A, P188A, P237A, P238A}$	[157]
pSTW53	GST-YscP$_{1-137}$	pGEX-6P-1-yscP$_{1-137}$ yscP$_{1-137}$ was amplified from pLJ6 using oligos 4428 and 5112 and cloned into pGEX-6P-1 using restriction sites BamHI/XhoI	This study
pSTW55	YscI$_{Q84A}$	pBADMycHisA-yscI$_{Q84A}$ Introduction of pointmutation Q84A in YscI by overlapping PCR using primer pairs 3521/5158 and 5157/3522 on pKEM4. Ligation into pBADMycHisA using restriction sites NcoI/HindIII	This study

Plasmid	encoded Protein	Genotype or Description	Source or Reference
pSTW56	$YscI_{L96A}$	pBADMycHisA-$yscI_{L96A}$ Introduction of pointmutation L96A in YscI by overlapping PCR using primer pairs 3521/5160 and 5159/3522 on pKEM4. Ligation into pBADMycHisA using restriction sites NcoI/HindIII	This study
pSTW57	GST-$YscP_{\Delta 500-515}$	pGEX-6P-1-$yscP_{\Delta 500-515}$ $yscP_{\Delta 500-515}$ was amplified from pLJ6 using oligos 4428 and 3064 and cloned into pGEX-6P-1 using restriction sites BamHI/EcoRI	This study
pSTW58	$YscP_{siteIΩYscP222-381 +siteIIIΩFliK151-270 + YscPΔ46-96+Δ222-306}$	pBADMycHisA-$yscP_{siteIΩYscP222-381 +siteIIIΩFliK151-270 + YscPΔ46-96+Δ222-306}$ $yscP_{\Delta 46-96+\Delta 222-306}$ was amplified from pCA20 using oligos 5320 and 5321 and cloned into pSTW26 using restriction sites EcoRI/SalI	This study
pSTW59	$YscP_{\Delta 46-96+\Delta 222-306 + YscPsiteIΩYscP222-381 +siteIIIΩFliK151-270}$	pBADMycHisA-$yscP_{\Delta 46-96+\Delta 222-306 + YscPsiteIΩYscP222-381 +siteIIIΩFliK151-270}$ $yscP_{siteIΩYscP222-381+siteIIIΩFliK151-270}$ was amplified from pSTW26 using oligos 5320 and 5321 and cloned into pCA20 using restriction sites EcoRI/SalI	This study
pSTW60	$YscP_{+C516}$	pBADMycHisA-$yscP_{+C516}$ Addition C516 C-terminal end of YscP using oligos 3344 and 5417 on pLJ6. Ligation into pBADMycHisA using restriction sites NcoI/EcoRI	This study
pSTW61	$YscU_{N263A, S351C}$	pBADMycHisA-$yscU_{N263A, S351C}$ Introduction of pointmutation S351C in $YscU_{N263A}$ using oligos 3724 and 5416 on pSTW7. Ligation into pBADMycHisA using restriction sites NcoI/EcoRI	This study
pSTW62	GST-$YscU_{211-354, N263A, S351C}$	pGEX-6P-1-$yscU_{N263A, S351C}$ Introduction of pointmutation S351C in $YscU_{211-354,N263A}$ using oligos 4337 and 5416 on pISO117. Ligation into pGEX-6P-1 using restriction sites BamHI/EcoRI	This study
pSTW63	$YscU_{S351C}$	pBADMycHisA-$yscU_{S351C}$ Introduction of pointmutation S351C in $YscU_{WT}$ using oligos 3724 and 5416 on pLY7. Ligation into pBADMycHisA using restriction sites NcoI/EcoRI	This study

Plasmid	encoded Protein	Genotype or Description	Source or Reference
pSTW64	GST-YscU$_{211-354, S351C}$	pGEX-6P-1-yscU$_{S351C}$ Introduction of pointmutation S351C in YscU$_{211-354}$ using oligos 4337 and 5416 on pISO116. Ligation into pGEX-6P-1 using restriction sites BamHI/EcoRI	This study
pSTW65	YscP$_{siteIIIΩYscP241-374 + YscPΔ46-96+Δ222-306}$	pBADMycHisA-yscP$_{siteIIIΩYscP241-374 + YscPΔ46-96+Δ222-306}$ yscP$_{Δ46-96+Δ222-306}$ from pSTW58 was cloned into pSTW14 using restriction sites EcoRI/SalI	This study

Oligonucleotides

Oligonucleotides used for clonings

No.	Sequence	Restriction site
3064	gatcgaattcttactcctgttcactgtcac	EcoRI
3081	gatcccatgggcagccatcatcatcatcataataaaatcaccactcgt	NcoI
3170	gggccagatctattattctgatggttgtg	
3171	gatcgaattccctccttgtcttttacag	
3321	aataccaagccgactgttcag	
3344	gatcccatggccaataaaatcaccactcgt	NcoI
3345	gatcgaattcttattcttcagcctcccactc	EcoRI
3410	gactccatggccacacaattagaggagcaactg	NcoI
3521	gatcccatggctccgaacatagaaatagct	NcoI
3522	gatcaagctttcacccccccttcgacaag	HindIII
3522	gatcaagctttcacccccccttcgacaag	HndIII
3672	ccttccattgtaactgtaat	
3704	gatcgaattcttataacatttcggaatg	EcoRI
3724	gatcccatggccagcggagaaaagacagag	NcoI
3973	ggtaatcgtcatcccaaactagtgccgcgtggatcccctgtacgtccgcatgac	
3974	gtcatgcggacgtacaggggatccacgcggcactagtttgggatgacgattacc	
3975	ccgactgttcagccattggttcctcgaggtagcggcgcagaggttcagcaa	
3976	ttgctgaacctctgcgccgctacctcgaggaaccaatggctgaacagtcgg	

No.	Sequence	Restriction site
3989	gatccatggtgagcaagggcg	NcoI
3992	gatcgaattcttacttgtacagctcgtccatg	EcoRI
4141	acgcgtcgacgtggaattgaatgtattacccc	SalI
4216	aatagcaatagctaccaccactgatga	
4217	gtggtagctattgctattggtattctt	
4218	ccggaattcttacggattagctaccaccactga	EcoRI
4337	actgggatccattaaggaacttaaaatgagcaag	BamHI
4338	actgctcgagttataacatttcggaatgctgttt	XhoI
4397	acgcgtcgactcccaagtaacccaatta	SalI
4398	acgtgatcactgttcactgtcaccgct	
4399	agtgaacagtgatcacgtcagaagcgccac	
4400	gctctagatcccttccattgtaactg	XbaI
4401	ttgatcgatgcgactagtaatcctgcagctgacggcgcagag	ClaI-SpeI
4402	gcaatcgatgcgactagtagatggtgtgctactcctgtggct	ClaI-SpeI
4403	gtcatcgatgcgactagtacgccgggtgatcacctattagca	ClaI-SpeI
4404	attactagtcgcatcgatcaatggctgaacagtcggcttggt	ClaI-SpeI
4405	tctactagtcgcatcgattgctaccaaatgatcattcggtgt	ClaI-SpeI
4406	cgtactagtcgcatcgatgacaaccggtgctgtaaaagacaa	ClaI-SpeI
4407	ccatcgatgatagcaggcaaaaacgccttgca	ClaI
4408	ggactagtttcgcgcggaagtaacagttcttc	SpeI
4409	ccgctcgagtcattcttcagcctcccactcctc	XhoI
4412	ccatcgatctgcccggacaacctgtcgcg	ClaI
4413	ggactagttaacggcgcgctgagtaccgg	SpeI
4428	cgcggatccaataaaatcaccactcgt	BamHI
4429	cgcggatccgaagaactgttacttccg	BamHI
4432	gctctagagatggtcaccaagccc	XbaI
4433	ataagaatgcggccgccagggcgaagccgtagttcatgatcttggt	NotI
4443	ggaattctcatgttgctaataggtgatc	EcoRI
4448	gatcccatgggcagccatcatcatcatcatatgcgcgcgacgaggctgacatcagtctcagag	NcoI
4628	ccatcgatatggtcaccaagccc	ClaI

No.	Sequence	Restriction site
4629	ggactagtcagggcgaagccgtagttcatgatcttggt	SpeI
4719	acgcgtcgactatgaactggagtgcgcc	SalI
4720	ggaacgagtggtgattttattcattaggcgttcct	
4721	aggaacgcctaatgaataaaatcaccactcgttcc	
4722	ggttaacaaactcattcttcagcctcccactc	
4723	gagtgggaggctgaagaatgagtttgttaacc	
4781	gcgggccccccagttagccagatcatc	ApaI
4875	actaactgccgcggcacatacctctgg	
4876	ccagaggtatgtgccgcggcagttagt	
4877	atcattcgctgtggcactaactgccgcggcacatacctctgg	
4878	acagcgaatgatcatttggtagcaagatggtgtgctactgctgtggctga	
4879	catgccatgggccatcatcatcatcatcatagtgaacaggagtcacgtcagaagcgccacgtctatgaggagtgggaggctgaagaatgagaattccg	NcoI EcoRI
4880	cggaattctcattcttcagcctcccactcctcatagacgtggcgcttctgacgtgactcctgttcactatgatgatgatgatggcccatggcatg	NcoI EcoRI
4881	cgcggatccagtgaacaggagtcacgtcagaagcgccacgtctatgaggagtgggaggctgaagaatgactcgagcgg	BamHI XhoI
4882	ccgctcgagtcattcttcagcctcccactcctcatagacgtggcgcttctgacgtgactcctgttcactggatccgcg	BamHI XhoI
4883	catgccatggacagtgaacaggagtcacgtcagaagcgccacgtctatgaggagtgggaggctgaagaatgagaattccg	NcoI EcoRI
4884	cggaattctcattcttcagcctcccactcctcatagacgtggcgcttctgacgtgactcctgttcactctccatggcatg	NcoI EcoRI
4947	gcaaaaaacccgcgcgatagcaggccaaaacgcctt	
4948	aaggcgttttggcctgctatcgcgcgggtttttgc	
4949	gagctggcggatcggtcacaacatcttactgatggcgttgatagcagcaaagataccatcgaaccaccgcgaccagaagaaccgttacctctt	
4950	ttgtgaccgatccgccagctcggtcacgtccagttgctctgactgcactatcgctttgtgcggaaaacgtgcagatttttctgctacctcagc	
4951	gagccggcggatcggtcacaacatcttactgatggcgttgatagcagcaaagataccatcgaaccaccgcgaccagaagaaccgttacctctt	
4952	ttgtgaccgatccgccggctcggtcacgtccagttgcggtgactgcactatcgctttgtgcggaaaacgtgcagatttttctgctacctcagc	
4962	cgcgaaccaaccttgctgccgatgtattcc	

No.	Sequence	Restriction site
4963	atacatcggcagcaaggttggttcgcgcgga	
4972	gactgtcgacgacctaaattagaactggtcaatgtcg	SalI
4973	ctcattcgcccggctgtcttatcgaggtttacctccattgagc	
4974	gctcaatggaggtaaacctcgataagacagccgggcgaatgag	
4975	gactctagagcttaatcttcccatctttgtctg	XbaI
4989	ccctgcgagccgtctggacatgatgagccatttgttccgcaatcgcctata	
4990	tccagacggctcgcaggggagggacttgatgtccccgtgggacaagtcac	
4995	gcaaaaaacgggcgcgatagcaggggaaaacgcctt	
4996	aaggcgttttcccctgctatcgcgcccgtttttgc	
4997	cgcgaaggaaccttgctggggatgtattcc	
4998	atacatccccagcaaggttccttcgcgcgga	
4999	aataccaaggcgactgttcaggcattgaatgctgcagctga	
5000	ctgaacagtcgccttggtattcaattgaactgcctgaacgga	
5112	ccgctcgagtcagggcgccaatggcatgag	XhoI
5157	cctgatgctaatggcatggtcacttatcc	
5158	ggataagtgaccatgccattagcatcagg	
5159	atccaagaagaagctatcgccaagaca	
5160	ctgtcttggcgatagcttcttcttggat	
5161	ctagtctagattataacatttcggaatgctgtttctc	XbaI
5201	ggaattccatatggccaataaaatcaccactcgt	NdeI
5202	ccgctcgagtcattcttcagcctccca	XhoI
5306	catgccatggatgaacacgatt	NcoI
5307	ggaattcttacgcgaacgcga	EcoRI
5320	gatcgaattcaggaggaattaaccatgaataaaatcaccactcgttccccattag	EcoRI
5320	gatcgaattcaggaggaattaaccatgaataaaatcaccactcgttccccattag	EcoRI
5321	acgcgtcgacttattcttcagcctcccactc	SalI
5321	acgcgtcgacttattcttcagcctcccactc	SalI
5416	gatcgaattcttataacatttcgcaatgctgtttc	EcoRI
5417	gatcgaattcttagcattcttcagcctcccactc	EcoRI
5437	ccgctcgagctacttgtacagctcgtc	XhoI

No.	Sequence	Restriction site
5444	ggaattccatatggtgagcaagggcgaggag	NdeI

Oligonucleotides used for sequencing

No.	Sequence	Binding site
1108	ATGCCATAGCATTTTTATCC	pBAD
3431	GATTTAATCTGTATCAGG	pBAD
4449	GTGAAACGGGGACAT	YscP
4452	CGCTAGTCGCTGTGC	YscP
4488	AGTGCCACACCGAAT	YscP
4489	TACCTCAGCCACAGG	YscP
4496	GGGCTGGCAAGCCACGTTTGGTG	pGEX
4497	CCGGGAGCTGCATGTGTCAGAGG	pGEX
5322	GAAGAATAAGAATTCAGG	YscP
5323	AGGTTGTCCGGGCAGATC	YscP
5324	CTCAGCGCGCCGTTAAC	YscP
5325	ATTCTGATGGTTGTG	YscP
5326	GCAGCGGCCGCTTGTCTAG	YscP
5327	TTCTTCGTCTAGACAAG	YscP

Antisera

No.	Name	Antigen	Dilution	Source
57	anti-YscP	YscP (polyclonal)	1:3000	rabbit, Laboratoire d'Hormonologie, Belgium
83	anti-YscI	YscI (polyclonal)	1:100	rabbit, Laboratoire d'Hormonologie, Belgium
96	anti-YopD	YopD (monoclonal)	1:2000	rat
98	anti-YopB	YopB (monoclonal)	1:2000	rat
120	anti-His	N-terminal His-tag (moonoclonal)	1:3000	Amersham
168	anti-rabbit	2ndary AB swine anti-rabbit-HRP	1:5000	DAKO

No.	Name	Antigen	Dilution	Source
182	anti-rat	goat anti-rat-HRP	1:4000	Southern Biotech
220	anti-LcrV	LcrV (polyclonal)	1:2000	rabbit, Laboratoire d'Hormonologie, Belgium
221	anti-YscU	YscU (polyclonal)	1:1000	rabbit, Laboratoire d'Hormonologie, Belgium
223	anti-YscF	YscF (polyclonal)	1:1000	rabbit, Laboratoire d'Hormonologie, Belgium

References

1. Troisfontaines, P. and Cornelis, G. R. (2005). Type III secretion: more systems than you think *Physiology (Bethesda),* **20**, 326-39.

2. Gophna, U., Ron, E. Z., and Graur, D. (2003). Bacterial type III secretion systems are ancient and evolved by multiple horizontal-transfer events *Gene,* **312**, 151-63.

3. Michiels, T., Wattiau, P., Brasseur, R., Ruysschaert, J. M., and Cornelis, G. (1990). Secretion of Yop proteins by Yersiniae *Infect Immun,* **58(9)**, 2840-9.

4. Sory, M. P. and Cornelis, G. R. (1994). Translocation of a hybrid YopE-adenylate cyclase from Yersinia enterocolitica into HeLa cells *Mol Microbiol,* **14(3)**, 583-94.

5. Pettersson, J., Nordfelth, R., Dubinina, E., Bergman, T., Gustafsson, M., Magnusson, K. E., and Wolf-Watz, H. (1996). Modulation of virulence factor expression by pathogen target cell contact *Science,* **273(5279)**, 1231-3.

6. Rosqvist, R., Magnusson, K. E., and Wolf-Watz, H. (1994). Target cell contact triggers expression and polarized transfer of Yersinia YopE cytotoxin into mammalian cells *EMBO J,* **13(4)**, 964-72.

7. Rosqvist, R., Bölin, I., and Wolf-Watz, H. (1988). Inhibition of phagocytosis in Yersinia pseudotuberculosis: a virulence plasmid-encoded ability involving the Yop2b protein *Infect Immun,* **56(8)**, 2139-43.

8. China, B., N'Guyen, B. T., de Bruyere, M., and Cornelis, G. R. (1994). Role of YadA in resistance of Yersinia enterocolitica to phagocytosis by human polymorphonuclear leukocytes *Infect Immun,* **62(4)**, 1275-81.

9. Visser, L. G., Annema, A., and van Furth, R. (1995). Role of Yops in inhibition of phagocytosis and killing of opsonized Yersinia enterocolitica by human granulocytes *Infect Immun,* **63(7)**, 2570-5.

10. Ruckdeschel, K., Roggenkamp, A., Schubert, S., and Heesemann, J. (1996). Differential contribution of Yersinia enterocolitica virulence factors to evasion of microbicidal action of neutrophils *Infect Immun,* **64(3)**, 724-33.

11. Fällman, M., Andersson, K., Håkansson, S., Magnusson, K. E., Stendahl, O., and Wolf-Watz, H. (1995). Yersinia pseudotuberculosis inhibits Fc receptor-mediated phagocytosis in J774 cells *Infect Immun,* **63(8)**, 3117-24.

12. Grosdent, N., Maridonneau-Parini, I., Sory, M., and Cornelis, G. R. (2002). Role of Yops and adhesins in resistance of Yersinia enterocolitica to phagocytosis *Infect Immun,* **70(8)**, 4165-76.

13. Une, T. (1977). Studies on the pathogenicity of Yersinia enterocolitica. I. Experimental infection in rabbits *Microbiol Immunol,* **21(7)**, 341-63.

14. Simonet, M., Richard, S., and Berche, P. (1990). Electron microscopic evidence for in vivo extracellular localization of Yersinia pseudotuberculosis harboring the pYV plasmid *Infect Immun,* **58(3)**, 841-5.

15. Marketon, M. M., DePaolo, R. W., DeBord, K. L., Jabri, B., and Schneewind, O. (2005). Plague bacteria target immune cells during infection *Science,* **309(5741)**, 1739-41.

16. Grützkau, A., Hanski, C., Hahn, H., and Riecken, E. O. (1990). Involvement of M cells in the bacterial invasion of Peyer's patches: a common mechanism shared by Yersinia enterocolitica and other enteroinvasive bacteria *Gut,* **31(9)**, 1011-5.

17. Autenrieth, I. B. and Firsching, R. (1996). Penetration of M cells and destruction of Peyer's patches by Yersinia enterocolitica: an ultrastructural and histological study *J Med Microbiol,* **44(4)**, 285-94.

18. Bakour, R., Balligand, G., Laroche, Y., Cornelis, G., and Wauters, G. (1985). A simple adult-mouse test for tissue invasiveness in Yersinia enterocolitica strains of low experimental virulence *J Med Microbiol,* **19(2)**, 237-46.

19. Cover, T. L. and Aber, R. C. (1989). Yersinia enterocolitica *N Engl J Med,* **321(1)**, 16-24.

20. Bockemühl, J. (1982). [Intestinal yersinia infection: pathogenesis, clinical course, epidemiology and diagnosis] *Immun Infekt,* **10(5)**, 180-6.

21. Smego, R. A., Frean, J., and Koornhof, H. J. (1999). Yersiniosis I: microbiological and clinicoepidemiological aspects of plague and non-plague Yersinia infections *Eur J Clin Microbiol Infect Dis,* **18(1)**, 1-15.

22. Laroche, Y., van Bouchaute, M., and Cornelis, G. (1984). A restriction map of virulence plasmid pVYE439-80 from a serogroup 9 Yersinia enterocolitica strain *Plasmid,* **12(1)**, 67-70.

23. Cornelis, G. R. and Wolf-Watz, H. (1997). The Yersinia Yop virulon: a bacterial system for subverting eukaryotic cells *Mol Microbiol,* **23(5)**, 861-7.

24. Wattiau, P., Woestyn, S., and Cornelis, G. R. (1996). Customized secretion chaperones in pathogenic bacteria *Mol Microbiol,* **20(2)**, 255-62.

25. Neyt, C., Iriarte, M., Thi, V. H., and Cornelis, G. R. (1997). Virulence and arsenic resistance in Yersiniae *J Bacteriol,* **179(3)**, 612-9.

26. Hoiczyk, E. and Blobel, G. (2001). Polymerization of a single protein of the pathogen Yersinia enterocolitica into needles punctures eukaryotic cells *Proc Natl Acad Sci U S A,* **98(8)**, 4669-74.

27. Kubori, T., Matsushima, Y., Nakamura, D., Uralil, J., Lara-Tejero, M., Sukhan, A., Galán, J. E., and Aizawa, S. I. (1998). Supramolecular structure of the Salmonella typhimurium type III protein secretion system *Science,* **280(5363)**, 602-5.

28. Kubori, T., Sukhan, A., Aizawa, S. I., and Galán, J. E. (2000). Molecular characterization and assembly of the needle complex of the Salmonella typhimurium type III protein secretion system *Proc Natl Acad Sci U S A,* **97(18)**, 10225-30.

29. Blocker, A., Gounon, P., Larquet, E., Niebuhr, K., Cabiaux, V., Parsot, C., and Sansonetti, P. (1999). The tripartite type III secreton of Shigella flexneri inserts IpaB and IpaC into host membranes *J Cell Biol,* **147(3)**, 683-93.

30. Blocker, A., Jouihri, N., Larquet, E., Gounon, P., Ebel, F., Parsot, C., Sansonetti, P., and Allaoui, A. (2001). Structure and composition of the Shigella flexneri "needle complex", a part of its type III secreton. *Mol Microbiol,* **39(3)**, 652–663.

31. Tamano, K., Aizawa, S., Katayama, E., Nonaka, T., Imajoh-Ohmi, S., Kuwae, A., Nagai, S., and Sasakawa, C. (2000). Supramolecular structure of the Shigella type III secretion machinery: the needle part is changeable in length and essential for delivery of effectors *EMBO J,* **19(15)**, 3876-87.

32. Mota, L. J., Journet, L., Sorg, I., Agrain, C., and Cornelis, G. R. (2005). Bacterial injectisomes: needle length does matter. *Science,* **307(5713)**, 1278.

33. Van Gijsegem, F., Vasse, J., Camus, J. C., Marenda, M., and Boucher, C. (2000). Ralstonia solanacearum produces hrp-dependent pili that are required for PopA secretion but not for attachment of bacteria to plant cells *Mol Microbiol,* **36(2)**, 249-60.

34. Knutton, S., Rosenshine, I., Pallen, M. J., Nisan, I., Neves, B. C., Bain, C., Wolff, C., Dougan, G., and Frankel, G. (1998). A novel EspA-associated surface organelle of enteropathogenic Escherichia coli involved in protein translocation into epithelial cells *EMBO J,* **17(8)**, 2166-76.

35. Daniell, S. J., Takahashi, N., Wilson, R., Friedberg, D., Rosenshine, I., Booy, F. P., Shaw, R. K., Knutton, S., Frankel, G., and Aizawa, S. (2001). The filamentous type III secretion translocon of enteropathogenic Escherichia coli *Cell Microbiol,* **3(12)**, 865-71.

36. Crepin, V. F., Shaw, R., Abe, C. M., Knutton, S., and Frankel, G. (2005). Polarity of enteropathogenic Escherichia coli EspA filament assembly and protein secretion *J Bacteriol,* **187(8)**, 2881-9.

37. Marlovits, T. C., Kubori, T., Sukhan, A., Thomas, D. R., Galan, J. E., and Unger, V. M. (2004). Structural insights into the assembly of the type III secretion needle complex. *Science,* **306(5698)**, 1040–1042.

38. Morita-Ishihara, T., Ogawa, M., Sagara, H., Yoshida, M., Katayama, E., and Sasakawa, C. (2006). Shigella Spa33 is an essential C-ring component of type III secretion machinery *J Biol Chem,* **281(1)**, 599-607.

39. Koster, M., Bitter, W., de Cock, H., Allaoui, A., Cornelis, G. R., and Tommassen, J. (1997). The outer membrane component, YscC, of the Yop secretion machinery of Yersinia enterocolitica forms a ring-shaped multimeric complex *Mol Microbiol,* **26(4)**, 789-97.

40. Burghout, P., van Boxtel, R., Van Gelder, P., Ringler, P., Müller, S. A., Tommassen, J., and Koster, M. (2004). Structure and electrophysiological properties of the YscC secretin from the type III secretion system of Yersinia enterocolitica *J Bacteriol,* **186(14)**, 4645-54.

41. Kimbrough, T. G. and Miller, S. I. (2000). Contribution of Salmonella typhimurium type III secretion components to needle complex formation *Proc Natl Acad Sci U S A,* **97(20)**, 11008-13.

42. Sukhan, A., Kubori, T., Wilson, J., and Galán, J. E. (2001). Genetic analysis of assembly of the Salmonella enterica serovar Typhimurium type III secretion-associated needle complex *J Bacteriol,* **183(4)**, 1159-67.

43. Woestyn, S., Allaoui, A., Wattiau, P., and Cornelis, G. R. (1994). YscN, the putative energizer of the Yersinia Yop secretion machinery *J Bacteriol,* **176(6)**, 1561-9.

44. Akeda, Y. and Galán, J. E. (2005). Chaperone release and unfolding of substrates in type III secretion *Nature,* **437(7060)**, 911-5.

45. Broz, P., Mueller, C. A., Müller, S. A., Philippsen, A., Sorg, I., Engel, A., and Cornelis, G. R. (2007). Function and molecular architecture of the Yersinia injectisome tip complex *Mol Microbiol,* **65(5)**, 1311-20.

46. Deane, J. E., Roversi, P., Cordes, F. S., Johnson, S., Kenjale, R., Daniell, S., Booy, F., Picking, W. D., Picking, W. L., Blocker, A. J., and Lea, S. M. (2006). Molecular model of a type III secretion system needle: Implications for host-cell sensing *Proc Natl Acad Sci U S A,* **103(33)**, 12529-33.

47. Mueller, C. A., Broz, P., Müller, S. A., Ringler, P., Erne-Brand, F., Sorg, I., Kuhn, M., Engel, A., and Cornelis, G. R. (2005). The V-antigen of Yersinia forms a distinct structure at the tip of injectisome needles *Science,* **310(5748)**, 674-6.

48. Håkansson, S., Schesser, K., Persson, C., Galyov, E. E., Rosqvist, R., Homblé, F., and Wolf-Watz, H. (1996). The YopB protein of Yersinia pseudotuberculosis is essential for the translocation of Yop effector proteins across the target cell plasma membrane and displays a contact-dependent membrane disrupting activity *EMBO J,* **15(21)**, 5812-23.

49. Nilles, M. L., Fields, K. A., and Straley, S. C. (1998). The V antigen of Yersinia pestis regulates Yop vectorial targeting as well as Yop secretion through effects on YopB and LcrG *J Bacteriol,* **180(13)**, 3410-20.

50. Pettersson, J., Holmström, A., Hill, J., Leary, S., Frithz-Lindsten, E., von Euler-Matell, A., Carlsson, E., Titball, R., Forsberg, A., and Wolf-Watz, H. (1999). The V-antigen of Yersinia is surface exposed before target cell contact and involved in virulence protein translocation *Mol Microbiol,* **32(5)**, 961-76.

51. Tardy, F., Homblé, F., Neyt, C., Wattiez, R., Cornelis, G. R., Ruysschaert, J. M., and Cabiaux, V. (1999). Yersinia enterocolitica type III secretion-translocation system: channel formation by secreted Yops *EMBO J,* **18(23)**, 6793-9.

52. Marenne, M., Journet, L., Mota, L. J., and Cornelis, G. R. (2003). Genetic analysis of the formation of the Ysc-Yop translocation pore in macrophages by Yersinia enterocolitica: role of LcrV, YscF and YopN *Microb Pathog,* **35(6)**, 243-58.

53. Journet, L., Agrain, C., Broz, P., and Cornelis, G. R. (2003). The needle length of bacterial injectisomes is determined by a molecular ruler. *Science,* **302(5651)**, 1757–1760.

54. Katsura I. *Lambda II.* Cold Spring Harbor Labotatory Press, New York; 1983.

55. Buchwald, M., Murialdo, H., and Siminovitch, L. (1970). The morphogenesis of bacteriophage lambda. II. Identification of the principal structural proteins *Virology,* **42(2)**, 390-400.

56. Casjens, S. R. and Hendrix, R. W. (1974). Locations and amounts of major structural proteins in bacteriophage lambda *J Mol Biol,* **88(2)**, 535-45.

57. Campbell, A. (1961). Sensitive mutants of bacteriophage lambda *Virology,* **14**, 22-32.

58. Parkinson, J. S. (1968). Genetics of the left arm of the chromosome of bacteriophage lambda *Genetics,* **59(3)**, 311-25.

59. Mount, D. W., Harris, A. W., Fuerst, C. R., and Siminovitch, L. (1968). Mutations in bacteriophage lambda affecting particle morphogenesis *Virology,* **35(1)**, 134-49.

60. Weigle, J. (1966). Assembly of phage lambda in vitro *Proc Natl Acad Sci U S A,* **55(6)**, 1462-6.

61. Kellenberger E. *Principles of Biomolecular Organization.* Little, Brown, Boston; 1966.

62. Caspar, D. L. (1980). Movement and self-control in protein assemblies. Quasi-equivalence revisited *Biophys J,* **32(1)**, 103-38.

63. Anderson, T. F. and Stephens, R. (1964). Decomposition of T6 bacteriophage in alkaline solutions *Virology,* **23(1)**, 113-7.

64. King, J. (1971). Bacteriophage T4 tail assembly: four steps in core formation *J Mol Biol,* **58(3)**, 693-709.

65. Katsura, I. (1976). Isolation of lambda prophage mutants defective in structural genes: their use for the study of bacteriophage morphogenesis *Mol Gen Genet,* **148(1)**, 31-42.

66. Katsura, I. and Hendrix, R. W. (1984). Length determination in bacteriophage lambda tails *Cell,* **39(3 Pt 2)**, 691-8.

67. Katsura, I. (1987). Determination of bacteriophage lambda tail length by a protein ruler *Nature,* **327(6117)**, 73-5.

68. Katsura, I. (1990). Mechanism of length determination in bacteriophage lambda tails *Adv Biophys,* **26**, 1-18.

69. Katsura, I. and Kühl, P. W. (1975). Morphogenesis of the tail of bacteriophage lambda. III. Morphogenetic pathway *J Mol Biol,* **91(3)**, 257-73.

70. Katsura, I. (1976). Morphogenesis of bacteriophage lambda tail. Polymorphism in the assembly of the major tail protein *J Mol Biol,* **107(3)**, 307-26.

71. Hendrix, R. W. and Casjens, S. R. (1974). Protein cleavage in bacteriophage lambda tail assembly *Virology,* **61(1)**, 156-9.

72. Tsui, L. C. and Hendrix, R. W. (1983). Proteolytic processing of phage lambda tail protein gpH: timing of the cleavage *Virology,* **125(2)**, 257-64.

73. Abuladze, N. K., Gingery, M., Tsai, J., and Eiserling, F. A. (1994). Tail length determination in bacteriophage T4 *Virology,* **199(2)**, 301-10.

74. Ishimoto, L. K., Ishimoto, K. S., Cascino, A., Cipollaro, M., and Eiserling, F. A. (1988). The structure of three bacteriophage T4 genes required for tail-tube assembly *Virology,* **164(1)**, 81-90.

75. Vianelli, A., Wang, G. R., Gingery, M., Duda, R. L., Eiserling, F. A., and Goldberg, E. B. (2000). Bacteriophage T4 self-assembly: localization of gp3 and its role in determining tail length *J Bacteriol,* **182(3)**, 680-8.

76. Zhao, L., Kanamaru, S., Chaidirek, C., and Arisaka, F. (2003). P15 and P3, the tail completion proteins of bacteriophage T4, both form hexameric rings *J Bacteriol,* **185(5)**, 1693-700.

77. Pedulla, M. L., Ford, M. E., Houtz, J. M., Karthikeyan, T., Wadsworth, C., Lewis, J. A., Jacobs-Sera, D., Falbo, J., Gross, J., Pannunzio, N. R., Brucker, W., Kumar, V., Kandasamy, J., Keenan, L., Bardarov, S., Kriakov, J., Lawrence, J. G., Jacobs, Jr, W. R., Hendrix, R. W., and Hatfull, G. F. (2003). Origins of highly mosaic mycobacteriophage genomes *Cell,* **113(2)**, 171-82.

78. Pedersen, M., Ostergaard, S., Bresciani, J., and Vogensen, F. K. (2000). Mutational analysis of two structural genes of the temperate lactococcal bacteriophage TP901-1 involved in tail length determination and baseplate assembly *Virology,* **276(2)**, 315-28.

79. Duda, R. L., Gingery, M., and Eiserling, F. A. (1986). Potential length determiner and DNA injection protein is extruded from bacteriophage T4 tail tubes in vitro *Virology,* **151(2)**, 296-314.

80. Piuri, M. and Hatfull, G. F. (2006). A peptidoglycan hydrolase motif within the mycobacteriophage TM4 tape measure protein promotes efficient infection of stationary phase cells *Mol Microbiol,* **62(6)**, 1569-85.

81. Boulanger, P., Jacquot, P., Plançon, L., Chami, M., Engel, A., Parquet, C., Herbeuval, C., and Letellier, L. (2008). Phage T5 straight tail fiber is a multifunctional protein acting as a tape measure and carrying fusogenic and muralytic activities *J Biol Chem,* **283(20)**, 13556-64.

82. Berg, H. C. and Anderson, R. A. (1973). Bacteria swim by rotating their flagellar filaments *Nature,* **245(5425)**, 380-2.

83. Macnab, R. M. (2003). How bacteria assemble flagella *Annu Rev Microbiol,* **57**, 77-100.

84. Macnab, R. M. (2004). Type III flagellar protein export and flagellar assembly *Biochim Biophys Acta,* **1694(1-3)**, 207-17.

85. Kojima, S. and Blair, D. F. (2004). The bacterial flagellar motor: structure and function of a complex molecular machine *Int Rev Cytol,* **233**, 93-134.

86. Homma, M., Komeda, Y., Iino, T., and Macnab, R. M. (1987). The flaFIX gene product of Salmonella typhimurium is a flagellar basal body component with a signal peptide for export *J Bacteriol,* **169(4)**, 1493-8.

87. Jones, C. J., Macnab, R. M., Okino, H., and Aizawa, S. (1990). Stoichiometric analysis of the flagellar hook-(basal-body) complex of Salmonella typhimurium *J Mol Biol,* **212(2)**, 377-87.

88. Ueno, T., Oosawa, K., and Aizawa, S. (1992). M ring, S ring and proximal rod of the flagellar basal body of Salmonella typhimurium are composed of subunits of a single protein, FliF *J Mol Biol,* **227(3)**, 672-7.

89. Khan, I. H., Reese, T. S., and Khan, S. (1992). The cytoplasmic component of the bacterial flagellar motor *Proc Natl Acad Sci U S A,* **89(13)**, 5956-60.

90. Homma, M., Kutsukake, K., Hasebe, M., Iino, T., and Macnab, R. M. (1990). FlgB, FlgC, FlgF and FlgG. A family of structurally related proteins in the flagellar basal body of Salmonella typhimurium *J Mol Biol,* **211(2)**, 465-77.

91. Macnab, R. M. (1999). The bacterial flagellum: reversible rotary propellor and type III export apparatus *J Bacteriol,* **181(23)**, 7149-53.

92. Morgan, D. G., Macnab, R. M., Francis, N. R., and DeRosier, D. J. (1993). Domain organization of the subunit of the Salmonella typhimurium flagellar hook *J Mol Biol,* **229(1)**, 79-84.

93. Morgan, D. G., Owen, C., Melanson, L. A., and DeRosier, D. J. (1995). Structure of bacterial flagellar filaments at 11 A resolution: packing of the alpha-helices *J Mol Biol,* **249(1)**, 88-110.

94. Mimori, Y., Yamashita, I., Murata, K., Fujiyoshi, Y., Yonekura, K., Toyoshima, C., and Namba, K. (1995). The structure of the R-type straight flagellar filament of Salmonella at 9 A resolution by electron cryomicroscopy *J Mol Biol,* **249(1)**, 69-87.

95. Minamino, T. and Macnab, R. M. (1999). Components of the Salmonella flagellar export apparatus and classification of export substrates *J Bacteriol,* **181(5)**, 1388-94.

96. Fan, F. and Macnab, R. M. (1996). Enzymatic characterization of FliI. An ATPase involved in flagellar assembly in Salmonella typhimurium *J Biol Chem,* **271(50)**, 31981-8.

97. Homma, M. and Iino, T. (1985). Excretion of unassembled hook-associated proteins by Salmonella typhimurium *J Bacteriol,* **164(3)**, 1370-2.

98. Ikeda, T., Asakura, S., and Kamiya, R. (1985). "Cap" on the tip of Salmonella flagella *J Mol Biol,* **184(4)**, 735-7.

99. Ikeda, T., Oosawa, K., and Hotani, H. (1996). Self-assembly of the filament capping protein, FliD, of bacterial flagella into an annular structure *J Mol Biol,* **259(4)**, 679-86.

100. Ohnishi, K., Ohto, Y., Aizawa, S., Macnab, R. M., and Iino, T. (1994). FlgD is a scaffolding protein needed for flagellar hook assembly in Salmonella typhimurium. *J Bacteriol,* **176(8)**, 2272–2281.

101. Suzuki, T., Iino, T., Horiguchi, T., and Yamaguchi, S. (1978). Incomplete flagellar structures in nonflagellate mutants of Salmonella typhimurium *J Bacteriol,* **133(2)**, 904-15.

102. Suzuki, T. and Komeda, Y. (1981). Incomplete flagellar structures in Escherichia coli mutants *J Bacteriol,* **145(2)**, 1036-41.

103. Hirano, T., Yamaguchi, S., Oosawa, K., and Aizawa, S. (1994). Roles of FliK and FlhB in determination of flagellar hook length in Salmonella typhimurium. *J Bacteriol,* **176(17)**, 5439–5449.

104. Kawagishi, I., Homma, M., Williams, A. W., and Macnab, R. M. (1996). Characterization of the flagellar hook length control protein fliK of Salmonella typhimurium and Escherichia coli. *J Bacteriol,* **178(10)**, 2954–2959.

105. Williams, A. W., Yamaguchi, S., Togashi, F., Aizawa, S. I., Kawagishi, I., and Macnab, R. M. (1996). Mutations in fliK and flhB affecting flagellar hook and filament assembly in Salmonella typhimurium. *J Bacteriol,* **178(10)**, 2960–2970.

106. Patterson-Delafield, J., Martinez, R. J., Stocker, B. A., and Yamaguchi, S. (1973). A new fla gene in Salmonella typhimurium--flaR--and its mutant phenotype-superhooks *Arch Mikrobiol,* **90(2)**, 107-20.

107. Minamino, T., Ferris, H. U., Moriya, N., Kihara, M., and Namba, K. (2006). Two parts of the T3S4 domain of the hook-length control protein FliK are essential for the substrate specificity switching of the flagellar type III export apparatus. *J Mol Biol,* **362(5)**, 1148–1158.

108. Muramoto, K., Makishima, S., Aizawa, S. I., and Macnab, R. M. (1998). Effect of cellular level of FliK on flagellar hook and filament assembly in Salmonella typhimurium. *J Mol Biol,* **277(4)**, 871–882.

109. Minamino, T., Saijo-Hamano, Y., Furukawa, Y., Gonzalez-Pedrajo, B., Macnab, R. M., and Namba, K. (2004). Domain organization and function of Salmonella FliK, a flagellar hook-length control protein. *J Mol Biol,* **341(2)**, 491–502.

110. Agrain, C., Callebaut, I., Journet, L., Sorg, I., Paroz, C., Mota, L. J., and Cornelis, G. R. (2005). Characterization of a Type III secretion substrate specificity switch (T3S4) domain in YscP from Yersinia enterocolitica. *Mol Microbiol,* **56(1)**, 54–67.

111. Minamino, T., Gonzalez-Pedrajo, B., Yamaguchi, K., Aizawa, S. I., and Macnab, R. M. (1999). FliK, the protein responsible for flagellar hook length control in Salmonella, is exported during hook assembly. *Mol Microbiol,* **34(2)**, 295–304.

112. Hirano, T., Shibata, S., Ohnishi, K., Tani, T., and Aizawa, S. (2005). N-terminal signal region of FliK is dispensable for length control of the flagellar hook. *Mol Microbiol,* **56(2)**, 346–360.

113. Shibata, S., Takahashi, N., Chevance, F. F. V., Karlinsey, J. E., Hughes, K. T., and Aizawa, S. (2007). FliK regulates flagellar hook length as an internal ruler. *Mol Microbiol,* **64(5)**, 1404–1415.

114.Suzuki, T. and Iino, T. (1981). Role of the flaR gene in flagellar hook formation in Salmonella spp *J Bacteriol,* **148(3)**, 973-9.

115.Kutsukake, K., Minamino, T., and Yokoseki, T. (1994). Isolation and characterization of FliK-independent flagellation mutants from Salmonella typhimurium. *J Bacteriol,* **176(24)**, 7625–7629.

116.Minamino, T. and Macnab, R. M. (2000). Domain structure of Salmonella FlhB, a flagellar export component responsible for substrate specificity switching. *J Bacteriol,* **182(17)**, 4906–4914.

117.Makishima, S., Komoriya, K., Yamaguchi, S., and Aizawa, S. I. (2001). Length of the flagellar hook and the capacity of the type III export apparatus. *Science,* **291(5512)**, 2411–2413.

118.Moriya, N., Minamino, T., Hughes, K. T., Macnab, R. M., and Namba, K. (2006). The type III flagellar export specificity switch is dependent on FliK ruler and a molecular clock. *J Mol Biol,* **359(2)**, 466–477.

119.Chevance, F. F. V. and Hughes, K. T. (2008). Coordinating assembly of a bacterial macromolecular machine *Nat Rev Microbiol,* **6(6)**, 455-65.

120.Samatey, F. A., Matsunami, H., Imada, K., Nagashima, S., Shaikh, T. R., Thomas, D. R., Chen, J. Z., Derosier, D. J., Kitao, A., and Namba, K. (2004). Structure of the bacterial flagellar hook and implication for the molecular universal joint mechanism *Nature,* **431(7012)**, 1062-8.

121.Koroyasu, S., Yamazato, M., Hirano, T., and Aizawa, S. I. (1998). Kinetic analysis of the growth rate of the flagellar hook in Salmonella typhimurium by the population balance method *Biophys J,* **74(1)**, 436-43.

122.Minamino, T., Moriya, N., Hirano, T., Hughes, K. T., and Namba, K. (2009). Interaction of FliK with the bacterial flagellar hook is required for efficient export specificity switching *Mol Microbiol,* **74(1)**, 239-51.

123.Marlovits, T. C., Kubori, T., Lara-Tejero, M., Thomas, D., Unger, V. M., and Galan, J. E. (2006). Assembly of the inner rod determines needle length in the type III secretion injectisome. *Nature,* **441(7093)**, 637–640.

124.Magdalena, J., Hachani, A., Chamekh, M., Jouihri, N., Gounon, P., Blocker, A., and Allaoui, A. (2002). Spa32 regulates a switch in substrate specificity of the type III secreton of Shigella flexneri from needle components to Ipa proteins. *J Bacteriol,* **184(13)**, 3433–3441.

125.Stainier, I., Bleves, S., Josenhans, C., Karmani, L., Kerbourch, C., Lambermont, I., Totemeyer, S., Boyd, A., and Cornelis, G. R. (2000). YscP, a Yersinia protein required for Yop secretion that is surface exposed, and released in low Ca2+. *Mol Microbiol,* **37(5)**, 1005–1018.

126.Agrain, C., Sorg, I., Paroz, C., and Cornelis, G. R. (2005). Secretion of YscP from Yersinia enterocolitica is essential to control the length of the injectisome needle but not to change the type III secretion substrate specificity. *Mol Microbiol,* **57(5)**, 1415–1427.

127. Russmann, H., Kubori, T., Sauer, J., and Galan, J. E. (2002). Molecular and functional analysis of the type III secretion signal of the Salmonella enterica InvJ protein. *Mol Microbiol,* **46(3)**, 769–779.

128. Edqvist, P. J., Olsson, J., Lavander, M., Sundberg, L., Forsberg, A., Wolf-Watz, H., and Lloyd, S. A. (2003). YscP and YscU regulate substrate specificity of the Yersinia type III secretion system. *J Bacteriol,* **185(7)**, 2259–2266.

129. Lavander, M., Sundberg, L., Edqvist, P. J., Lloyd, S. A., Wolf-Watz, H., and Forsberg, A. (2002). Proteolytic cleavage of the FlhB homologue YscU of Yersinia pseudotuberculosis is essential for bacterial survival but not for type III secretion. *J Bacteriol,* **184(16)**, 4500–4509.

130. Sorg, I., Wagner, S., Amstutz, M., Muller, S. A., Broz, P., Lussi, Y., Engel, A., and Cornelis, G. R. (2007). YscU recognizes translocators as export substrates of the Yersinia injectisome. *EMBO J,* **26(12)**, 3015–3024.

131. Cornelis, G. R. (2006). The type III secretion injectisome *Nat Rev Microbiol,* **4(11)**, 811-25.

132. Botteaux, A., Sani, M., Kayath, C. A., Boekema, E. J., and Allaoui, A. (2008). Spa32 interaction with the inner-membrane Spa40 component of the type III secretion system of Shigella flexneri is required for the control of the needle length by a molecular tape measure mechanism. *Mol Microbiol,* **70(6)**, 1515–1528.

133. Raetz, C. R. H. and Whitfield, C. (2002). Lipopolysaccharide endotoxins *Annu Rev Biochem,* **71**, 635-700.

134. Hitchcock, P. J. and Brown, T. M. (1983). Morphological heterogeneity among Salmonella lipopolysaccharide chemotypes in silver-stained polyacrylamide gels *J Bacteriol,* **154(1)**, 269-77.

135. Munford, R. S., Hall, C. L., and Rick, P. D. (1980). Size heterogeneity of Salmonella typhimurium lipopolysaccharides in outer membranes and culture supernatant membrane fragments *J Bacteriol,* **144(2)**, 630-40.

136. Palva, E. T. and Mäkelä, P. H. (1980). Lipopolysaccharide heterogeneity in Salmonella typhimurium analyzed by sodium dodecyl sulfate polyacrylamide gel electrophoresis *Eur J Biochem,* **107(1)**, 137-43.

137. Samuel, G. and Reeves, P. (2003). Biosynthesis of O-antigens: genes and pathways involved in nucleotide sugar precursor synthesis and O-antigen assembly *Carbohydr Res,* **338(23)**, 2503-19.

138. Batchelor, R. A., Haraguchi, G. E., Hull, R. A., and Hull, S. I. (1991). Regulation by a novel protein of the bimodal distribution of lipopolysaccharide in the outer membrane of Escherichia coli *J Bacteriol,* **173(18)**, 5699-704.

139. Batchelor, R. A., Alifano, P., Biffali, E., Hull, S. I., and Hull, R. A. (1992). Nucleotide sequences of the genes regulating O-polysaccharide antigen chain length (rol) from Escherichia coli and Salmonella typhimurium: protein homology and functional complementation *J Bacteriol,* **174(16)**, 5228-36.

140.Wugeditsch, T., Paiment, A., Hocking, J., Drummelsmith, J., Forrester, C., and Whitfield, C. (2001). Phosphorylation of Wzc, a tyrosine autokinase, is essential for assembly of group 1 capsular polysaccharides in Escherichia coli *J Biol Chem,* **276(4)**, 2361-71.

141.Collins, R. F., Beis, K., Dong, C., Botting, C. H., McDonnell, C., Ford, R. C., Clarke, B. R., Whitfield, C., and Naismith, J. H. (2007). The 3D structure of a periplasm-spanning platform required for assembly of group 1 capsular polysaccharides in Escherichia coli *Proc Natl Acad Sci U S A,* **104(7)**, 2390-5.

142.Morona, R., Van Den Bosch, L., and Daniels, C. (2000). Evaluation of Wzz/MPA1/MPA2 proteins based on the presence of coiled-coil regions *Microbiology,* **146 (Pt 1)**, 1-4.

143.Bastin, D. A., Stevenson, G., Brown, P. K., Haase, A., and Reeves, P. R. (1993). Repeat unit polysaccharides of bacteria: a model for polymerization resembling that of ribosomes and fatty acid synthetase, with a novel mechanism for determining chain length *Mol Microbiol,* **7(5)**, 725-34.

144.Morona, R., van den Bosch, L., and Manning, P. A. (1995). Molecular, genetic, and topological characterization of O-antigen chain length regulation in Shigella flexneri *J Bacteriol,* **177(4)**, 1059-68.

145.Becker, A. and Pühler, A. (1998). Specific amino acid substitutions in the proline-rich motif of the Rhizobium meliloti ExoP protein result in enhanced production of low-molecular-weight succinoglycan at the expense of high-molecular-weight succinoglycan *J Bacteriol,* **180(2)**, 395-9.

146.Doublet, P., Grangeasse, C., Obadia, B., Vaganay, E., and Cozzone, A. J. (2002). Structural organization of the protein-tyrosine autokinase Wzc within Escherichia coli cells *J Biol Chem,* **277(40)**, 37339-48.

147.Franco, A. V., Liu, D., and Reeves, P. R. (1998). The wzz (cld) protein in Escherichia coli: amino acid sequence variation determines O-antigen chain length specificity *J Bacteriol,* **180(10)**, 2670-5.

148.Klee, S. R., Tzschaschel, B. D., Timmis, K. N., and Guzman, C. A. (1997). Influence of different rol gene products on the chain length of Shigella dysenteriae type 1 lipopolysaccharide O antigen expressed by Shigella flexneri carrier strains *J Bacteriol,* **179(7)**, 2421-5.

149.Tocilj, A., Munger, C., Proteau, A., Morona, R., Purins, L., Ajamian, E., Wagner, J., Papadopoulos, M., Van Den Bosch, L., Rubinstein, J. L., Féthière, J., Matte, A., and Cygler, M. (2008). Bacterial polysaccharide co-polymerases share a common framework for control of polymer length *Nat Struct Mol Biol,* **15(2)**, 130-8.

150.Larue, K., Kimber, M. S., Ford, R., and Whitfield, C. (2009). Biochemical and structural analysis of bacterial O-antigen chain length regulator proteins reveals a conserved quaternary structure *J Biol Chem,* **284(11)**, 7395-403.

151. Marolda, C. L., Haggerty, E. R., Lung, M., and Valvano, M. A. (2008). Functional analysis of predicted coiled-coil regions in the Escherichia coli K-12 O-antigen polysaccharide chain length determinant Wzz *J Bacteriol,* **190(6)**, 2128-37.

152. Nilsson, C., Skoglund, A., Moran, A. P., Annuk, H., Engstrand, L., and Normark, S. (2006). An enzymatic ruler modulates Lewis antigen glycosylation of Helicobacter pylori LPS during persistent infection *Proc Natl Acad Sci U S A,* **103(8)**, 2863-8.

153. Fraser, G. M., Hirano, T., Ferris, H. U., Devgan, L. L., Kihara, M., and Macnab, R. M. (2003). Substrate specificity of type III flagellar protein export in Salmonella is controlled by subdomain interactions in FlhB. *Mol Microbiol,* **48(4)**, 1043–1057.

154. Ferris, H. U., Furukawa, Y., Minamino, T., Kroetz, M. B., Kihara, M., Namba, K., and Macnab, R. M. (2005). FlhB regulates ordered export of flagellar components via autocleavage mechanism. *J Biol Chem,* **280(50)**, 41236–41242.

155. Ferris, H. U. and Minamino, T. (2006). Flipping the switch: bringing order to flagellar assembly. *Trends Microbiol,* **14(12)**, 519–526.

156. Allaoui, A., Woestyn, S., Sluiters, C., and Cornelis, G. R. (1994). YscU, a Yersinia enterocolitica inner membrane protein involved in Yop secretion. *J Bacteriol,* **176(15)**, 4534–4542.

157. Wagner, S., Sorg, I., Degiacomi, M., Journet, L., Dal Peraro, M., and Cornelis, G. R. (2009). The helical content of the YscP molecular ruler determines the length of the Yersinia injectisome. *Mol Microbiol,* **71(3)**, 692–701.

158. Wiesand, U., Sorg, I., Amstutz, M., Wagner, S., van den Heuvel, J., Luhrs, T., Cornelis, G. R., and Heinz, D. W. (2009). Structure of the type III secretion recognition protein YscU from Yersinia enterocolitica. *J Mol Biol,* **385(3)**, 854–866.

159. Lavander, M., Sundberg, L., Edqvist, P. J., Lloyd, S. A., Wolf-Watz, H., and Forsberg, A. (2003). Characterisation of the type III secretion protein YscU in Yersinia pseudotuberculosis. YscU cleavage--dispensable for TTSS but essential for survival. *Adv Exp Med Biol,* **529**, 109–112.

160. Zarivach, R., Deng, W., Vuckovic, M., Felise, H. B., Nguyen, H. V., Miller, S. I., Finlay, B. B., and Strynadka, N. C. J. (2008). Structural analysis of the essential self-cleaving type III secretion proteins EscU and SpaS *Nature,* **453(7191)**, 124-7.

161. Wood, S. E., Jin, J., and Lloyd, S. A. (2008). YscP and YscU switch the substrate specificity of the Yersinia type III secretion system by regulating export of the inner rod protein YscI. *J Bacteriol,* **190(12)**, 4252–4262.

162. Sani, M., Allaoui, A., Fusetti, F., Oostergetel, G. T., Keegstra, W., and Boekema, E. J. (2007). Structural organization of the needle complex of the type III secretion apparatus of Shigella flexneri. *Micron,* **38(3)**, 291–301.

163.Zhu, K., Gonzalez-Pedrajo, B., and Macnab, R. M. (2002). Interactions among membrane and soluble components of the flagellar export apparatus of Salmonella. *Biochemistry,* **41(30)**, 9516–9524.

164.Deane, J. E., Graham, S. C., Mitchell, E. P., Flot, D., Johnson, S., and Lea, S. M. (2008). Crystal structure of Spa40, the specificity switch for the Shigella flexneri type III secretion system *Mol Microbiol,* **69(1)**, 267-76.

165.Lountos, G. T., Austin, B. P., Nallamsetty, S., and Waugh, D. S. (2009). Atomic resolution structure of the cytoplasmic domain of Yersinia pestis YscU, a regulatory switch involved in type III secretion *Protein Sci,* **18(2)**, 467-74.

166.Vanderkooi, J. M., Ierokomas, A., Nakamura, H., and Martonosi, A. (1977). Fluorescence energy transfer between Ca2+ transport ATPase molecules in artificial membranes *Biochemistry,* **16(7)**, 1262-7.

167.Sharma, N., Hewett, J., Ozelius, L. J., Ramesh, V., McLean, P. J., Breakefield, X. O., and Hyman, B. T. (2001). A close association of torsinA and alpha-synuclein in Lewy bodies: a fluorescence resonance energy transfer study *Am J Pathol,* **159(1)**, 339-44.

168.Palmer, B. R. and Marinus, M. G. (1994). The dam and dcm strains of Escherichia coli--a review *Gene,* **143(1)**, 1-12.

169.Metcalf, W. W., Jiang, W., and Wanner, B. L. (1994). Use of the rep technique for allele replacement to construct new Escherichia coli hosts for maintenance of R6K gamma origin plasmids at different copy numbers *Gene,* **138(1-2)**, 1-7.

170.Miller, V. L. and Mekalanos, J. J. (1988). A novel suicide vector and its use in construction of insertion mutations: osmoregulation of outer membrane proteins and virulence determinants in Vibrio cholerae requires toxR *J Bacteriol,* **170(6)**, 2575-83.

171.Sory, M. P., Boland, A., Lambermont, I., and Cornelis, G. R. (1995). Identification of the YopE and YopH domains required for secretion and internalization into the cytosol of macrophages, using the cyaA gene fusion approach *Proc Natl Acad Sci U S A,* **92(26)**, 11998-2002.

172.Cornelis, G., Vanootegem, J. C., and Sluiters, C. (1987). Transcription of the yop regulon from Y. enterocolitica requires trans acting pYV and chromosomal genes *Microb Pathog,* **2(5)**, 367-79.

173.Kaniga, K., Delor, I., and Cornelis, G. R. (1991). A wide-host-range suicide vector for improving reverse genetics in gram-negative bacteria: inactivation of the blaA gene of Yersinia enterocolitica *Gene,* **109(1)**, 137-41.

174.Tabor, S. and Richardson, C. C. (1985). A bacteriophage T7 RNA polymerase/promoter system for controlled exclusive expression of specific genes *Proc Natl Acad Sci U S A,* **82(4)**, 1074-8.

Acknowledgement

I am grateful to Prof. Dr. Guy R. Cornelis for his support, his trust in me, his ideas, our discussions, coffee-breaks and the open door.

I thank Prof. Dr. Urs Jenal and Prof. Dr. Christoph Dehio for being my PhD committee and the inspiring discussions during the committee meetings.

Lab members I want to thank all the past and present members of the Cornelis lab for the pleasant atmosphere, for coffee breaks and after work beers, for scientific discussions and mental support, for inspiring ruler models and BBQs. Special thanks to Lisa Metzger, Dr. Caroline Montagner, Dr. Francesco Renzi, Dr. Fabian M. Commichau, Pablo Manfredi, Dr. Manuela Mally, Andreas Diepold, Cecile Pfaff, Marina Kuhn, Cedric Cattin, Dr. Isabel Sorg, Dr. Hwain Shin, Dr. Michel Letzelter and Dr. Jaime Mota.

Collaborators I am grateful to Prof. Dr. Matteo Dal Peraro, Matteo Degiacomi and Dr. Marco Stenta from the EPF Lausanne for our fruitful collaboration and for giving me a completely different view on my project.

Biozentrum colleagues Thank you for the good atmosphere on the floor and for scientific support. Special thanks to Michaela Hanisch, Roger Sauder, Gianni Morson, Vesna Olivieri, Ursula Sauder, Roland Gut, Andreas Hefti and Loredana D'Anna.

My friends Thanks a lot for your infinite support, your friendship, your patience. Special thanks to Kerstin & Michel, Helo, Rainer, David, Caro, Tina, Emilio and Yücel.

Meine Familie Ein ganz besonderer Dank gilt meiner Familie, ohne die diese Arbeit nicht möglich gewesen wäre. Danke, dass ihr für mich da seit, mich unterstützt und an mich glaubt.

Alex "Happiness is only real when shared."- Into the wild.
Danke das Du an meiner Seite, und immer für mich da bist.

Curriculum vitae

Stefanie Wagner

Bungestrasse 18
4055 Basel
Switzerland
Phone: +41-(0)61-3215867
Email: stefanie.wagner@unibas.ch

Date of birth: October, 2nd 1979
Place of birth: Frankfurt/Höchst, Germany
Nationality: German
Marital status: Single

Education

10.1999 - 09.2001	Basic studies in biology, Darmstadt Technical University, Germany
10.2001 - 03.2004	Main studies in biology, Darmstadt Technical University, Germany
10.2004 – 12.2004	Oral diploma examinations
01.2005 – 09.2005	Diploma thesis with Prof. W. Keller, Biozentrum, University of Basel, Division of Cell Biology, Switzerland
09.2005	Graduation Degree: Diplom-Biologin
10.2005 – 12.2009	PhD thesis with Prof. Guy R. Cornelis Biozentrum, University of Basel, Basel, Infection Biology, Switzerland
Gap in the CV	03.2004 - 07.2004 Journey to Argentina, Chile, Bolivia, Peru, Brasil and the U.S.A.

Professional Experience

05.2002	Practical Traineeship with Priv.-Doz. Dr. A. Robitzki Fraunhofer Institute for Biomedical Engineering, St. Ingbert, Germany
10.2003 - 11.2003	Practical Training with Prof. H. U. Göringer Institute of Microbiology and Genetics, Darmstadt Technical University, Germany
12.2003 - 01.2004	Effect of mutations in *yscP* on type III secretion Practical training with Prof. G. Cornelis Biozentrum, University of Basel, Division of Molecular Microbiology, Switzerland
01.2005 – 09.2005	Genetic interactions between a new poly(A) polymerase complex and RNA processing factors in *S. cerevisiae* Diploma thesis with Prof. W. Keller Biozentrum, University of Basel, Division of Cell Biology, Switzerland
10.2005 – 12.2009	Length control of the Yersinia injectisome needle PhD thesis with Prof. Guy R. Cornelis

	Biozentrum, University of Basel, Basel, Infection Biology, Switzerland
01.2010 – present	Length control of the Salmonella injectisome needle Post-Doc with Prof. Guy R. Cornelis Biozentrum, University of Basel, Basel, Infection Biology, Switzerland
06.2007	FEBS/EMBO Advanced Lecture Course Cellular and Molecular Biology of Membranes Cargese, Corsica, France

Teaching Experience

Assistant and supervisor of an experiment in the annual students Blockkurs: 1 week per year
Practical training with 3rd year students in Molecular Microbiology

Co-supervision of Project work: Cedric Cattin (09.2007 - 11.2007)
Evaluation of the AFM to test the hypothesis of a molecular ruler controlling bacterial injectisome needle length

Supervision of Master Thesis: Lisa Metzger (08.2008 - 10.2009)
The assembly of one injectisome needle involves only one molecule of YscP ruler

Publications and Posters

Stefanie Wagner, Marco Stenta, Lisa Metzger, Matteo Dal Peraro and Guy R. Cornelis. Control of the length of the injectisome needle requires only one molecule of YscP. (revised version submitted to EMBO Reports)

Stefanie Wagner, Isabel Sorg, Matteo Degiacomi, Laure Journet, Matteo Dal Peraro and Guy R. Cornelis. The helical content of the YscP molecular ruler determines the length of the Yersinia injectisome. (2009) *Mol Microbiol*., 71(3), 692-701

Ulrich Wiesand, Isabel Sorg, Marlise Amstutz, Stefanie Wagner, Joop van den Heuvel, Thorsten Lührs, Guy R. Cornelis and Dirk W. Heinz. Structure of the Type III secretion recognition protein YscU from Yersinia enterocolitica. (2009) *J Mo. Biol*, 385(3), 854-866

Isabel Sorg, Stefanie Wagner, Marlise Amstutz, Shirley A. Müller, Petr Broz, Yvonne Lussi, Andreas Engel and Guy R. Cornelis. YscU recognizes translocators as export substrates of the Yersinia injectisome. (2007) *EMBO J*., 26, 3015-3024

Stefanie Wagner, Isabel Sorg, Laur Journet, Cecile Pfaff and Guy R. Cornelis. Needle length control in the Yersinia type III secretion system. Biozentrum Symposium, Oktober 2007

Stefanie Wagner, Isabel Sorg, Céline Agrain and Guy R. Cornelis. Needle length control in the Yersinia type III secretion system – How does the ruler work?. FEBS / EMBO Advanced Lecture Course, Juni 2007

Stefanie Wagner, Isabel Sorg, Céline Agrain, Laure Journet, Luis Jaime Mota, Petr Broz and Guy R. Cornelis. Length control of the Yersinia injectisome needle. Biozentrum Symposium, Oktober 2006

Scholarship

FEBS Travel-Scholarship